

Methanotrophy under extreme conditions

**Biochemistry and physiology of
Methylacidiphilum fumariolicum SolV**

Khadem, A. F. (2012). Methanotrophy under extreme conditions: Biochemistry and physiology of *Methylacidiphilum fumariolicum* SolV. *Ph.D. thesis, Radboud University Nijmegen, Nijmegen, the Netherlands*, **220** pages. This thesis includes summaries in English, Dutch and Arabic.

This research was supported
by the Netherlands
Organisation for Scientific
Research (NWO) under
project number:
017.005.113.



Cover: A fumarole at Campi Flegrei, near Naples, Italy.
Picture by Dr. Arjan Pol. Design by Ahmad F. Khadem.

Printed by Ipskamp Drukkers, Enschede, the Netherlands.

ISBN 978-94-6191-417-0 / NUR 922 - Biologie algemeen.

Methanotrofie onder extreme condities

Biochemie en fysiologie van *Methylophilum thermophilum* SolV

Proefschrift

ter verkrijging van de graad van doctor aan de
Radboud Universiteit Nijmegen op gezag van
rector magnificus prof. mr. S. C. J. J. Kortmann,
volgens besluit van het college van decanen
in het openbaar te verdedigen op
woensdag 5 december 2012
om 10:30 uur precies.

Door

Ahmad Fouad Khadem
geboren op 15 april 1981
te Bagdad (Irak).

Promotor:

prof. dr. ir. Mike S. M. Jetten.

Copromotoren:

dr. Huub J. M. Op den Camp.

dr. Arjan Pol.

Manuscriptcommissie:

prof. dr. Titti Mariani.

prof. dr. ir. Fons Stams (Wageningen Universiteit).

dr. Paul L. E. Bodelier (Nederlands Instituut voor Ecologie (NIOO-KNAW), Wageningen).

Methanotrophy under extreme conditions

Biochemistry and physiology of *Methylophilum thermophilum* SolV

Doctoral Thesis

to obtain the degree of doctor from
Radboud University Nijmegen on the authority of the
Rector Magnificus Prof. dr. S. C. J. J. Kortmann,
according to the decision of the Council of Deans
to be defended in public on
Wednesday, December 5, 2012
at 10:30 hours.

By

Ahmad Fouad Khadem
Born on April 15, 1981
in Baghdad (Iraq).

Supervisor:

Prof. dr. ir. Mike S. M. Jetten.

Co-supervisors:

Dr. Huub J. M. Op den Camp.

Dr. Arjan Pol.

Doctoral Thesis Committee:

Prof. dr. Titti Mariani.

Prof. dr. ir. Fons Stams (Wageningen University).

Dr. Paul L. E. Bodelier (The Netherlands Institute of Ecology (NIOO-KNAW), Wageningen).

Table of Contents

Chapter One..... (9)

General Introduction

Chapter Two..... (35)

Draft genome sequence of the
volcano-inhabiting thermoacidophilic methanotroph
Methylacidiphilum fumariolicum strain SolV

Chapter Three..... (47)

Nitrogen fixation by the verrucomicrobial methanotroph
Methylacidiphilum fumariolicum SolV

Chapter Four..... (67)

Autotrophic methanotrophy in *Verrucomicrobia*:
Methylacidiphilum fumariolicum SolV uses the
Calvin-Benson-Bassham cycle for carbon dioxide fixation

Chapter Five..... (101)

Genomic and physiological analysis of
carbon storage in the verrucomicrobial methanotroph
“*Ca. Methylacidiphilum fumariolicum*” SolV

Chapter Six..... (131)

Metabolic regulation of
“*Ca. Methylacidiphilum fumariolicum*” SolV cells
grown under different nitrogen and oxygen limitations

Table of Contents (continuation)

Chapter Seven.....	(169)
---------------------------	--------------

Summary & Outlook

References.....	(181)
------------------------	--------------

Nederlandse samenvatting (Dutch summary).....	(195)
--	--------------

Dankwoord (Acknowledgments).....	(203)
---	--------------

Curriculum Vitae & List of publications.....	(207)
---	--------------

الاهداء (Arabic acknowledgments).....	(٢)
--	------------

في نهاية الكتاب

الملخص (Arabic summary).....	(٥)
-------------------------------------	------------

في نهاية الكتاب

Chapter One

General Introduction



Introduction

Methane

Methane (CH₄) is an important fossil fuel for households and industry, but also a climate-affecting trace gas in the atmosphere (Forster *et al.*, 2007; Houghton *et al.*, 1996). Methane shows a strong infrared absorption and the atmospheric methane acts as a greenhouse gas, being 25 to 30 times more effective than carbon dioxide (CO₂) on 100 years-scale (Denman *et al.*, 2007; Shindell *et al.*, 2009). Due to man-made activity the concentration of methane in the atmosphere has raised exponentially over the past 200 years. However, according to a recent report of the Intergovernmental Panel on Climate Change, the rise in atmospheric methane concentration had declined significantly during the last (2-3) years (Singh, 2011). It is not clear if the decline rate is caused by a decrease in emission or an increase in methane sink activity. Global warming is a worldwide concern and therefore it is important to increase knowledge of the sources and sinks of methane.

About 70 to 80 % of the methane emitted to the atmosphere originates from natural ecosystems (wetlands, ruminants, termites) and anthropogenic activities (rice paddies, landfills, coal mining) (Table 1). This biogenic methane is produced by methanogenic Archaea during decomposition of organic matter under anaerobic conditions (Conrad, 2009; Etiope *et al.*, 2011; Schink, 1997; Thauer, 1998). The other 20 to 30 % is the result of thermal decomposition of organic matter (> 80 °C) within the Earth's crust (Conrad, 2009; Etiope & Klusman, 2002; Etiope *et al.*, 2011). This (geological) methane is emitted to the atmosphere from geothermal areas like seeps, mud volcanoes, mud pots and fumaroles.

Pictures (previous page). The Solfatara volcano located at Pozzuoli near Naples (southern Italy). Left-top, overview of the Solfatara; left-bottom, Dr. Arjan Pol is sampling the fangaia; right, fumarole with metal sulfide precipitates. Pictures by Dr. Arjan Pol.

Although methane emission from geothermal areas needs to be quantified more accurately (Etiope & Klusman, 2002), these environments add 45 to 75 Tg methane per year on the total emission of about 600 Tg methane per year (Castaldi & Tedesco, 2005; Kvenvolden & Rogers, 2005). Fortunately, not all the methane produced reaches the atmosphere, since a considerable part is oxidized by aerobic and anaerobic methane-oxidizing bacteria, also known as methanotrophs (Table 1). These microorganisms are assumed to be the major players in keeping the methane balance on our planet.

Atmospheric methane, that has escaped methanotrophic oxidation, is mainly oxidized in the troposphere by the hydroxyl radical (OH^\cdot), by far the major radical in this part of the atmosphere, leading to the formation of carbon dioxide and water vapor. In the presence of sufficiently high levels of nitrogen oxides (NO_x), methane oxidation with the hydroxyl radical leads to the formation of formaldehyde (CH_2O), carbon monoxide (CO) and ozone (O_3). This reaction is responsible for the removal of about 445 to 530 Tg methane per year, making the concentration of hydroxyl radical the most important determinant of the rate at which methane is removed from the atmosphere. About 30 Tg methane per year is removed through dry soil oxidation due to the activity of aerobic methanotrophs and about 40 Tg methane per year is transported to the stratosphere (Houweling *et al.*, 1999; Khalil & Shearer, 2000; Lelieveld *et al.*, 1998; Moss *et al.*, 2000) (Table 1).

Recently it was shown that volcanoes are also acting as important methane sinks, due to methane oxidation activity of aerobic verrucomicrobial methanotrophs. These microorganisms were isolated independently from volcanic regions in Italy, New Zealand and Russia (Dunfield *et al.*, 2007; Islam *et al.*, 2008; Pol *et al.*, 2007).

In this study the main focus will be on the biochemistry and physiology of *Methyacidiphilum fumariolicum* SolV, one of those recently isolated aerobic verrucomicrobial methanotrophs.

Table 1. Sources and sinks for methane on the Earth and atmosphere

Methane sources	Methane sinks		Teragram ^a methane per year					
Natural								
Wetlands			265	100	225	145		92-237
Termites				20	20	20		20
Oceans			5	4	15	15		10-15
Anaerobic marine sediments				5			75	320
Geological sources				14	10	10		
Wild fires				2				
Agricultural anthropogenic								
Ruminants			75	81	115	93		80-115
Rice cultivations			110	60				25-100
Non-agricultural anthropogenic								
Energy					110	89		75-110
Natural gas			95	30				
Coal mining			35	46				
Other fossil fuels				30				
Landfills			40		40	73		35-73

Table 1 proceeds on next page.

Table 1. Sources and sinks for methane on the Earth and atmosphere (continuation)

Methane sources	Methane sinks				Teragram ^a methane per year			
Non-agricultural anthropogenic								
Waste water treatment							25	14-25
Biomass burning	40	50	40	40			40	23-55
Waste disposal	25	61	25					
Other							20	
Total sources								
	690	518	600	340				500-600
Chemical processes								
Reaction with tropospheric hydroxyl radicals (OH [•])	530	445	510					
Removal to stratosphere	40	40	40					
Biological aerobic oxidation								
Soil uptake	30	30	30	30				
Biological anaerobic oxidation								
Marine sediments							70	300
Total sinks	600	515	580					

^a 1 Teragram equals 10¹² gram.

Data were collected from Etiope *et al.* (2011), Hinrichs & Boetius (2002), Houweling *et al.* (1999), Khalil & Shearer (2000), Lelieveld *et al.* (1998), Liu & Whitman (2008), Moss *et al.* (2000), Reeburgh (1996) and references therein.

Methanotrophs

Anaerobic methanotrophs

Anaerobic oxidation of methane can be performed either by consortia of methane-oxidizing Archaea and sulfate-reducing bacteria (Boetius *et al.*, 2000; Valentine & Reeburgh, 2000) or by nitrite-reducing bacteria (Ettwig *et al.*, 2008; Raghoebarsing *et al.*, 2006). Table 2 gives an overview of sites where the anaerobic oxidation of methane has been studied.

First geochemical evidence for sulfate-driven methane oxidation was derived from profile analyses in anoxic organic-rich sediments (Barnes & Goldberg, 1976; Martens & Berner, 1974; Reeburgh, 1976). However, the process stayed controversial, because neither mechanism nor responsible microorganism could be identified. In 2000 it was shown that consortia of anaerobic methanotrophic Archaea and sulfate-reducing bacteria were performing the process in deep sea environments (Boetius *et al.*, 2000). Research progress from that time on is excellently reviewed by Knittel & Boetius (2009).

The first report on nitrite-driven anaerobic methane oxidation (n-damo) hypothesized a consortium with Archaea conducting reverse methanogenesis in association with a denitrifying bacterial partner (Raghoebarsing *et al.*, 2006). Subsequently it was shown that the complete process could be performed by the bacterial partner on its own (Ettwig *et al.*, 2008). The dominant bacterium responsible for the n-damo process belonged to the candidate division ‘NC10’ (Rappe & Giovannoni, 2003). Its genome could be assembled from the metagenome of an enrichment culture and the bacterium was tentatively named ‘*Candidatus Methyloirabilis oxyfera*’ (Ettwig *et al.*, 2010). The n-damo process follows a classical aerobic methane oxidation pathway (see also below) in the total absence of externally supplied oxygen (O₂) (Ettwig *et al.*, 2010). It was demonstrated that ‘*Candidatus Methyloirabilis oxyfera*’ has the unique ability to produce intracellular oxygen through an alternative denitrification pathway.

Already quite some time circumstantial evidence exists for iron (III)-driven anaerobic methane oxidation as a thermodynamically favorable process (Beal *et al.*, 2009; Sivan *et al.*, 2007; Zehnder & Brock, 1980). Recently geochemical evidence was published for this process in deep lake sediments being located below

a depth of 20-cm, which is well below the depths where nitrate and sulfate are available (Sivan *et al.*, 2011). The process was further studied using iron (III)-amended mesocosm studies with intact sediment cores.

Aerobic methanotrophs

The obligate aerobic methanotrophs form a unique group of microorganisms among the methylotrophs. They utilize methane as sole source of energy and carbon (Hanson & Hanson, 1996). So far within the bacterial phylum *Proteobacteria*, 18 genera of aerobic methanotrophs have been described (Table 3). These proteobacterial methanotrophs are further divided into two subphyla, the *Alphaproteobacteria* and the *Gammaproteobacteria* (Table 3). The methanotrophic members of the *Alphaproteobacteria* (also known as type II methanotrophs), are represented by two families, the *Methylocystaceae* and the *Beijerinckiaceae*. The members of the *Gammaproteobacteria* (also known as type I methanotrophs), are represented by the family *Methylococcaceae*.

The type I and II classification of methanotrophs is based on their cell morphology, ultrastructure (internal membrane structure), phylogeny (*Alphaproteobacteria* versus *Gammaproteobacteria*), the dominant phospholipid fatty acids (16C versus 18C) and the metabolic pathways used for biomass production (ribulose monophosphate [RuMP] pathway versus serine pathway) (Chistoserdova, 2011; Chistoserdova *et al.*, 2009; Hanson & Hanson, 1996). However, not all genera described fit into these classifications, e.g. *Methylocella*, *Methylohalobius* and *Methylovulum* (Dedysh *et al.*, 2000; Heyer *et al.*, 2005; Iguchi *et al.*, 2011). Although in the past the terms type I and type II methanotroph were preferably used, they now have become synonyms for *Gammaproteobacteria* and *Alphaproteobacteria*, respectively (Op den Camp *et al.*, 2009). So far the family *Methylococcaceae* of the *Gammaproteobacteria* harbors the most genera of the proteobacterial methanotrophs, but not all the genera perfectly fit into this family. The genera *Methylohalobius* and *Methylothermus* are classified in this family, but analysis of the 16S ribosomal RNA and *pmoA* genes show that these microorganisms may not be monophyletic with this family (Heyer *et al.*, 2005; Tsubota *et al.*, 2005). In addition the family *Crenotrichaceae* (with *Crenothrix* and *Clonothrix*, two filamentous and sheathed microorganisms as the genera) is

validated, but it is phylogenetically a subset of the *Methylococcaceae* (Op den Camp *et al.*, 2009; Stoecker *et al.*, 2006; Vigliotta *et al.*, 2007).

There are several detailed literature reviews available about the physiology and ecology of the aerobic proteobacterial methanotrophs (Conrad, 1996; Dunfield, 2006; Hanson & Hanson, 1996; McDonald *et al.*, 2008; Trotsenko & Khmelenina, 2002). These microorganisms are widespread in natural and man-made environments such as fresh and marine waters and sediments, soils, landfills and rice paddies where they typically consume 10-90 % of the methane produced by methanogenic Archaea in the anoxic zones of these environments (Segers, 1998).

Aerobic methanotrophs are also found in symbioses with marine invertebrates (the sponge *Cladorhiza methanophila*, tubeworms of the *Siboglinum* genus, the hydrothermal vent snails *Ifremeria nautiliei* and *Alviniconcha hessleri*, and deep-sea bathymodiolin mussels of two genera, *Bathymodiolus* and *Idas*) at hydrothermal vents and cold seeps in the deep Sea (Petersen & Dubilier, 2009 and references therein). The methods applied to show that symbionts are methanotrophs included ultrastructure analysis of the internal cytoplasmic membrane system, 16S ribosomal RNA analyzed, activity assays with crucial enzymes of the methane oxidation pathway and physiological experiments using labeled methane in whole animals or tissues containing the methanotrophic symbionts. So far only type I methanotrophs seems to be involved in the symbiosis with the marine invertebrates. This may be caused by the efficiency of the pathway used for carbon assimilation, the serine pathway used by type II methanotrophs being less efficient (Leak *et al.*, 1985). The marine invertebrate fully rely on their symbiont for most or even all there carbon and energy needs, so it is advantageous to be in association with type I methanotrophs. However, type II methanotrophs are found in association with wetland plants (Raghoebarsing *et al.*, 2005), which are autotrophs and much less dependent for their organic carbon. In these associations, type II methanotrophs supply the plant with up to 15 % of the cellular carbon.

Table 2. List of sites where anaerobic oxidation of methane has been studied

Sediment location	Depth in meters	CH ₄ source	Coupled to	References
Pearl River estuary, Pacific Ocean	3- 4	Organic matter decomposition/ Methanogenesis	SO ₄ ²⁻ reduction	Wu <i>et al.</i> , 2006
Haakon Mosby, Mud Volcano, Atlantic Ocean	1250	Fossil methane	SO ₄ ²⁻ reduction	Damm & Budéus, 2003
Chilean continental margin, Pacific Ocean	800-4600	Organic matter decomposition/ Methanogenesis	SO ₄ ²⁻ reduction	Treude <i>et al.</i> , 2005
Eckemförde Bay, Baltic Sea	25-28	Organic matter decomposition/ Methanogenesis	SO ₄ ²⁻ reduction	Treude <i>et al.</i> , 2005
The Green Canyon area of the Gulf of Mexico	540-560	Gas hydrates	SO ₄ ²⁻ reduction	Joye <i>et al.</i> , 2004
Eel River Basin, Pacific Ocean	516-556	Gas hydrates	SO ₄ ²⁻ reduction	Orphan <i>et al.</i> , 2002
Black Sea	250	Fossil methane	SO ₄ ²⁻ reduction	Treude <i>et al.</i> , 2007
Aarhus Bay, Denmark	16	Organic matter decomposition/ Methanogenesis	SO ₄ ²⁻ reduction	Thomsen <i>et al.</i> , 2001
Hydrate Ridge, Pacific Ocean	700	Gas hydrates	SO ₄ ²⁻ reduction	Boetius <i>et al.</i> , 2000
Gulf of Cadiz, Atlantic Ocean	400-3000	Mud Volcano	SO ₄ ²⁻ reduction	Niemann <i>et al.</i> , 2006
Namibian margin, Atlantic Ocean	25	Organic matter decomposition/ Methanogenesis	SO ₄ ²⁻ reduction	Niewöhner <i>et al.</i> , 1998
Monterey Bay, Pacific Ocean	800-1000	Cold seep	SO ₄ ²⁻ reduction	Girguis <i>et al.</i> , 2003; Girguis <i>et al.</i> , 2005
Kattegat, Baltic Sea	0.5	Organic matter decomposition/ Methanogenesis	SO ₄ ²⁻ reduction	Dando <i>et al.</i> , 1994

Table 2 proceeds on next page.

Table 2. List of sites where anaerobic oxidation of methane has been studied (continuation)

Sediment location	Depth in meters	CH ₄ source	Coupled to	References
Spiekeroog, North Sea	0-5	Organic matter decomposition/ Methanogenesis	SO ₄ ²⁻ reduction	Böttcher <i>et al.</i> , 1998
Twente kanaal, the Netherlands receiving agricultural runoff	1	Organic matter decomposition /Methanogenesis	NO ₃ ⁻ and NO ₂ ⁻ reduction	Raghoebarsing <i>et al.</i> , 2006
The Ooijpolder, a floodplain of the River Rhine in the Netherlands	-	Organic matter decomposition /Methanogenesis	NO ₂ ⁻ reduction	Ettwig <i>et al.</i> , 2009
Mixed sample of sediments from a local freshwater lake, anaerobic digester sludge and return sludge from the Luggage Point wastewater treatment plant (Brisbane, Australia)	-	Organic matter decomposition /Methanogenesis	NO ₂ ⁻ reduction	Hu <i>et al.</i> , 2009
In waste water treatment plants located in the Netherlands	-	Organic matter decomposition /Methanogenesis	NO ₂ ⁻ reduction	Luesken <i>et al.</i> , 2011

Table 3. Comparison of all described families of aerobic methanotrophs (modified from Op den Camp *et al.* (2009))

Phylum and class	Proteobacteria (Alphaproteobacteria)	Proteobacteria (Alphaproteobacteria)	Proteobacteria (Gammaproteobacteria)	Verrucomicrobia
Family	Methylocystaceae	Beijerinckiaceae	Methylococcaceae	Methylocidiphilaceae
Genera	Methylocystis, Methylosinus	Methylocella, Methylocapsa, Methyloferula	Methylococcus, Methylocaldum, Methylobacter, Methylobacterium, Methylomonas, Methylosarcina, Methylosphaera, Methylosoma, Methylohalobius, Methylothermus, Crenothrix, Clonothrix, Methylovulum	Methylocidiphilum
Internal membrane structures or compartments	Type II: membrane stacks along the cell periphery, parallel to the cell envelope	Methylocella and Methyloferula: cytoplasmic membrane invaginations or vesicles Methylocapsa: single membrane stack parallel to the long axis	Type I: membrane bundles perpendicular to the cell envelope	Carboxysome-like structures or vesicular membranes
Lowest reported growth pH	4.4 (<i>Methylocystis heyeri</i>)	3.5 (<i>Methyloferula stellata</i>)	5.0 (many species)	0.8 (<i>Methylocidiphilum fumariolicum</i> strain SolV)
Highest reported growth pH	7.5 (<i>Methylocystis heyeri</i>)	7.5 (<i>Methylocella</i> spp.)	11 (<i>Methylobacterium buryatense</i>)	6.0 (<i>Methylocidiphilum infernum</i> strain V4)
Lowest reported growth temperature (°C)	5 (<i>Methylocystis heyeri</i>)	4.0 (<i>Methylocella silvestris</i> and <i>Methyloferula stellata</i>)	3.5 (<i>Methylobacter psychrophilus</i>)	37 (<i>Methylocidiphilum kamchatkense</i> strain Kaml)
Highest reported growth temperature (°C)	40 (many species)	33 (<i>Methyloferula stellata</i>)	67 (<i>Methylothermus thermalis</i>)	65 (<i>Methylocidiphilum fumariolicum</i> strain SolV)

Table 3 proceeds on next page.

Table 3. Comparison of all described families of aerobic methanotrophs (modified from Op den Camp *et al.* (2009)) (continuation)

Phylum and class	Proteobacteria (<i>Alphaproteobacteria</i>)	Proteobacteria (<i>Alphaproteobacteria</i>)	Proteobacteria (<i>Gammaproteobacteria</i>)	<i>Verrucomicrobia</i>
Major PLFAs (more than 15 % of total in any species)	16:1 ω 8c (0-29 %) 18:1 ω 7c (10-37 %) 18:1 ω 8c (32-74 %)	18:1 ω 7c (59-86 %) 16:0 (3-8 %)	14:0 (1-34 %), 16:1 ω 8c (0-41 %), 16:0 (4-63 %), 18:1 ω 7c (0-60 %), 16:1 ω 5t (0-30 %), 18:1 ω 9c (0-35 %), 16:1 ω 7c (8-57 %)	i14:0 (7-22 %) a15:0 (13-31 %) 18:0 (14-42 %)
Carbon fixation pathway	Serine cycle	Serine cycle, Calvin-Benson-Bassham cycle ^a	Ribulose monophosphate pathway, Calvin-Benson-Bassham cycle (rarely)	Serine cycle ^b , Calvin-Benson-Bassham cycle ^a
G+C mol %	60-67	55-63	43-65	40.8-45.5
N ₂ fixation ^c	+/-	+	+/-	+/-
sMMO ^c	+/-	+/-	+/-	-
pMMO ^c	+	+/-	+	+
Obligately methylophilic ^c	+	+/-	+	+

^a Based on genome data for *Methylocella silvestris* BL2, *Methylocandidiphilum infernorum*, *Methylocandidiphilum fumarolicum* and RuBisCO activity in *Methyloferula stellata*.

^b A variant of the serine cycle may operate, using glyoxylate shunt enzymes to regenerate glyoxylate (Hou *et al.*, 2008).

^c (+) all species positive, (-) all species negative, (+/-) some species positive.

Data are collected from Bowman *et al.* (1993), Chen *et al.* (2010), Dedysh *et al.* (2007), Dedysh *et al.* (2002), Dedysh *et al.* (2004), Dunfield *et al.* (2003), Dunfield *et al.* (2007), Heyer *et al.* (2005), Hou *et al.* (2008), Iguchi *et al.* (2011), Islam *et al.* (2008), Kaluzhnaya *et al.* (2001), Pol *et al.* (2007), Rahalkar *et al.* (2007), Stoecker *et al.* (2007), Trotsenko & Khmelenina (2002), Tsubota *et al.* (2005), Vigliotta *et al.* (2007), Vorobev *et al.*, 2011, Wise *et al.* (2001) and references therein.

The discovery of the aerobic verrucomicrobial methanotrophs

Most of the known genera within the aerobic proteobacterial methanotrophs are mesophiles and neutrophils. Exceptions on that are the genera found in geothermal springs (*Methylothermus*, *Methylococcus* and *Methylocaldum*), for which temperatures of 45-58 °C for optimal growth was reported. In addition, there are reports on mild acidophilic genera (*Methylocystis*, *Methylocapsa*, *Methylocella* and *Methyloferula*), which are abundant in soil environments, such as peat bogs. These microorganisms are capable of growth at pH values between 3.5 and 7.5 (Dedysh *et al.*, 2002; Dedysh *et al.*, 2000; Dedysh *et al.*, 2007; Trotsenko & Khmelenina, 2002; Tsubota *et al.*, 2005; Vorobev *et al.*, 2011) (Table 3).

A significant amount of methane consumption has been reported in geothermal areas, characterized by high temperatures (50-95 °C) and a very low pH (below 1.8) (Castaldi & Tedesco, 2005). This pointed into the direction of methanotrophy under more extreme conditions. This geological evidence was supported and validated in late 2007 to early 2008, by three independent isolations in pure culture of novel aerobic methane oxidizing bacteria from volcanic regions (Dunfield *et al.*, 2007; Islam *et al.*, 2008; Pol *et al.*, 2007) (Table 3). Inocula were obtained from the Solfatara at Pozzuoli near Naples (Italy), Hell's Gate, Tikitere (New Zealand) and the Uzon Caldera, Kamchatka, (Russia). Excitingly, based on 16S ribosomal RNA gene sequences, all three isolates (strains SolV, V4 and Kam1) could be identified as members of the *Verrucomicrobia* phylum and they belong to a single genus for which the name *Methylacidiphilum* was proposed (Op den Camp *et al.*, 2009) (Fig. 1). This was the first time that the widely distributed *Verrucomicrobia* phylum is coupled to a geochemical cycle. Although environmental clone libraries show large biodiversity in *Verrucomicrobia* and their presence in many ecosystems (soils, peat bogs, acid rock drainage and landfill leachate) often in relative high numbers, most members remain uncultivated and their physiology is poorly understood (Wagner & Horn, 2006).

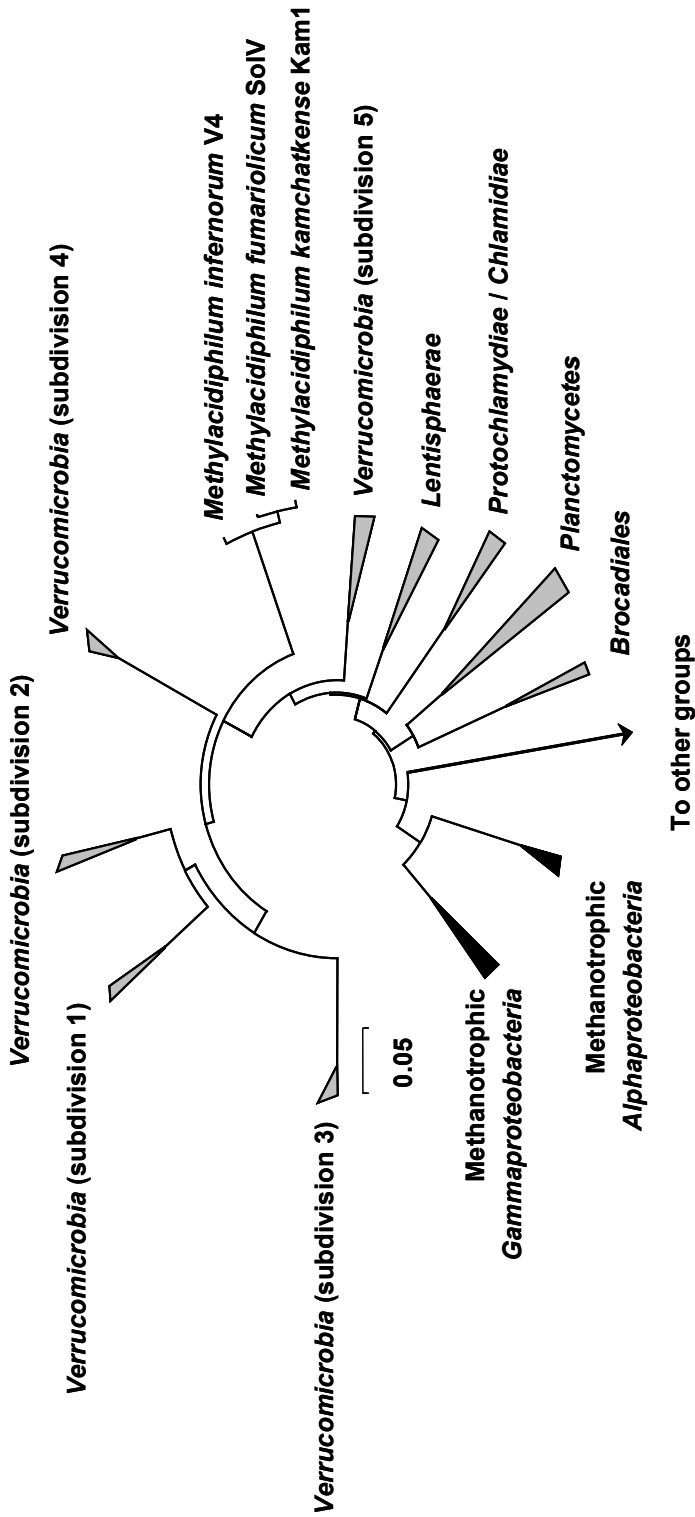


Figure 1. Phylogenetic tree showing the position of the verrucomicrobial aerobic methanotrophs (strains V4, SolV and Kam1) relative to the proteobacterial aerobic methanotrophs (modified from Op den Camp *et al.* (2009)).

In addition to the several verrucomicrobial genome assemblies (van Passel *et al.*, 2011) a complete genome sequence was published for *Methylophilum infernorum* strain V4 (Hou *et al.*, 2008) and a draft genome was available for *Methylophilum fumariolicum* strain SolV (Op den Camp *et al.*, 2009; Pol *et al.*, 2007). Initial analysis of *Methylophilum* strains (V4, SolV and Kam1) showed similarities, but also major differences with the proteobacterial aerobic methanotrophs, e.g. distinct enzymes of the methane oxidation and carbon dioxide fixation pathways (see below) (Table 3). The stacked membrane structures characteristic for methanotrophs expressing particulate methane monooxygenase (pMMO) were not observed in *Methylophilum* strains with transmission electron micrograph. Instead circular bodies of about 50-70 nm were observed (Fig. 2). It was postulated that these circular bodies in *Methylophilum* strains may resemble carboxysomes or a novel subcellular compartments for methane oxidation (Islam *et al.*, 2008; Op den Camp *et al.*, 2009). Carboxysomes are compartments found in cyanobacteria and in limited numbers of chemoautotrophs and thought to enhance the concentration of carbon dioxide for the enzyme ribulose 1,5 bisphosphate carboxylase/oxygenase (RuBisCO), which has a low affinity for carbon dioxide (Yeates *et al.*, 2008).

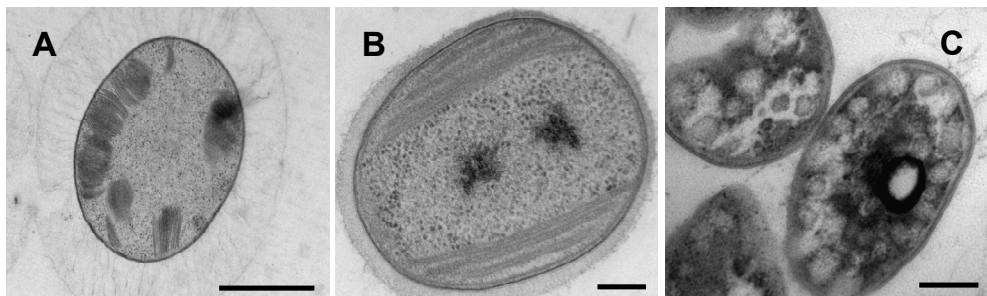
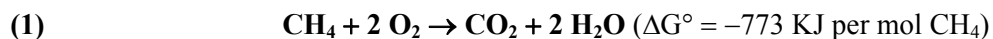


Figure 2. (A) Transmission electron micrograph of type I (scale bar, 1 μ m) and (B) type II (scale bar, 200 nm) proteobacterial aerobic methanotrophs, showing the disc-shaped and the parallel membranes in these microorganisms, respectively. (C) In *Methylophilum fumariolicum* strain SolV circular bodies of about 50-70 nm were observed (scale bar, 200 nm). Pictures were modified from Kip *et al.* (2011) and Pol *et al.* (2007).

Genome comparison: proteobacterial versus verrucomicrobial methanotrophs

Energy metabolism in aerobic methanotrophs

The aerobic oxidation of methane proceeds according to equation 1. During this oxidation, energy is obtained at the level of methanol (CH₃OH), formaldehyde (CH₂O) and formate (CHOOH) oxidation (Chistoserdova *et al.*, 2009; Hanson & Hanson, 1996) (Fig. 3). In these reactions, electrons are transferred to a membrane-bound electron transport chain via a pyrroloquinoline quinone cofactor to cytochrome *c* (methanol dehydrogenase) or NAD (in formaldehyde oxidation systems and formate dehydrogenase). With oxygen as the terminal electron acceptor, electron flow through the membrane produces a proton motive force that is converted to the cellular energy carrier ATP by the ATPase enzyme complex.



Enzymes involved in methane oxidation

Methane monooxygenase (MMO) catalyzes the first step in methane oxidation, converting methane into methanol. Proteobacterial aerobic methanotrophs are known to possess two distinct form of this enzyme; the soluble cytoplasmic form (sMMO, NADH-dependent) and the particulate membrane-associated form (pMMO, cytochrome *c* dependent) (Figs. 3A and 3B) (Hanson & Hanson, 1996). The pMMO is present in all genera of methanotrophs, except for the *Methylocella silvestris* BL2, *Methylocella palustris* gen. nov., sp. nov., and *Methyloferula stellata* gen. nov., sp. nov., that only possess the sMMO variant (Chen *et al.*, 2010; Dedysh *et al.*, 2000; Vorobev *et al.*, 2011). The soluble cytoplasmic methane monooxygenase is only found in limited number of methanotrophs, in addition to pMMO (Chistoserdova, 2011).

Proteobacterial aerobic methanotrophs contain multiple copies of *pmo* operons. In both type I and type II proteobacterial methanotrophs two nearly sequence-identical copies of *pmoCAB1* are found (Murrell *et al.*, 2000; Semrau *et al.*, 1995). It is thought that sequence-identical copies have arisen through gene duplications

and insertions. The requirement of both sequence-identical copies of pMMO was demonstrated by mutation studies in *Methylococcus capsulatus* Bath (Stolyar *et al.*, 1999).

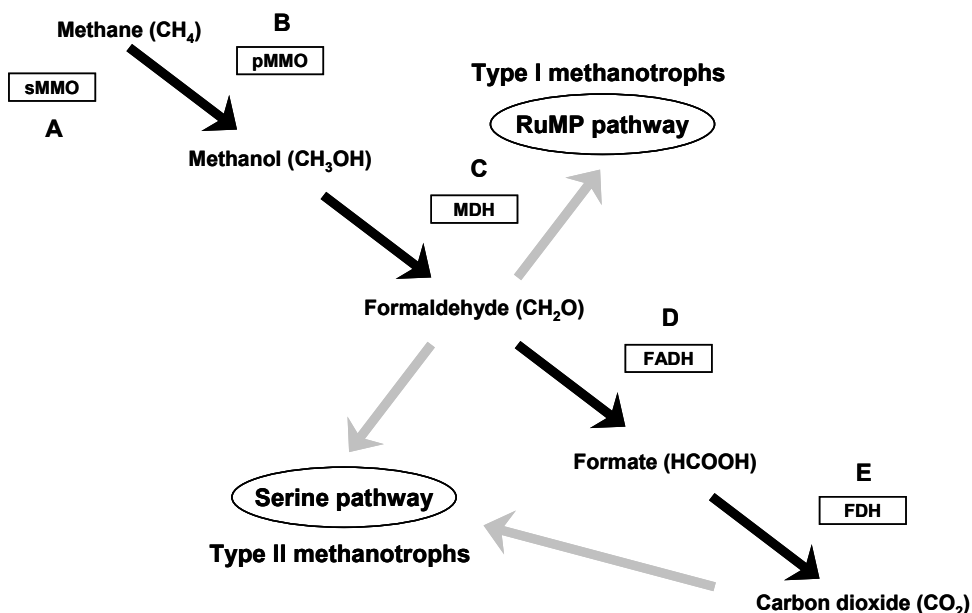


Figure 3. Established pathways for the oxidation of methane (black arrows) and assimilation of formaldehyde (grey arrows) in type I and type II proteobacterial aerobic methanotrophs (modified from Hanson & Hanson, 1996). The enzymes involved in methane oxidation are indicated within the boxes. (A) The soluble methane monooxygenase (sMMO). (B) The particulate methane monooxygenase (pMMO). (C) The methanol dehydrogenase (MDH). (D) The formaldehyde dehydrogenase (FADH). (E) The formate dehydrogenase (FDH). The formaldehyde, produced during the oxidation of methane can be assimilated via the serine pathway or the ribulose monophosphate (RuMP) pathway.

The sequence-divergent copy of *pmoCAB1* (*pmoCAB2*) was shown to be widely but not universally distributed in type II proteobacterial methanotrophs and is

absent in type I proteobacterial methanotrophs (Baani & Liesack, 2008). Recently it was found that the genera of type I proteobacterial methanotrophs encode for a new sequence-divergent *pmo*. Unlike the CAB order for pMMO and ammonia monooxygenase (AMO) operon, it was encoded in the *pxmABC* operon (Tavormina *et al.*, 2011). The presence of sequence-divergent copies suggests alternative physiological function under different environmental conditions. *Methylocystis* sp. strain SC2 was shown to possess two pMMO isozymes, encoded by *pmoCAB1* and *pmoCAB2* operons. The *pmoCAB2* operon encoded pMMO, oxidized methane at lower apparent K_m (Baani & Liesack, 2008).

Based on the complete genome of *M. infernorum* strain V4 and the draft genome of *M. fumariolicum* strain SolV, none of the genes encoding for the sMMO subunits were found in these verrucomicrobial aerobic methanotrophs (Hou *et al.*, 2008; Op den Camp *et al.*, 2009; Pol *et al.*, 2007). However, three complete *pmoCAB* operons were identified in these strains and an extra copy of *pmoC*. The draft genome analysis for *M. kamchatkense* strain Kam1 reveled orthologues of each of the three *pmo* operons found in strains V4 and SolV, in addition to a forth *pmoCA* operon (Op den Camp *et al.*, 2009). Based on phylogenetic analysis of the verrucomicrobial *pmoA* genes, high similarity was found between the genes *pmoA1*, *pmoA2* and *pmoA3* of each strain and the *pmoA4* of Kam1 and they represented a new branch, which is distinct from *pmoA* and *amoA* genes of other cultured organisms (Op de Camp *et al.*, 2009).

By using quantitative polymerase chain reaction (qPCR), recently it was demonstrated that *pmoA2* in *M. kamchatkense* strain Kam1 was highly expressed, and this expression dropped by factor of 10 when grown on methanol (Erikstad *et al.*, 2012).

Enzymes involved in methanol oxidation

Methanol dehydrogenase (MDH) is involved in the second step in methane oxidation, converting methanol into formaldehyde (Fig. 3C). This enzyme was first characterized in the proteobacterial methylotroph *Methylobacterium extorquens* and was later detected in most of the methylotrophs (Chistoserdova, 2011 and references therein). This enzyme consist of a large and small subunits encoded by the *mxoFI* genes and requires pyrroloquinoline quinone as cofactor, and a

cytochrome *c* electron acceptor, the later encoded by *mxg* gene. In addition this enzyme requires calcium (Ca^{2+}) insertion to its active center. The accessory genes *mxACKL* are required for this insertion. Although the genes *mxRS* are also required for an active MDH, their function is still unknown (Chistoserdova, 2011 and reference therein).

MDH activity in the verrucomicrobial methanotroph *M. fumariolicum* strain SolV could be demonstrated (Pol *et al.*, 2007), but the gene cluster encoding this enzyme in this strain and in *M. infernorum* V4 seems to be rather different compared to proteobacterial aerobic methanotrophs. The *mxFJGIRSACKLDEHB* cluster, encoding MDH (Chen *et al.*, 2010; Chistoserdova *et al.*, 2003) was absent and replaced by *mxFJG* predicted along with the cluster *pqqABCDEF* for biosynthesis of the cofactor pyrroloquinoline quinone in these verrucomicrobial aerobic methanotrophic strains (Hou *et al.*, 2008; Op den Camp *et al.*, 2009).

Formaldehyde oxidation pathways

Formaldehyde is an intermediate of the methane oxidation pathway and its oxidation in methanotrophs is important for energy generation, but also to keep intracellular formaldehyde concentrations at non-toxic levels (Chistoserdova, 2011). Methylotrophs are known to have variety of formaldehyde oxidizing systems, which are nicely reviewed by Chistoserdova (2011). Formaldehyde oxidation can be performed by single enzyme; the NAD or mycothiol-linked formaldehyde dehydrogenases (FADH) (Fig. 3D) or by multienzyme cofactor linked C1 transfer pathways. One of the most widespread pathways for formaldehyde oxidation in methylotrophs is the one requiring tetrahydromethanopterin (H_4MPT) as a cofactor and is encoded by at least 20 genes (Chistoserdova *et al.*, 2009). Another important pathway is the C1 transfer pathway, requiring tetrahydrofolate (H_4F) as cofactor.

Based on available genome data of the verrucomicrobial methanotrophs (Hou *et al.*, 2008; Op den Camp *et al.*, 2009; Pol *et al.*, 2007) conversion of formaldehyde in *Methylophilum* strains (V4 and SolV) seems to be mediated by a H_4F dependent pathway or directly by formaldehyde dehydrogenase, which makes these microorganisms the first fully sequenced methylotrophs to lack the H_4MPT pathway for formaldehyde oxidation.

Formate oxidation

The last step in methane oxidation is the conversion of formate into carbon dioxide by formate dehydrogenase (FDH) (Fig. 3E). Methylotrophs are known to have more than one type of this enzyme. For example the methylotroph *M. extorquens* have four different functional FDH enzymes; a tungsten-containing FDH, a predicted molybdenum-containing FDH, a predicted cytochrome-linked FDH that is likely periplasmic, and a novel type of FDH (Chistoserdova, 2011 and references therein). Although, first it was thought that formate oxidation step is less critical for methylotrophs, which oxidize formaldehyde via the RuMP pathway (Anthony, 1982), later studies in RuMP pathway containing methylotrophs, showed that this oxidation step is important (Hendrickson *et al.*, 2010).

The genome data of the verrucomicrobial methanotrophs (strains V4 and SolV) indicate that formate oxidation is probably conducted by NAD-dependent formate dehydrogenase (Hou *et al.*, 2008; Pol *et al.*, 2007).

Carbon assimilation in aerobic methanotrophs

Carbon assimilation in proteobacterial aerobic methanotrophs takes place at the level of formaldehyde (Chistoserdova *et al.*, 2009; Hanson & Hanson, 1996). The members of the *Gammaproteobacteria* (also known as type I methanotrophs), use the RuMP pathway for the assimilation of formaldehyde to form glyceraldehyde-3-phosphate as an intermediate of central metabolism (Fig. 3). Two key enzymes, specific for RuMP pathway are required to enable this carbon fixation pathway; hexulose-6-phosphate synthase and hexulose-6-phosphate isomerase, in addition to the enzymes of glycolysis, pentose phosphate cycle and Entner-Doudoroff pathways (Chistoserdova, 2011).

The members of the *Alphaproteobacteria* (also known as type II), use the serine pathway, in which formaldehyde and carbon dioxide are utilized to produce acetyl-coenzyme A for biosynthesis. Key enzymes that are typically measured to indicate active serine pathway are hydroxypyruvate reductase and serine glyoxylate aminotransferase (Chistoserdova, 2011).

Analyses of the available genome data of the verrucomicrobial methanotrophs (strains SolV and V4) revealed that the key genes needed for an operational RuMP

and serine pathways are absent. Instead, genes encoding for Calvin-Benson-Bassham (CBB) cycle are present (Hou *et al.*, 2008; Op den Camp *et al.*, 2009; Pol *et al.*, 2007). This suggests that these verrucomicrobial aerobic methanotrophs fix carbon dioxide into biomass.

Although genome data of some proteobacterial aerobic methanotrophs (*M. capsulatus* Bath, *M. silvestris* BL2) and the non proteobacterial aerobic methanotroph '*Candidatus Methyloirabialis oxyfera*' (Chen *et al.*, 2010; Ettwig *et al.* 2010; Ward *et al.*, 2004), also revealed the presence of RuBisCO, the key enzyme of the CBB cycle, autotrophic growth in liquid cultures has not been reported and any physiological evidence for an active CBB cycle in these methanotrophs is lacking.

Nitrogen fixation in aerobic methanotrophs

In addition to the important role of methanotrophs in the carbon cycle (methane oxidation), their ability to fix atmospheric nitrogen (N_2) suggest their role in nitrogen cycling in many environments (Auman *et al.*, 2001). However the coupling between methane and nitrogen cycles are not yet understood (Kalyuzhnaya *et al.*, 2009; Murrell & Jetten, 2009). First it was thought that nitrogen fixation is the property of only type II and the type I moderately thermophilic *Methylococcus* strains (Oakley & Murrell, 1988). However, later on genetic and biochemical evidence was provided to show that atmospheric nitrogen fixation capabilities are broadly distributed among methanotrophs (Table 3). This was done by demonstrating of both the presence of *nifH* gene fragments and acetylene reduction activity in a variety of type I and type II strains of the proteobacterial aerobic methanotrophs (Auman *et al.*, 2001). Recently, it was also demonstrated that the deep-sea anaerobic methane-oxidizing Archaea fix nitrogen and share the products with their sulfate-reducing bacterial symbionts (Dekas *et al.*, 2009).

Genomic data of the verrucomicrobial methanotrophic strains (V4 and SolV) indicated the ability of atmospheric nitrogen fixation like most proteobacterial aerobic methanotrophs (Hou *et al.*, 2008; Op den Camp *et al.*, 2009).

Aim & research questions

The discovery of *M. fumariolicum* strain SolV and the other verrucomicrobial methanotrophs (strains V4 and Kam1) was a surprise to most microbiologists. It has revealed that the ability of bacteria to oxidize methane is much more diverse than has previously been assumed in terms of ecology, phylogeny and physiology. These microbes may be significant players in geochemical carbon and nitrogen cycling, and will harbor biochemically very exciting pathways. Taken together the newly discovered extremophilic methanotrophs with their new metabolic features are a good starting point for exciting and innovative research.

The aim of this thesis is to answer the question how *M. fumariolicum* strain SolV is able to survive and live under the extreme conditions (acid, hot and low oxygen) of its natural environment. Furthermore it was investigated which pathways are used and how are they regulated.

Approach & outline

This research was performed by using a complementary array of methods including genomics, electron microscopy, mRNA analyses, and ^{13}C -labeling, to unravel the biochemistry and physiology of the novel extremophilic methanotroph *M. fumariolicum* SolV in molecular detail. These combined approaches will provide the basic understanding that is necessary to assess the environmental importance of these microbes as a methane sink.

Chapter Two: Draft genome sequence of the volcano-inhabiting thermoacidophilic methanotroph *Methylacidiphilum fumariolicum* strain SolV.

In this chapter the genome of *M. fumariolicum* strain SolV was sequenced, by using next generation sequencing methods and finally presented as 109 contigs. Based on the genome data the important pathways involved in carbon and nitrogen metabolism were predicted.

Chapter Three: Nitrogen fixation by the verrucomicrobial methanotroph *Methylacidiphilum fumariolicum* SolV.

In this chapter growth experiments both in batch and chemostat were combined with nitrogenase activity measurements and phylogenetic analysis of the nitrogenase to document N_2 fixation by *M. fumariolicum* SolV.

Chapter Four: Autotrophic methanotrophy in *Verrucomicrobia*: *Methylacidiphilum fumariolicum* SolV uses the Calvin-Benson-Bassham cycle for carbon dioxide fixation.

In this chapter growth experiments were performed with ^{13}C -labeled methane or ^{13}C -labeled carbon dioxide in batch and chemostat cultures to show that carbon dioxide is the only carbon source for *M. fumariolicum* strain SolV during growth on methane. This was further supported by a transcriptome study in which the expression of all the genes necessary for a complete CBB cycle was shown. In addition, a novel ^{13}C stable isotope enzyme assay was developed to demonstrate the activity of RuBisCO in strain SolV.

Chapter Five: Genomic and physiological analysis of carbon storage in the verrucomicrobial methanotroph “*Ca. Methylacidiphilum fumariolicum*” SolV.

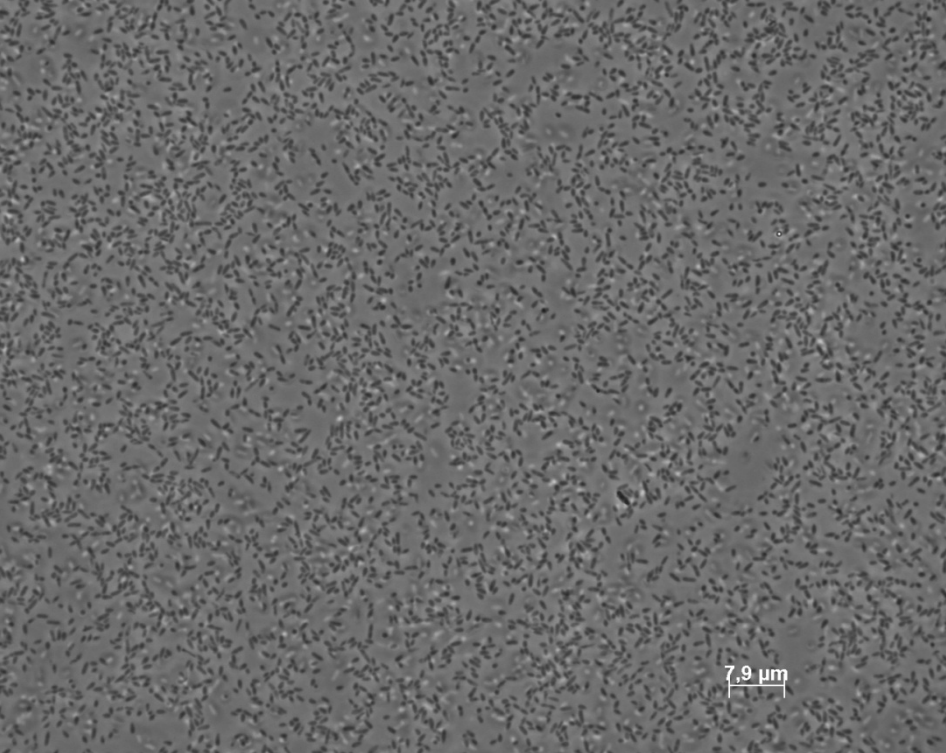
In this chapter *M. fumariolicum* strain SolV was grown in fed-batch to study the response of this microorganism upon ammonium depletion. The cells, which were harvested at different time intervals during growth, were used for electron microscopy, elementary analysis, and biochemical analysis of protein and glycogen levels. Oxygen concentration in this culture did not support N₂ fixation.

Chapter Six: Metabolic regulation of “*Ca. Methylacidiphilum fumariolicum*” SolV cells grown under different nitrogen and oxygen limitations.

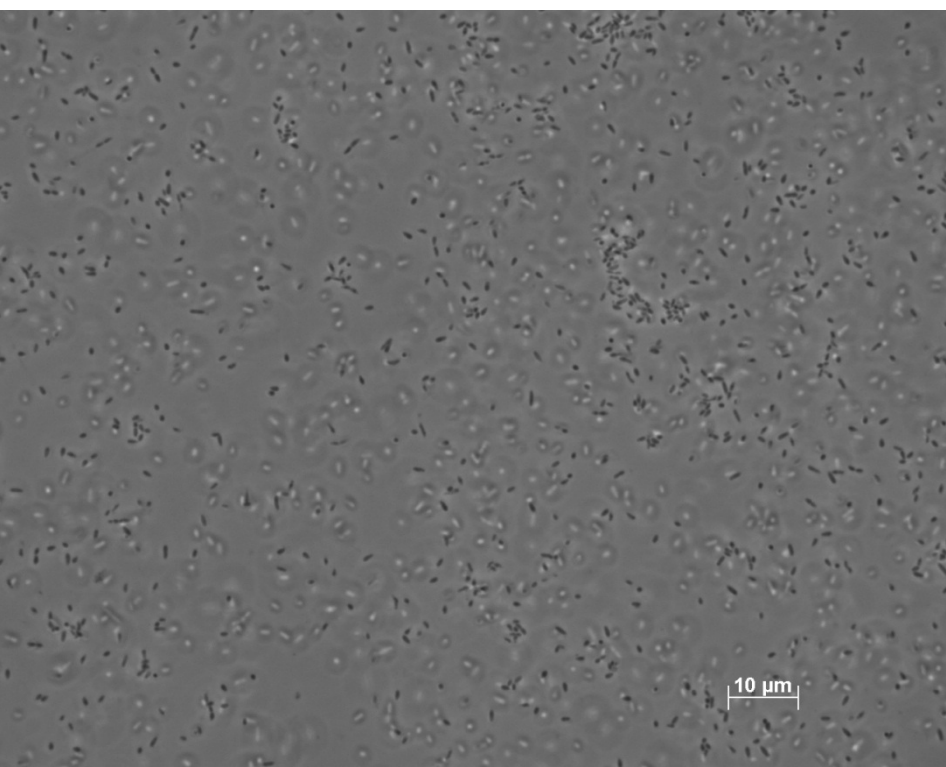
Cells grown under different conditions are the basis for the transcriptome analysis described in this chapter. Exponentially growing cells in bottles (methane, carbon dioxide, oxygen and ammonium in excess), nitrogen-fixing cells in the chemostat (no ammonium, and 0.5 % dissolved oxygen) and oxygen-limited cells in the chemostat (with ammonium, methane and carbon dioxide in excess) were compared with each other.

Chapter Seven: Summary & Outlook.

This chapter summarizes and gives several ideas about further studies to be done in the future.



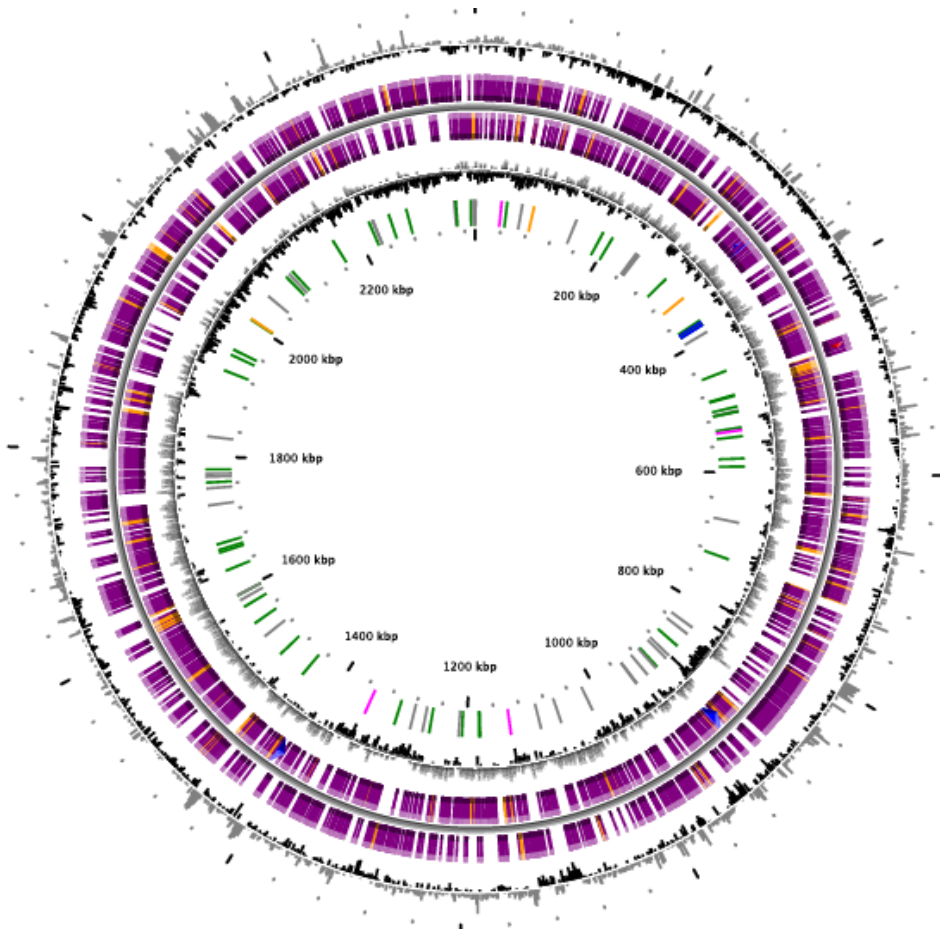
Methylophilum thermophilum strain SolV
cells, obtained from transition phase I (Chapter Five).
These pictures were taken by Ahmad F. Khadem,
using an Axioplan 2 imaging phase contrast microscope.



Chapter Two

Draft genome of *Methylophilum fumariolicum* SolV

A modified version of this chapter was published in:
Journal of Bacteriology **194**, 3729-3730 (2012).



Circular representation of the *Methylobacillus fumariolicum* SolV chromosome (Mfum). Circles display (from the outside): (1) GC percent deviation (GC window-mean GC) in a 1,000-bp window. (2) Predicted CDSs transcribed in the clockwise direction. (3) Predicted CDSs transcribed in the counter clockwise direction. *Genes displayed in (2) and (3) are color-coded according different categories*: red and blue: MaGe validated annotations; orange: MicroScope automatic annotation with a reference genome; purple: Primary/Automatic annotations. (4) GC skew (G+C/G-C) in a 1,000-bp window. (5) rRNA (blue), tRNA (green), misc_RNA (orange), transposable elements (pink) and pseudo genes (grey).

Draft genome sequence of the volcano-inhabiting thermoacidophilic methanotroph *Methylophilum thermophilum* strain SolV

Ahmad F. Khadem¹, Adam S. Wiczorek¹, Arjan Pol¹, Stéphane Vuilleumier², Harry R. Harhangi¹, Peter F. Dunfield³, Marina G. Kalyuzhnaya⁴, J. Colin Murrell⁵, Kees-Jan Francoijs⁶, Henk G. Stunnenberg⁶, Lisa Y. Stein⁷, Alan A. DiSpirito⁸, Jeremy D. Semrau⁹, Aurélie Lajus¹⁰, Claudine Médigue¹⁰, Martin G. Klotz¹¹, Mike S. M. Jetten¹ & Huub J. M. Op den Camp¹

¹Department of Microbiology, IWR, Radboud University Nijmegen, Nijmegen, the Netherlands.

²Université de Strasbourg, UMR 7156 CNRS, Strasbourg, France.

³Department of Biological Sciences, University of Calgary, Calgary, Alberta, Canada.

⁴Department of Microbiology, University of Washington, Seattle, Washington, USA.

⁵School of Environmental Sciences, University of East Anglia, Norwich Research Park, Norwich, United Kingdom.

⁶Department of Molecular Biology, Nijmegen Centre for Molecular Life Sciences, Radboud University Nijmegen, Nijmegen, the Netherlands.

⁷Department of Biological Sciences, University of Alberta, Edmonton, Alberta, Canada.

⁸Department of Biochemistry, Biophysics and Molecular Biology, Iowa State University, Ames, Iowa, USA.

⁹Department of Civil and Environmental Engineering, the University of Michigan, Ann Arbor, Michigan, USA.

¹⁰Laboratoire d'Analyses Bioinformatiques pour la Génomique et le Métabolisme (LABGeM), Genoscope-IG-CEA, Evry, France.

¹¹Department of Biology, University of North Carolina, Charlotte, North Carolina, USA.

Abstract

Methylophilum thermophilum SolV is a novel thermoacidophilic aerobic methanotroph of the *Verrucomicrobia* phylum that was isolated from the central mud pot of the Solfatara volcano near Naples, Italy. Here we present the draft genome sequence of this strain, the second genome available from the cohort of methane-oxidizing *Verrucomicrobia*. Genome sequence annotation has allowed prediction of pathways for one-carbon (C1), nitrogen, and hydrogen catabolism and respiration as well as the central metabolic pathways. The genome encodes three orthologues of particulate methane monooxygenase and the inventory required for nitrification and has led to new insights into methane cycling in volcanic environments.

Introduction

Methane oxidizing bacteria are a subset of the physiological group of methylotrophs, and are unique in using methane (CH₄) as carbon and energy source (Hanson & Hanson, 1996). Until 2007 the phylogenetic distribution of the aerobic methanotrophs was limited to the *Alphaproteobacteria* and *Gammaproteobacteria* (Hanson & Hanson, 1996).

In late 2007 to early 2008, novel thermoacidophilic aerobic methanotrophs were discovered in geothermal areas in Italy, New Zealand and Russia (Dunfield *et al.*, 2007; Islam *et al.*, 2008; Pol *et al.*, 2007). The isolation of these strains was performed by the floating filter technique or by serial dilution using media supplemented with soil extract. These methanotrophs represented a distinct phylogenetic lineage within the *Verrucomicrobia* for which the genus name *Methylacidiphilum* was proposed (Op den Camp *et al.*, 2009). So far the genus *Methylacidiphilum* is represented by three strains; *M. fumariolicum* strain SolV, *M. infernorum* strain V4 and *M. kamchatkense* strain Kam1. The *Methylacidiphilum* species have been shown to be well adapted to the harsh volcanic environment (Op den Camp *et al.*, 2009; Pol *et al.*, 2007) in that they can thrive at very low methane and oxygen concentrations and pH values as low as 1.

Environmental clone libraries show that there is a large biodiversity within the *Verrucomicrobia* and representatives are encountered in many ecosystems like soils, peat bogs, acid rock drainage and landfill leachate, often in relative high numbers but having an unknown physiology (Wagner & Horn, 2006). However, the verrucomicrobial methanotrophs were obtained in pure cultures and a complete genome sequence was published for *M. infernorum* strain V4 (Hou *et al.*, 2008). This was for the first time that members of the verrucomicrobial methanotrophs were shown to be involved in a geochemical cycle.

In this study a draft genome sequence of *M. fumariolicum* SolV is presented. Together with the strain V4 genome, this will lead to new insights into methane cycling in volcanic environments as well as non-proteobacterial methanotrophy and nitrification.

Materials & methods

Growth conditions & DNA isolation

Genomic DNA was extracted from an exponentially growing *Methylophilum thermophilum* cell culture according to Juretschko *et al.* (1998).

The composition and preparation of the growth medium were described previously (Khadem *et al.*, 2010).

Genome sequencing & annotation

The high-quality draft genome of *M. thermophilum* SolV was assembled from Illumina and Roche 454 reads using CLCbio (<http://www.clcbio.com>) and manual adjustments.

Auto-annotation was performed based on comparison to public databases using the MicroScope platform (Genoscope, France, Vallenet *et al.*, 2009).

The nucleotide genome sequence of *M. thermophilum* SolV has been deposited in the European Nucleotide Archive (ENA) under accession numbers CAHT01000001 to CAHT01000109.

Results & discussion

Classification & features of *Methylobacillus fumariolicum*

The *M. fumariolicum* strain SolV used in this study was originally isolated from the volcanic region Campi Flegrei, near Naples, Italy (Pol *et al.*, 2007). Classification and features of *M. fumariolicum* are presented in Table 1. Strain SolV was able to grow with ammonium (doubling time 10 h), nitrate (doubling time 17 h) or dinitrogen gas (doubling time 27 h) as nitrogen source (Khadem *et al.*, 2010; Pol *et al.*, 2007). For biomass carbon, strain SolV fixes CO₂ via the Calvin-Benson-Bassham cycle, with methane as the energy source (Khadem *et al.*, 2011).

Genomic properties

The genome was assembled into 109 contigs. The draft genome is 2.36 Mbp in size with a GC content of 40.9 %, and was very similar to the genome of *M. infernorum* strain V4 (Fig. 1). Auto-annotation identified 2283 protein-encoding gene models. For 623 of these, full-length homologs (> 80 % identity at the protein level) were located in the complete genome of *M. infernorum* V4, with 619 of them organised in synteny in both strains. Synthetic pathways for tRNA of all 20 amino acids were present together with a single rRNA operon.

Carbon metabolism

Genome sequence annotation has allowed prediction of genes involved in one-carbon (C1) metabolism (Table 2). Key genes for the ribulose monophosphate pathway and the serine cycle were absent. However, genes encoding the Calvin-Benson-Bassham cycle enzymes were present. The genome encodes all three central pathways: Embden-Meyerhof-Parnas glycolytic pathways, the pentose phosphate pathway and the tricarboxylic acid cycle. Genes encoding keto-deoxygluconate catabolism of the Entner-Doudoroff pathway were absent. Three particulate methane monooxygenase operons (*pmoCAB*) were predicted, while genes encoding a soluble methane monooxygenase were not found. The *mxnFI*

genes encoding methanol dehydrogenase (Chen *et al.*, 2010; Chistoserdova *et al.*, 2009) were absent, but a homologous *xoxFJG* gene cluster and a *pqqABCDEF* operon for the biosynthesis of the cofactor pyrroloquinoline quinone were detected. H₄MTP-linked C1-transfer genes are not present. The H₄Folate-linked pathway inventory includes *metF*, *folD* and *ftfL* genes. The genes *mtaA*, *fch* or *purU* were not present. Genes encoding NAD-linked formate dehydrogenase (*fdsABCD*) were identified (Oh & Bowien, 1998). Should the identified genes encoding acetate kinase and acetyl-coenzyme A synthase prove functional, strain SolV may be able to assimilate C2 compounds, and thus be physiologically classified as a facultative methanotroph (Semrau *et al.*, 2011). The presence of a hydrogenase gene cluster points towards possible chemolithotrophic growth or the use of hydrogen to provide reducing equivalents for methane oxidation (Hanczár *et al.*, 2002). A complex IV-type heme-copper oxidase gene cluster predicted the respiratory role of a terminal cytochrome *c* oxidase.

Nitrogen metabolism

Strain SolV was able to grow with ammonium, nitrate or dinitrogen gas as nitrogen source (see above). Coincidentally, genes were predicted for direct ammonium uptake (*amtB*) and assimilation (e.g. glutamine synthase, *glnA*; glutamate synthase, *gltB*; alanine dehydrogenase, *ald*) as well as for urea metabolism (urea hydrolase, *ureABCDHFG*; carbamoyl phosphate synthase, *carA* and *carB*). As in most other methanotrophs, however, the urea cycle is incomplete (i.e. lack of arginase; (Boden *et al.*, 2011)). A full complement of genes for dinitrogen fixation, nitrate/nitrite transport and assimilation was also found. In addition, genes for nitrite reduction (*nirK*) and nitric oxide reduction (*norB*, *norC*), were identified but the inventory to encode nitrous oxide reduction was missing. Like in the genome of *M. infernorum* V4, a *haoAB* gene cluster encoding hydroxylamine oxidase was identified, suggesting the capability of nitrification and nitrosative stress handling (Nyerges *et al.*, 2010; Nyerges & Stein, 2009; Stein & Klotz, 2011).

Table 1. Classification and general features of *Methyloacidiphilum fumariolicum* SolV

Property	Term
Current classification	Domain <i>Bacteria</i>
	Phylum <i>Verrucomicrobia</i>
	Order <i>Methyloacidiphilales</i>
	Family <i>Methyloacidiphilaceae</i>
	Genera <i>Methyloacidiphilum</i>
	Type strain SolV
Site	Thermal mud pot, (fangaia) Solfatara, Italy (pH 1-2, 50 °C)
Gram stain	Negative
Cell shape	Rod-shaped
Cell width × Length	0.4-0.6 µm × 0.8-2.0 µm
Motility	Non-motile
Resting stages (cysts, spores)	Not observed
Energy source	CH ₄ , with K _s of 6 µM
Oxygen requirements	Aerobic, with K _s of 0.7 µM
Carbon source	CO ₂
Nitrogen source	Ammonium, nitrate and N ₂
Temperature range	40-65 °C
Temperature optimum	55 °C
pH range	0.8-5.8
pH optimum	2

Data were collected from Khadem *et al.* (2010), Khadem *et al.* (2011), Op den Camp *et al.* (2009) and Pol *et al.* (2007).

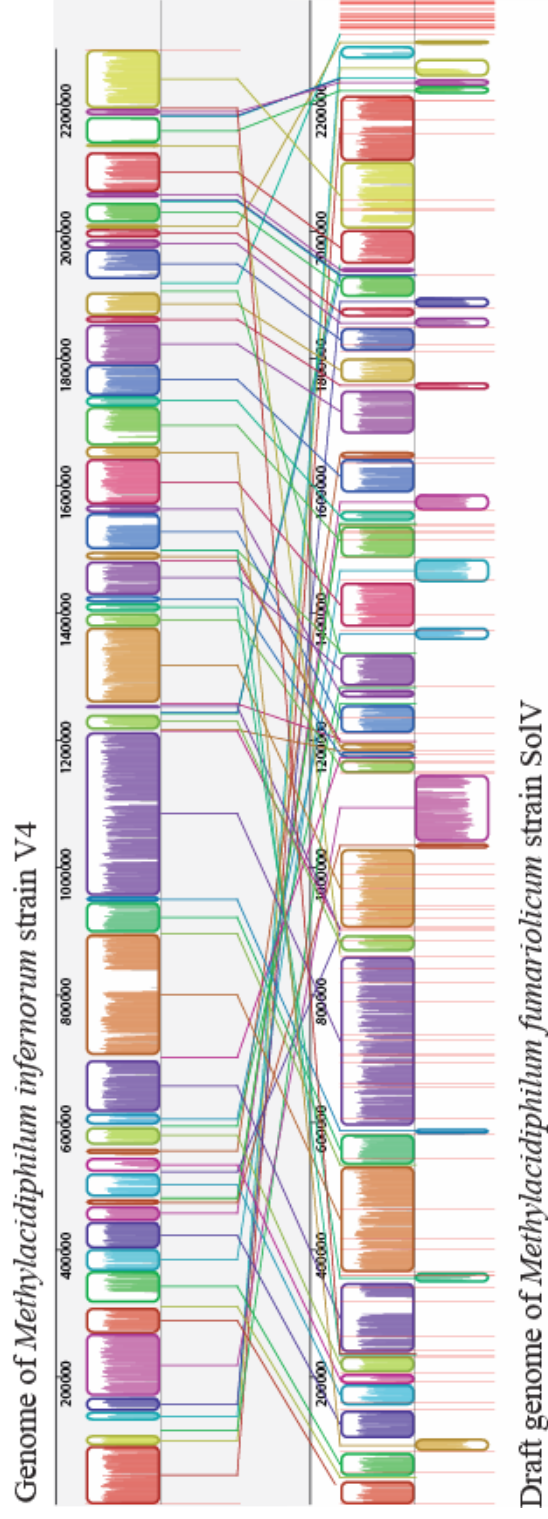


Figure 1. Alignment of the draft genome of *Methylobacillus fumariolicum* strain SolV, against the complete genome of *Methylobacillus infernorum* strain V4. The vertical red lines of the SolV draft genome resemble the contig boundaries.

Table 2. Genes of one-carbon (C1) metabolism of *Methylobacillus thermophilus* SolV

Enzyme	Gene name	Enzyme Commission (E.C.) number	GenBank accession no.	BLASTP search against <i>Methylobacillus thermophilus</i> V4	
				Identity %	Expected (E)-value
Methane monooxygenase_3	<i>pmoC3</i>		Mfumv1_480007	92	0
	<i>pmoA3</i>		Mfumv1_480006	97	6×10^{-175}
	<i>pmoB3</i>		Mfumv1_480005	81	0
Methane monooxygenase_2	<i>pmoC2</i>	1.14.13.25	Mfumv1_780001	96	9×10^{-166}
	<i>pmoA2</i>	1.14.13.25	Mfumv1_770004	99	0
	<i>pmoB2</i>		Mfumv1_770003	93	0
Methane monooxygenase_1	<i>pmoC1</i>	1.14.13.25	Mfumv1_790003	93	2×10^{-180}
	<i>pmoA1</i>	1.14.13.25	Mfumv1_790002	94	2×10^{-176}
	<i>pmoB1</i>		Mfumv1_790001	88	0
Methanol dehydrogenase	<i>mxhF/xoxF</i>	1.1.99.8	Mfumv1_190005	96	0
Cytochrome c family protein	<i>mxhG/xoxG</i>		Mfumv1_190003	83	2×10^{-166}
Periplasmic binding protein	<i>mxhJ/xoxJ</i>		Mfumv1_190004	82	9×10^{-162}
Zn-dependent alcohol dehydrogenase	<i>adhP1</i>		Mfumv1_310051	72	0
Formate dehydrogenase	<i>fdsA</i>		Mfumv1_80015	89	0

Table 2 proceeds on next page.

Table 2. Genes of one-carbon (C1) metabolism of *Methylobacillus thermophilus* SolV (continuation)

Enzyme	Gene name	Enzyme Commission (E.C.) number	GenBank accession no.	BLASTP search against <i>Methylobacillus thermophilus</i> V4	
				Identity %	Expected (E)-value
Formate dehydrogenase	<i>fdsB</i>		Mfumv1_80014	84	0
Formate dehydrogenase	<i>fdsD</i>		Mfumv1_80016	68	3×10^{-36}
Formate dehydrogenase	<i>fdh</i>	1.2.1.2	Mfumv1_50001	94	0
NAD-dependent formate dehydrogenase gamma subunit	<i>nuoE</i>		Mfumv1_80013	80	8×10^{-94}
Formate-tetrahydrofolate ligase	<i>fhs</i>	6.3.4.3	Mfumv1_300027	74	0
Serine hydroxymethyltransferase	<i>ghyA</i>	2.1.2.1	Mfumv1_720018	82	0
5-formyltetrahydrofolate cyclo-ligase	<i>ygfA</i>		Mfumv1_800009	75	2×10^{-108}
Serine-glyoxylate aminotransferase	<i>sgaA</i>		Mfumv1_750005	84	0
Methylenetetrahydrofolate dehydrogenase/methylenetetrahydrofolate cyclohydrolase	<i>folD</i>	1.5.1.5 / 3.5.4.9	Mfumv1_210029	83	0
Ribulose biphosphate carboxylase large subunit	<i>cbbL</i>	4.1.1.39	Mfumv1_70006	98	0
Ribulose biphosphate carboxylase small subunit	<i>cbbS</i>	4.1.1.39	Mfumv1_70007	91	3×10^{-97}
Glyceraldehyde-3-phosphate dehydrogenase	<i>cbbG</i>	1.2.1.12	Mfumv1_170031	90	0
Phosphoribulokinase	<i>udk</i>	2.7.1.19	Mfumv1_70009	97	0
Phosphoglycerate kinase	<i>pgk</i>	2.7.2.3	Mfumv1_170032	80	0

Conclusion

The information provided by the draft genome sequence of *M. fumariolicum* SolV reported here will enable further transcriptomic and proteomic studies to unravel the fascinating metabolism of these and related verrucomicrobial methanotrophs.

Acknowledgements

The work of Ahmad F. Khadem was supported by Mosaic grant 62000583 from the Netherlands Organisation for Scientific Research (NWO).

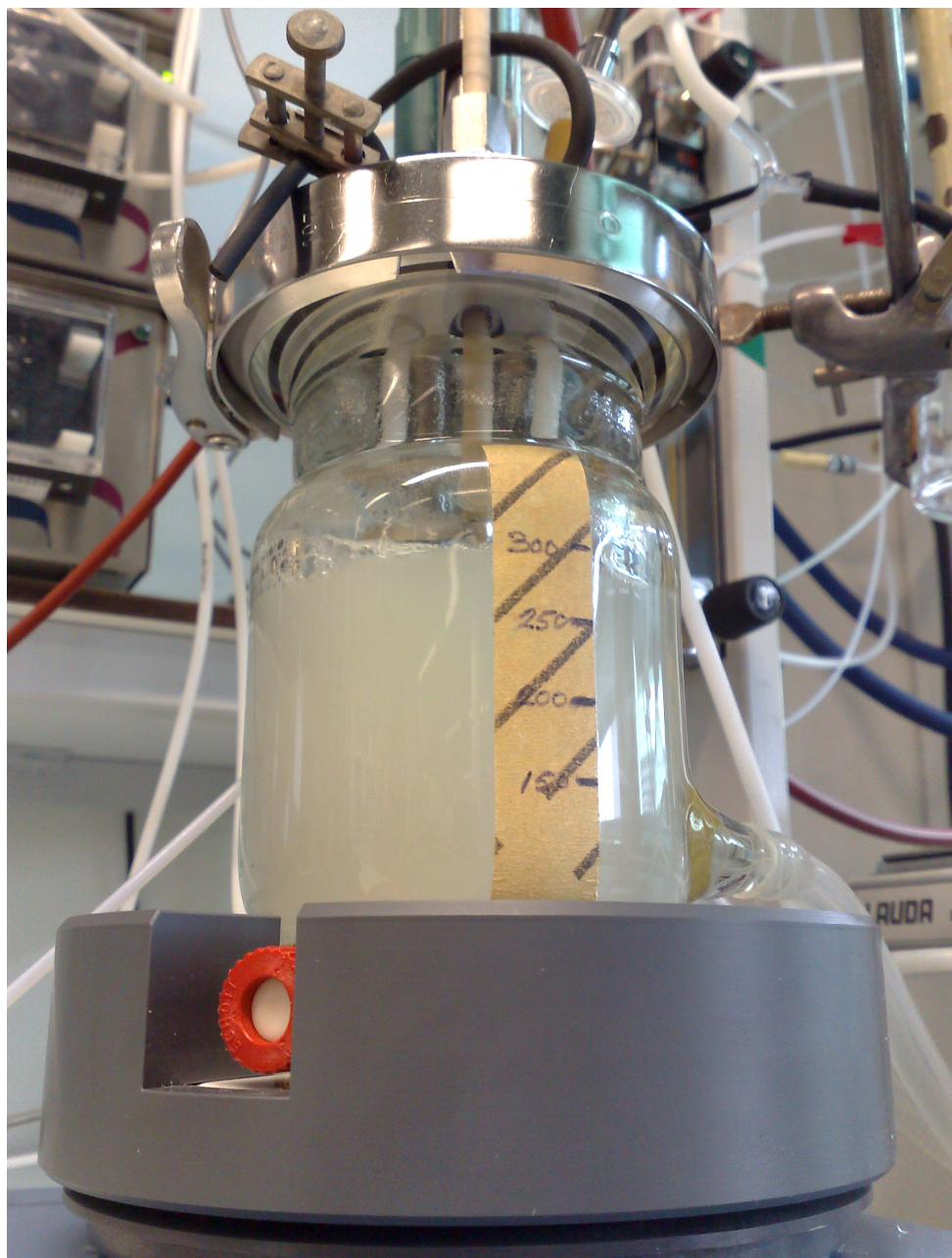
Adam S. Wieczorek and Mike S. M. Jetten were supported by grant 232937 from the European Research Council.

Chapter Three

Nitrogen fixation by *Methylophilum fumariolicum* SolV

Published in:

Microbiology-Sgm **156**, 1052-1059 (2010).



Nitrogen fixing chemostat culture of *Methylophilum thermophilum* strain SolV.

Picture by Ahmad F. Khadem.

Nitrogen fixation by the verrucomicrobial methanotroph *Methyloacidiphilum fumariolicum* SolV

Ahmad F. Khadem¹, Arjan Pol¹, Mike S. M. Jetten¹ & Huub J. M. Op den Camp¹

¹Department of Microbiology, IWW, Radboud University Nijmegen, Heyendaalseweg 135, NL-6525 AJ, Nijmegen, the Netherlands.

Abstract

The ability to utilize atmospheric nitrogen (N₂) as a sole nitrogen source is an important trait for prokaryotes. Knowledge on N₂ fixation by methanotrophs is needed to understand their role in nitrogen cycling in different environments. The verrucomicrobial methanotroph, *Methyloacidiphilum fumariolicum* strain SolV was investigated for its ability to fix N₂. Physiological studies were combined with nitrogenase activity measurements and phylogenetic analysis of the *nifD* genes, encoding the subunits of the nitrogenase. *M. fumariolicum* SolV was able to fix N₂ at low oxygen (O₂) concentration (0.5 %, v/v) in chemostat cultures. This low oxygen concentration was also required for an optimal nitrogenase activity [47.4 nmol ethylene h⁻¹ (mg cell dry weight)⁻¹]. Based on the acetylene (C₂H₂) reduction assay and growth experiments, the nitrogenase of strain SolV seems extremely oxygen sensitive compared to most proteobacterial methanotrophs. The activity of nitrogenase was not inhibited by ammonium concentrations up to 94 mM. This is the first report on physiology of N₂ fixation within the phylum *Verrucomicrobia*.

Introduction

Biological N₂ fixation is essential to life. In this process nitrogen is taken from its relatively inert molecular form (N₂) in the atmosphere and converted into ammonium according to the equation: $\text{N}_2 + 8\text{H}^+ + 8\text{e}^- + 16 \text{ATP} \rightarrow 2\text{NH}_3 + \text{H}_2 + 16 \text{ADP} + 16 \text{P}_i$ (Dixon & Kahn, 2004; Howard & Rees, 1996). The microorganisms performing this process are known as diazotrophs and they provide about 60 % of the annual nitrogen input into the biosphere (Newton, 2007). Diazotrophs are found in the domains Bacteria and Archaea and their lifestyle varies from free-living, loosely associated to symbiotic. The first methane-oxidizing bacteria, or methanotrophs, capable of N₂ fixation were isolated in 1964, referred to as *Pseudomonas methanitrificans* (Davis *et al.*, 1964). Methanotrophs form an important sink for the greenhouse gas methane but the coupling between methane and nitrogen cycles is poorly understood (Murrell & Jetten, 2009).

The microbial oxidation of methane may be coupled to the reduction of sulfate, nitrite or oxygen (Boetius *et al.*, 2000; Hanson & Hanson, 1996; Raghoebarsing *et al.*, 2006). The oxygen-consuming obligate aerobic methanotrophs are widespread in many natural environments (Conrad, 2009; Hanson & Hanson, 1996), where they feed on the methane produced by methanogens in the anoxic zones of these ecosystems. Until recently, all methanotrophs could be phylogenetically placed into 13 genera, belonging to the *Gammaproteobacteria* (type I) and the *Alphaproteobacteria* (type II) (Hanson & Hanson, 1996). However, in 2007, three research groups independently described novel thermoacidophilic methanotrophs isolated from geothermal areas in Italy, New Zealand, and Russia (Dunfield *et al.*, 2007; Islam *et al.*, 2008; Pol *et al.*, 2007). These methanotrophs represented a distinct phylogenetic lineage within the *Verrucomicrobia* and they belong to a single genus for which the name *Methylocidiphilum* was proposed (Op den Camp *et al.*, 2009). Environmental clone libraries show that there is a large biodiversity in *Verrucomicrobia* and they are encountered in many ecosystems like soils, peat bogs, acid rock drainage, and landfill leachate, often in relative high numbers but having an unknown physiology (Wagner & Horn, 2006). However, the verrucomicrobial methanotrophs were obtained in pure cultures and a complete genome sequence was published for *Methylocidiphilum infernorum* strain V4 (Hou *et al.*, 2008) while a draft genome analyses were made for *Methylocidiphilum*

fumariolicum strain SolV (Pol *et al.*, 2007). As nitrogen is one of the compounds that limits bacterial growth in most ecosystems, the ability to utilize N₂ as a sole nitrogen source is an important trait. Knowledge on N₂ fixation by methanotrophs will help to understand their role in carbon and nitrogen cycling in different environments. Although it was first assumed that only type II and the type I moderately thermophilic *Methylococcus* strains were capable of N₂ fixation (Oakley & Murrell, 1988), later the presence of both *nifH* gene fragments and acetylene reduction activity was demonstrated in a variety of type I and type II strains (Auman *et al.*, 2001). Genetic and biochemical evidence was provided to show that N₂ fixation capabilities are broadly distributed among methanotrophs. Recently, it was also demonstrated that the deep-sea anaerobic methane-oxidizing Archaea fix N₂ and share the products with their sulfate-reducing bacterial symbionts (Dekas *et al.*, 2009).

Preliminary growth experiments and genome analyses indicated that also the *Methyloacidiphilum* strains should be able to fix N₂ (Op den Camp *et al.*, 2009). The genomes of strain SolV and strain V4 show a complete set of necessary genes for N₂ fixation (Op den Camp *et al.*, 2009; Hou *et al.*, 2008). Most of these genes and their organization in putative operons resemble those of *Methylococcus capsulatus* Bath (Ward *et al.*, 2004), a Gammaproteobacterial methanotroph that has been shown to fix N₂ (Oakley & Murrell, 1991).

The aim of the research study was to elucidate N₂ fixation by *Methyloacidiphilum fumariolicum* SolV in more detail. Physiological studies were combined with nitrogenase activity measurements and analysis of the *nifH* gene encoding one of the subunits of the nitrogenase.

Materials & methods

Organism

Methylophilum fumariolicum, strain SolV used in this study was originally isolated from the volcanic region, Campi Flegrei, near Naples, Italy (Pol *et al.*, 2007). The pH and temperature optima for growth were 2 and 55 °C, respectively.

Medium composition for growth

The medium used in this study to grow strain SolV contained in g l⁻¹: MgCl₂·6H₂O, 0.08; CaHPO₄·2H₂O, 0.44; Na₂SO₄, 0.14; K₂SO₄, 0.35; (NH₄)₂SO₄, 0.26 and 1 ml l⁻¹ trace element solution (Schönheit *et al.*, 1979) and 2 % (v/v) autoclaved fangaia soil extract (liquid obtained from the Fangaia mud pool at Pozzuoli in Italy), unless stated otherwise. The medium was brought to a pH value of 2 with 1 M H₂SO₄ before autoclaving. To prevent precipitations, CaHPO₄·2H₂O was dissolved in fangaia soil extract and was sterilized separately and added to the bulk of the medium after autoclaving and cooling. The concentration of ammonium (NH₄⁺) in the fangaia soil extract may vary from 1 to 28 mM. Most of the experiments were performed with an extract containing 28 mM.

Gas & ammonium analyses

Methane (CH₄), oxygen (O₂), nitrogen (N₂) and carbon dioxide (CO₂) were analyzed on an Agilent series 6890 gas chromatograph (Agilent, USA) equipped with a Porapak Q and a Molecular sieve column and a thermal conductivity detector as described before (Ettwig *et al.*, 2008). Ethylene (C₂H₄) and acetylene (C₂H₂) were analyzed with a Varian star 3400 gas chromatograph using a flame ionization detector and a Porapak N column (1.8 m × 2 mm) with helium (He) as carrier gas. The injection, detector and oven temperature were 125, 250 and 90 °C, respectively. The gas chromatograph instruments were calibrated quantitatively for each gas by injecting dilutions of pure gasses or mixtures. For all gas analyses 100 µl gas samples were injected with a glass syringe.

Ammonium concentrations were measured using the ortho-phthalaldehyde (OPA) method (Taylor *et al.*, 1974).

Batch cultivation

The effect of O₂ concentrations on N₂ fixation by strain SolV was tested in 1 liter serum bottles, sealed with red butyl rubber stoppers. The batch incubations were performed in 50 ml nitrogen-free medium, without fangaia soil extract. The medium was inoculated with cells obtained from the early stationary phase and the inoculum size was always adjusted to achieve the same low initial optical density (OD₆₀₀), varying between 0.08 and 0.12. The gas composition in the headspace was adjusted to 13 % and 8 % (v/v) for CH₄ and CO₂, respectively. O₂ concentrations between 1 and 10 % (v/v) were tested. The experiment was started by incubating the bottles at 50 °C with shaking at 200 r.p.m. During the experiment, gas samples were removed from the bottle headspace and analyzed as described above.

Chemostat cultivation

The growth yield and stoichiometry of CH₄ conversion to CO₂ of strain SolV was determined using a chemostat, under N₂ fixing conditions. The chemostat, liquid volume 300 ml, was operated at 55 °C with stirring at 750 r.p.m. with a stirrer bar. The chemostat was supplied with medium at a flow rate of 5.1 ml h⁻¹, using a peristaltic pump. The cell-containing medium was removed automatically from the chemostat by a peristaltic pump, when the liquid level reached the sensor in the reactor. Supply of CH₄ (0.72 ml min⁻¹), N₂ (0.46 ml min⁻¹) and CO₂ (2.1 ml min⁻¹) took place by mass flow controllers through a sterile filter and sparged into the medium just above the stirrer bar. An O₂ sensor in the liquid was coupled to an ADI1030 Biocontroller (Applikon) regulating the O₂ mass controller to achieve a O₂ saturation of 0.5 %. After steady state was reached, CH₄ and O₂ consumption and CO₂ production were determined by measuring the ingoing and outgoing gas flows and the gas concentrations. The ingoing gas mixture now contained (all v/v) 14 % CH₄, 19 % O₂, 12 % N₂ and 54 % CO₂ at a flow rate of 3.8 ml h⁻¹. The outgoing gas passed through a sterile filter with a flow rate of 2.8 ml h⁻¹, and contained (all v/v) 3 % CH₄, 2.8 % O₂, 16 % N₂ and 79 % CO₂. To determine the

dry weight concentration, triplicate 5 ml samples from the culture suspension were filtered through pre-weighed 0.45 μm filters and dried to constant weight in a vacuum oven at 70 °C.

Nitrogenase assay

Acetylene (C_2H_2) reduction has been shown to be a suitable assay for N_2 fixation in methanotrophs (Dalton & Whittenbury, 1976; Murrell & Dalton, 1983; Toukdarian & Lidstrom, 1984). The nitrogenase activity assay was performed in 120 ml serum bottles, sealed with grey butyl rubber stoppers. The black rubber stoppers proved to be inhibitory. For this assay 0.5 to 2 ml culture (1 mg dry weight) were used. For the acetylene assay routinely C_2H_2 and O_2 in the headspace were set to be 2 % and 0.5 % (v/v), respectively. Because C_2H_2 is a potent inhibitor of the methane monooxygenase (MMO) (Dalton & Whittenbury, 1976; De Bont & Mulder, 1976), 0.1 % (v/v) methanol (CH_3OH) was provided to the cell suspension as an alternative electron donor. The experiment was started by incubations of the bottles at 50 °C with shaking at 200 r.p.m. To measure the ethylene (C_2H_4) production, the gas phase in the bottles was sampled at fixed time intervals and analysed by gas chromatography.

Phylogenetic analysis

Representative *nifH*, *nifD* and *nifK* gene sequences, encoding the functional proteins of the nitrogenase complex, were obtained from GenBank. The genes were also extracted from the preliminary genome data of strain SolV (GenBank accession number GU299762). Conceptual translations into amino acids were performed and a concatenated set was created for alignment and phylogenetic analysis using MEGA 4 (Tamura *et al.*, 2007). The evolutionary history was inferred using the neighbor-joining method (Saitou & Nei, 1987). The bootstrap consensus tree inferred from 500 replicates was taken to represent the evolutionary history of the taxa analysed (Felsenstein, 1985).

Results & discussion

N₂ fixation in batch cultures

Although N₂ fixation by the recently discovered methanotrophic *Verrucomicrobia* is claimed on basis of preliminary data (Dunfield *et al.*, 2007) and the presence of their genetic potential (Op den Camp *et al.*, 2009) there are no reports that show N₂ fixation.

Batch incubations of *M. fumariolicum* SolV in nitrogen-free medium (and without fangaia soil extract) showed that this methanotroph was able to fix N₂. When *M. fumariolicum* cells from batch cultures in the late exponential phase (when ammonium was already depleted) were transferred to media with N₂ as the sole source of nitrogen, and incubated at our standard oxygen concentrations (5-10 %, v/v) some increase in OD₆₀₀ was observed but this increase did not last long. We subsequently used cells that had reached the stationary phase. Transfers of these cells (at 5-10 % v/v O₂) never showed any growth within 10 weeks. However, when initial oxygen concentrations were reduced to 2 % (v/v) O₂ an increase in OD₆₀₀ could be observed (Fig. 1A), indicating N₂ fixation. In batch cultures such low oxygen concentrations cannot be maintained because of rapid oxygen consumption. Even at low cell densities (OD₆₀₀ 0.1), repeated additions of oxygen were necessary and concentrations fluctuated accordingly (Fig. 1B). This variation was also described by Dedysh *et al.* (2004). Such incubations at around 2 % of O₂ in the headspace resulted in linear growth (Fig. 1A). After decreasing the oxygen concentration to 1.3 % (v/v) and below, a short exponential growth phase was observed (Fig. 1B), but was experimentally difficult to reproduce. It was observed that in such bottles growth accelerated when oxygen concentrations were dropped below 1 % (v/v) and slowed down after adjusting the oxygen concentration to 1.5 % (v/v).

In the above-described experiments, it took 13 days before the bacteria started to grow. When these (already) N₂-fixing cultures were transferred into fresh nitrogen-free medium, their lag phase was reduced to one day. The long adaptation is probably required for induction of the nitrogenase. As there is no free nitrogen available for this protein synthesis, the organism probably relies on the recycling of other proteins or the presence of some stored nitrogen.

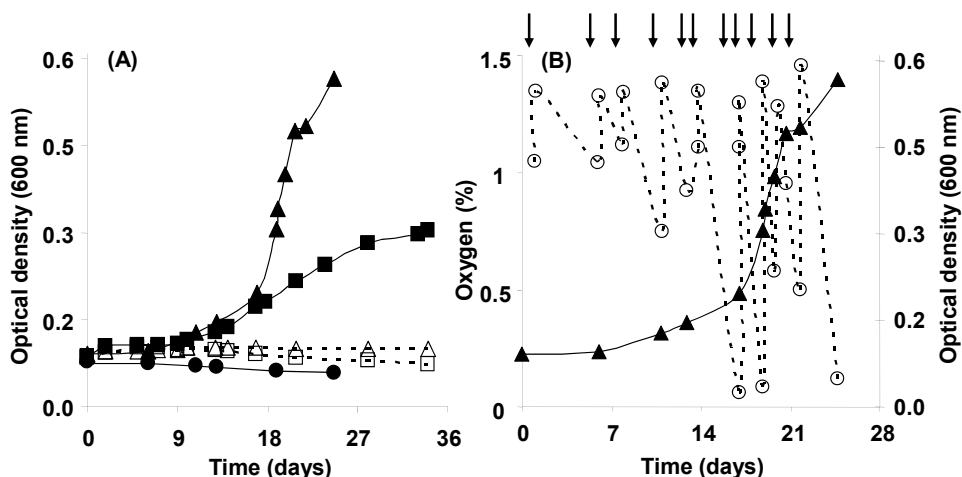


Figure 1. (A) Batch cultivation of strain SolV in nitrogen-free medium with nitrogen gas as nitrogen source. Incubation with oxygen concentrations of between 0.5 and 1.5 % (closed triangle), between 1 and 2 % (closed square), 5 % (open square) and 10 % (open triangle); and the control with 1 % oxygen in the absence of nitrogen (closed circle). (B) Due to practical limitation it was not possible to keep the oxygen concentration (open circle) constant in the batch bottles and frequently additions were required (arrows).

When the stationary cultures were transferred to ammonium-containing media, exponential growth restored within 1 day, indicating that the long lag phase is not caused by inactivation of the metabolism.

When a N_2 -free argon (Ar) gas phase was used no growth was observed, further supporting the conclusion that an active N_2 -fixing metabolism was present (Fig. 1A).

The requirement of low oxygen concentration for N_2 fixation has also been demonstrated for *Methylobacter luteus* (< 2 % v/v), *Methylocystis* strain T-1 (< 6 % v/v) and *Methylococcus capsulatus* Bath (< 10 % v/v) by batch cultivation under N_2 -fixing condition (Dedysh *et al.*, 2004; Murrell & Dalton, 1983; Takeda, 1988). In contrast some other known methanotrophs are able to fix N_2 at higher oxygen concentrations, like *Methylosinus trichosporium* OB3b (15-17 % v/v) and

Methylocapsa acidiphila B2^T (atmospheric oxygen concentration) (Dedysh *et al.*, 2002; Dedysh *et al.*, 2004).

Nitrogenase assays

The N₂-fixing *M. fumariolicum* cells described above were tested for nitrogenase activity. The acetylene reduction assay showed that these growing cultures indeed possessed nitrogenase activity. After 3 hours of incubation with acetylene, linear ethylene production started for more than 8 hours at rates of 11.1 nmol h⁻¹ (mg dry weight cells)⁻¹ for the cells growing at around 1 % (v/v) O₂. A linearly growing culture (up to 2 % v/v, O₂) showed a reduced nitrogenase activity of 3.7 nmol h⁻¹ (mg dry weight cells)⁻¹. Consistently, both the growth experiments and nitrogenase activity assays showed the detrimental effects of oxygen at concentration above 1 % (v/v).

The non-growing control culture with argon gas, where oxygen concentration was kept constant at around 1 % (v/v), also showed nitrogenase activity. After 3 hours of incubation with acetylene, this culture showed linear ethylene production for more than 8 hours at a rate of 5.5 nmol h⁻¹ (mg dry weight cells)⁻¹. This activity represents the induction of the nitrogenase. The 3 h incubation time required before that linear ethylene production started was also observed for *Methylococcus capsulatus* Bath (Zhivotchenko *et al.*, 1995).

The differences in nitrogenase activity between the cultures grown at 1-2 % (v/v) O₂ and below 1 % (v/v) O₂ can be explained as a toxic effect of oxygen. Nitrogenase is known to be an oxygen-sensitive enzyme and can be irreversibly damaged by oxygen (Robson & Postgate, 1980). So it is plausible that part of the activity of this enzyme is lost during growth at 1-2 % (v/v) O₂, resulting in the linear growth observed.

Our results are in accordance with the concept that molecular oxygen is an important repressor of the transcription of *nif* genes (Rudnick *et al.*, 1997) and that the presence of N₂ is not needed for their activation.

N₂-fixing chemostat cultures

In contrast to batch cultures, chemostat cultivation has the advantage of a much better oxygen control, especially at low concentrations. A chemostat with medium containing 2 % (v/v) fangaia soil extract (resulting in an initial ammonium concentration of 0.5 mM) was inoculated with *M. fumariolicum* SolV. In the first period of incubation (about 7 days), no medium was supplied to the chemostat; influent and effluent pumps were switched off. The oxygen concentration in the medium in the chemostat was controlled at 0.5 % saturation. Exponential growth was observed during 2 days. The maximum growth rate (μ_{\max}) was 0.07 h^{-1} (corresponding to a doubling time of 10 h) which is identical to that of a batch culture with 5-10 % (v/v) O₂ and indicates that oxygen is not limiting growth at 0.5 % saturation. Growth ceased (at an OD₆₀₀ of 0.35) when the amount of ammonium from the fangaia soil extract was depleted ($< 5 \text{ }\mu\text{M}$, Fig. 2A). After one day of adaptation the cells resumed exponential growth, but now with N₂ as the only nitrogen source at a μ_{\max} of 0.025 h^{-1} (doubling time 27 h) (Fig. 2A). The rapid onset of N₂ fixation is in contrast to the long lag phase in batch incubations, where only stationary-phase, nitrogen-depleted cells were able to start N₂ fixation. Apparently the actively growing cells in a chemostat are able to synthesize the nitrogenase protein more rapidly than the fully depleted stationary-phase cells in batch culture. After an OD₆₀₀ of 2 was reached, exponential growth ceased and the culture showed linear growth up to OD₆₀₀ 3.6, most likely due to CH₄ gas-liquid transfer limitations (Fig. 2A). At that time (day 7) the influent and effluent pumps of the chemostat were switched on. The chemostat was now supplied with medium, at a dilution rate of 0.017 h^{-1} (doubling time 40 h), well below the μ_{\max} observed in the batch phase. Although the soil extract added to the medium contains ammonium, the ammonium concentration in the chemostat remained below detection limit ($< 5 \text{ }\mu\text{M}$). A stable steady state was reached in about 18 days (Fig. 2B). In the presence of ammonium, N₂ fixation was not expected. Cells will start to fix N₂ when the availability of nitrogen compounds becomes limiting, as was demonstrated for *Methylococcus capsulatus* Bath by Zhivotchenko *et al.* (1995). Furthermore, ammonium is an important repressor of the transcription of *nif* genes, as it was observed for diazotrophic species of *Proteobacteria* (Rudnick *et al.*, 1997).

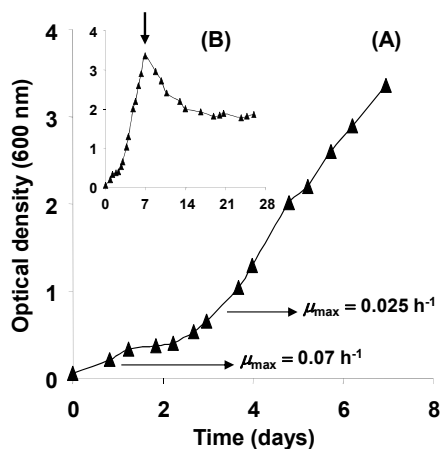


Figure 2. (A) Growth (OD_{600}) of strain SolV in chemostat, in nitrogen-free medium, with nitrogen gas as the only nitrogen source. After 2 days, ammonium from the fangaia soil extract had been consumed and exponential growth started. (B) On day 7 (arrow) the medium supply pump was switched on (dilution rate 0.017 h^{-1}) and the chemostat reached a steady state at day 18.

The μ_{\max} of strain SolV under N_2 -fixing conditions was 2.8 times slower compared to growth on ammonium as nitrogen source (Pol *et al.*, 2007). This was expected, because N_2 -fixation is an endergonic process, which needs about 16 mol of ATP per mol N_2 fixed (Dixon & Kahn, 2004). Accordingly, the growth yield of 3.5 g of dry weight cells per mol CH_4 under N_2 fixing conditions was almost two times lower than the yield with ammonium as nitrogen source (6.4 g dry weight per mol CH_4 ; Pol *et al.*, 2007). CH_4 was converted to CO_2 according to the stoichiometry $CH_4 + 1.62\text{ O}_2 \rightarrow 0.87\text{ CO}_2 + 1.5\text{ H}_2\text{O} + 0.13\text{ CH}_2\text{O}$ (biomass). When compared to the stoichiometry of ammonium-grown cells (Pol *et al.*, 2007), a slightly higher consumption of oxygen and production of carbon dioxide was found, which coincides with the lower cell yield.

N_2 fixation by cells of strain SolV grown in chemostat cultures, was confirmed by a nitrogenase activity assays. The incubation with acetylene showed linear ethylene production for more than 4 hours at a rate of $47.4\text{ nmol h}^{-1} (\text{mg dry weight cells})^{-1}$. The rate is sufficient to sustain N_2 assimilation in chemostat cultures with a doubling time of 40 h. Similar nitrogenase activity values were reported for type II and type X methanotrophs (Murrell & Dalton, 1983). The activity rate of the chemostat-grown cells is 4 times higher than for cells growing in batch culture at $< 1\%$ (v/v) O_2 , indicating that 1% (v/v) O_2 is still detrimental for N_2 fixation. In contrast to the inhibitory effect of ammonium on N_2 fixation in growing cultures, concentration of ammonium up to 94 mM, did not have an effect

on the acetylene reduction activity of the nitrogenase. Rates were linear for more than 2 h. This was also observed for several species of *Proteobacteria* able to fix N_2 (Rudnick *et al.*, 1997). However, Murrell & Dalton (1983), suggested that ammonium may affect the activity of nitrogenase and not the synthesis of this enzyme.

Oxygen optimum of SolV nitrogenase activity

The nitrogenase assay performed under 1 % (v/v) O_2 resulted in nonlinear ethylene production, with both batch-grown cells and chemostat-grown cells. Fig. 3 (A) shows ethylene production by batch-grown cells with pulse-wise addition of small amounts of oxygen. The effect of oxygen concentration on ethylene accumulation is clearly visible: e.g. addition of oxygen at day 3 slowed down production while the decreasing oxygen concentration from this point onwards resulted in an increase. This effect was explained by oxygen inhibition and was similar to the oxygen effect on growth in the N_2 -fixing batch incubations described above.

To determine the optimum oxygen concentration for the SolV nitrogenase activity in whole cells, acetylene and oxygen in the headspace were set to be 2 % (v/v) and 0.1-8 % (v/v), respectively. The optimum of oxygen concentration for SolV nitrogenase activity was found at 0.5 % (v/v) (Fig. 3B). At lower oxygen concentrations the activity decreased, possibly due to oxygen limitation for energy generation. Nitrogenase activity was still observed at oxygen concentrations up to 1 % (v/v), but at oxygen concentrations above 2 % (v/v) no nitrogenase activity was detected. This is in agreement with the results of batch incubations, where no growth was observed at head-space oxygen concentrations above 2 % (v/v) (Fig. 1A) and favors the 0.5 % O_2 saturation we used for the chemostat culture liquid medium as being optimal for growth under N_2 -fixing conditions. The oxygen requirement for the nitrogenase activity for other methanotrophs was 6 % (v/v) for *Methylococcus capsulatus* Bath, 2 % (v/v) for *Methylosinus* strain 6 and 0.5-1 % (v/v) for *Methylocystis* strain T-1 (Zhivotchenko *et al.*, 1995; Toukdarian & Lidstrom, 1984; Takeda, 1988). If we compare the nitrogenase assay with growth experiments in nitrogen-free medium, no activity of nitrogenase was observed in assays at oxygen concentrations above 1 % (v/v), while growth was observed even

at 2 % (v/v) O₂. This might be explained as a result of metabolic activity, which reduces the oxygen concentration in the cells.

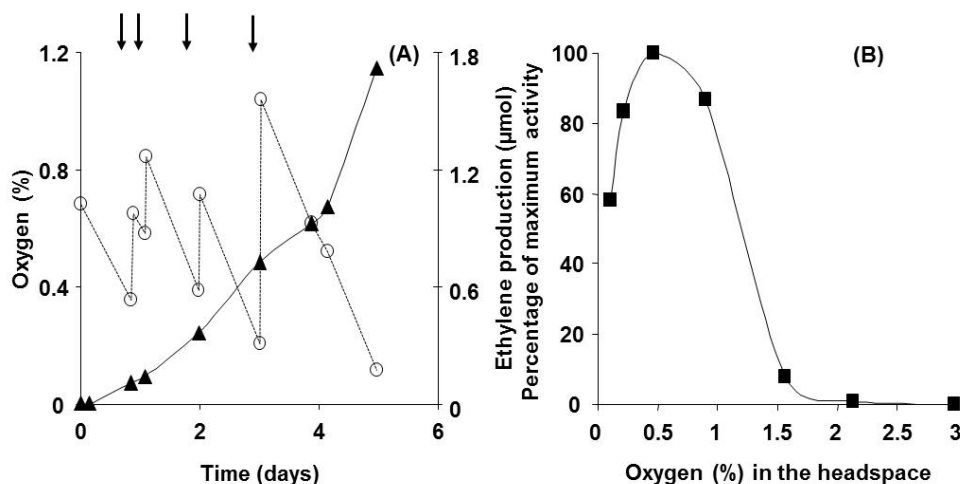


Figure 3. (A) Effect of oxygen concentration (open circle) on nitrogenase activity (closed triangle) of a N₂-fixing batch of strain SolV. Additions of oxygen are indicated by arrows. (B) Cell suspensions of N₂-fixing strain SolV were incubated at different oxygen concentrations, with methanol as the oxidizable carbon substrate. Ethylene production from acetylene was measured (closed square); 100 % activity is equal to 47.4 nmol C₂H₄ h⁻¹ (mg dry weight)⁻¹.

Phylogenetic analysis of the nitrogenase

From the preliminary genome data it was clear that the important genes for N₂ fixation were present in strain SolV. The genes encoding the structural protein (*nifH*, *nifD* and *nifK*) and the genes encoding cofactor biosynthesis (*nifE*, *nifN* and *nifX*) are located in a putative operon (Fig. 4). BlastP searches with the translated genes from the operon revealed an 89 ± 6 % identity with the proteins of the closely related *Methyloacidiphilum infernorum* V4. Proteins from α- and γ-proteobacterial methanotrophs showed 72 ± 10 % identity. The Fe-protein from

strain SolV, encoded by *nifH*, was shown to possess the cysteines involved in 4Fe-4S cluster coordination and the residues of the two Walker motifs (Howard & Rees, 1996). The other two structural proteins, encoded by *nifD* and *nifK*, also contain the conserved residues depicted by Howard & Rees (1996).

Based upon NifH phylogeny the verrucomicrobial genes can be grouped with Cluster I NifH proteins (Zehr *et al.*, 2003, Fig. 5). This cluster contains the conventional Mo-containing NifH proteins. The nitrogenase is believed to be an evolutionarily conserved protein complex (Howard & Rees, 1996). The high degree of sequence similarity among nitrogenase proteins may suggest either an early origin or lateral gene transfer among prokaryotic lineages (Postgate & Eady, 1988). Although the early origin is supported by phylogenetic analysis of large sets of nitrogenase and 16S rRNA gene sequences (Postgate & Eady, 1988; Young, 1992), comparative genomics analysis supports a scenario in which nitrogenases could have been dispersed by lateral gene-transfer mechanisms.

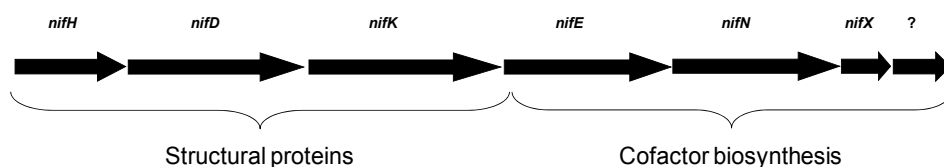
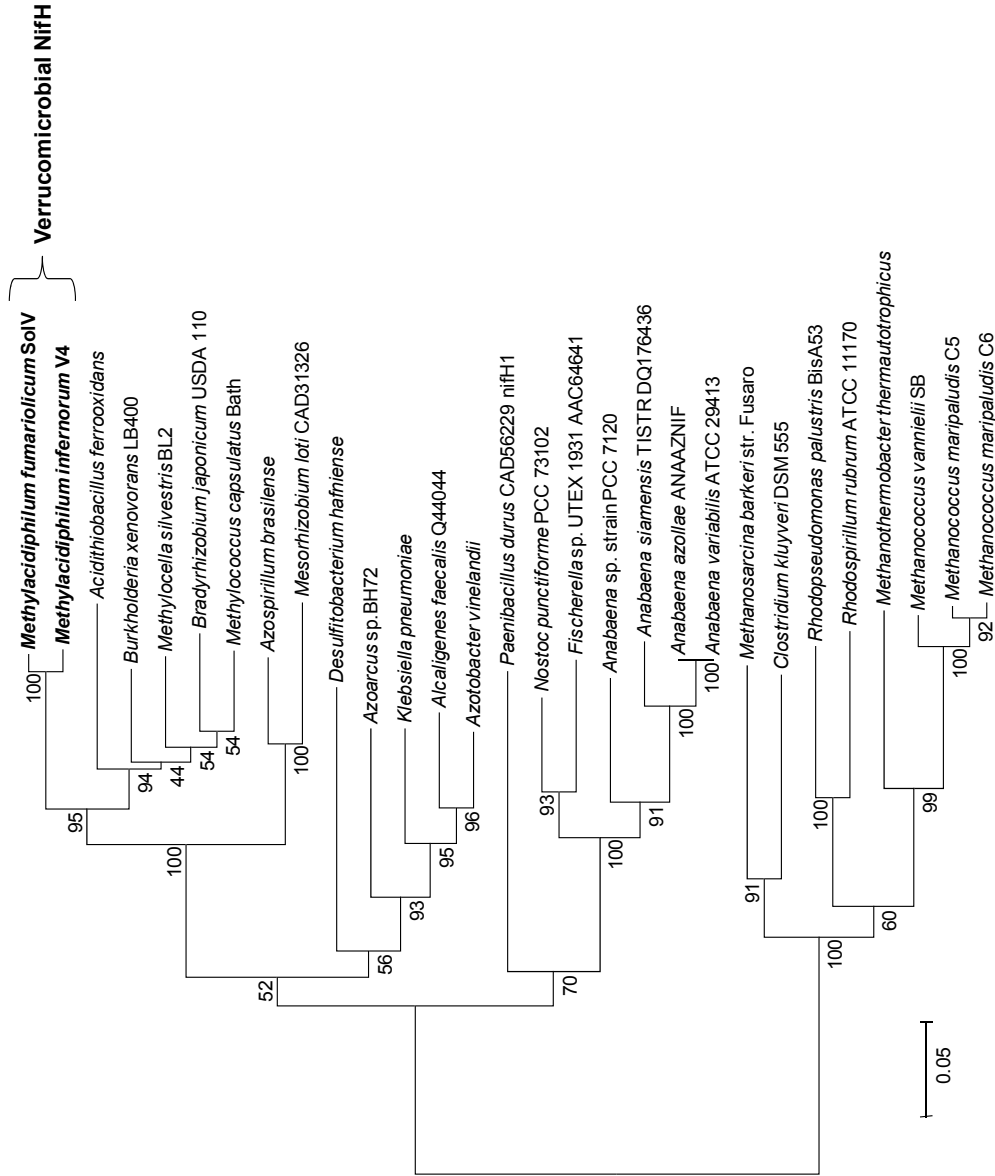


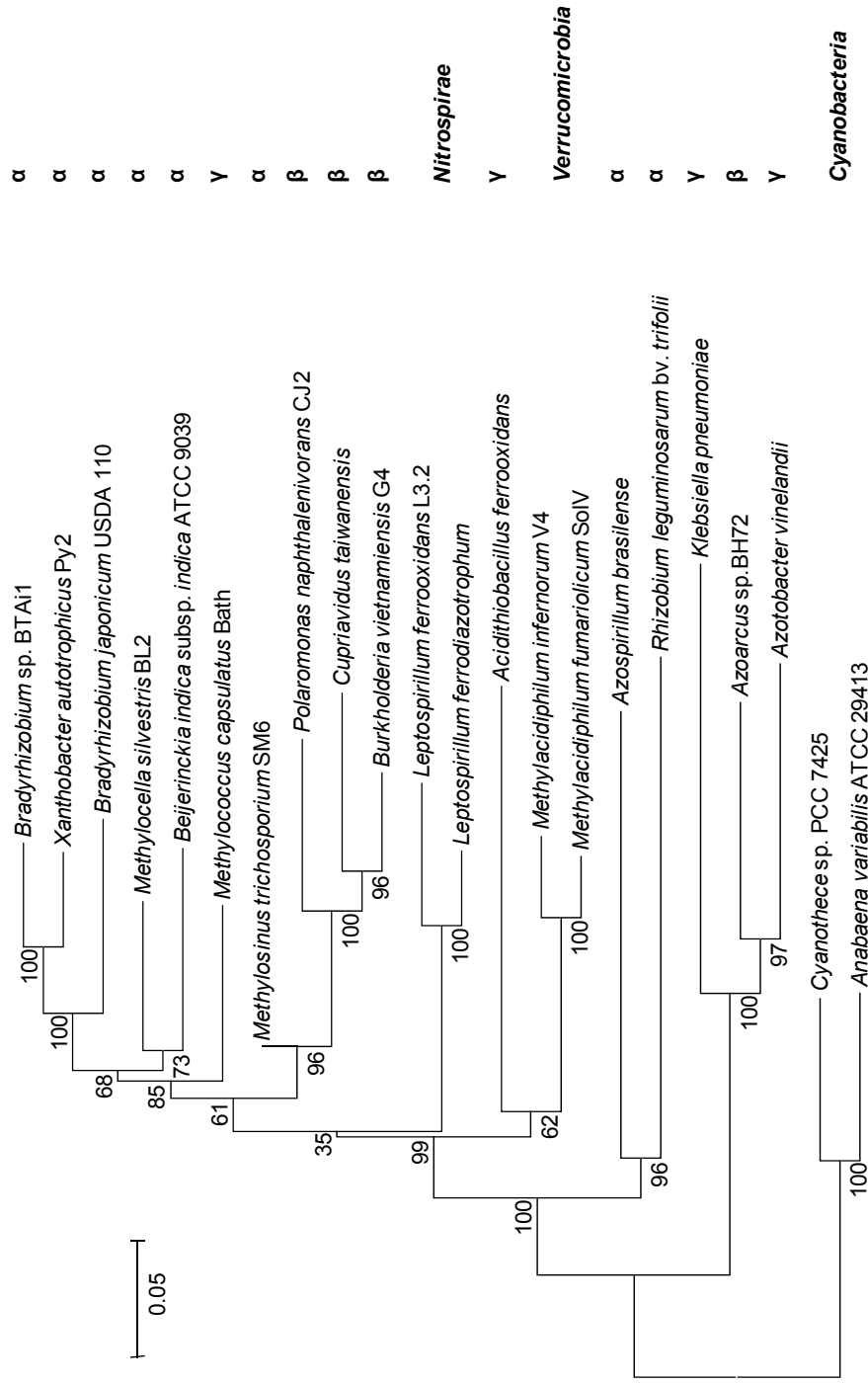
Figure 4. Schematic representation of the *nif* operon organization in the genome of *Methylophilum thermophilum* SolV (GenBank accession number GU299762).

Figure 5 (next page). Phylogenetic analysis of a representative set of NifH proteins. Bootstrap values (500 replicates) are shown at the branches. The bar represents 5 % sequence divergence. The neighbor-joining tree is drawn to scale and the evolutionary distances were computed using the Dayhoff matrix-based method and are in units of the number of amino acid substitutions per site. All positions containing alignment gaps and missing data were eliminated only in pairwise sequence comparisons (pairwise deletion option). There were a total of 332 positions in the final dataset. Phylogenetic analyses were conducted in MEGA 4 (Tamura *et al.*, 2007).



The relation of verrucomicrobial nitrogenase to that of the Archaea and *Proteobacteria* was investigated by analysis of a concatenated set of the translated structural genes *nifH*, *nifD* and *nifK*, taken from representative available bacterial genome sequences. Two cyanobacteria were chosen as an out-group. The neighbor-joining phylogenetic tree (Fig. 6) calculated from the alignment showed that the verrucomicrobial nitrogenases group with those of *Proteobacteria* and acidophilic *Leptospirillum* species, the latter being members of the *Nitrospirae* that inhabit acid mine drainage. This finding seems to be more supportive of the lateral gene transfer scenario also in view of the grouping in the tree with a proteobacterial acidophile, *Acidithiobacillus ferrooxidans*. Based on growth experiments and the acetylene reduction assay, diazotrophy was demonstrated for *Acidithiobacillus ferrooxidans* and *Leptospirillum ferrooxidans* (Mackintosh, 1978; Norris *et al.*, 1995). It is believed that the acidophilic biofilms in acid mine drainage receive limited fixed carbon and nitrogen from external sources and therefore have to fix atmospheric CO₂ and N₂ (Tyson *et al.*, 2005). For the Solfatara ecosystem less is known about the nitrogen availability. We have observed a high variety of ammonium concentrations in soil extract (see above).

Figure 6 (next page). Phylogenetic analysis of a concatenated set of the derived amino acid sequences of the *nifH*, *nifD* and *nifK* genes. Representative sequences were obtained from sequenced genomes (<http://www.ncbi.nlm.nih.gov/genomes/lproks.cgi>). Bootstrap values (500 replicates) are shown at the branches. The bar represents 5 % sequence divergence. The neighbor-joining tree is drawn to scale; the evolutionary distances were computed using the Dayhoff matrix-based method and are in units of the number of amino acid substitutions per site. All positions containing alignment gaps and missing data were eliminated only in pairwise sequence comparisons (pairwise deletion option). There were a total of 1419 positions in the final dataset.



Conclusion

Methylophilum fumariolicum SolV was able to fix N₂ under low oxygen concentration (0.5 % O₂ saturation) in chemostat cultures at a dilution rate of 0.017 h⁻¹. Based on the acetylene reduction assay and the growth experiments we conclude that the nitrogenase of strain SolV is extremely oxygen sensitive compared to most other proteobacterial methanotrophs.

To our knowledge, this is the first report on the physiology of N₂ fixation within the phylum *Verrucomicrobia*.

Acknowledgments

Ahmad F. Khadem was supported by Mosaic grant 62000583 from the Netherlands Organisation for Scientific Research (NWO).

Chapter Four

Autotrophic methanotrophy in *Verrucomicrobia*

Published in:

Journal of Bacteriology **193**, 4438-4446 (2011).



French press.
Picture by Ahmad F. Khadem.

Autotrophic methanotrophy in *Verrucomicrobia*: *Methylacidiphilum fumariolicum* SolV uses the Calvin-Benson-Bassham cycle for carbon dioxide fixation

**Ahmad F. Khadem¹, Arjan Pol¹, Adam Wieczorek¹, Seyed S. Mohammadi¹,
Kees-Jan Francoijs², Henk G. Stunnenberg², Mike S. M. Jetten¹ &
Huub J. M. Op den Camp¹**

¹Department of Microbiology, IWW, Radboud University Nijmegen, Heyendaalseweg 135, NL-6525 AJ, Nijmegen, the Netherlands.

²Department of Molecular Biology, Nijmegen Centre for Molecular Life Sciences, Radboud University Nijmegen, Geert Grooteplein-Zuid 26, NL-6525 GA, Nijmegen, the Netherlands.

Abstract

Genome data of the extreme acidophilic verrucomicrobial methanotroph *Methylacidiphilum fumariolicum* strain SolV indicated the ability of autotrophic growth. This was further validated by transcriptome analysis, which showed that all genes required for a functional Calvin-Benson-Bassham (CBB) cycle were transcribed. Experiments with $^{13}\text{CH}_4$ or $^{13}\text{CO}_2$ in batch and chemostat cultures demonstrated that CO_2 is the sole carbon source for growth of strain SolV. In the presence of CH_4 , CO_2 concentrations in the headspace below 1 % (vol/vol) were growth limiting and no growth was observed when CO_2 concentrations were below 0.3 % (vol/vol). The activity of the key enzyme of the CBB cycle, ribulose-1,5-bisphosphate carboxylase/oxygenase (RuBisCO), measured with a ^{13}C stable-isotope method was about $70 \text{ nmol CO}_2 \text{ fixed min}^{-1} (\text{mg of protein})^{-1}$. An immune reaction with antibody against the large subunit of RuBisCO on Western blots was found only in the supernatant fractions of cell free extracts. The apparent native mass of the RuBisCO complex in strain SolV was about 482 kDa, probably consisting of 8 large (53-kDa) and 8 small (16-kDa) subunits. Based on phylogenetic analysis of the corresponding RuBisCO gene, we postulate that RuBisCO of the verrucomicrobial methanotrophs represent a new type of form I RuBisCO.

Introduction

Methanotrophs are a unique group of microorganisms within the methylotrophs that oxidize methane (CH_4) to carbon dioxide (CO_2). Until 2007, the phylogenetic distribution of the aerobic methanotrophs was limited to the α and γ subclasses of the *Proteobacteria* (Hanson & Hanson, 1996). In 2007, novel thermoacidophilic aerobic methanotrophs were discovered in geothermal areas in New Zealand, Russia and Italy (Dunfield *et al.*, 2007; Islam *et al.*, 2008; Pol *et al.*, 2007). These methanotrophs represented a distinct phylogenetic lineage within the *Verrucomicrobia*, for which the genus name *Methylacidiphilum* was proposed (Op den Camp *et al.*, 2009).

Recently, methanotrophy was discovered in a member of the NC10 phylum. It was shown that '*Candidatus Methylomirabilis oxyfera*', enriched under strict anoxic conditions, produces its own oxygen from nitrite (Ettwig *et al.*, 2010). This oxygen is then used for CH_4 oxidation in a biochemical pathway comparable to those of aerobic methanotrophs.

During the aerobic oxidation of CH_4 and methanol by proteobacterial methanotrophs, formaldehyde is produced. This central metabolite can be further oxidized to CO_2 or directly assimilated via intermediates of the central metabolism. Based on the pathway used for formaldehyde assimilation, methanotrophs were divided into type I and type II. Type II methanotrophs use the serine pathway, in which formaldehyde and CO_2 are utilized in a one-to-one ratio to produce acetyl coenzyme A (acetyl-CoA) for biosynthesis (Chistoserdova *et al.*, 2009), while type I methanotrophs use the ribulose monophosphate pathway for the assimilation of formaldehyde to form glyceraldehyde-3-phosphate as an intermediate of central metabolism (Hanson & Hanson, 1996). In the latter pathway, all cellular carbon is assimilated at the oxidation level of formaldehyde. Genome data of some proteobacterial methanotrophs (*Methylococcus capsulatus* Bath, *Methylocella silvestris* BL2 [Chen *et al.*, 2010; Ward *et al.*, 2004]) and non-proteobacterial aerobic methanotrophs (*Methylacidiphilum infernorum* V4, *Methylacidiphilum fumariolicum* SolV and '*Candidatus Methylomirabilis oxyfera*' [Ettwig *et al.*, 2010; Hou *et al.*, 2008; Op den Camp *et al.*, 2009]), revealed the presence of ribulose-1,5-bisphosphate carboxylase/oxygenase (RuBisCO), the key enzyme of the Calvin-Benson-Bassham (CBB) cycle. *M. capsulatus* Bath was found to

contain RuBisCO in an active form (Stanley & Dalton, 1982), and genome analysis suggested that a variant of the CBB cycle may operate (Kelly *et al.*, 2005; Ward *et al.*, 2004). Although hydrogen seems to support moderate growth with CO₂ on agar plates for *M. capsulatus* Bath and some other methanotrophs (Baxter *et al.*, 2002), autotrophic growth in liquid cultures has not been reported. Marker exchange mutagenesis deleting the genes encoding RuBisCO may give definite answers on the exact role of RuBisCO, but unfortunately, a good genetic system for manipulation of these bacteria is lacking.

Analyses of the complete genome sequence of *M. infernorum* strain V4 (Hou *et al.*, 2008) and a draft genome of *M. fumariolicum* strain SolV showed that these two verrucomicrobial methanotrophs lack the key enzymes for both the ribulose monophosphate and serine pathways (Op den Camp *et al.*, 2009). However, in this study, we show that a complete set of genes encoding the enzymes of the CBB cycle are present, which suggests that these methanotrophs may be able to fix CO₂, probably using CH₄ mainly as an energy source. The CBB cycle has been associated with a large use of ATP per mol of CO₂ fixed (Chistoserdova *et al.*, 2009) and was thus never considered to be a likely pathway to support growth on CH₄. In the present paper, we show, by applying ¹³CH₄ or ¹³CO₂ in growth experiments, that CO₂ is the only carbon source for *M. fumariolicum* strain SolV during growth on CH₄. With a transcriptome study of strain SolV, we show that all genes necessary for a complete CBB cycle are transcribed. The large and small subunits of RuBisCO turned out to be highly expressed. In addition, we developed a novel ¹³C stable-isotope enzyme assay to demonstrate the activity of RuBisCO.

Materials & methods

Organism & medium composition for growth

The *M. fumariolicum* strain SolV used in this study was originally isolated from the volcanic region Campi Flegrei, near Naples, Italy (Pol *et al.*, 2007). The composition and preparation of the growth medium were described previously (Khadem *et al.*, 2010).

Transcriptome analysis

The available draft genome of strain SolV (Pol *et al.*, 2007) was improved by adding data (30×10^6 75-nucleotide reads) from an Illumina sequencing run. Genes encoding the enzymes of the CBB cycle were identified by BLAST searches, and their DNA and protein sequences were used for transcriptome analysis. Exponentially growing cells were harvested by centrifugation, 3.1 mg (dry weight) cells was used for isolation of mRNA, and subsequent synthesis of cDNA (328 ng) was done as described before (Ettwig *et al.*, 2010). The cDNA was used for single-end Illumina sequencing (Ettwig *et al.*, 2010). Expression analysis was performed with the RNA-Seq analysis tool from the CLC Genomics Workbench software (version 4.0; CLC bio, Aarhus, Denmark).

Gas & protein analyses

Gas samples (100 μ l) were analyzed for CH₄ and CO₂ on an Agilent series 6890 gas chromatograph (GC) equipped with Porapak Q and molecular Sieve columns and a thermal conductivity detector (Ettwig *et al.*, 2008). To quantify the molecular masses for ¹²CH₄ and ¹³CH₄ (16 and 17 Da) and for ¹²CO₂ and ¹³CO₂ (44 and 45 Da), the same gas chromatograph was coupled with a mass spectrometer (GC-MS) (Agilent 5975C GC MSD; Agilent, Santa Carla, CA) (Ettwig *et al.*, 2010). All gas concentrations are given in volume percentages (volume/volume). Protein concentrations were measured using the Bio-Rad protein assay kit (Bio-Rad Laboratories B.V., Veenendaal, the Netherlands).

$^{13}/^{12}\text{C}$ IRMS analysis

The $^{13}/^{12}\text{C}$ ratio of biomass samples was determined using isotope ratio mass spectrometry (IRMS). The cells were harvested by centrifugation, and the pellet was washed with acidified water (pH 3) and dried overnight in a vacuum oven at 70 °C. The dried material (about 0.04 mg) was analyzed on a Thermo Fisher Scientific EA 1110 CHN element analyzer coupled with a Finnigan DeltaPlus mass spectrometer.

Batch cultivation

The effect of CO_2 concentration on the growth of strain SolV was studied in batch cultures using 1-liter serum bottles containing 50 ml of medium and sealed with red butyl rubber stoppers. Incubations were performed in duplicate and at 55 °C with shaking at 180 r.p.m., and mixtures contained 5 % CH_4 and air as the only source of O_2 and CO_2 . To remove dissolved CO_2 originating from the inoculum, the cell suspension was flushed with sterile air for 10 min before inoculation.

$^{13}\text{CH}_4$ experiments were done in 150-ml serum bottles containing 10 ml of culture medium, 40 % CO_2 , and 5 ml of $^{13}\text{CH}_4$ (99 atom % ^{13}C ; Sigma-Aldrich). The bottles were inoculated with 0.25 ml of a culture of strain SolV. Initial and final gas concentrations and amounts, as well as mass ratios, were verified by gas chromatographic analysis using a pressure lock syringe. Recovery of ^{13}C was calculated from $^{13}\text{C}/^{12}\text{C}$ ratio of CO_2 and the total amount (moles) of gasses in the bottle. For calculating CO_2 in the liquid phase, a partition coefficient of 1.066 (gas/liquid ratio) at 21 °C was assumed (Weiss, 1974). At the end of the experiment, the biomass was used for the IRMS analysis.

Chemostat cultivation

$^{13}\text{CH}_4$ - and $^{13}\text{CO}_2$ -labeling experiments were performed in continuous chemostat cultures under N_2 -fixing conditions as described before (Khadem *et al.*, 2010). In the first experiment, $^{13}\text{CH}_4$ (99 atom % ^{13}C ; Sigma-Aldrich) replaced the unlabeled CH_4 in the inlet gas mixture of the chemostat. After a steady state was obtained, the ^{13}C -labeling percentage of the gases in the outlet of the chemostat was determined.

The ingoing gas now contained 4.7 % $^{13}\text{CH}_4$ and 3.5 % $^{12}\text{CO}_2$ at a flow rate of 10.7 ml min $^{-1}$. The outgoing gas (10.3 ml min $^{-1}$) contained 2.5 % $^{13}\text{CH}_4$, 3.1 % $^{12}\text{CO}_2$, and 2.2 % $^{13}\text{CO}_2$.

In the second experiment, $^{13}\text{CO}_2$ replaced the unlabeled CO_2 . $^{13}\text{CO}_2$ was prepared by pumping a 0.6 M $\text{NaH}^{13}\text{CO}_3$ (99 % ^{13}C) solution into a stirred solution (450 ml) of 1.2 M HCl in a closed 500-ml serum bottle. The argon gas supply of the chemostat was led via the headspace of this bottle, and once the $^{13}\text{CO}_2$ concentration was constant, it was supplied into the chemostat. The ingoing gas contained 4.6 % $^{12}\text{CH}_4$, 0.07 % $^{12}\text{CO}_2$, and 3.6 % $^{13}\text{CO}_2$ at flow rate of 10.4 ml min $^{-1}$. The outgoing gas, with a flow rate of 10.3 ml min $^{-1}$, contained 2.3 % $^{12}\text{CH}_4$, 1.95 % $^{12}\text{CO}_2$, and 3.2 % $^{13}\text{CO}_2$. During the experiments, samples of chemostat culture were collected and used for the IRMS analysis of the biomass.

Assuming that carbon in new biomass is labeled according to the label percentage of the CO_2 present (X^{CO_2}) in the chemostat (i.e. gas outlet), the ^{13}C -label percentage of biomass in the chemostat will develop over time according to the formula: $X^{\text{CO}_2} \times (1 - e^{-Dt})$, in which D represents the dilution rate (h $^{-1}$) of the reactor and t represents time (h).

The “old” biomass in the chemostat at the moment we started the calculations washed out according to the formula $X^{\text{old}} \times (e^{-Dt})$. X^{old} is the ^{13}C label percentage of biomass of the first sample taken, at the moment that the $^{13}\text{CO}_2$ gas concentrations in the outlet reached steady state. This value was still close to the natural abundance of ^{13}C in the biomass, as only a little $^{13}\text{CO}_2$ was incorporated. The sum of new and old biomass percentages was taken as the predicted average ^{13}C -label percentage of the chemostat biomass in the course of time during the supply of labeled gasses: $X_t = X^{\text{CO}_2} \times (1 - e^{-Dt}) + X^{\text{old}} \times (e^{-Dt})$.

Recovery calculation of ^{13}C from $^{13}\text{CH}_4$ in CO_2 & biomass

The ^{13}C recovery in biomass (see results [Table 1]) was calculated using the following formula: (mole fraction of formaldehyde $\times 0.34 \times 100$) + (mole fraction of $\text{CO}_2 \times 0.34 \times 42$). In this formula, the mole fraction refers to incorporation ratio of formaldehyde and CO_2 into biomass, depending on the carbon assimilation pathway. The values 100 and 42 refer to the labelling percentages of formaldehyde

and CO₂, respectively. The value 0.34 refers to the biomass produced according to the observed stoichiometry of CH₄ oxidation (see Results).

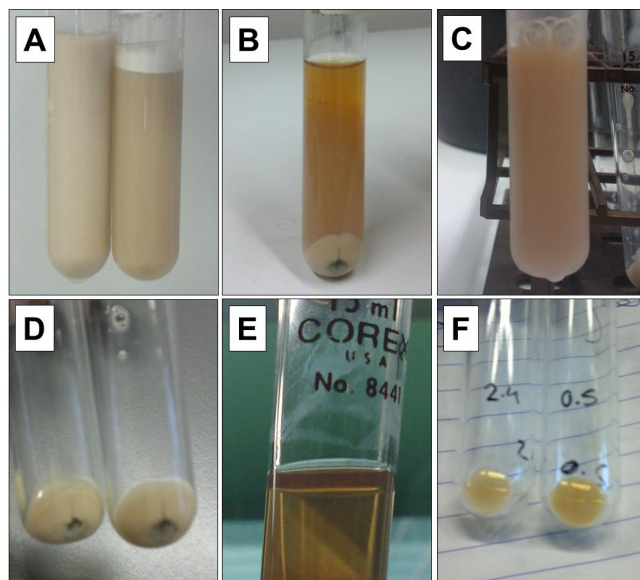
Cell extracts

Cells of an exponentially growing culture (9 liters, optical density at 600 nm [OD₆₀₀] = 0.56) were collected by centrifugation (4,000 × *g*, 4 °C, 10 min) and washed two times with 70 ml buffer {25 mM PIPES [piperazine-*N,N'*-bis-(2-ethanesulfonic acid)]-NaOH, pH 7.5}. Finally, the cell pellet (9.6 g [wet weight]) was resuspended in 10 ml of PIPES-NaOH buffer. To this suspension (pH 7), one tablet of protease inhibitor cocktail (Boehringer, Mannheim, Germany) and 1 mg DNase I were added. Cells were broken by passing the cell suspension 3 times through a French press at 20,000 lb/in². Unbroken cells and cell debris were removed from the resulting crude extract by centrifugation at 12,000 × *g* for 20 min (4 °C, Sorvall SS-34 rotor). This resulted in a turbid supernatant, with increasing turbidity toward the bottom of the tube. The turbid cell extract was centrifuged again at 48,000 × *g* for 40 min (4 °C). This resulted in clear reddish supernatant and a yellowish pellet (see picture 1). The clarified cell extract obtained was further ultracentrifuged, using a Sorvall Discovery with a 70.1 Ti rotor (150,000 × *g*, 4 °C, 60 min). This resulted in clear reddish supernatant and a tiny yellow transparent pellet (the same observation as the 48,000 × *g* centrifugation step).

Protein gel electrophoresis

Sodium dodecyl sulfate-polyacrylamide gel electrophoresis (SDS-PAGE) and native-PAGE were performed using a Mini-Protean 3 Cell (Bio-Rad) according to the method of Laemmli (Laemmli, 1970). Molecular weight standards were obtained from Fermentas and Invitrogen. For SDS-PAGE, protein samples (25 µg) were incubated at 95 °C for 10 min in loading buffer (6.5 % [vol/vol], glycerol, 0.016 M Tris-HCl [pH 6.8], 0.5 % [wt/vol] SDS, 0.003 % [wt/vol] bromophenol blue and 1.3 % [vol/vol] β-mercaptoethanol). For native-PAGE, loading buffer without SDS and β-mercaptoethanol was used. Proteins in the gel were stained overnight by Coomassie brilliant blue G-250.

Protein bands from native gels were cut out and further analyzed by SDS-PAGE; bands (8.5 mm³) were incubated in 100 μ l SDS-PAGE loading buffer at 95 °C for 10 min, and incubated further overnight at 4 °C with gentle shaking. The eluted proteins were 10-fold concentrated and washed several times with Tris-HCl buffer (0.5 M, pH 6.8) using a 3k Vivaspın column (Sartorius Stedim Biotech) before loading on the SDS-PAGE gel.



Picture 1. (A, left) Cell suspension of *Methylophilum fumariolicum* SolV. (A, right) Crude extract obtained by passing the cell suspension through a French press. (B) The reddish turbid supernatant with increasing turbidity toward the bottom of the tube, obtained after centrifugation of the crude extract at 12,000 \times g. (C) 12,000 \times g supernatant. (D) 12,000 \times g pellet. (E) 48,000 \times g supernatant. (F) 48,000 \times g pellet.

Molecular mass determination of RuBisCO

For mass determination of RuBisCO, native-PAGE (see above) and size exclusion chromatography were applied. Clarified cell extract of strain SolV was passed through a column (16 mm by 130 cm) of Sephacryl S-300 HR (VWR). The column was preequilibrated with 20 mM phosphate buffer-100 mM NaCl (pH 7.2). After loading, the column was eluted with the same buffer at 0.5 ml min⁻¹ and column effluent was monitored at 280 nm. Protein fractions were collected using an automated fraction collector. Peak fractions were then subjected to SDS-PAGE

analysis. Calibration proteins obtained from Sigma were albumin egg (45-kDa), albumin bovine (66-kDa), alcohol dehydrogenase (150-kDa), apoferritin (443-kDa), thyroglobulin (669-kDa), and blue dextran (2,000-kDa).

MALDI-TOF MS analysis

Identification of the protein bands on the SDS-PAGE gels were performed by matrix-assisted laser desorption ionization-time of flight mass spectrometry (MALDI-TOF MS). Gel spots (about 5 mm³) were destained (solutions contained acetonitrile [30, 50, and 100 % vol/vol], diluted with 25 mM ammonium bicarbonate [NH₄HCO₃]), and dried, and the proteins were in-gel digested with 5 µl of trypsin (the solution contained 15 ng trypsin µl⁻¹ in a mixture of 25 mM NH₄HCO₃ and 5 mM *n*-octyl-β-D-glucopyranoside) on ice for 1 h. The excess trypsin solution was removed, and the gel spot was covered with a solution containing 25 mM NH₄HCO₃ and 5 mM *n*-octyl-β-D-glucopyranoside and was incubated overnight at 37 °C. The peptides were extracted by adding 4 µl of a mixture containing (all volume/volume) 50 % acetonitrile, 0.5 % trifluoroacetic acid (TFA), and 49.5 % 5 mM *n*-octyl-β-D-glucopyranoside, followed by 1 h incubation at room temperature. The liquid was sonicated for 2 min in a water bath and dried in a vacuum centrifuge. The peptides were solved in 4 µl of TFA (0.1 %). The dissolved peptides (3 µl) were mixed with 0.3 µl of matrix solution (20 mg α-cyano-4-hydroxycinnamic acid in 0.5 ml 0.1 % TFA and 0.5 ml acetonitrile), spotted on a stainless steel target plate, and analyzed on a Biflex III MALDI-TOF mass spectrometer (Bruker, Bremen, Germany) operating in the reflectron mode. Data analysis was performed using X-TOF software (Bruker, Bremen, Germany), and the Mascot search engine (Matrix Science Ltd., Boston, MA) was used to identify the proteins.

Immunoblotting

The proteins from SDS-PAGE and native-PAGE gels were transferred to a nitrocellulose membrane by electroblotting at 100 mA for 45 min. The obtained blots were then prepared for immune reaction as previously described (van Niftrik *et al.*, 2009). The polyclonal anti-RuBisCO, raised in rabbit using a synthetic

peptide, was used as primary antibody (product AS03 037; Agrisera, Vännäs, Sweden). This antibody was 3,300-fold diluted in blocking buffer. The monoclonal mouse anti-rabbit IgG alkaline phosphatase conjugate (Sigma catalog no. A2556) was used as the secondary antibody.

Activity assay for RuBisCO. (i) Carboxylase activity

As an alternative to the radioisotope method, we developed a stable-isotope method for measuring RuBisCO activity. This was based on the incorporation of $^{13}\text{CO}_2$ into 3-phosphoglycerate (3-PGA) and subsequent destruction of 3-PGA by acid permanganate oxidation. The $^{13}\text{CO}_2$ liberated was quantified by GC-MS as described above. The destruction of 3-PGA to liberate the carboxyl group was performed analogously to the destruction of lactate with permanganate and phosphoric acid (H_3PO_4), as previously described (Bird *et al.*, 1978), which produces CO_2 and acetate. We used 1 % potassium permanganate (KMnO_4) in 0.1 M H_3PO_4 instead of 5 % KMnO_4 in 0.07 M H_3PO_4 , and the temperature was lowered from 80 °C to 50 °C. Under such conditions, 15 min of incubation yielded 1 mol of CO_2 per mol of 3-PGA. This was verified by a series of 0.1 to 2 μmol of 3-PGA in 3-ml Exetainer vials (Labco Limited, High Wycombe, United Kingdom). Ice-cold KMnO_4 (500 μl) was added, and the vial was immediately closed with a screw cap with a rubber seal and incubated at 50 °C. A linear relation between the amount of 3-PGA and CO_2 produced was measured (GC-MS analysis). Under stronger oxidative conditions, the initial production of CO_2 was more rapid but followed by a continuous slow evolution of CO_2 . Apparently, the oxidation product of 3-PGA is prone to further oxidation. The final destruction conditions applied were 0.1 % KMnO_4 in 0.1 M H_3PO_4 for 25 min at 50 °C.

To limit the background production of CO_2 and increase the sensitivity of the method, we used 20 mM phosphate buffer in the assay mixtures to replace the commonly used organic buffers. The only organic material present in the assay mixture now originated from the RuBisCO-containing samples. Apart from some CO_2 from air, the major part of CO_2 (> 80 %) present in the Exetainer vial after destruction resulted from the RuBisCO assay samples. As it reflects the sample amount, this CO_2 could act as an internal standard when the ratio of $^{13}\text{CO}_2$ to $^{12}\text{CO}_2$ was taken. This resulted in better time curves than those obtained using the

absolute amounts of $^{13}\text{CO}_2$ produced in the destruction vial. Moreover, the GC-MS response for CO_2 was varied over time, while the ratio of $^{13}\text{CO}_2$ to $^{12}\text{CO}_2$ was very constant. The ratio multiplied by the average total amount of CO_2 in the destruction bottles from a time series was used to calculate the amount of $^{13}\text{CO}_2$ produced. Time series were linear for 2 min. The standard RuBisCO assay was performed in a 2-ml vial (VersaVial; Alltech) containing 200 μl of Mg-phosphate buffer (20 mM potassium phosphate, 10 mM MgCl_2 , pH 6.9). Cell extracts diluted in 25 mM PIPES-NaOH, pH 7.5, to a total volume of 25 μl and $\text{NaH}^{13}\text{CO}_3$ (99 % ^{13}C) (20 μl of a 100 mM stock) were added. The vial was closed immediately with a thin rubber cap (Alltech) to prevent the loss of CO_2 . The final pH in this mixture was pH 7.25 (at 50 °C), and the CO_2 gas concentration was calculated to be 1.5 %. The vial was preincubated for 10 min at 50 °C in a water bath and the RuBisCO activity assay was started by adding 5 μl of stock solution of ribulose-1,5-bisphosphate (25 mM) by a syringe through the rubber cap. The mixture was vortexed for 2 s and incubated further at 50 °C. Samples of 50 μl were taken through the stopper by a syringe every 30 s for 2 min. Samples were mixed with 20 μl of 0.5 M HCl in 3-ml Exetainer tubes and dried under vacuum at 45 °C. After destruction with 0.5 ml permanganate solution as described above and cooling down to room temperature, the vials were stirred on a vortex device to allow CO_2 to equilibrate. The gas phase was measured for $^{13}\text{CO}_2$ and $^{12}\text{CO}_2$ by GC-MS analysis.

Activity assay for RuBisCO. (ii) Oxygenase activity

The oxygenase reaction of RuBisCO was assayed in a Strathkelvin RC350 respiration cell at a working volume of 0.7 ml. The assay buffer contained 50 mM HEPES and 10 mM MgCl_2 (pH 7.2) and was air saturated at 50 °C. Unlabeled NaHCO_3 was added in the range of 0 to 10 mM, and after addition of cell extract (12,000 $\times g$ supernatant, 1 mg protein), the background O_2 consumption was followed for 10 min before the addition of ribulose 1,5-bisphosphate (0.4 mM). After this addition, consumption rates increased immediately but then slowed down.

pH optimum for RuBisCO assay

The effect of pH on the activity was determined by setting the initial pH value of the Mg-phosphate buffer at values of 6.45, 6.6, 6.85 and 7.05. $\text{NaH}^{13}\text{CO}_3$ was added at 7, 9, 12 and 16 mM final concentrations, respectively. The final pH was verified at 50 °C in an up-scaled situation (10-ml tubes) to be 7.0, 7.22, 7.5 and 7.75, respectively. Taking a dissociation constant (pK_a) of 6.1 for carbonic acid (H_2CO_3) at 50 °C, the CO_2 percentage in the gas phase was calculated to be between 1.4 and 1.7 %.

Phylogenetic analysis

Representative *CbbL* and *CbbS* sequences, encoding the large and small subunits of RuBisCO, were obtained from GenBank and aligned using MUSCLE (Edgar, 2004) in MEGA 5.0 (www.megasoftware.net). Phylogenetic trees were calculated using the neighbor-joining method (Saitou & Nei, 1987) with 1,000 bootstraps (Felsenstein, 1985) to infer the evolutionary relationship. Positions containing alignment gaps and missing data were eliminated only in pairwise sequence comparisons (pairwise deletion option). The Dayhoff matrix-based method was used to compute the evolutionary distances.

Nucleotide sequence accession numbers

The *M. fumariolicum* SolV genes reported in this study were extracted from the draft genome and submitted to GenBank under accession numbers JF706245 to JF706259 and JF714482.

Results

Growth of strain SolV at different CO₂ concentrations

Standard batch incubations of *M. fumariolicum* strain SolV with CO₂ and CH₄, both 5 %, resulted in exponential growth within one day. However, incubations without CO₂ did not result in any growth on CH₄, even after 40 days of incubation, indicating that CO₂ was necessary for growth. This dependency was further investigated in a series of batch incubations in 1-liter bottles with air as the only source of CO₂ (0.04 %) and 5 % CH₄. In all incubations, we observed CO₂ production from CH₄ during the initial period, at a rate directly depending on the inoculum size. As the CH₄ oxidation was not coupled to growth, the CO₂ production rate decreased with time (Fig. 1A). Growth resumed only after CO₂ had reached levels above 0.3 % (Figs. 1B and 1C). This indicated that growth of strain SolV is dependent on a minimum concentration of CO₂ in the headspace.

In order to circumvent endogenous CO₂ production and to test the effect of non-growth conditions on the viability of strain SolV, a culture was starved for CH₄ for 35 days (at 55 °C). When CH₄ was subsequently added, CO₂ production was hardly measurable, and no growth was observed for 7 days. Thereafter, when CO₂ was added, growth resumed within 3 days (Fig. 2).

From various growing cultures of strain SolV, the growth rate was determined at different prevailing CO₂ concentrations. This was done for time intervals of about 6 h, in which CO₂ concentrations in the headspace did not changed more than 15 %. The results clearly showed the dependency of the growth rate on CO₂ concentration (Fig. 3). The lowest CO₂ concentration at which growth was observed was 0.3 % (doubling time, about 80 h), and the growth rate increased towards its maximal (doubling time, 10 h) at 1 % CO₂.

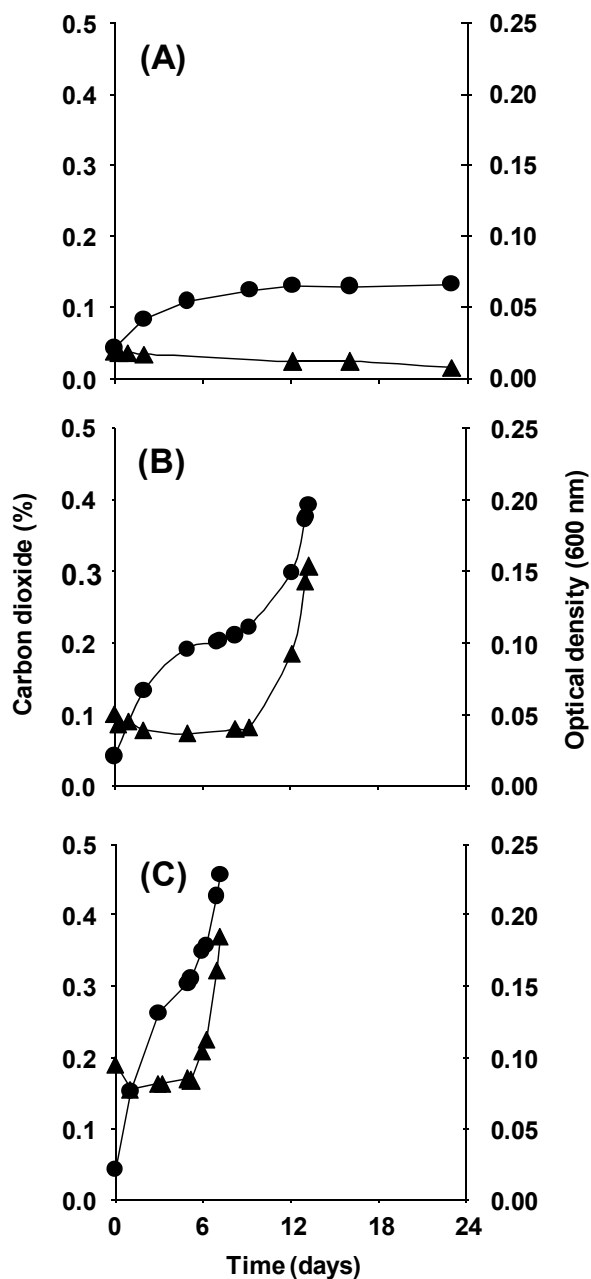


Figure 1. Effect of CO₂ concentration (closed circles) on growth of *M. fumariolicum* strain SolV in batch (closed triangles). Batch incubation with initial OD₆₀₀ of 0.02 (A), 0.05 (B) and 0.1 (C) were started with 5 % (vol/vol) CH₄ and with air as the only O₂ and CO₂ source.

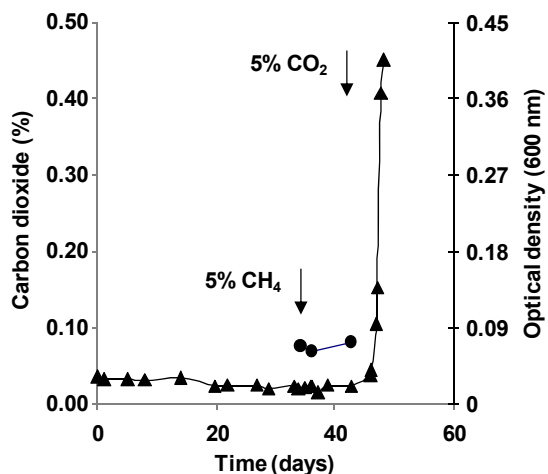
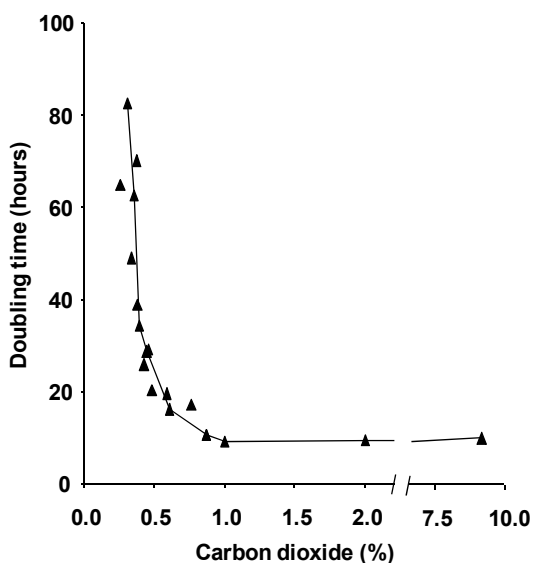


Figure 2. The effect of non-growth conditions on viability of *M. fumariolicum* strain SolV was tested in batch culture. SolV cells were starved for 35 days for CH₄. On day 35 CH₄ (5 % [volume/volume]) was added and 7 days later CO₂ was adjusted to 5 % (volume/volume) in the headspace. CH₄ and CO₂ additions are indicated with arrows. CO₂ % (closed circles), OD₆₀₀ (closed triangles).

Figure 3. Doubling time of *M. fumariolicum* strain SolV at different CO₂ concentrations (triangles). The growth rates of various growing cultures of strain SolV were determined at different prevailing CO₂ concentrations. This was done for time intervals of about 6 hours, in which CO₂ concentrations in the headspace did not change more than 15 %.



¹³C-labeling experiments in chemostat cultures

Labeling experiments were performed to determine whether CO₂ was the only carbon source in *M. fumariolicum* strain SolV. A CH₄-limited chemostat culture at a dilution rate (*D*) of 0.016 h⁻¹ was used for this purpose. At steady state, gas concentrations in the inlet and outlet were analyzed, and CH₄ consumption rate (ml min⁻¹ ± standard error of the mean [SEM]) was calculated to be 0.254 ± 0.009 (*n* = 4). The CO₂ production rate (ml min⁻¹ ± SEM) was 0.167 ± 0.01 (*n* = 4). This results in the following stoichiometry for carbon: 1 CH₄ → 0.66 CO₂ + 0.34 biomass (CH₂O). The biomass carbon can be derived either from CH₄ oxidation intermediates or from CO₂.

In the first experiment, the unlabeled CH₄ supply of the chemostat was changed to ¹³CH₄. The labeling percentages of the gases in the chemostat headspace reached steady state after 1.5 hours (42 % ¹³C for CO₂ and > 99 % ¹³C for CH₄), and the ¹³CH₄ consumption and ¹³CO₂ production rates (ml min⁻¹ ± SEM) were calculated (0.254 ± 0.009 and 0.226 ± 0.002, respectively), thus resulting in a recovery (mean ± SEM) of 89 % ± 3.3 % of the ¹³CH₄ consumed.

Even when all ¹³CH₄ consumed is converted into ¹³CO₂ and all biomass is derived from CO₂, a total recovery in ¹³CO₂ is not expected, as part of the ¹³CO₂ produced in the chemostat is incorporated into the biomass. With the above stoichiometry for carbon and a measured 42 % ¹³C-labeling percentage for CO₂ in the chemostat, still 14 % (measured ¹³C-labelling percentage × moles of biomass) of the label will be incorporated into the biomass, and so only 86 % can be recovered as ¹³CO₂ (Table 1).

The measured ¹³C-labeling percentage of CO₂ in the chemostat was in good agreement with the calculated value of about 40 %. This was calculated on the basis of the unlabeled CO₂ in the inlet gas and the amount of ¹³CH₄ converted into ¹³CO₂.

Table 1. Recovery calculation of ^{13}C from $^{13}\text{CH}_4$ in CO_2 and biomass

Pathway	^{13}C -labeled CH_4	^{13}C -labeled formaldehyde	^{13}C % of CO_2 in pool	^{13}C recovery in biomass	^{13}C recovery in ^{13}C -labeled CO_2	References
RuMP ^a	100 %	100 %		34 %	66 %	(Hanson & Hanson, 1996)
serine ^b	100 %	100 %	42 %	21 %	79 %	(Hanson & Hanson, 1996)
serine ^c	100 %	100 %	42 %	24 %	76 %	(Chistoserdova <i>et al.</i> , 2009)
CBB ^d	100 %		42 %	14 %	86 %	This study

^a According to the ribulose monophosphate (RuMP) pathway, all biomass is produced from formaldehyde.

^b According to the serine pathway, formaldehyde and CO_2 are incorporated into biomass in a 1 to 2 ratio.

^c According to the serine pathway, formaldehyde and CO_2 are incorporated into biomass in a 1 to 1 ratio.

^d According to the Calvin-Benson-Bassham (CBB) cycle, all biomass is produced from CO_2 .

The increase in ^{13}C percentage of the biomass in the chemostat culture in the course of time (Fig. 4A) was predicted under the assumption that all biomass was derived from CO_2 , at the current ^{13}C label percentage of 42 %. Before the reactor was supplied with the ^{13}C label, the percentage was 1.1, close to the natural abundance of ^{13}C in CO_2 gas (1.17 %). Measured values of the increase of the ^{13}C percentage of the biomass followed exactly the predicted curve (Fig. 4B).

The experiment was repeated with $^{13}\text{CO}_2$ in the inlet gas of the chemostat and unlabeled CH_4 . The labeling percentage of CO_2 in the outlet increased to 62 % after 1.5 h (steady state). Unlabeled CO_2 originated from oxidation of the unlabeled CH_4 . Again, the increase of the ^{13}C percentage of the biomass followed the predicted curve (Fig. 4B), with the assumption that CO_2 was the only carbon source.

Within the first hours of the experiment, the increase of the ^{13}C label percentage into biomass was assumed to be linear, and the ^{13}C incorporation rate of the predicted curve for the $^{13}\text{CO}_2$ experiment was calculated to be 1.5 times higher than the predicted curve for the $^{13}\text{CH}_4$ experiment (Fig. 4B), in accordance with the 1.5-times-higher label percentage (62 % versus 42 %).

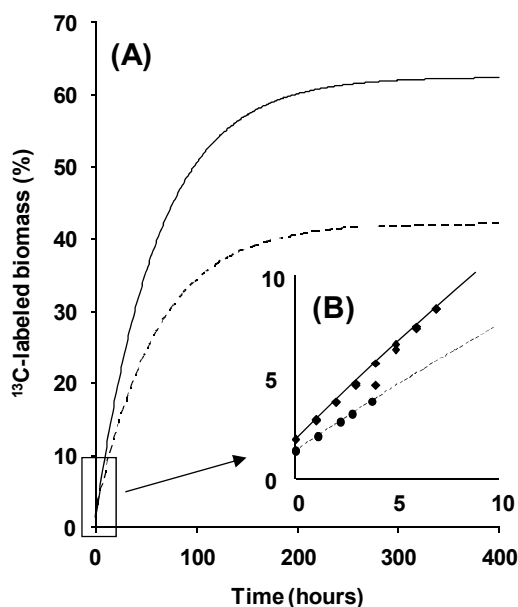


Figure 4. (A) Predicted percentage of ^{13}C -labeled biomass, for a *M. fumariolicum* strain SolV chemostat culture supplied with $^{13}\text{CH}_4$ (dashed line) and $^{13}\text{CO}_2$ (solid line). (B) Measured percentages of ^{13}C -labeled biomass in the first 10 hours for a SolV culture supplied with $^{13}\text{CH}_4$ (circles) and $^{13}\text{CO}_2$ (squares), combined with the predicted percentages.

¹³C-labeling experiments in batch cultures

The labeling study with ¹³CH₄ in the chemostat culture always resulted in high ¹³CO₂ production from ¹³CH₄ oxidation. This could have been circumvented by sparging much larger gas volumes through the reactor. This option was not used, since this is technically not feasible in our chemostat setup; instead, labeling experiments in two batch cultures with a high concentration (40 %) of unlabeled ¹²CO₂ and a relatively limited amount (3.2 %) of ¹³CH₄ were performed. If all ¹³CH₄ was converted to ¹³CO₂, the CO₂ pool would be labeled for an additional 7.4 % only (3.2 % / 40 % × 100). Concentrations of gasses and ¹³C/¹²C mass ratios of CO₂ at the start of and after growth, when 80 to 95 % of the added CH₄ was converted, were carefully measured. It could be calculated that in both bottles, at least 96 % of the label of ¹³CH₄ was recovered as ¹³CO₂. This pointed to complete oxidation of CH₄ and the sole use of CO₂ as the carbon source.

If we assume that carbon assimilation by fixation of CO₂ and that 0.34 mol CO₂ incorporated into biomass per mole CH₄ converted, then close to 2 % of the total ¹³C produced would have been incorporated. This makes the total ¹³C recovery at least 98 %. At the end of the experiment, the ¹³C/¹²C ratio of the biomass in both bottles was determined by IRMS. The analysis showed that 4.6 % of the biomass carbon was ¹³C labeled. This percentage was in very good agreement with the average measured ¹³C percentage of the CO₂ during growth (1.2 % at the start of and 7.7 % at the end of growth, so an average 4.5 %) and again confirms that CO₂ is the main carbon source.

RuBisCO in strain SolV

The labeling experiments described above showed that *M. fumariolicum* strain SolV fixes CO₂, and the draft genome data of strain SolV contained a RuBisCO gene, encoding the key enzyme of the CBB cycle (see below). Therefore, cell extracts of strain SolV were tested for the presence of RuBisCO activity and analyzed by SDS-PAGE (13 % gel) and native-PAGE (5 % gel).

For the activity assay, we developed a method based on the $^{13}\text{CO}_2$ incorporation into 3-PGA and its subsequent destruction in closed vials with acid permanganate solution. $^{13}\text{CO}_2$ concentrations in the vial were quantified on basis of $^{13}\text{C}/^{12}\text{C}$ ratios as measured by GC-MS.

Activity was proportional to the amount of turbid cell extract added (concentrations of 10 to 250 μg protein per 250 μl assay mixture were tested) and linear for 2 min (Fig. 5). No $^{13}\text{CO}_2$ was incorporated without extract or the substrate ribulose-1,5-biphosphate (0.5 mM). Activity was optimal between pHs 7.2 and 7.5. At pHs 7.7 and 7.0, activity dropped by about 10 %. When kept on ice, the activity in extracts was stable for at least a month. The specific activity of the turbid cell extract was 55 to 70 $\text{nmol CO}_2 \text{ fixed min}^{-1} (\text{mg of protein})^{-1}$. The oxygenase activity of RuBisCO measured at an oxygen concentration of around 150 μM was about 4.5 $\text{nmol O}_2 \text{ min}^{-1} (\text{mg of protein})^{-1}$, and this activity was inhibited by the addition of NaHCO_3 (50 % inhibition at 4 mM NaHCO_3 [results not shown]). Virtually all the RuBisCO activity (> 90 %) appeared to be present in the clarified cell extract ($48,000 \times g$ supernatant). The corresponding pellet contained only very small amounts of RuBisCO activity that could be attributed to a residual soluble fraction (Fig. 5).

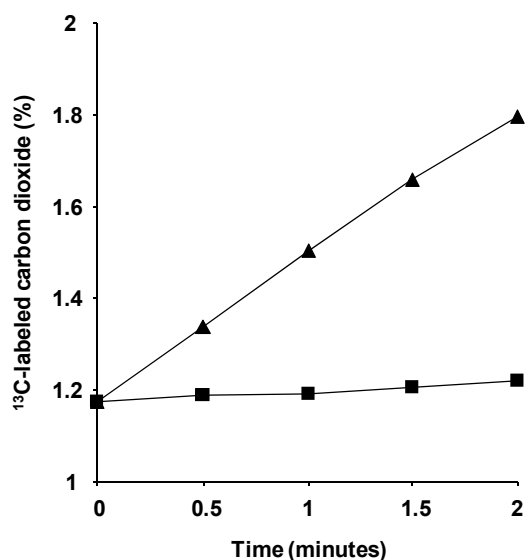


Figure 5. $^{13}\text{CO}_2$ incorporation into 3-PGA and its subsequent destruction in closed vials with acid permanganate solution. $^{13}\text{CO}_2$ concentrations quantified in the vial represents *M. fumariolicum* strain SolV RuBisCO activity in turbid cell extract ($12,000 \times g$ supernatant, [triangles]) and in the pellet after centrifugation at $48,000 \times g$ (squares).

When the proteins in the crude extract were analyzed by 13 % SDS-PAGE, a consistent pattern of proteins was observed, which did not change upon subsequent centrifuging steps (Fig. 6A). Dominant bands (indicated with arrows) were cut out of the gel and identified by tryptic digestion and MALDI-TOF MS peptide mass analysis. The results showed that the upper band corresponded with the large subunit of RuBisCO, with a predicted mass of 53,930 Da, and the lower band corresponded to the small subunit of RuBisCO, with a predicted mass of 16,550 Da (Fig. 6A). The pellets obtained after the different centrifugation steps did not contain these bands (data not shown). In addition to the MALDI-TOF MS identification, immunoblotting with an antibody against the RuBisCO large subunit was done, and only the 53,930-Da band specifically reacted with this antibody (Fig. 6B, lanes 1 to 4). After being washed extensively with PIPES-NaOH buffer, pellets of $12,000 \times g$ and $48,000 \times g$ centrifugation steps (yielding intact cells and membranes) showed only a weak reaction with this antibody. In contrast, after washing of the $150,000 \times g$ pellet, a clear immune response band remained visible (data not shown), suggesting that RuBisCO is present as a high-molecular-mass complex that partly sediments at this high centrifugation speed. This was verified by analyzing all supernatants on a 5 % native-PAGE gel (Fig. 7A). The prominent band at about 536 kDa (Fig. 7A) showed an immunoreaction with the RuBisCO antibody (Fig. 7B). The corresponding protein band from an unstained native gel part was cut out of the gel. Proteins from the gel pieces were denatured, eluted, and loaded on a 13 % SDS-PAGE gel. This resulted in only 2 protein bands with molecular weights corresponding to the large and small subunits of RuBisCO (Fig. 7C, lane 1). This was confirmed by the MALDI-TOF analysis and antibody reaction (data not shown). The native mass of RuBisCO was also determined by size exclusion chromatography, which showed a somewhat apparent lower molecular mass of about 482 kDa. Most likely, the native RuBisCO protein complex is composed of 8 small and 8 large subunits, with a calculated molecular mass of 563,840 Da.

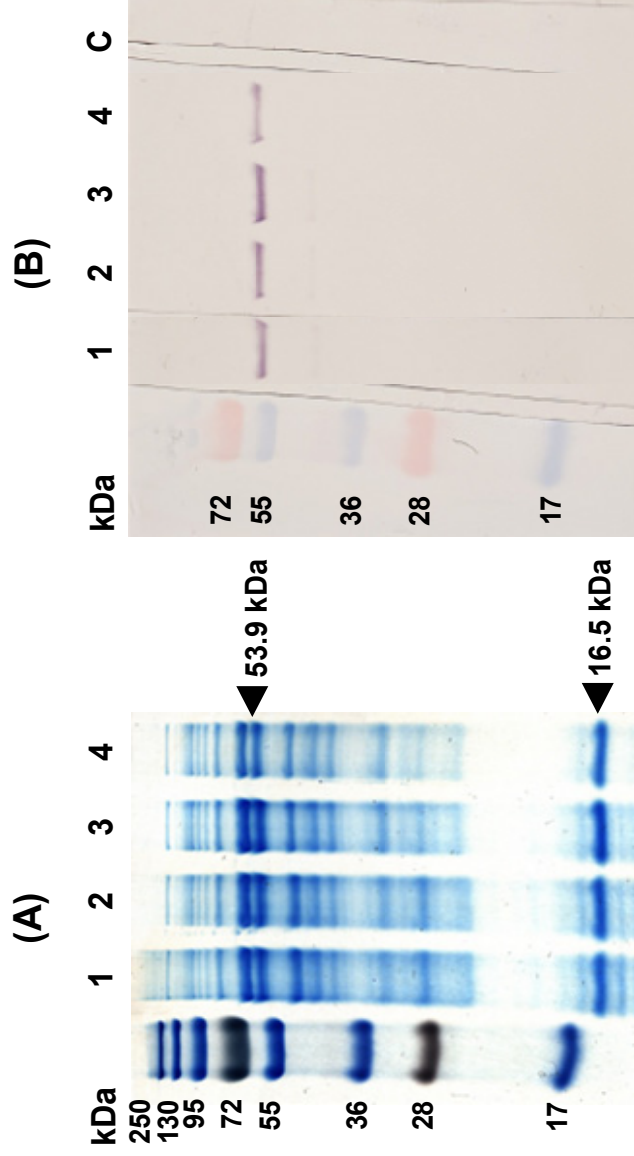


Figure 6. (A) *M. fumariolicum* strain SolV proteins in the crude extract were analyzed by 13 % SDS-PAGE after subsequent centrifuging steps. (B) The proteins were then transferred onto a nitrocellulose membrane and tested for the presence of RuBisCO, using a peptide antibody against the large subunit of this enzyme. Lane numbers in both figures are the same. Lane 1, crude extract; lane 2, $12,000 \times g$ supernatant; lane 3, $48,000 \times g$ supernatant; lane 4, $150,000 \times g$ supernatant; lane C, control (crude extract without peptide antibody). The upper and lower bands indicated with arrows correspond to the large and small subunits of RuBisCO, respectively, identified by MALDI-TOF MS analysis.

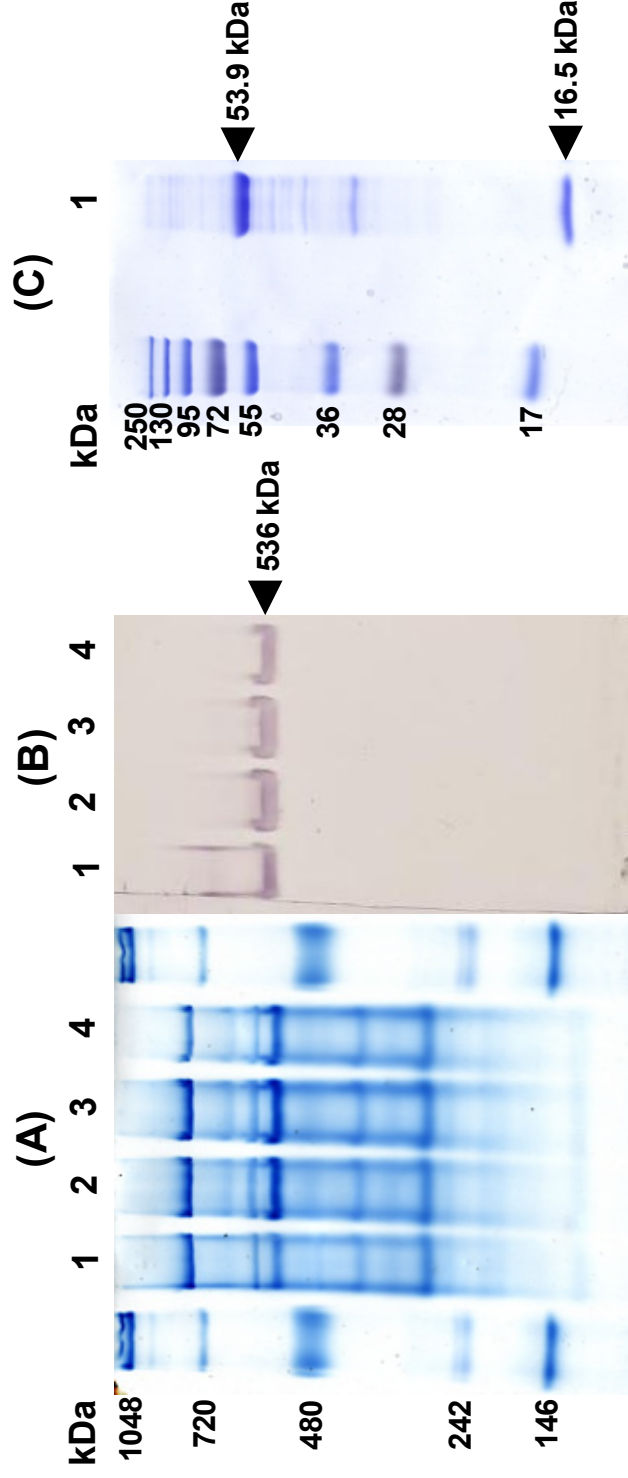


Figure 7. (A) *M. fumariolicum* strain SolV proteins in the crude extract were analyzed on 5 % native-PAGE after subsequent centrifuging steps. (B) The proteins were then transferred onto nitrocellulose membrane and tested for the presence of RuBisCO, using the peptide antibody against the large subunit of this enzyme. Lane numbers in both figures (A and B) are identical. Lane 1, crude extract; lane 2, 12,000 \times g supernatant; lane 3, 48,000 \times g supernatant; lane 4, 150,000 \times g supernatant. (C) The native band corresponding to the RuBisCO complex (indicated with an arrow in panel B) was analyzed on a 13 % SDS-PAGE gel (lane 1).

Transcriptomics

Analyses of the draft genome of *M. fumariolicum* strain SolV revealed that the key genes needed for an operational ribulose monophosphate pathway, the hexulose-6-phosphate synthase and hexulose-6-phosphate isomerase genes, were absent (Pol *et al.*, 2007). In addition, the crucial genes encoding key enzymes of the serine pathway, the malyl-coenzyme A lyase and glycerate kinase genes were not found. However, the genes needed for a full operational CBB cycle were present. All these genes were also transcribed (Table 2), as was verified by transcriptome analysis of exponentially growing cells, especially the genes encoding the large and small subunits of RuBisCO, which were highly transcribed. These results, together with the physiological and biochemical experiments described above, fully support the conclusion that strain SolV makes use of the CBB cycle to fix CO₂ for carbon assimilation.

Phylogenetic analysis of RuBisCO

RuBisCO enzymes can be grouped according to the structures, catalytic properties and gene arrangement into type I (A, B, C and D), II, III and IV (RuBisCO-like) (Badger & Bek, 2008). A neighbor-joining tree (Fig. 8) was constructed using representative *cbbL* sequences of each group. Also, for this analysis, the sequences of three (uncharacterized) mesophilic verrucomicrobial methanotrophs available from GenBank (accession numbers JF706245, JF706246 and JF706247) were added. The verrucomicrobial RuBisCO enzymes formed a distinct group in the phylogenetic tree. The RuBisCO operons in *M. fumariolicum* strain SolV and *M. infernorum* strain V4 are arranged in the gene order *cbbL cbbS cbbX* (Fig. 9), which is typical for the type IC (Badger & Bek, 2008). In both strains, no genes involved in carboxysome formation were detected. The remaining genes of the CBB cycle (Table 2) are spread through the genome of strain V4, sometimes with two or three CBB cycle genes clustered. BLASTP searches with the *M. fumariolicum* SolV RuBisCO large subunit in environmental data sets did not result in sequences fitting into the distinct verrucomicrobial group.

Table 2. Genes involved in the Calvin-Benson-Bassham cycle in *M. fumariolicum* strain SolV^a

Enzyme	Gene name	EC no. ^b	GenBank accession no.	Relative expression mRNA
Ribulose 1,5-bisphosphate carboxylase, large subunit	<i>cbbL</i>	EC 4.1.1.39	JF706253	21.6
Ribulose 1,5-bisphosphate carboxylase, small subunit	<i>cbbS</i>	EC 4.1.1.39	JF706253	14.4
RuBisCO accessory protein CbbX, AAA ATPase	<i>cbbX</i>		JF706253	14.3
Ribulose-phosphate 3-epimerase	<i>rpe</i>	EC 5.1.3.1	JF706259	1.1
Phosphoribulokinase	<i>prkB</i>	EC 2.7.1.19	JF706255 JF706253	1.8 3.8
Ribose 5-phosphate isomerase B	<i>rpiB</i>	EC 5.3.1.6	JF706256	1.5
Triosephosphate isomerase	<i>tpiA</i>	EC 5.3.1.1	JF714482	1.2
Putative phosphoketolase			JF706257	0.7
Transketolase	<i>tktA</i>	EC 2.2.1.1	JF706253	4.3
Fructose-1,6-bisphosphatase II / sedoheptulose 1,7-bisphosphatase	<i>glpX</i> -SEBP gene	EC 3.1.3.11 EC 3.1.3.37	JF706249	1.3
Fructose-1,6-bisphosphatase	<i>fbp</i>	EC 3.1.3.11	JF706254	2.5
Fructose-bisphosphate aldolase, class I	<i>fbaA</i>	EC 4.1.2.13	JF706258	0.5
Fructose-bisphosphate aldolase, class II	<i>fba2</i>	EC 4.1.2.13	JF706254	4.4
Glyceraldehyde-3-phosphate dehydrogenase	<i>gapA</i>	EC 1.2.1.59	JF714482	5.1
Phosphoglycerate kinase	<i>pgk</i>	EC 2.7.2.3	JF714482	1.8

Table 2 proceeds on next page.

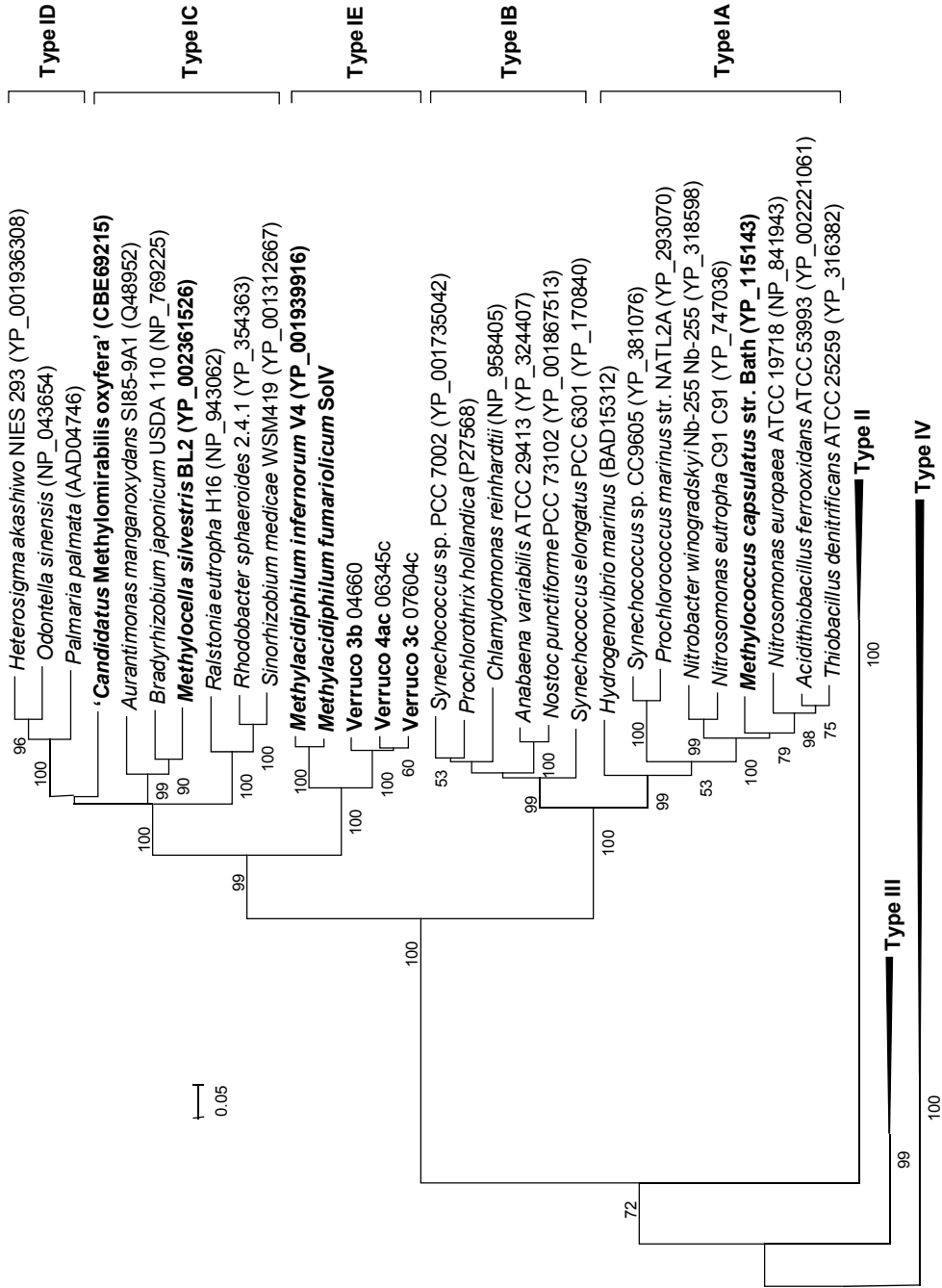
Table 2. Genes involved in the Calvin-Benson-Bassham cycle in *M. fumariolicum* strain SolV^a (continuation)

Enzyme	Gene name	EC no ^b	GenBank accession no.	Relative expression mRNA
6-Phosphogluconolactonase	<i>nagB</i>	EC 3.1.1.31	JF706252	0.3
6-Phosphogluconate dehydrogenase	<i>gnd</i>	EC 1.1.1.44	JF706256	1.2
Glucose-6-phosphate 1-dehydrogenase	<i>zwf</i>	EC 1.1.1.49	JF706252	1.0
Glucose-6-phosphate isomerase	<i>pgi</i>	EC 5.3.1.9	JF706248	0.4
Fructose-6-phosphate aldolase 1	<i>mipB</i>	EC 4.1.2.-	JF706251	0.8

^a The relative levels of transcription of the genes were obtained by a transcriptome analysis of an exponentially growing liquid culture (see Materials & methods).

^b Enzyme commission number.

Figure 8 (next page). Phylogenetic analysis of the RuBisCO large subunit (*CbbL*). Representative amino acid sequences were obtained from GenBank. Bootstrap values (1,000 replicates) are shown at the branches. The bar represents 20 % sequence divergence. The neighbor-joining tree is drawn to scale; the evolutionary distances were computed using the Dayhoff matrix-based method, and units are the numbers of amino acid substitutions per site. All positions containing alignment gaps and missing data were eliminated only in pairwise sequence comparisons (pairwise deletion option). There were a total of 539 positions in the final dataset.



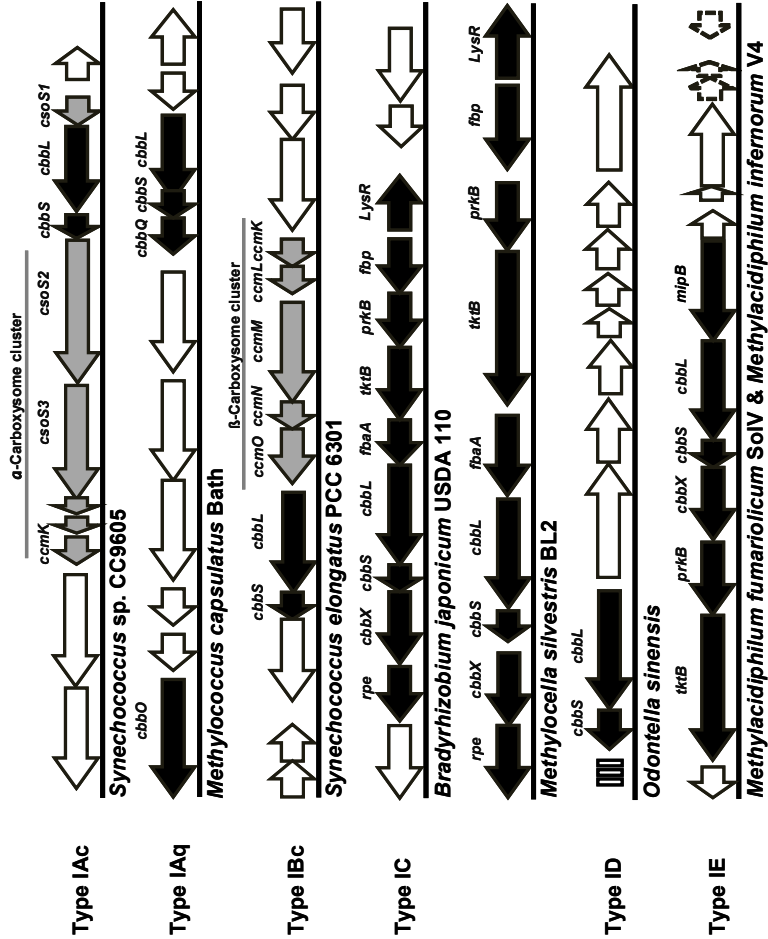


Figure 9. Arrangement of genes encoding for the Calvin-Benson-Bassham (CBB) cycle (black arrows) in *Methylobacterium furiosus* strain V4 and *Methylobacterium infernorum* strain V4, compared to all types of form I RuBisCO (A, B, C and D). Genes involved in carboxysome formation are indicated with grey arrows. Other genes are indicated with white arrows.

Discussion

Carbon fixation by methanotrophs has been a topic of research for decades, and the assimilation via the CBB cycle by proteobacterial methanotrophs is unlikely, because CBB is associated with high ATP requirements (Chistoserdova *et al.*, 2009). Although *M. capsulatus* Bath possesses CBB cycle genes (Ward *et al.*, 2004), physiological evidence for an active CBB cycle is lacking thus far. However, available genome data from verrucomicrobial methanotrophs (Hou *et al.*, 2008; Pol *et al.*, 2007) point to an autotrophic lifestyle of these microbes.

In the present study, the transcriptome analysis of *M. fumariolicum* strain SolV showed that all of the genes for the enzymes necessary for a CBB cycle are expressed, most prominently the genes encoding for RuBisCO. The *cbbR* gene (encoding the RuBisCO operon transcriptional regulator) is present, but its expression is low (only 0.1). On the V4 genome, this gene seems to be coupled to nitrate transport and reduction (Hou *et al.*, 2008). Whether this gene is involved in regulation of the RuBisCO operon needs to be resolved.

On SDS-PAGE gels, RuBisCO was identified as one of the most dominant proteins in the cell extracts of strain SolV. Using a novel $^{13}\text{CO}_2$ incorporation assay, we showed the high specific activity of RuBisCO [$70 \text{ nmol CO}_2 \text{ fixed min}^{-1} (\text{mg of protein})^{-1}$]. This activity is similar to that reported for other autotrophic bacteria (Cannon & Shively, 1983) and corresponds well with the maximum specific growth rate of 0.07 h^{-1} (doubling time, 10 h), assuming dry cells contain 50 % carbon and 70 % protein.

As RuBisCO was found only in the clarified cell extract, we conclude that RuBisCO is not densely packed into polyhedral inclusion bodies (carboxysomes), which generally sediment upon centrifugation at $10,000 \times g$ and $40,000 \times g$ (Gonzales *et al.*, 2005; Price *et al.*, 1992). In addition, the genome data did not show any proteins that could encode carboxysomal shell proteins. Carboxysomes are encountered in cyanobacteria and in a limited number of chemoautotrophs like sulfur- or sulfide-oxidizing and nitrifying bacteria (Yeates *et al.*, 2008). These compartments are thought to enhance the concentration of CO_2 for RuBisCO, which has a low affinity for CO_2 . Microorganisms, which contain carboxysomes, are able to grow at ambient CO_2 concentration; however, our batch incubations have demonstrated that strain SolV needs a high CO_2 concentration for growth

(above 0.3 %), in agreement with a free form of RuBisCO. Furthermore, the volcanic regions from which the verrucomicrobial methanotrophs were isolated exhibit high CO₂ concentrations (Castaldi & Tedesco, 2005). In these environments, there is apparently no need to sequester CO₂.

Based on the apparent molecular masses of the native RuBisCO protein and the two subunits, we predict that it forms an octomeric complex (L₈S₈). This form of RuBisCO is typical for all form I RuBisCOs, which are composed of four large-subunit dimers (L2) with small subunits (S) decorating the top and bottom of the L8 octomeric core (Tabita *et al.*, 2008).

Phylogenetic analysis and the gene arrangement of the RuBisCOs from two thermophilic *Methylocidiphilum* strains positions them in a separate cluster within form I RuBisCOs, for which we propose the name type IE. Based on gene arrangement, the verrucomicrobial RuBisCO is most closely related to RuBisCO type IC (Badger & Bek, 2008). The *cbbX cbbS cbbL* operon arrangement is typical for type IC and type IE and not typical for other form I enzymes. The IC form has medium to low affinity for CO₂, indicating an adaptation to environments with medium to high CO₂ but with O₂ present, and microorganisms having type IC RuBisCO do not possess carboxysomes (Badger & Bek, 2008). This verrucomicrobial RuBisCO type has not been detected before by molecular approaches. This can be explained by the mismatches we observed when comparing the *Methylocidiphilum*-type *cbbL* sequence with all the available RuBisCO primers sets (Alfreider *et al.*, 2009; Elsaied *et al.*, 2007; Selesi *et al.*, 2007; Tourova *et al.*, 2010).

The ¹³C label percentage in the biomass of both the batch and the chemostat experiments was in complete accordance with the ¹³C label percentage of CO₂ in the cultures and confirms that biomass carbon was derived exclusively from CO₂. If CO₂ is the only carbon source in *M. fumariolicum* strain SolV, it can be anticipated that CH₄ is completely oxidized into CO₂. This was demonstrated by the recovery study of ¹³CH₄ (see Results). If intermediates of CH₄ oxidation (which are fully ¹³C labeled) were incorporated, the recovery of label into CO₂ would have been much lower: about 66 % for the ribulose monophosphate pathway and 79 % or 76 % for the serine pathway (see results [Table 1]).

The autotrophic nature of verrucomicrobial methanotrophs has large consequences for their detection in the environment. The presence of active methanotrophs has been assessed by isotope-based techniques, like stable isotope probing and phospholipid fatty-acid labeling, which rely on the incorporation of labeled CH_4 into DNA/RNA or lipids, respectively. Such methods will overlook the involvement of these autotrophic methanotrophs, especially in environments with high CO_2 concentrations.

Conclusion

M. fumariolicum strain SolV is an autotrophic methanotroph. It fixes CO₂ via the CBB cycle, with CH₄ as the energy source.

It uses a non-carboxysome-associated RuBisCO, in agreement with a high requirement for CO₂. RuBisCO in verrucomicrobial methanotrophs form a new group most closely related to type IC.

To proof that *M. fumariolicum*, is an autotrophic microorganism, using the CBB cycle, knockout and complementation studies are required, but this has to await the development of a genetic system.

Acknowledgments

This work was supported by Mosaic grant 62000583 from the Netherlands Organisation for Scientific Research (NWO).

We are grateful to Jelle Eygensteyn for help with the IRMS analyses, and would like to thank Mingliang Wu for help with the Western blotting and immunoblotting techniques, Naomi de Almeida for help with the SDS-PAGE and native-PAGE techniques, and Dick van Aalst for photography.

Chapter Five

Carbon storage in “*Ca. Methylacidiphilum fumariolicum*” strain SolV

Key words:

“*Methylacidiphilum*”,
methane, *Verrucomicrobia*,
carbon storage, glycogen &
survival.

This chapter was submitted for publication in:

Frontiers in Microbiology



Gas chromatograph, coupled to a thermal conductivity detector and mass spectrometer (GC-MS).

Picture by Ahmad F. Khadem.

Genomic and physiological analysis of carbon storage in the verrucomicrobial methanotroph “*Ca. Methylacidiphilum fumariolicum*” SolV

Ahmad F. Khadem^{1a}, Muriel C. F. van Teeseling^{1a}, Laura van Niftrik¹,
Mike S. M. Jetten¹, Huub J. M. Op den Camp¹ & Arjan Pol¹

¹Department of Microbiology, IWW, Radboud University Nijmegen, Heyendaalseweg 135, NL-6525 AJ, Nijmegen, the Netherlands.

^a Both authors contributed equally.

Abstract

“*Candidatus Methylacidiphilum fumariolicum*” SolV is a verrucomicrobial methanotroph that can grow in extremely acidic environments at high temperature. Strain SolV fixes carbon dioxide (CO₂) via the Calvin-Benson-Bassham cycle with methane as energy source, a trait so far very unusual in methanotrophs. In this study, the ability of “*Ca. M. fumariolicum*” to store carbon was explored by genome analysis, physiological studies and electron microscopy. When cell cultures were depleted for nitrogen, glycogen storage was clearly observed in cytoplasmic storage vesicles by electron microscopy. After cessation of growth, the dry weight kept increasing and the bacteria were filled up almost entirely by glycogen. This was confirmed by biochemical analysis, which showed that glycogen accumulated to 36 % of the total dry weight of the cells. When methane was removed from the culture, this glycogen was consumed within 47 days. During the period of glycogen consumption, the bacteria kept their viability high when compared to bacteria without glycogen (from cultures growing exponentially). The latter bacteria lost viability already after a few days when starved for methane. Analysis of the draft genome of “*Ca. M. fumariolicum*” SolV demonstrated that all known genes for glycogen storage and degradation were present and also transcribed. Phylogenetic analysis of these genes showed that they form a separate cluster with “*Ca. M. infernorum*” V4, and the most closely related other sequences only have an identity of 40 %. This study presents the first physiological evidence of glycogen storage in the phylum *Verrucomicrobia* and indicates that carbon storage is important for survival at times of methane starvation.

Introduction

The use of methane (CH₄) as carbon and energy source distinguishes the aerobic methanotrophs as a unique group within the methylotrophs. Aerobic methanotrophs are found within the *Proteobacteria*, *Verrucomicrobia* and the NC10 phylum (Ettwig *et al.*, 2010; Hanson & Hanson, 1996; Op den Camp *et al.*, 2009; Semrau *et al.*, 2010).

The verrucomicrobial methanotrophs, for which the genus name “*Methylacidiphilum*” was proposed (Op den Camp *et al.*, 2009), were recently discovered. They were isolated in pure cultures from volcanic regions (Dunfield *et al.*, 2007; Islam *et al.*, 2008; Pol *et al.*, 2007), which may be important natural sources of methane (Castaldi & Tedesco, 2005; Kvenvolden & Rogers, 2005). The verrucomicrobial methanotrophic bacteria are able to grow in these highly acidic and hot conditions and might have an essential role in reducing global methane emissions into the atmosphere.

“*Ca. Methylacidiphilum fumariolicum*” strain SolV is one of the thermoacidophilic verrucomicrobial methanotrophs and its physiology has been studied in some detail. This microorganism can use ammonium, nitrate or atmospheric nitrogen as nitrogen source (Khadem *et al.*, 2010; Pol *et al.*, 2007), and fixes carbon dioxide (CO₂) into biomass via the Calvin-Benson-Bassham cycle, using methane as its energy source (Khadem *et al.*, 2011). The latter is in contrast to proteobacterial methanotrophs that use formaldehyde in the ribulose monophosphate pathway (type I) or the serine pathway (type II) for carbon assimilation (Chistoserdova *et al.*, 2009; Semrau *et al.*, 2010).

This study focuses on the growth response of “*Ca. M. fumariolicum*” during nitrogen depletion. When nitrogen is limited and carbon compounds are in excess, methanotrophs, as many other bacteria (Wanner & Egli, 1990 and references therein), start to accumulate carbon-rich reserve polymers, such as poly-3-hydroxybutyrate (PHB) or glycogen (Eshinimaev *et al.*, 2002; Linton & Cripps, 1978; Pieja *et al.*, 2011 a and references therein). The cells of “*Ca. M. fumariolicum*” are rod-shaped and have a length of 0.8-2.0 μm and a width of 0.4-0.6 μm (Op den Camp *et al.*, 2009). Electron microscopy demonstrated the presence of intracellular inclusions in all three “*Methylacidiphilum*” strains (Islam *et al.*, 2008; Op den Camp *et al.*, 2009; Pol *et al.*, 2007), which might represent

storage material. Genes encoding for PHB synthesis are absent from the genomes of the “*Methylacidiphilum*” strains, as is also the case for type I proteobacterial methanotrophs (Hou *et al.*, 2008; Khadem *et al.*, 2012 b; Pieja *et al.*, 2011 a). However, based on the draft genome of “*Ca. M. fumariolicum*”, genes encoding for glycogen metabolism are predicted (Khadem *et al.*, 2012 b).

This study combines growth experiments, transcriptome analysis, electron microscopy and biochemical analysis to elucidate the ability of glycogen storage in “*Ca. M. fumariolicum*” SolV.

Materials & methods

Organism & medium composition for growth

“*Ca. Methylacidiphilum fumariolicum*” strain SolV used in this study was originally isolated from the Solfatara volcano, near Naples, Italy (Pol *et al.*, 2007).

“*Ca. M. fumariolicum*” was grown in the standard medium (pH 2) as described before (Khadem *et al.*, 2010), with 10 % (v/v) liquid mud pool extract and 2 mM of ammonium.

Materials

^{13}C -labeled CO_2 was prepared by injecting a 0.6 M $\text{NaH}^{13}\text{CO}_3$ (99 % ^{13}C) solution into a solution of 1.2 M HCl in a closed 60 ml serum bottle. The headspace was then used as source of ^{13}C -labeled CO_2 . ^{13}C -labeled CH_4 (99 % atom % ^{13}C) was obtained from Sigma-Aldrich.

Fed-batch cultivation

Cultivation of “*Ca. M. fumariolicum*” SolV was performed in a 10 L fermentor (Applikon, Schiedam, the Netherlands). The medium (5 liter) contained 1.2 mM ammonium. A gas mixture of (all in v/v); 9.5 % methane (CH_4), 23.9 % carbon dioxide (CO_2) and 66.6 % air, was supplied to the fermentor in a continuous flow. The oxygen sensor showed a dissolved oxygen level of 8.8 % at the onset of cultivation. The pH of the medium was set with sulfuric acid at pH 2 and remained close to pH 2 during growth. The temperature and agitation speed were set to 55 °C and 1,000 r.p.m., respectively.

To determine the dry weight, samples of 10 ml from the culture suspension were filtered through pre-weighed 0.45 μm filters and dried to constant weight in a vacuum oven at 70 °C.

Batch cultivation

Batch incubations were performed in serum bottles containing 5 % (v/v) medium. The bottles were sealed with red butyl rubber stoppers (Rubber B.V.,

Hilversum, the Netherlands). The headspace contained air as the source of oxygen, and CH₄ and CO₂ concentrations of 10 % and 5 % (v/v), respectively. The incubations were performed in duplicate at 55 °C with shaking at 180 r.p.m.

In the experiments where methane was removed from the bottles, the cell suspension was sparged with air for about 5 min and 5 % (v/v) CO₂ was added after sealing.

Cell extracts

Cells were collected by centrifugation (4,000 × g, 4 °C, 10 min). The cell pellet was washed twice in phosphate-buffer (20 mM, pH 7.1) and resuspended in the same buffer. The suspension, which had a final pH of 6, was passed 4 times through a French press at 20,000 psi and cell lysis (at least 90 %) was confirmed by counting DAPI stained cells with light microscopy. Unbroken cells and cell debris were removed from the resulting crude extract by centrifugation at 12,000 × g for 30 min (4 °C, Sorvall SS-34 rotor).

Gas analysis

Methane (CH₄) was analyzed on a HP 5890 gas chromatograph (Agilent, USA) equipped with a Porapak Q column (1.8 m × 2 mm) and a flame ionization detector. ¹²C and ¹³C-labeled carbon dioxide (CO₂) were analyzed on an Agilent series 6890 gas chromatograph (Agilent, USA) equipped with a Porapak Q and a Molecular sieve column, coupled to a thermal conductivity detector and mass spectrometer (GC-MS) (Agilent 5975C inert MSD; Agilent, USA) as described before (Ettwig *et al.*, 2008). For all gas analyses, 100 µl sample of gas was injected into the gas chromatograph.

Elemental analysis

The cells were harvested by centrifugation, after which the pellet was washed with demineralized water and dried overnight in a vacuum oven at 70 °C. The dried material (about 0.4 mg) was analyzed on a Thermo Fisher Scientific EA 1110 CHN element analyzer coupled to a Finnigan DeltaPlus mass spectrometer.

Ammonium & protein analyses

Ammonium concentrations were measured using the ortho-phthaldialdehyde (OPA) method (Taylor *et al.*, 1974). Protein concentrations were measured using the bicinchoninic acid (BCA) assay as described before (Ettwig *et al.*, 2008).

Light microscopy

Cell numbers were determined by counting cells in 30 fields (volume per field $2.5 \times 10^{-8} \text{ cm}^3$) of a hemocytometer slide, using an Axioplan 2 imaging phase contrast microscope (Carl Zeiss B.V.).

Glycogen assay

The concentration of glycogen in the crude extracts was determined by a two-step enzymatic assay. To enhance the enzyme accessibility of the glycogen granules, crude extracts were first shaken for 10 minutes at 30 s^{-1} with glass beads (80–110 μm in diameter) in a Retsch MM 301 ball mill. The bead-beaten crude extracts (in triplicate) were then incubated with amyloglucosidase (35 units per ml crude extract in the case of transition phase I and II cells, and 17.5 units per ml crude extract for the exponential phase cells) from *Aspergillus niger* (Sigma Aldrich) in 0.05 M acetate buffer (pH 4.8) for 4 h at 45°C to convert glycogen into glucose. In the second step the resulting glucose was quantified by the glucose oxidase kit (Sigma Aldrich). To correct for the amount of glucose already present in the crude extracts, controls of bead-beaten crude extracts that did not undergo amyloglucosidase incubation were also analyzed.

Chemical fixation & Epon embedding

“*Ca. M. fumariolicum*” cells were fixed in Karnovsky fixative (2 % paraformaldehyde, 2.5 % glutaraldehyde, 0.025 mM CaCl_2 and 0.05 mM MgCl_2 in 0.08 M sodiumcacodylate buffer pH 7.4) at 4°C for a maximum of 17 days. The cells were then resuspended in 0.1 M sodiumcacodylate buffer (pH 7.4) for 15 min, followed by a post-fixation for 2 h in 1 % OsO_4 and 1.5 % K_4FeCN_6 in 0.08 M sodiumcacodylate buffer (pH 7.4) on ice in the dark. After washing with MilliQ

water, the cells were dehydrated in a graded ethanol series (70-100 %). Samples were gradually infiltrated with Epon resin. Polymerization of Epon took place at 60 °C for 72 hours. Ultrathin sections (60-70 nm) of the Epon-embedded cells were cut with the use of a glass knife in a Leica Ultracut UCT microtome.

Before investigation, the sections were post-stained by incubating the grids on drops of 4 % uranyl acetate in MilliQ water (30 min in the dark) and 2 min in Reynolds lead citrate stain (Reynolds, 1963), with MilliQ washing in between and afterwards. The sections were then investigated in a TEM 1010, JEOL transmission electron microscope. 50 cells were used for each analysis.

Polysaccharide (glycogen) stain

Ultrathin sections of chemically fixed “*Ca. M. fumariolicum*” cells (as described above) were treated with the polysaccharide stain as described previously (van Niftrik *et al.*, 2008). In this method, electron dense silver albumin aggregates indicate the presence of polysaccharide molecules.

Glycogen metabolism genes

Genes encoding proteins involved in glycogen metabolism were identified in the available draft genome of strain SolV by Blast searches, (Khadem *et al.*, 2012 b) which also showed amino acid identities to homologous proteins. Representative reference *glgA* sequences, encoding the glycogen synthase, were obtained from GenBank and aligned using the MUSCLE aligner in MEGA 5.0 (Tamura *et al.*, 2011). Phylogenetic trees were calculated using the neighbor-joining method with 1,000 bootstraps to infer the evolutionary relationship. Positions containing alignment gaps and missing data were eliminated only in pairwise sequence comparisons (pairwise deletion option). The Dayhoff matrix-based method was used to compute the evolutionary distances.

For transcriptome analysis RNA was extracted from exponentially growing cells as described before (Khadem *et al.*, 2011). After synthesis of cDNA, single-end Illumina sequencing was performed and transcription analysis was performed using the RNA-Seq Analysis tool from the CLC Genomic Workbench software (version 5.0, CLC-Bio, Aarhus, Denmark) and values are expressed as RPKM (Reads Per Kilobase of exon model per Million mapped reads; Mortazavi *et al.*, 2008).

Results

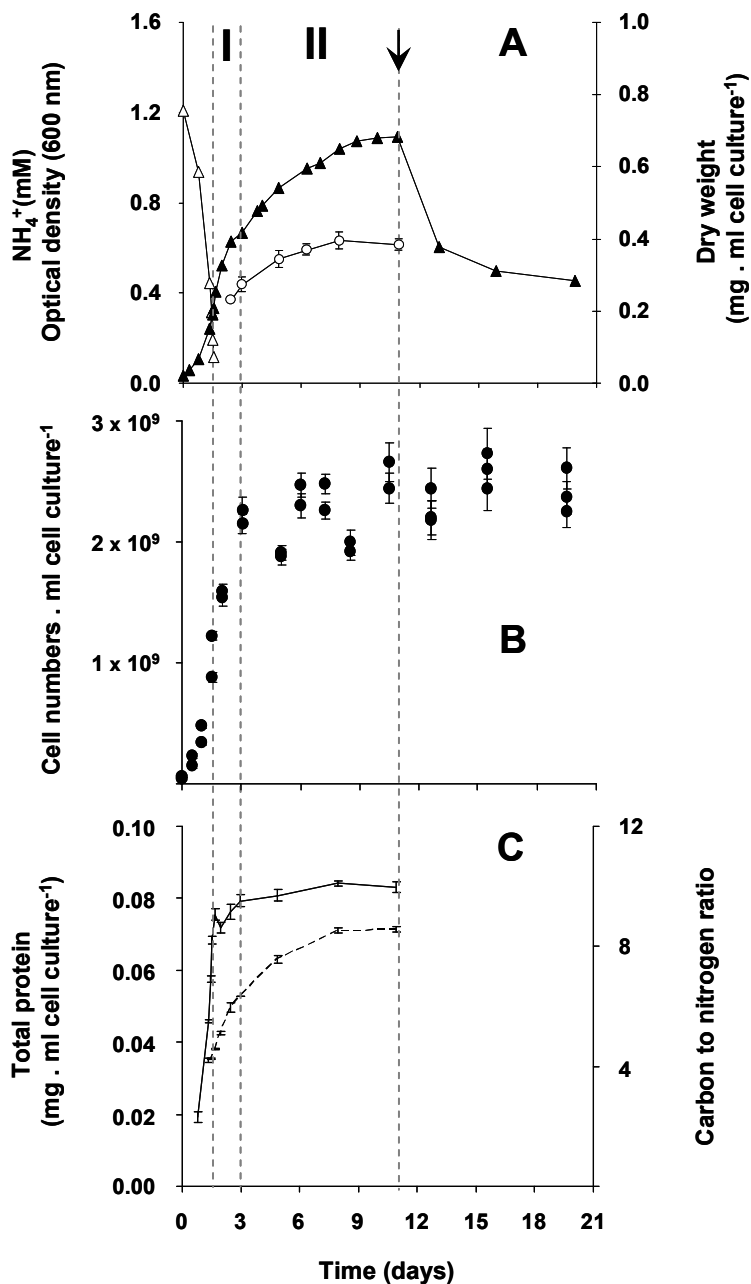
Growth response of “*Ca. M. fumariolicum*” upon nitrogen depletion

In order to study the growth response of “*Ca. M. fumariolicum*” SolV upon nitrogen depletion, the bacteria were cultivated in a fermentor with methane in excess and ammonium as nitrogen source. The dissolved oxygen concentration in the culture was always maintained above 2 % O₂ which prohibits nitrogen fixation to occur (Khadem *et al.*, 2010). After ammonium was depleted, an unexpectedly large increase in optical density was observed that occurred in two phases (Fig. 1A). During the first phase (transition phase I) that lasted 1.5 days, both the cell numbers and optical density doubled. At the end of this phase a shoulder in the optical density curve was observed. This seemed to be caused by the fact that growth of the culture stopped, because cell numbers remained more or less constant (Figs. 1A and 1B). However, the optical density still increased for 7 more days (transition phase II).

To exclude any possibility of nitrogen fixation following ammonium depletion, the nitrogen in the headspace of the batch incubations was replaced by argon. Before starting the batch incubation, the cultures undergoing exponential growth were washed and put in an ammonium-free medium (methane was present). In these bottles, the same growth pattern was observed as in bottles with nitrogen in the headspace.

Figure 1 (next page). Growth response of “*Ca. M. fumariolicum*” SolV upon ammonium depletion. (A) Growth was monitored by measuring increase in optical density (closed triangles) and dry weight (open circles). Error bars represent S.E.M. ($n = 4$). Concentration of ammonium is represented by open triangles. After 1.5 days of exponential growth ($\mu_{\max} = 0.07 \text{ h}^{-1}$) ammonium was depleted and two phases were observed, indicated by dashed lines and the symbols I and II. At day 11 (arrow), cell cultures were diluted into ammonium containing medium, but without methane added. To compare with the original optical density and cell numbers, values were multiplied by the dilution factor. (B) Cell numbers per ml cell culture of “*Ca. M. fumariolicum*” SolV (solid circles). Error bars represent S.E.M. ($n = 30$). (C) Total

protein (solid line), determined in the crude extracts prepared from harvested cells and carbon to nitrogen ratio of the harvested cells (dashed line). Error bars represent S.E.M. ($n = 4-5$).



In addition, growth by uptake of exogenous sources of nitrogen (produced during the exponential phase by “*Ca. M. fumariolicum*”) was excluded. This was done by incubating washed cultures from the exponential phase in medium obtained from a culture at the end of transition phase II. Since no increase in growth parameters was observed in these transition phase II cultures, it could be concluded that all nitrogen in the medium was depleted by the cultures. Again, the same growth pattern was observed as for transition phase I. Moreover, the protein content of the culture remained constant after ammonium depletion (Fig. 1C).

The changes during transition phase I were studied in more detail in separate cultures with higher cell concentrations (higher initial ammonium concentration). These yielded more accurate dry weight values and allowed preparing adequate quantities of crude cell extracts. Cultures grew exponentially till ammonium was depleted, after which the metabolic rate changed abruptly as indicated by a sharp increase in the dissolved oxygen concentration and the growth rate dropped gradually (Fig. 2A). The total nitrogen content of the culture remained constant as inferred from analysis of crude extract of harvested cells (Fig. 2B). As cell numbers (Fig. 1B), total carbon and dry weight were all almost doubled during this phase (Figs. 2B and 2C) and cells maintained their normal size, the protein content per cell must have been reduced by half. The consequence of this change of protein content of the cell wall and cytosol was investigated by analyzing the pellet and supernatant fractions of crude extracts of cells at the start (exponentially grown) and the end of transition phase I. When expressed per ml culture, a clear shift of proteins and total nitrogen was observed from the supernatant to the pellet fraction, for which the protein content almost doubled (Figs. 3A and 3B). As the cell numbers in the culture doubled, it means that when results are expressed per cell, the protein and total nitrogen content of the pelleted fraction remained constant at the expense of the supernatant fraction of which the proteins content dropped by a factor of 3 (Figs. 4A and 4B). In contrast to total nitrogen, total carbon in the pellet fraction increased more than 4 times for the total culture and more than 2 times when expressed per cell (Figs. 3C and 4C). This high content of carbon pointed to intracellular particulate storage material.

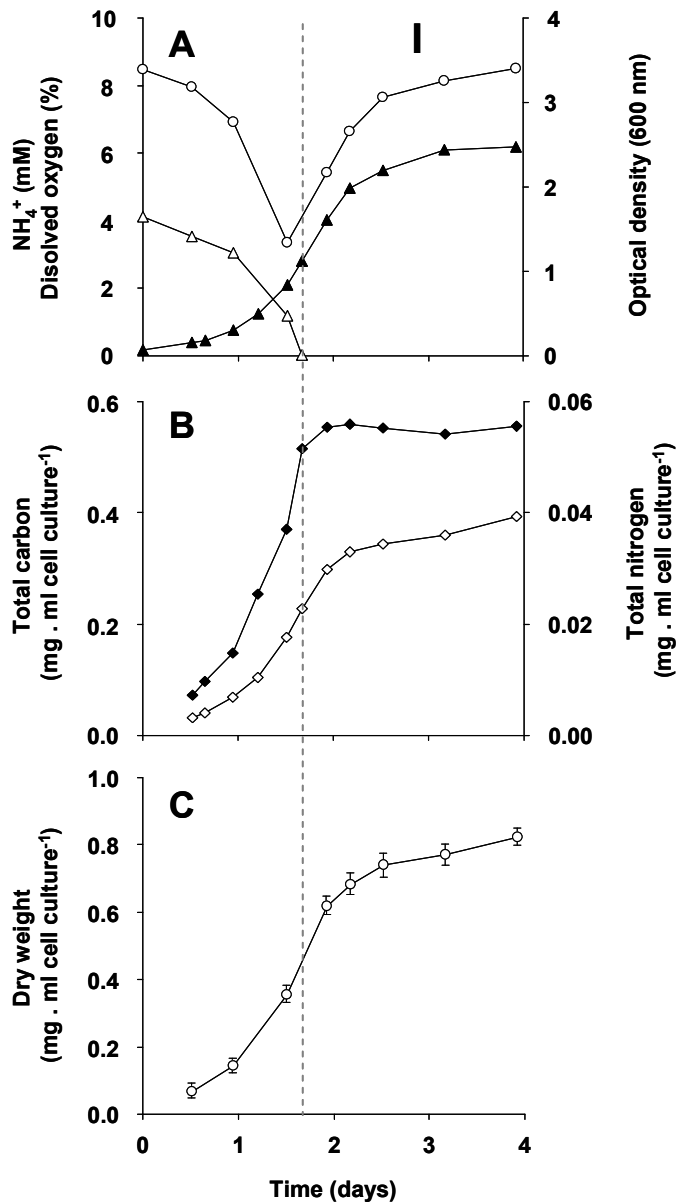


Figure 2. Growth response of “*Ca. M. fumariolicum*” SolV upon ammonium depletion during transition phase I (the start is indicated by the dashed line). (A) The optical density (closed triangles), ammonium (open triangles) and dissolved oxygen in culture medium (open circles). (B) Total nitrogen (closed squares) and total carbon (open squares). (C) Dry weight (open circles). Error bars represent S.E.M. ($n = 5$).

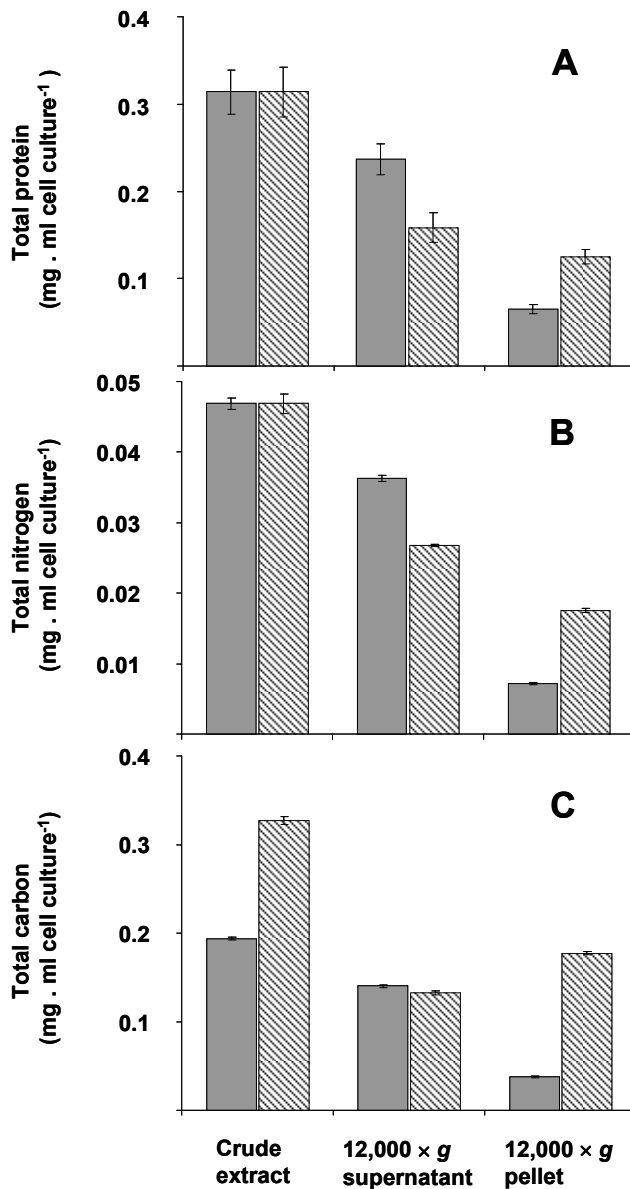


Figure 3. The distribution calculated per ml of cell culture of (A) total protein, (B) nitrogen and (C) carbon over cell wall and cytosol at the beginning (grey bars) and end (dashed bars) of transition phase I in the crude extract, 12,000 × g supernatant and 12,000 × g pellet. This experiment was performed with exponential cells that had reached an optical density of 0.5 (see Fig. 2A). The amount of total protein and total nitrogen in this exponential cells were normalized to values from cells obtained at the start of transition phase I, since total protein (see Fig. 1C) and total nitrogen (see Fig. 2B) stabilized after ammonium depletion. The total carbon of the exponential cells was normalized to values from cells obtained at the end of the exponential growth phase (at optical density of 1.12). Error bars represent S.E.M. ($n = 4$).

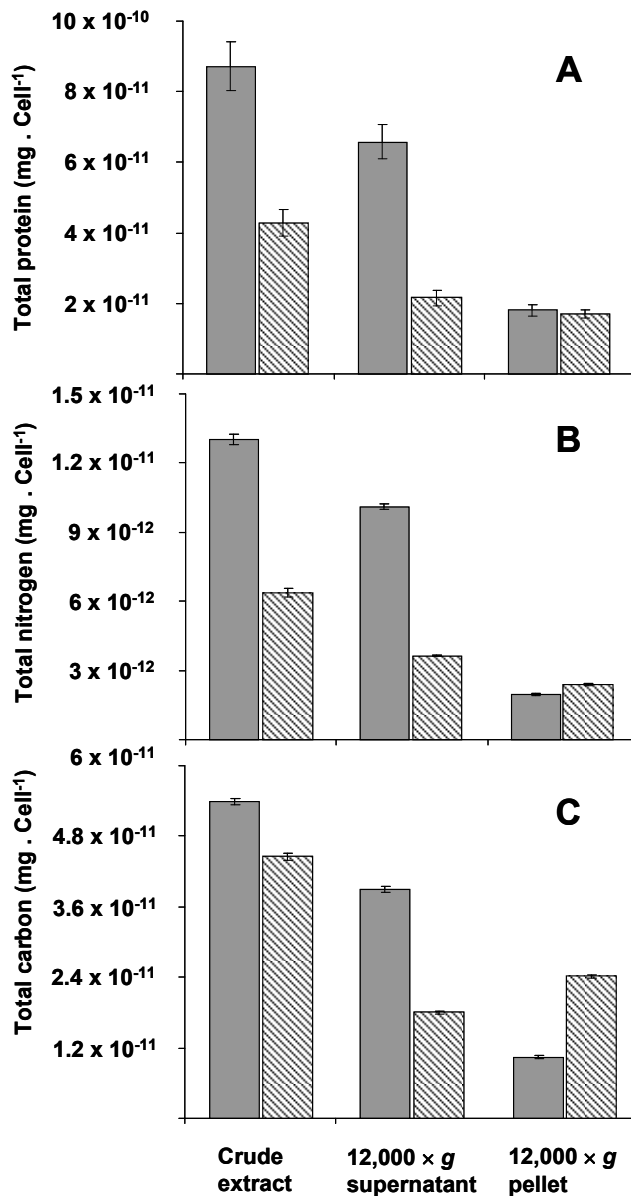


Figure 4. The distribution calculated per cell of (A) total protein, (B) nitrogen and (C) carbon over cell wall and cytosol at the beginning (grey bars) and end (dashed bars) of transition phase I in the crude extract, 12,000 × g supernatant and 12,000 × g pellet. This experiment was performed with exponential cells that had reached an optical density of 0.5 (see Fig. 2A). The amount of total protein and total nitrogen in this exponential cells were normalized to values from cells obtained at the start of transition phase I, since total protein (see Fig. 1C) and total nitrogen (see Fig. 2B) stabilized after ammonium depletion. The total carbon of the exponential cells was normalized to values from cells obtained at the end of the exponential growth phase (at optical density of 1.12). Error bars represent S.E.M. ($n = 4$).

This storage seems to continue in transition phase II, where the carbon to nitrogen ratio and dry weight increased at stabilizing cell numbers (Fig. 1). Storage of an insoluble form of carbon was most evident from the strong increase in the carbon to nitrogen ratio of the pellet fraction of crude cell extract in both phases (Fig. 5).

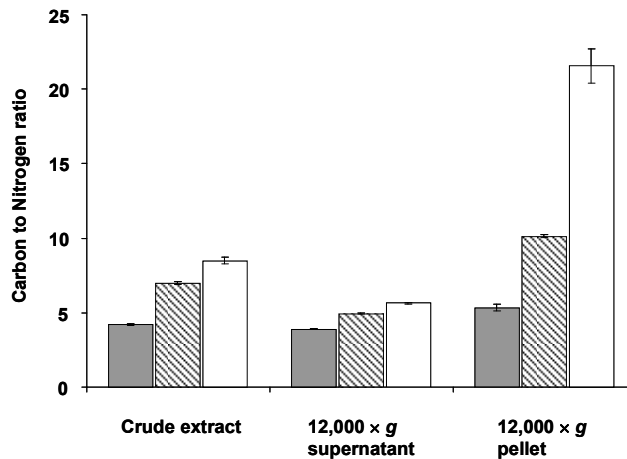


Figure 5. Carbon to nitrogen ratio (mg/mg) in the crude extract, 12,000 × g supernatant and 12,000 × g pellet prepared from cells harvested in the exponential phase (grey bars), at the end of transition phase I (dashed bars) and II (white bars). Error bars represent S.E.M. ($n = 3$).

Transmission electron microscopic investigation of the cells

The ultrastructure of “*Ca. M. fumariolicum*” cells from three different growth phases (exponential, end transition phase I and II) was studied by transmission electron microscopy. Circular or ellipsoid (electron light) bodies were observed in high amounts in cells at the end of transition phase I and II (Fig. 6 (white arrows) and Table 1). This resulted in a dense occupation of the whole cell area (as seen in the thin-sections) by these bodies. A specific electron microscopical stain performed on cells from transition phase II confirmed that these bodies consist of polysaccharide (Fig. 7). In exponential cells these bodies could be discriminated, but only in low numbers and smaller in size.

In addition, some “*Ca. M. fumariolicum*” cells feature an elliptical to circular body (100-200 nm in diameter) of high electron density (appears black in images; Fig. 6 (black arrows)). In most cases only one of these electron dense bodies seems to be present per “*Ca. M. fumariolicum*” cell, although dividing cells occasionally show two electron dense bodies.

Table 1. Amount and diameter of electron light bodies per cell in different growth phases as observed with transmission electron microscopy of chemically fixed cells

Growth phase	Amount of electron light bodies per cell area (1/ μm^2) ^a	Diameter of electron light bodies (nm) ^b
Exponential	8 ± 8	48 ± 15
End transition phase I	51 ± 19	84 ± 27
End transition phase II	44 ± 13	96 ± 35

^a Analysis performed on 50 cells.

^b Analysis performed on 50 electron light bodies.

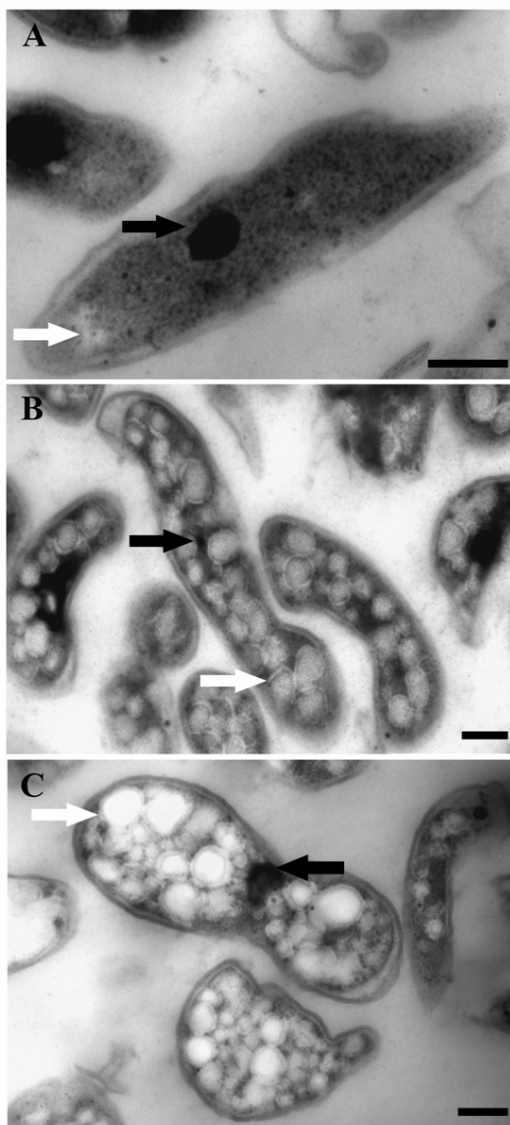


Figure 6. Transmission electron micrographs showing chemically fixed, Epon-embedded thin sections of *M. fumariolicum* cells in different growth phases. (A) Cell from the exponential phase. (B) Cells taken at the end of transition phase I. (C) Cells taken at the end of transition phase II. Electron light particles (white arrows) are seen in all growth phases, but are especially abundant in cells of transition phase I and II. Electron dense particles (black arrows) are present in all growth phases. Scale bars, 200 nm.

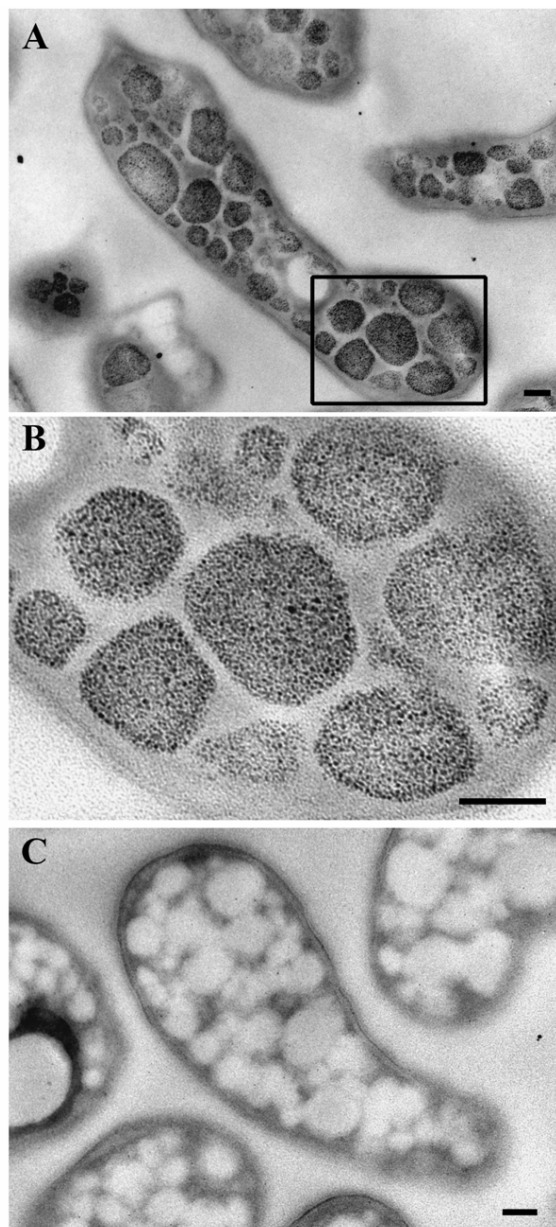


Figure 7. Transmission electron micrographs showing glycogen staining of chemically fixed, Epon-embedded thin sections of *M. fumariolicum* cells in transition phase II. (A) Glycogen staining is seen in the otherwise electron light particles abundantly present in the cytoplasm. (B) Zoom-in of the box drawn in (A). (C) Negative control incubated with water instead of periodic acid. Scale bars, 100 nm.

Glycogen metabolism genes

In the draft genome of strain SolV (Khadem *et al.*, 2012 b) genes encoding for glycogen synthesis (*glgA*, *glgB* and *glgC*) and degradation (*glgP*, *glgX*, *gdb* and *pgm*) were present (Table 2). All genes were present in a single copy except for *glgP* encoding the glycogen phosphorylase for which strain SolV possesses 3 copies. All genes showed orthologs in “*Ca. M. infernorum*” V4 (Hou *et al.*, 2008) with amino acid identities ranging from 70-89 %. Compared to this, identities to other more distantly related species were always below 47-61 %. Phylogenetic analysis of the glycogen synthase (encoded by *glgA*) showed that the verrucomicrobial methanotrophs form a separate cluster (Fig. 8).

Messenger RNA analysis of cells from an exponentially growing culture by RNA-Seq showed transcription of the aforementioned genes comparable to house-keeping genes (Table 2 and Khadem *et al.*, 2012 a). RNA-Seq analysis of nitrogen fixing cells and cells under low oxygen concentration showed comparable transcription levels of glycogen synthesis/degradation genes (Khadem *et al.*, 2012 a). Key genes involved in poly-3-hydroxybutyrate (PHB) synthesis (*phaC*, *phaA*, *phaB*) are absent.

Figure 8 (next page). Phylogenetic analysis of glycogen synthases (*glgA*). Representative amino acid sequences were obtained from GenBank. The evolutionary history was inferred using the maximum-likelihood method based on the Dayhoff matrix-based model. The consensus bootstrap tree is shown. Initial tree(s) for the heuristic search were obtained automatically as follows. When the number of common sites was < 100 or less than one fourth of the total number of sites, the maximum parsimony method was used; otherwise BIONJ method with MCL distance matrix was used. The tree is drawn to scale, with branch lengths measured in the number of substitutions per site. The bar represents 20 % sequence divergence. The analysis involved 39 amino acid sequences. All positions containing gaps and missing data were eliminated. There were a total of 434 positions in the final dataset.

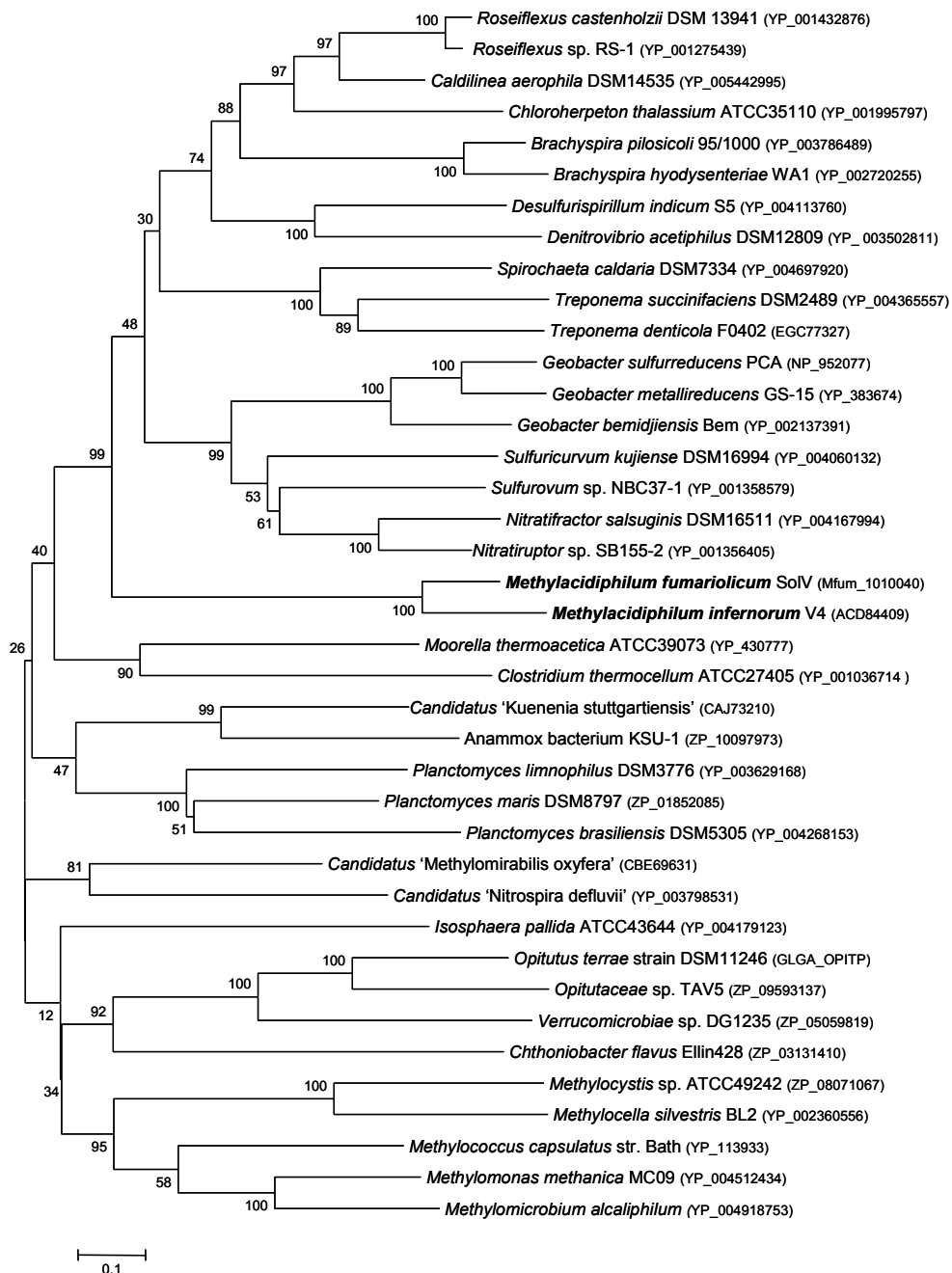


Table 2. Genes involved in glycogen synthesis and degradation in “*Ca. Methylocandidiphilum fumariolicum*” strain SoIV and their expression levels

Enzyme	Gene name	E.C. number ^a	Accession nr.	Identity to V4 ortholog (%) ^b	Expression (RPKM value) ^c
Glycogen synthase	<i>glgA</i>	2.4.1.21	Mfumv1_1010040	74	306
1,4-alpha-glucan-branching enzyme	<i>glgB</i>	2.4.1.18	Mfumv1_170041	70	154
Glucose-1-phosphate adenylyltransferase	<i>glgC</i>	2.7.7.27	Mfumv1_1020013	89	391
Glycogen phosphorylase	<i>glgP1</i>	2.4.1.1	Mfumv1_1020098	81	656
	<i>glgP2</i>		Mfumv1_220010	86	113
	<i>glgP3</i>		Mfumv1_880004	88	447
Glycogen debranching enzyme	<i>glgX</i>	3.2.1.-	Mfumv1_40003	70	381
Amylo-alpha 1,6 glucosidase	<i>gdb</i>	3.2.1.33	Mfumv1_200059	84	256
Glycosyl transferase (group 1)	<i>rfaG</i>	2.4.1.-	Mfumv1_200060	81	43
Phosphoglucomutase	<i>pgm</i>	5.4.4.2	Mfumv1_550015	73	398

^a Enzyme commission number.

^b Comparison with proteins encoded in the genome of “*Ca. Methylocandidiphilum infernorum*” strain V4.

^c mRNA expression in exponentially growing cells as determined by RNA-Seq is expressed as RPKM (Mortazavi *et al.*, 2008).

Glycogen assay

To confirm the presence of glycogen as a carbon storage compound in “*Ca. M. fumariolicum*”, a glycogen assay was performed on crude cell extracts prepared from bacteria from an exponentially growing culture and from a culture obtained at the end of transition phase I and II. The glycogen amount as a percentage of dry weight in the crude extracts was 2 % for the exponentially growing culture, 26 % and 36 % for the culture obtained at the end of transition phase I and II, respectively.

Glycogen consumption & function

The consumption of glycogen was detected by the release of ^{13}C -labeled CO_2 from cells that had accumulated ^{13}C -labeled glycogen. Accumulation of ^{13}C containing glycogen was achieved by growing cultures till late transition phase II in the presence of both ^{13}C -labeled methane and carbon dioxide. When such cells are transferred to a medium without methane, stored glycogen is likely to be consumed to meet the energy requirement of the starving cells, and thus ^{13}C -labeled CO_2 is produced. The ratio of $^{12}\text{C}/^{13}\text{C}$ was determined accurately by GC-MS analysis, against a background of 10 % unlabeled CO_2 in the culture bottles. During the first day a rapid $^{13}\text{CO}_2$ production was observed (initial rate of $5 \mu\text{mol } ^{13}\text{CO}_2 \text{ produced (mg dry weight of cells)}^{-1} \text{ day}^{-1}$; Fig. 9). This rate dropped gradually to a linear rate of $0.2 \mu\text{mol } ^{13}\text{CO}_2 \text{ produced (mg dry weight of cells)}^{-1} \text{ day}^{-1}$, which did not change at least till day 28. The total amount of $^{13}\text{CO}_2$ produced over this period was calculated to be $51.4 \pm 1.9 \mu\text{mol of } ^{13}\text{CO}_2$ ($n = 4$). On basis of the glycogen content of the cells (36 % of 4.4 mg dry weight of cells), $9.8 \mu\text{mol}$ of ^{13}C -labeled glycogen was introduced in the incubation. This could result in a maximum of $58.6 \mu\text{mol}$ of $^{13}\text{CO}_2$ to be produced. This means that about 88 % of the ^{13}C -labeled glycogen was recovered as $^{13}\text{CO}_2$. In a parallel experiment it was shown that $^{13}\text{CO}_2$ production ceased after about 47 days of starvation and during this extended period an additional 9 % of the glycogen was converted to $^{13}\text{CO}_2$ (data not shown). The control incubations with ^{13}C -labeled cells from the exponential phase produced only small amounts of $^{13}\text{CO}_2$, and at lower initial rate ($1 \mu\text{mol } ^{13}\text{CO}_2 \text{ produced (mg dry weight of cells)}^{-1} \text{ day}^{-1}$), and this production

ceased after 3 days. This corresponded with the observation that cells from cultures growing exponentially contained little glycogen (based on both electron microscopy and biochemical analysis).

The possibility of growth on stored glycogen was investigated in a similar experiment as described above without ^{13}C -labeling. For this study, cultures that had accumulated glycogen (obtained at the end of transition phase II; Figs. 1A and 1B) were diluted and transferred to a medium without methane but with 2 mM of ammonium in order to allow growth. During 10 days of starvation, in which the ^{13}C -labeling experiments suggested that most of the glycogen was already consumed, no growth was observed as cell numbers remained the same (Fig. 1B). The optical density decreased rapidly during this incubation (Fig. 1A), probably as a result of glycogen consumption. In a parallel experiment in presence of methane (and no ammonium), the optical density was stable in this period (data not shown). Apparently glycogen in the cell caused some more light scattering; this effect was also observed during the transition phase II, where only glycogen was produced, the optical density increased while cell numbers remained constant (size differences of the bacteria at the different growth phases were only marginal).

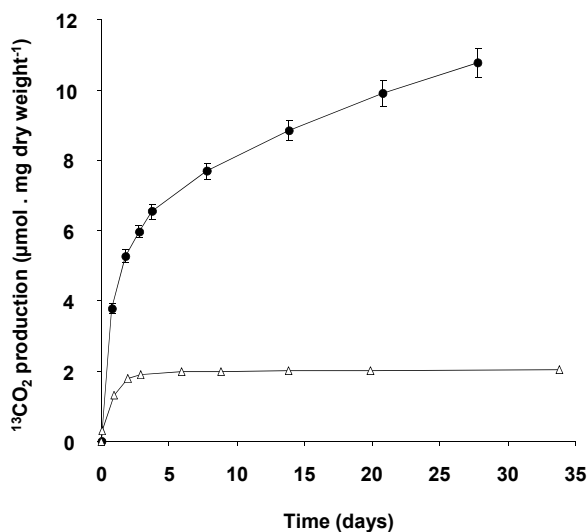
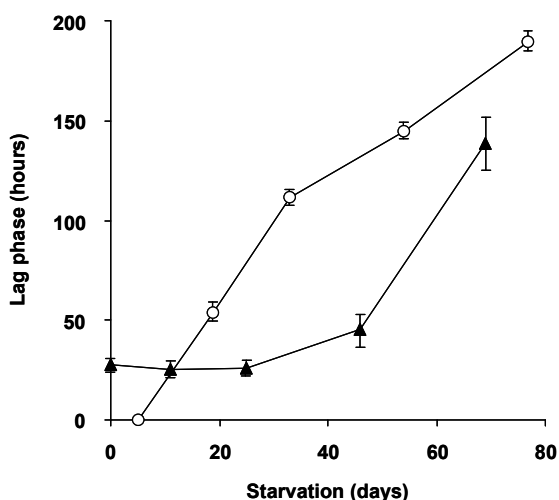


Figure 9. $^{13}\text{CO}_2$ production originating from ^{13}C -glycogen loaded cells (4.4 mg dry weight), obtained at the end of the transition phase II (closed circles). Exponential cells (2.1 mg dry weight; open triangles) served as a control. $^{13}\text{CO}_2$ measured after 1 hour of incubation at 55 °C, was subtracted from all measured values during the experiment. Error bars represent S.E.M. ($n = 4$).

To study the role of glycogen in viability of the cells, a long-term (70 days) starvation experiment for methane was performed with cultures undergoing exponential growth and cultures that were in transition phase II for 20 days. Exponentially growing cultures were grown till the moment that all ammonium was consumed and the starvation for both cell types was initiated by removing methane from the headspace of the bottles. During the starvation period, cell numbers of both cell types gradually decreased during methane starvation. The cell numbers decreased by a factor of 4.5 in the case of cells obtained from exponentially grown cultures and by a factor 2.4 in the case of cells obtained at the end of transition phase II. The lag phase observed upon recultivation in optimal growth conditions was taken as a measure of viability of the remaining cultures of both types. Exponentially grown cultures were losing viability rapidly after 4 days of methane starvation (Fig. 10). Recultivation starting from glycogen loaded cultures showed a lag phase (28 h) from the start. This lag phase remained unchanged for about 40 days of methane starvation (Fig. 10). Only after 45 days the lag phase of glycogen loaded cells increased, pointing to a depletion of the stored glycogen (Fig. 10). This is well in accordance with the results of ^{13}C -labeled glycogen consumption experiment, which showed that in about 47 days all glycogen in the cells was consumed.

Figure 10. Viability and recovery of glycogen containing “*Ca. M. fumariolicum*” SolV cells (closed triangles) and exponential growing cells (open circles) after methane and ammonium starvation for different periods of time. At time 0, cells were inoculated into optimal medium (4 mM ammonium and methane in the headspace) and lag phases were recorded. Error bars represent S.E.M. ($n = 4$).



Discussion

Many bacteria store carbon when nitrogen becomes growth limiting (Wanner & Egli, 1990 and references therein). Methanotrophs are also known for their ability to store carbon, either in the form of poly-3-hydroxybutyrate (PHB), glycogen or by exopolysaccharide (EPS) production. Many studies have focused on PHB storage and its role in methanotrophs, and the genes involved in its synthesis (Pieja *et al.*, 2011 a and b). In addition, EPS production in multiple methanotrophs has been studied in some detail (Malashenko *et al.*, 2001). However, detailed studies about glycogen production and its role in methanotrophs are scarce (Eshinimaev *et al.*, 2002; Khmelenina *et al.*, 1999; Linton & Cripps, 1978). In these studies, usually only the presence of glycogen is reported in these microorganisms based on basic electron microscopic observations, without specific staining.

Although the electron microscopic polysaccharide stain used in our study is not specific for glycogen (Bradbury & Stoward, 1967), our results in combination with the biochemical assay clearly show the presence of glucose polymers in strain SolV. As all the genes for glycogen production and consumption were shown to be present and transcribed, this glucose polymer is most likely glycogen. For more definite proof a biochemical analysis of chain length and type of branching will be necessary.

Based on the growth experiments, it can be assumed that glycogen storage starts soon after ammonium depletion in the medium. However, the glycogen measurements, electron microscopic observations and the transcriptome data suggest that there was a little bit of glycogen produced during exponential phase. Electron microscopy showed that at the end of the transition phase I (1.5 days after ammonium depletion), cells were packed with glycogen bodies. In addition, the strong increase in total amount of carbon in the pellet fraction per cell, pointed to glycogen storage in phase I.

The increase in dry weight and total carbon (mg per ml cell culture) in transition phase I was not only due to glycogen storage (26 % of the dry weight), but also to cell growth, since cell numbers doubled. This growth was not due to other nitrogen sources present in the medium or nitrogen fixation. Nitrogen fixation would also be impossible since dissolved oxygen concentrations in the cultures were too high to support nitrogen fixation by “*Ca. M. fumariolicum*” (Khadem *et al.*, 2010).

Moreover, the total protein and nitrogen content (mg per ml cell culture) stabilized immediately after ammonium depletion. The observation that the amount of protein and total nitrogen (mg per ml cell culture) in the pellet fraction of the crude extracts doubled, was in accordance with the doubling of cell numbers.

Completion of cell division once DNA replication has started, seems to be a strong regulating factor when growth substrates are limiting as has been documented before (Wanner & Egli, 1990 and references therein). While some bacteria become smaller under such conditions (reductive cell division), strain SolV maintained its normal shape and size.

On basis of the carbon percentages, the changes in carbon to nitrogen ratio and assuming a constant amount of nitrogen at the start and end of transition phase II we calculated that dry weight in this phase should have increased about 20 %. The measured increase (based on weighing) was about 30 %. The increase of the glycogen percentage from 26 to 36 % can account for only 15 % of the dry weight increase. The observed biomass increase may have resulted from some ongoing growth in this phase, but the increase in cell numbers was too small to result in a significant difference.

Under the circumstances tested (nitrogen depletion), the maximum amount of glycogen measured in the cells of strain SolV was 36 % of the dry weight. Under nitrogen limitation, a similar percentage of glycogen was found in the halotolerant methanotroph *Methylobacter alcaliphilus* 20Z (Khmelenina *et al.*, 1999). Under other growth conditions, percentages of 16 % (calcium limitation) and 35 % (growth on methanol) are reported for methanotrophs (Eshinimaev *et al.*, 2002; Linton & Cripps, 1978). However, under nitrogen depletion PHB can account for up to 50 % of the dry weight in *Methylocystis parvus* OBBP (Pieja *et al.*, 2011 b).

Glyceraldehyde-3-phosphate produced from CO₂ via the Calvin-Benson-Bassham cycle (Khadem *et al.*, 2011), is the most likely precursor of glucose-6-phosphate in strain SolV. The consecutive action of triosephosphate isomerase, fructose 1,6-bisphosphate aldolase, fructose 1,6-bisphosphate phosphatase and glucose-6-phosphate isomerase results in glucose-6-phosphate. The presence of a gene encoding for phosphoglucumutase (*pgm*), suggest that the latter enzyme in turn can convert glucose-6-phosphate and its product glucose-1-phosphate can be used for glycogen synthesis (Wayne *et al.*, 2010). The same route (in reverse) can be used for the degradation of glycogen.

The benefit of accumulated glycogen for “*Ca. M. fumariolicum*” under energy-limiting conditions (no methane) was shown by the fact that cell numbers declined less and that the viability of remaining cells was maintained much better for glycogen loaded cells compared to cells without glycogen (exponentially grown). Glycogen loaded cells showed an initial lag phase which could be expected because the bacteria were in very different metabolic state as a result of the nitrogen depletion, with much lower cytosolic protein content. This lag phase however became longer only after 40 days of starvation. During this period the glycogen was almost fully consumed, as was shown by ^{13}C -labeling experiments. These cells produced $^{13}\text{CO}_2$ in amounts that equal the initial glycogen content of the cells, while the headspace of exponential cells only showed a small increase in $^{13}\text{CO}_2$ during the first few days. Growth was only observed in presence of methane and it can therefore be concluded that glycogen was not used for cell growth. Similar results were found for *Methylocystis parvus* OBBP, where no growth on PHB was observed (Pieja *et al.*, 2011 b). Therefore, we conclude that the glycogen storage enhances the viability of “*Ca. M. fumariolicum*” during methane starvation.

Regulation of glycogen synthesis/degradation seems not to be at the transcriptional level. There are good arguments for having a regulation on protein/enzyme level since strain SolV needs to be ready for acting rapidly to two situations: 1) when starved for nitrogen, cells can directly make profit of the energy/carbon source still available for immediate storage of carbon. This can be accomplished only when necessary proteins are already present, as mRNA or protein synthesis is hardly possible when there is no nitrogen source available; 2) when starved for methane, an energy deprived conditions in which cells have difficulty to produce (new) proteins, cells already have the proteins available for glycogen degradation. So, depending on the level of substrates (e.g. glucose-6-phosphate) the route may operate in a biosynthetic or degradative direction.

Conclusion

The thermoacidophilic verrucomicrobial methanotroph “*Ca. M. fumariolicum*” strain SolV is able to store glycogen in the case of nitrogen depletion.

This accumulated glycogen may be consumed in response to energy limitation. It is hypothesized that the bacteria use accumulated glycogen to enhance viability, since growth on accumulated glycogen was not observed.

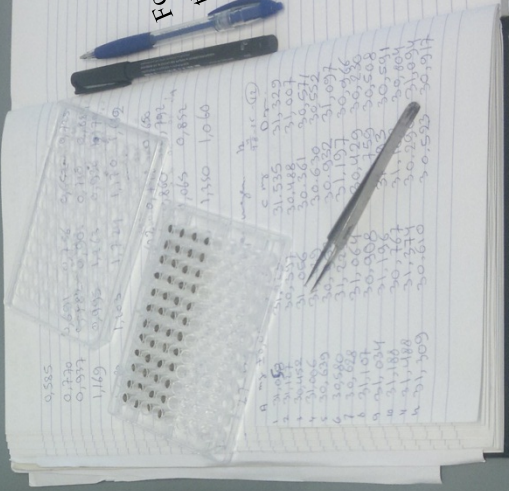
To the best of our knowledge this is the first experimental validation of glycogen storage in the phylum *Verrucomicrobia*.

Acknowledgments

We are grateful to Jelle Eygensteyn for help with the elemental analyses and Elly G. van Donselaar for help with the polysaccharide staining for electron microscopy.

Ahmad F. Khadem was supported by Mosaic grant 62000583 and Laura van Niftrik by VENI grant 86309009, both from the Netherlands Organisation for Scientific Research (NWO).

Mike S. M. Jetten and Muriel C. F. van Teeseling were supported by European Research Council, grant number 232937.



Picture by Ahmad F. Khadem.
Sartorius microbalance.
For the IRMS analysis
the samples
weighed in tin or silver
containers, using the



Chapter Six

Whole genome transcriptome analysis of “*Ca. Methylacidiphilum fumariolicum*” strain SolV

Keywords:

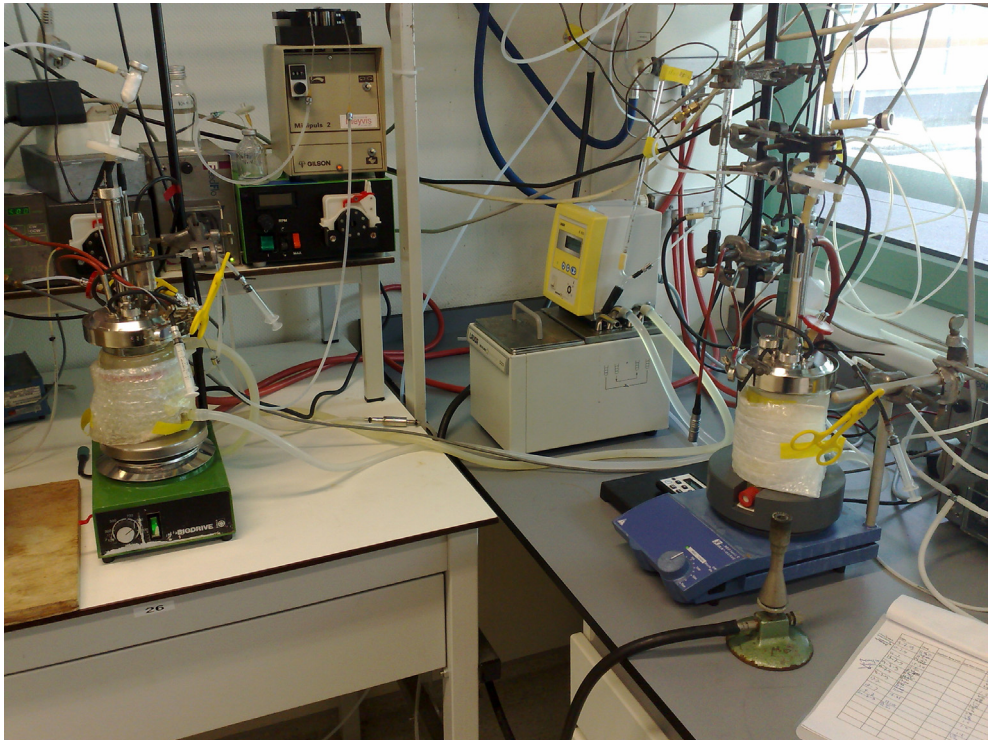
metabolic regulation

“*Methylacidiphilum*”, *Verrucomicrobia*

methane, nitrogen, RNA-Seq &
pMMO.

Published in:

Frontiers in Microbiology **3**, 266 (2012).



Nitrogen fixing (right side) and oxygen limited (left side) chemostat cultures.
Picture by Ahmad F. Khadem.

Metabolic regulation of “*Ca. Methylacidiphilum fumariolicum*” SolV cells grown under different nitrogen and oxygen limitations

Ahmad F. Khadem¹, Arjan Pol¹, Adam S. Wiczorek¹, Mike S. M. Jetten¹ &
Huub J. M. Op den Camp¹

¹Department of Microbiology, Institute of Water and Wetland Research, Radboud University Nijmegen,
Heyendaalseweg 135, NL-6525 AJ, Nijmegen, the Netherlands.

Abstract

Aerobic methanotrophic bacteria can use methane as their sole energy source. The discovery of “*Ca. Methylacidiphilum fumariolicum*” strain SolV and other verrucomicrobial methanotrophs has revealed that the ability of bacteria to oxidize CH₄ is much more diverse than has previously been assumed in terms of ecology, phylogeny and physiology. A remarkable characteristic of the methane-oxidizing *Verrucomicrobia* is their extremely acidophilic phenotype, growing even below pH 1. In this study we used RNA-Seq to analyze the metabolic regulation of “*Ca. M. fumariolicum*” SolV cells growing at μ_{\max} in batch culture or under nitrogen fixing or oxygen limited conditions in chemostats, all at pH 2. The analysis showed that two of the three *pmoCAB* operons each encoding particulate methane monooxygenases were differentially expressed, probably regulated by the available oxygen. The hydrogen produced during N₂ fixation is apparently recycled as demonstrated by the up-regulation of the genes encoding a Ni/Fe-dependent hydrogenase. These hydrogenase genes were also up-regulated under low oxygen conditions. Handling of nitrosative stress was shown by the expression of the nitric oxide reductase encoding genes (*norB* and *norC*) under all conditions tested, the up-regulation of nitrite reductase (*nirK*) under oxygen limitation and of hydroxylamine oxidoreductase (*hao*) in the presence of ammonium. Unraveling the gene regulation of carbon and nitrogen metabolism helps to understand the underlying physiological adaptations of strain SolV in view of the harsh conditions of its natural ecosystem.

Introduction

Methanotrophs are an unique group of microorganisms that can use methane (CH₄) as sole carbon and energy source (Hanson & Hanson, 1996). Methanotrophs are found both in aerobic and anaerobic natural environments (Boetius *et al.*, 2000; Conrad, 2009; Hanson & Hanson, 1996; Raghoebarsing *et al.*, 2006). Aerobic methane oxidizing bacteria are represented by members of the *Alphaproteobacteria*, the *Gammaproteobacteria*, the *Verrucomicrobia* and the NC10 phylum (Ettwig *et al.*, 2010; Hanson & Hanson, 1996; Op den Camp *et al.*, 2009). “*Candidatus Methylomirabilis oxyfera*”, a representative of the latter phylum and growing anaerobically in the absence of oxygen, has the unique ability to produce intracellular oxygen through an alternative denitrification pathway (Ettwig *et al.*, 2010).

During aerobic CH₄ oxidation, energy is conserved during the oxidation of methanol, formaldehyde and formate (Chistoserdova *et al.*, 2009; Hanson & Hanson, 1996). In the oxidation of methanol, electrons are transferred to a membrane-bound electron transport chain via a pyrroloquinoline quinone cofactor to cytochrome *c* and the bc₁ complex by the enzyme methanol dehydrogenase. During formaldehyde and formate oxidation, NAD is reduced to NADH and transferred to NADH-oxidoreductase complex I (*nuo* genes). Electrons flow via the membrane protein complexes, Nuo, bc₁, to the cytochrome *c* oxidases and produce a proton motive force that is converted to the cellular energy carrier ATP by the ATPase enzyme complex.

Verrucomicrobial methanotrophs were isolated from volcanic areas in Italy, New Zealand and Russia (Dunfield *et al.*, 2007; Islam *et al.*, 2008; Pol *et al.*, 2007) and the genus name “*Methylacidiphilum*” was proposed since 16S rRNA gene sequences of the three independent isolates had 98-99 % sequence identity (Op den Camp *et al.*, 2009). Although environmental clone libraries from many ecosystems show a large abundance and biodiversity of *Verrucomicrobia* (Wagner & Horn, 2006), little is known about their *in situ* physiology. There are now several verrucomicrobial genome assemblies available (van Passel *et al.*, 2011) including two of the verrucomicrobial methanotrophs (Hou *et al.*, 2008; Khadem *et al.*, 2012 b). The genome data of strains V4 and SolV showed some similarities but also major differences in the C1-utilization pathways compared to proteobacterial and

NC10 methanotrophs. The functional significance of these differences can only be validated by a combination of physiological and expression studies.

Physiological studies of “*Ca. M. fumariolicum*” strain SolV have demonstrated that this microorganism was able to grow with ammonium, nitrate or dinitrogen gas as nitrogen source (Khadem *et al.*, 2010; Pol *et al.*, 2007). ¹³C-labeling studies showed that strain SolV growing on CH₄, fixed CO₂ into biomass exclusively via the Calvin-Benson-Bassham (CBB) cycle (Khadem *et al.*, 2011). Based on these results we expect that genes involved in nitrogen fixation are only expressed in the absence of ammonium/nitrate and genes involved in the CBB cycle are constitutively expressed. To evaluate this in more detail, analysis of the complete set of transcripts (the transcriptome) and their quantity present in cells grown under different condition is needed.

With the development of microarrays (Malone & Oliver, 2011) high-throughput quantification of the transcriptome became possible, improving the low throughput mRNA data from Northern blots or reverse-transcription PCR (RT-PCR) analysis. More recently, next generation sequencing has been shown to be a very powerful method to analyze the transcriptome of cells by what is known as RNA-Seq (Wang *et al.*, 2009). Furthermore, this technique can detect transcripts without corresponding genomic sequences and can detect very low abundance transcripts (Croucher & Thomson, 2010; Malone & Oliver, 2011).

In this study we used RNA-Seq to analyze the genome wide transcriptome of “*Ca. M. fumariolicum*” SolV cells grown under different conditions at pH 2. Expression profiles of exponentially growing SolV batch cultures (at μ_{\max}) were compared to nitrogen fixing or oxygen limited chemostat cultures and used to unravel the gene and genome regulation of carbon and nitrogen metabolism which may reflect the underlying physiological adaptations of SolV.

Materials & methods

Organism & medium composition for growth

“*Ca. Methylacidiphilum fumariolicum*” strain SolV used in this study was originally isolated from the Solfatara volcano, Campi Flegrei, near Naples, Italy (Pol *et al.*, 2007). Preparation and composition of the growth medium (pH 2) was described previously (Khadem *et al.*, 2010). Mineral salts composition and concentration were changed for oxygen limited SolV chemostat cultures: 0.041 g l⁻¹ MgCl₂·6H₂O was added (instead of 0.08 g l⁻¹) and CaHPO₄·2H₂O was replaced by 0.138 g l⁻¹ NaH₂PO₄·H₂O to limit precipitation.

Chemostat cultivation

Chemostat cultivation of strain SolV under nitrogen fixing condition at pH 2 was performed as described previously (Khadem *et al.*, 2010). Growth yield and stoichiometry of CH₄ conversion to CO₂ of strain SolV were also determined for oxygen limited SolV chemostat cultures. The chemostat liquid volume was 300 ml and the system was operated at 55 °C with stirring at 900 r.p.m. with a stirrer bar. The chemostat was supplied with medium at a flow rate of 5.1 ml h⁻¹, using a peristaltic pump. Culture liquid level was controlled by a peristaltic pump actuated by a level sensor. A gas mixture containing (v/v) 5.8 % CH₄, 2.3 % O₂, 0.4 % N₂ and 91.1 % CO₂ was supplied to the chemostat by mass flow controllers through a sterile filter and sparged into the medium just above the stirrer bar. Oxygen concentrations in the liquid were measured with a Clarke-type electrode. After steady state was reached, CH₄ and O₂ consumption and CO₂ production were determined by measuring the ingoing and outgoing gas flows and the gas concentrations. The outgoing gas passed through a sterile filter at a flow rate of 11.9 ml h⁻¹, and contained (v/v) a mixture of approximately 4.8 % CH₄, 0.72 % O₂, 0.7 % N₂ and 92.7 % CO₂. The dissolved oxygen concentration (dO₂) was below 0.03 % oxygen saturation. To determine biomass dry weight concentration, triplicate 5 ml samples from the culture suspension were filtered through pre-weighed 0.45 µm filters and dried to constant weight in a vacuum oven at 70 °C.

After steady state, both chemostats were sampled for mRNA isolation and Illumina sequencing.

Batch cultivation

Cells of SolV grown at maximal growth rate (μ_{\max}), without any nitrogen, O₂ and CH₄ limitation were obtained in 1 liter serum bottles, containing 50 ml medium (with 4 mM ammonium, 2 % fangaia soil extract and at pH 2, (Khadem *et al.*, 2010)) and sealed with red butyl rubber stoppers. Incubations were performed in duplicate and contained in (v/v) 10 % CH₄, 5 % CO₂ and 18 % O₂ at 55 °C with shaking at 180 r.p.m. Exponentially growing cells were collected for mRNA isolation and Illumina sequencing.

Gas & ammonium analyses

Gas samples (100 µl) were analyzed for methane (CH₄), carbon dioxide (CO₂) and oxygen (O₂) on an Agilent series 6890 gas chromatograph (GC) equipped with Porapak Q and Molecular Sieve columns and a thermal conductivity detector as described before (Ettwig *et al.*, 2008).

Ammonium concentrations were measured using the ortho-phthaldialdehyde (OPA) method (Taylor *et al.*, 1974).

Transcriptome analysis

The draft genome sequence of strain SolV (Khadem *et al.*, 2012 b) was used as the template for the transcriptome analysis. Cells were harvested by centrifugation and 3.1 mg dry weight cells were used for isolation of mRNA, and subsequent synthesis of cDNA (328 ng) was done as described before (Ettwig *et al.*, 2010). The cDNA was used for Illumina sequencing (RNA-Seq) as described before (Ettwig *et al.*, 2010; Kartal *et al.*, 2011). Expression analysis was performed with the RNA-Seq Analysis tool from the CLC Genomic Workbench software (version 4.0, CLC-Bio, Aarhus, Denmark) and values are expressed as RPKM (Reads Per Kilobase of exon model per Million mapped reads) (Mortazavi *et al.*, 2008).

Results & discussion

Physiology of “*Ca. M. fumariolicum*” SolV growing with & without nitrogen source & under oxygen limitation

Prior to the expression studies the physiological properties of strain SolV were examined in batch and chemostat continuous culture. These studies showed that strain SolV in batch culture had a maximum growth rate of 0.07 h^{-1} and 0.04 h^{-1} , with ammonium or nitrate as nitrogen source, respectively (Table 1). In the absence of ammonium and nitrate “*Ca. M. fumariolicum*” SolV cells were able to fix atmospheric N_2 only at headspace oxygen concentration below 1 % (Khadem *et al.*, 2010). The additional reduction steps of nitrate to ammonium could explain the observed increase in doubling time with nitrate compared to ammonium. The slower growth rate with N_2 as nitrogen source was expected, since N_2 -fixation is an endergonic process, which needs about 16 mol ATP per mol N_2 fixed (Dixon & Kahn, 2004). Based on the μ_{\max} data obtained, strain SolV seems to prefer ammonium, which is also the most likely nitrogen source in its natural environment.

Continuous cultivation of strain SolV cells in a chemostat at pH 2 under nitrogen fixing conditions, was performed at dissolved oxygen concentrations (dO_2) equal to 0.5 % oxygen saturation and without ammonium or nitrate (Table 1). Growth was limited by CH_4 liquid-gas transfer in this chemostat culture (Khadem *et al.*, 2010). The growth rate (0.017 h^{-1}) is 68 % of the μ_{\max} (0.025 h^{-1}) obtained in N_2 fixing batch cultures.

For continuous cultivation of strain SolV under oxygen limitation and in the presence of excess methane and ammonium, the chemostat was supplied with medium at a dilution rate of 0.017 h^{-1} (Table 1). This resulted in a dO_2 equal to 0.03 % oxygen saturation ($< 0.24\text{ }\mu\text{mol l}^{-1}$).

After a steady state was obtained in the chemostat, the stoichiometry of CH_4 oxidation and cell yield under N_2 fixing and O_2 limiting conditions were determined. Under O_2 limitation the stoichiometry of CH_4 oxidation was the same as reported for excess ammonium and O_2 (Pol *et al.*, 2007). However, under N_2 fixing conditions, a slightly higher consumption of O_2 and production of CO_2 was

found (Khadem *et al.*, 2010). This coincides with the lower cell yield of the nitrogen fixing chemostat culture of strain SolV (Table 1).

Three of the above described physiological conditions were selected for a genome wide transcriptome analysis (Table 1), e.g. exponentially growing cells (batch culture at μ_{\max}) and cells from nitrogen or oxygen limited chemostat cultures.

Whole genome transcriptome analysis of “*Ca. M. fumariolicum*” SolV

The SolV transcriptome was characterized using RNA-Seq. RNA was prepared from the three different cell cultures (see above), converted to cDNA and sequenced. The Illumina Genome Analyser reads (75 bp) were first mapped to the ribosomal RNA operon and mapped reads were discarded. The unmapped reads (3.5×10^6 , 3.2×10^6 and 2.0×10^6 reads for μ_{\max} , N₂ fixing and O₂ limited cells, respectively) were mapped to the CDS, tRNA and ncRNA sequences extracted from the genome sequence of strain SolV (Khadem *et al.*, 2012 b). The total number of reads obtained and mapped for each sampled culture together with the calculated expression levels (RPKM) are provided in the Supplementary file (Data Sheet 2.XLS; RNA-Seq_SolV.xls). We selected a set of 394 housekeeping genes (in total 443 kbp) involved in energy generation, in ribosome assembly, carbon fixation (CBB cycle), C1 metabolism (except for *pmo*), amino acid synthesis, cell wall synthesis, translation, transcription, DNA replication and tRNA synthesis for the three conditions, to compare baseline expression levels (Supplementary file: Data Sheet 1.XLS; Housekeeping genes.xls). For this gene set all ratios of expression between conditions were > 0.5 and < 2 . The robustness of the transcriptome data were checked by the method of Chaudhuri *et al.* (2011) in which the expression levels ($\log_2(\text{RPKM}+1)$) of the 394 genes set for the three conditions were plotted against each other. This resulted in correlation coefficients of 0.70, 0.86 and 0.86 (Fig. 1), which are only slightly lower than those of technical replicates as reported by Chaudhuri *et al.* (2011).

In the following paragraphs, the differences in expression pattern under the various cultivation conditions with respect to energy, carbon, nitrogen and hydrogen metabolism of strain SolV will be presented and discussed.

Table 1. Description of batch and chemostat cultures of “*Ca. Methylococcoides burtonii*” strain SolV

Culture	Nitrogen source	Growth rate (h ⁻¹)	Doubling time (h)	Yield (g dry weight per mol CH ₄)	Limitation	O ₂ concentration ^b
Batch	Ammonium ^a	$\mu_{\max} = 0.07$	10	6.5	No	18 %
	Nitrate	$\mu_{\max} = 0.04$	17	n.d.	No	18 %
	N ₂	$\mu_{\max} = 0.025$	27	n.d.	Nitrogen	< 1 %
Chemostat	N ₂ ^a	$\mu = 0.017$	40	3.5	Methane	0.5 %
	Ammonium ^a	$\mu = 0.017$	40	4.9 ^c	Oxygen	< 0.03 %

^a Cells used for transcriptome analysis. In all other Tables referred to as “Cells at μ_{\max} ” “N₂ fixation” and “O₂ limitation”.

^b For batch cultures initial headspace oxygen concentration are given, while for the chemostat cultures measured dissolved oxygen concentration (dO₂) is expressed as % oxygen saturation (100 % equals 800 $\mu\text{mol l}^{-1}$ at 55 °C).

^c Calculated from optical density (measured at 600 nm) comparisons at steady state.

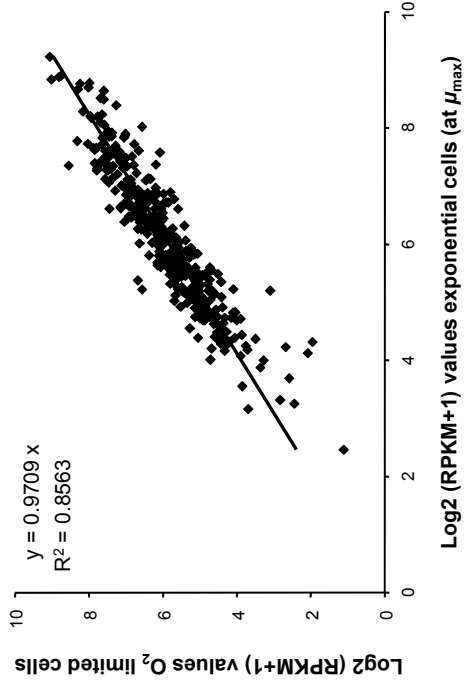
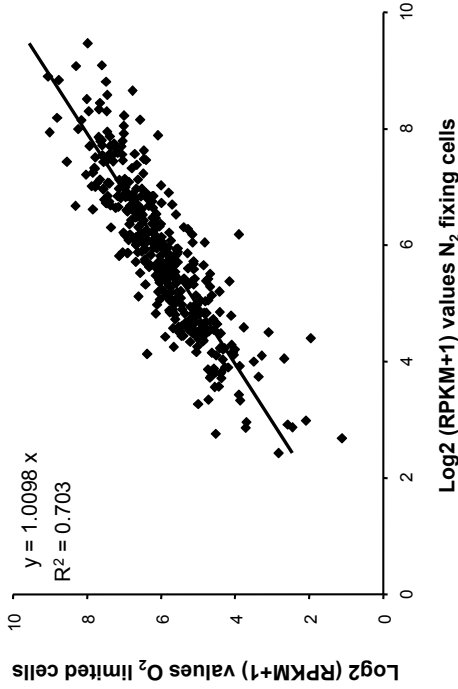
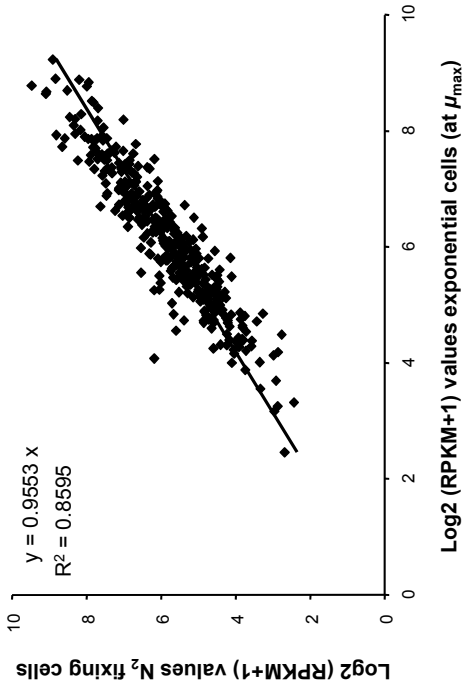


Figure 1. Plots of expression levels ($\text{log}_2 (\text{RPKM}+1)$) of 394 genes (in total 443 kbp) involved in energy generation, ribosomes, carbon fixation (Calvin-Benson-Bassham cycle), C1 metabolism (except for *pmo*), amino acid synthesis, cell wall synthesis, translation, transcription, DNA replication and tRNA synthesis.



Energy metabolism

Genes involved in CH₄ oxidation pathway (Chistoserdova *et al.*, 2009; Hanson & Hanson, 1996) and their RPKM values are presented in Table 2. In the genome data of the verrucomicrobial methanotrophs no genes encoding for the soluble cytoplasmic form of the methane monooxygenase (sMMO) were found (Hou *et al.*, 2008; Khadem *et al.*, 2012 b). However, three *pmoCAB* operons, encoding for the three subunits of particulate membrane-associated form (pMMO) were predicted.

Transcriptome analysis of “*Ca. M. fumariolicum*” SolV showed differential expression of two of the three different operons. One of the *pmoCAB* operons (*pmoCAB2*) was highly expressed (RPKM values 10.9×10^3 to 45×10^3 , Fig. 2) in cells growing at μ_{\max} with excess ammonium and oxygen (initial headspace concentration of 18 %). The other two *pmoCAB* operons were hardly expressed under this culture condition (RPKM 21 to 253). The cells from CH₄ limited, N₂ fixing chemostat culture and the O₂ limited chemostat culture with dO₂ of 0.5 % and 0.03 % oxygen saturation, respectively, showed a remarkable different expression pattern of the *pmoCAB* operons. Under these conditions the *pmoCAB1* operon was highly expressed (RPKM values 4.1×10^3 to 25×10^3) while expression of the *pmoCAB2* operon was down regulated 40 times compared to the batch culture. The *pmoCAB3* operon was hardly expressed in cells from the two chemostat cultures, expression values being identical to that of the cells at μ_{\max} . Although other factors like growth rate, cell density etc. could have an effect, the results point to a regulation of the *pmoCAB1/pmoCAB2* genes by the oxygen concentration. Since the *pmoCAB3* operon was not expressed under the conditions tested, other growth conditions have to be tested to elucidate the regulation and function of this pMMO. In a recent study, qPCR was used to investigate expression of the four *pmoA* genes of “*Ca. Methylacidiphilum kamchatkense*” Kam1 (Erikstad *et al.*, 2012). The *pmoA2* gene was 35-fold stronger expressed than the other copies. Suboptimal temperature and pH conditions did not change this pattern. Other limitations were not tested. Grow on methanol resulted in a 10-fold decreased expression of *pmoA2*.

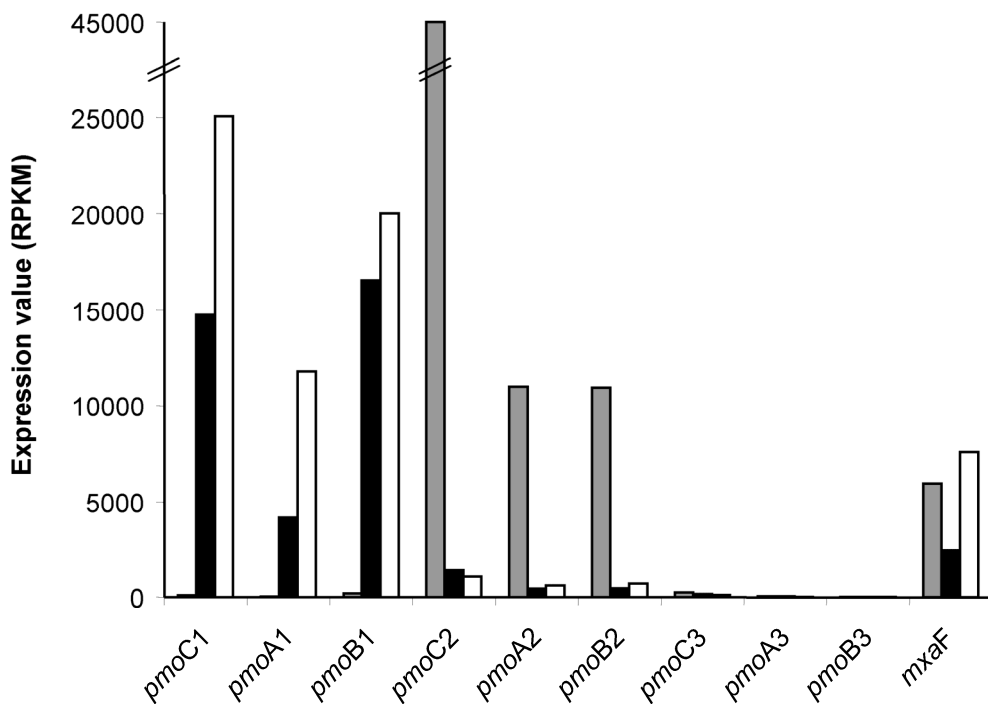


Figure 2. Expression of the three *pmoCAB* operons, encoding the three subunits of the particulate methane monooxygenase (pMMO). Values from exponential growing cells, at μ_{\max} (grey bars), N_2 fixing cells (black bars) and O_2 limited cells (open bars) are compared. Expression of *mxoF* (*xoxF*) encoding methanol dehydrogenase is shown for comparison.

Also some proteobacterial methanotrophs are known to contain multiple copies of *pmo* operons (Murrell *et al.*, 2000; Semrau *et al.*, 1995). Within sequenced genomes of gammaproteobacterial methanotrophs two nearly sequence-identical copies of *pmoCAB1* were found. It is thought that sequence-identical copies have arisen through gene duplications and insertions. Mutation studies in *Methylococcus capsulatus* Bath have demonstrated that both pMMO's were required for growth (Stolyar *et al.*, 1999). More sequence-divergent copies (*pmoCAB2*) were shown to be widely distributed in alphaproteobacterial methanotrophs (Yimga *et al.*, 2003). Recently it was found that some genera of gammaproteobacterial methanotrophs

also possess a sequence-divergent particulate methane monooxygenase, depicted as pXMO (Tavormina *et al.*, 2011). Unlike the CAB gene order of the *pmo* operon the *pxm* operon shows an ABC gene order. The presence of sequence-divergent copies suggests alternative physiological function under different environmental conditions. *Methylocystis* sp. strain SC2 was shown to possess two pMMO isozymes, encoded by *pmoCAB1* and *pmoCAB2* operons. The *pmoCAB1* operon was expressed by strain SC2 at mixing ratios > 600 ppmv CH₄, while growth and concomitant oxidation of methane at concentrations < 600-700 ppmv was due to the expression of *pmoCAB2* (Baani & Liesack, 2008). In this case the methane concentration seems to control the up- and down-regulation of the different pMMO's.

The second step in CH₄ oxidation pathway is the conversion of methanol to formaldehyde by methanol dehydrogenase. Methanol dehydrogenase activity in strain SolV could be demonstrated but the gene cluster encoding this activity seems to be rather different compared to proteobacterial methanotrophs. The *mxoFJGIRSACKLDEHB* cluster encoding the methanol dehydrogenase (*mxoF*), a cytochrome (*mxoG*), a solute binding protein (*mxoJ*) and accessory proteins (Chen *et al.*, 2010; Chistoserdova *et al.*, 2003; Ward *et al.*, 2004) was absent in the verrucomicrobial methanotrophs (Hou *et al.*, 2008; Khadem *et al.*, 2012 b) and found to be replaced by a *mxoFJG* operon. In addition the gene cluster *pqqABCDEFG* encoding proteins involved in biosynthesis of the methanol dehydrogenase cofactor pyrroloquinoline quinone was present. The expression of these genes did not vary much under the conditions tested (Table 2 and Fig. 2).

Formaldehyde, the product from the methanol dehydrogenase, is a key intermediate in methanotrophs. It may be oxidized for energy and detoxification, or fixed into cell carbon via the ribulose monophosphate pathway (RuMP) or serine cycle (see below, Chistoserdova *et al.*, 2009; Hanson & Hanson, 1996). The canonical formaldehyde oxidation pathway requires folate as a cofactor for C1 transfer and formate dehydrogenase complexes (see below). The classical gene *folA* involved in the last step of folate-biosynthesis (encoding dihydrofolate reductase) is absent in “*Ca. Methylacidiphilum*” strains V4 and SolV. Hou *et al.* (2008) suggested that the role of this enzyme could be taken over by an alternative dihydropteroate synthase (FolP). The gene encoding for this enzyme was also present in strain SolV and was constitutively expressed at RPKM values of 133 to

236. The presence of the *folD* gene in the “*Ca. Methylacidiphilum*” strains (V4 and SolV) and expression data of this gene in strain SolV (Table 2), indeed suggest that conversion of formaldehyde is tetrahydrofolate-dependent. The “archaeal” tetrahydromethanopterin cofactor-based pathway for C1 transfer found in other methylotrophs is not present in the genomes of the “*Ca. Methylacidiphilum*” strains (Hou *et al.*, 2008; Khadem *et al.*, 2012 b).

Formaldehyde can also directly be oxidized by a formaldehyde dehydrogenase. The genome data of strain SolV reveal several candidates for formaldehyde oxidation: a NADPH:quinone reductase (or related Zn-dependent oxidoreductases), Zn-dependent alcohol dehydrogenases or the NAD-dependent aldehyde dehydrogenases. The genes encoding for these enzymes were expressed under all conditions tested (Table 2). A role for these enzymes should be further supported by enzyme purification and characterization studies. Genes encoding for soluble and membrane bound NAD-dependent formate dehydrogenases were also predicted from the draft genome of strain SolV and their expression levels were not significantly different under all experimental conditions (Table 2). This enzyme performs the last step of CH₄ oxidation, converting formate into CO₂.

Table 2. Transcription of genes involved in oxidation of CH₄ in “*Ca. M. fumariolicum*” strain SolV

Enzyme	Gene name	GenBank identifier	Expression level (RPKM)		
			Cells at μ_{max}	N ₂ fixing cells	O ₂ limited cells
Methane monooxygenase_1	<i>pmoC1</i>	Mfum_790003	90	14764	25054
	<i>pmoA1</i>	Mfum_790002	37	4148	11804
	<i>pmoB1</i>	Mfum_790001	181	16550	20004
Methane monooxygenase_2	<i>pmoC2</i>	Mfum_780001	45059	1405	1087
	<i>pmoA2</i>	Mfum_770004	10994	454	598
	<i>pmoB2</i>	Mfum_770003	10930	467	712
	<i>pmoC3</i>	Mfum_480006	253	148	101
Methane monooxygenase_3	<i>pmoA3</i>	Mfum_480005	45	44	24
	<i>pmoB3</i>	Mfum_480007	21	17	15
	<i>mxoF/xoxF</i>	Mfum_190005	5945	2434	7554
Methanol dehydrogenase					
Periplasmic binding protein	<i>mxoJ</i>	Mfum_190004	941	1548	629
Cytochrome c family protein	<i>mxoG</i>	Mfum_190003	760	513	522
Coenzyme PQQ synthesis proteins	<i>pqqB</i>	Mfum_80011	483	288	677
	<i>pqqC</i>	Mfum_80010	589	645	1243
	<i>pqqD</i>	Mfum_710019	32	26	55

Table 2 proceeds on next page.

Table 2. Transcription of genes involved in oxidation of CH₄ in “*Ca. M. fumariolicum*” strain SolV (continuation)

Enzyme	Gene name	GenBank identifier	Expression level (RPKM)		
			Cells at μ_{max}	N ₂ fixing cells	O ₂ limited cells
NADPH:quinone reductase	<i>pqqD</i>	Mfum_80009	108	118	195
	<i>pqqE</i>	Mfum_80008	525	1078	766
	<i>pqqF</i>	Mfum_690050	527	339	737
	<i>qor1</i>	Mfum_270035	330	236	1092
	<i>qor2</i>	Mfum_300032	608	690	509
Zn-dependent alcohol dehydrogenase	<i>qor3</i>	Mfum_820025	117	77	128
	<i>adhP1</i>	Mfum_310051	216	397	218
	<i>adhP2</i>	Mfum_680019	165	96	196
Aldehyde dehydrogenase	<i>dhaS1</i>	Mfum_940074	58	68	73
	<i>dhaS2</i>	Mfum_840001	1345	1008	1337
7,8-dihydropteroate synthase	<i>folP1</i>	Mfum_690066	199	162	236
	<i>folP2</i>	Mfum_940066	163	236	133
Formate-tetrahydrofolate ligase	<i>fhs</i>	Mfum_300027	286	279	371
Bifunctional protein	<i>folD</i>	Mfumv1_210029	162	89	112
GTP cyclohydrolase	<i>folE</i>	Mfumv1_990006	993	501	1135

Table 2 proceeds on next page.

Table 2. Transcription of genes involved in oxidation of CH₄ in “*Ca. M. fumariolicum*” strain SolV (continuation)

Enzyme	Gene name	GenBank identifier	Expression level (RPKM)		
			Cells at μ_{\max}	N ₂ fixing cells	O ₂ limited cells
Formate dehydrogenase	<i>fdsA</i>	Mfumv1_80015	987	645	763
	<i>fdsB</i>	Mfumv1_80014	675	905	520
	<i>fdsC</i>	Mfumv1_80013	298	75	182
	<i>fdsD</i>	Mfumv1_80016	313	260	62
Formate dehydrogenase	<i>fdh</i>	Mfumv1_50001	233	186	257
Methylamine dehydrogenase	<i>mauA</i>	Mfumv1_700106	45	24	101
	<i>mauB</i>	Mfumv1_700109	220	199	168

The mRNA expression is expressed as RPKM according to Mortazavi *et al.* (2008). Changes in expression in the chemostat cultures (N₂ fixing cells or O₂ limited cells) compared to batch culture cells growing at μ_{\max} are indicated by shading: up-regulation > 2 times (dark grey), down-regulation < 0.5 (light grey).

Carbon metabolism

Carbon fixation

The genome data of the verrucomicrobial methanotrophs (Hou *et al.*, 2008; Khadem *et al.*, 2012 b) showed differences in carbon assimilation compared to proteobacterial methanotrophs (Chistoserdova *et al.*, 2009). Analyses of the draft genome of “*Ca. Methylophilum fumariolicum*” strain SolV revealed that the key genes needed for an operational RuMP pathway, hexulose-6-phosphate synthase and hexulose-6-phosphate isomerase were absent. In addition, the crucial genes encoding key enzymes of the serine pathway, malyl coenzyme A lyase and glycerate kinase, were not found (Khadem *et al.*, 2011). However, all genes required for an active CBB cycle could be identified in the SolV genome. These genes were highly expressed in both chemostat cultures (Table 3), to levels identical to those of cells in batch cultures growing at μ_{\max} (Khadem *et al.*, 2011). The constitutive expression in all cell cultures was expected, assuming biomass carbon in strain SolV growing on methane can only be derived from fixation of CO₂ via the CBB cycle (Khadem *et al.*, 2011). Our transcriptome data of the chemostat cultures and batch cultures showed low expression of the *cbbR* gene, encoding a possible RuBisCO operon transcriptional regulator. The *cbbR* gene product is a LysR-type transcriptional regulator and the key activator protein of *cbb* operons in facultative autotrophs (Bowien & Kusian, 2002). As an autotroph, strain SolV may not need much regulation of the CBB cycle genes. For strain V4 a coupling of this *cbbR* gene to nitrate reduction and transport was suggested (Hou *et al.*, 2008).

Although, the genes encoding for the ribulose-1,5-bisphosphate carboxylase/oxygenase (RuBisCO), the key enzyme of the CBB cycle was found in the genome of some proteobacterial methanotrophs like *M. capsulatus* Bath (Ward *et al.*, 2004) and *Methylocella silvestris* BL2 (Chen *et al.*, 2010) and the non-proteobacterial methanotroph “*Candidatus Methylophilum oxyfera*” (Ettwig *et al.*, 2010), autotrophic growth in liquid cultures has not been reported for these methanotrophs yet.

Carbohydrate metabolism

The presence and transcription of genes involved in the pentose phosphate pathway suggested the possibility of gluconeogenesis in strain SolV (Table 3). In *M. capsulatus* Bath, gluconeogenesis was suggested as follows: a putative phosphoketolase condenses pyruvate and glyceraldehyde-3-phosphate into xylulose-5-phosphate, which in turn is fed into the ribulose-5-phosphate pool for formation of glucose-6-phosphate through the pentose phosphate pathway (Ward *et al.*, 2004). Since a putative phosphoketolase is also present and expressed in strain SolV, gluconeogenesis might take place in the same way. Another possibility for the production of glucose-6-phosphate from glyceraldehyde-3-phosphate would be the consecutive action of triosephosphate-isomerase, fructose 1,6-bisphosphate aldolase, fructose 1,6-bisphosphate phosphatase and glucose-6-phosphate isomerase. All genes encoding these enzymes are expressed under the growth conditions tested (Table 3).

In many gammaproteobacterial methanotrophs, the tricarboxylic acid (TCA) cycle is believed to be incomplete, because they lack the α -ketoglutarate dehydrogenase activity (Hanson & Hanson, 1996). However in the *M. capsulatus* genome homologs of this enzyme were identified, suggesting that the TCA-cycle might operate in this microorganism (Ward *et al.*, 2004). Alphaproteobacterial methanotrophs are known to have a complete TCA cycle (Chen *et al.*, 2010; Dedysh *et al.*, 2002; Hanson & Hanson, 1996). The genes encoding for the TCA cycle enzymes were predicted from the genomes of strains V4 and SolV (Hou *et al.*, 2008; Khadem *et al.*, 2012 b). Our transcriptome analysis showed that these genes were expressed under the conditions applied, with slightly lower expression levels under N₂ fixing conditions (Table 4). The presence of an operational TCA cycle in strain SolV suggests that growth on two carbon compounds like acetate should be possible. The presence and transcription of a gene encoding acetyl-coenzyme A synthetase (*acs*), allows acetate to be activated and fed into the TCA cycle (Table 4). Three alphaproteobacterial genera; *Methylocella*, *Methylocapsa* and *Methylocystis*, which were shown to be able to grow or survive on acetate, also possess a TCA cycle (Belova *et al.*, 2011; Dedysh *et al.*, 2005; Dunfield *et al.*, 2010; Semrau *et al.*, 2011).

Table 3. Transcription of genes involved in carbon fixation and the pentose phosphate pathway in “*Ca. M. fumariolicum*” strain SolV

Enzyme	Gene name	GenBank identifier	Expression level (RPKM)		
			Cells at μ_{\max}	N ₂ fixing cells	O ₂ limited cells
6-Phosphogluconolactonase	<i>nagB</i>	Mfum_380003	166	70	285
Glucose-6-phosphate isomerase	<i>pgi</i>	Mfum_180006	218	156	112
Ribose-5-phosphate-3-epimerase	<i>rpe</i>	Mfum_830014	238	227	335
Transaldolase	<i>mipB</i>	Mfum_70005	279	301	256
Phosphoketolase	<i>xfp</i>	Mfum_200044	326	253	302
Transaldolase	<i>mipB</i>	Mfum_120006	380	205	187
Glucose-6-phosphate 1-dehydrogenase	<i>zwf</i>	Mfum_380002	569	478	469
Triosephosphate isomerase	<i>tpiA</i>	Mfum_170033	587	428	522
Fructose-1,6-bisphosphatase II	<i>glpX</i>	Mfum_1080012	591	670	750
6-Phosphogluconate dehydrogenase	<i>gnd</i>	Mfum_1020039	610	334	411
Glucose-6-phosphate 1-dehydrogenase	<i>zwf</i>	Mfum_1020106	686	302	794
Ribose 5-phosphate isomerase B	<i>rpiB</i>	Mfum_1020038	752	335	1250
Phosphoribulokinase, chromosomal	<i>cfxP</i>	Mfum_280006	829	682	662
Phosphoglycerate kinase	<i>pgk</i>	Mfum_170032	891	1066	671
Fructose-1,6-bisphosphatase class I	<i>fbp</i>	Mfum_280007	1174	974	1078

Table 3 proceeds on next page.

Table 3. Transcription of genes involved in carbon fixation and the pentose phosphate pathway in “*Ca. M. fumariolicum*” strain SolV (continuation)

Enzyme	Gene name	GenBank identifier	Expression level (RPKM)		
			Cells at μ_{\max}	N ₂ fixing cells	O ₂ limited cells
Phosphoribulokinase	<i>udk</i>	Mfum_70009	1798	938	1300
Glyceraldehyde-3-phosphate dehydrogenase	<i>cbbG</i>	Mfum_170031	1830	483	926
Fructose-bisphosphate aldolase	<i>fbaA</i>	Mfum_310038	2016	1688	1917
Transketolase (TK)	<i>cbbT</i>	Mfum_70010	2119	1527	2448
Protein CbxX	<i>cbbX</i>	Mfum_70008	6882	2807	8188
Ribulose biphosphate carboxylase small subunit	<i>cbbS</i>	Mfum_70007	7200	3606	6693
Ribulose biphosphate carboxylase large subunit	<i>cbbL</i>	Mfum_70006	10209	7348	8567
RuBisCO operon transcriptional regulator CbbR	<i>lysR</i>	Mfum_140011	47	41	28
Carbonic anhydrase	<i>cynT</i>	Mfum_890009	1832	2022	851
Ribose-phosphate pyrophosphokinase	<i>prs</i>	Mfum_870060	1105	1091	1055

The mRNA expression is expressed as RPKM according to Mortazavi *et al.* (2008). Changes in expression in the chemostat cultures (N₂ fixing cells or O₂ limited cells) compared to batch culture cells growing at μ_{\max} are indicated by shading: up-regulation > 2 times (dark grey), down-regulation < 0.5 (light grey).

Table 4. Transcription of genes involved in the TCA cycle in “*Ca. M. fumariolicum*” strain SolV

Enzyme	Gene name	GenBank identifier	Expression level (RPKM)		
			Cells at μ_{\max}	N ₂ fixing cells	O ₂ limited cells
Pyruvate 2-oxoglutarate dehydrogenase complex (E1), alpha subunit	<i>acoA</i>	Mfum_180024	1016	891	813
Pyruvate 2-oxoglutarate dehydrogenase complex (E1), beta subunit	<i>acoB</i>	Mfum_180023	922	937	987
Pyruvate 2-oxoglutarate dehydrogenase complex, dihydroliipoamide acyltransferase (E2)	<i>aceF</i>	Mfum_180020	877	813	297
Pyruvate 2-oxoglutarate dehydrogenase complex, dihydroliipoamide dehydrogenase (E3)	<i>lpdI</i>	Mfum_180019	478	241	322
	<i>lpd 2</i>	Mfum_720053	121	42	103
Succinate dehydrogenase flavoprotein subunit	<i>sdhA</i>	Mfum_300009	419	359	256
Succinate dehydrogenase catalytic subunit	<i>sdhB</i>	Mfum_300008	177	84	231
Succinate dehydrogenase cytochrome b subunit	<i>sdhC</i>	Mfum_300010	185	72	59
Succinyl-CoA synthetase subunit beta	<i>sucC</i>	Mfum_170019	279	227	214
Succinyl-CoA ligase [ADP-forming] subunit alpha	<i>sucD</i>	Mfum_170018	831	1248	751
Pyruvate kinase	<i>pykF1</i>	Mfum_940089	155	86	130
	<i>pykF2</i>	Mfum_990021	630	382	499
6-Phosphofructokinase	<i>pfkA</i>	Mfum_920021	413	288	540

Table 4 proceeds on next page.

Table 4. Transcription of genes involved in the TCA cycle in “*Ca. M. fumariolicum*” strain SolV (continuation)

Enzyme	Gene name	GenBank identifier	Expression level (RPKM)		
			Cells at μ_{\max}	N ₂ fixing cells	O ₂ limited cells
Deoxyribose-phosphate aldolase	<i>deoC</i>	Mfum_850005	100	44	92
Enolase	<i>eno</i>	Mfum_310014	1540	2423	1136
Fumarate hydratase class II	<i>fumC</i>	Mfum_220008	192	146	156
Phosphoenolpyruvate carboxykinase [ATP]	<i>pckA</i>	Mfum_200061	250	227	161
Isocitrate dehydrogenase [NADP]	<i>icd</i>	Mfum_200008	242	154	122
Aconitate hydratase	<i>acn</i>	Mfum_170037	343	170	156
Phosphoglycerate mutase (PhoE family)	<i>phoE</i>	Mfum_70011	530	282	306
Citrate synthase	<i>gltA</i>	Mfum_260030	830	404	368
Acyl-CoA synthetase (AMP forming)	<i>acs</i>	Mfum_1020005	448	297	414
Acetate kinase	<i>ackA</i>	Mfum_310026	256	180	161

The mRNA expression is expressed as RPKM according to Mortazavi *et al.* (2008). Changes in expression in the chemostat cultures (N₂ fixing cells or O₂ limited cells) compared to batch culture cells growing at μ_{\max} are indicated by shading: up-regulation > 2 times (dark grey), down-regulation < 0.5 (light grey).

Potential carbon & energy storage

Many bacteria start to accumulate reserve polymers when enough supply of suitable carbon is available, but nitrogen is limited (Wanner & Egli, 1990). This phenomenon is also known for methanotrophs (Pieja *et al.*, 2011b). Recently it was shown that type II methanotrophs contained the gene *phaC*, which encodes for the poly-3-hydroxybutyrate (PHB) synthase enable them to produce PHB (Pieja *et al.*, 2011b). At least three genes (*phaC*, *phaA*, *phaB*) were considered to be crucial for PHB synthesis. These genes are absent in type I methanotrophs and in the “*Ca. Methylacidiphilum*” strains (Hou *et al.*, 2008; Khadem *et al.*, 2012 b). However, genes encoding for glycogen synthesis, degradation and transport (glycogen synthase, glycogen debranching enzyme and ADP-glucose pyrophosphorylase) were predicted based on the draft genome of strain SolV. These genes were expressed under all conditions tested (Table 5). This supports the ability of carbon storage by strain SolV, but further physiological studies with cells growing under excess of carbon and nitrogen limitation are needed. Thus far literature on glycogen synthesis in methanotrophs is sparse, but several of the publicly available genomes (<http://www.ncbi.nlm.nih.gov/genomes>) of proteobacterial methanotrophs contain glycogen synthesis genes (*M. capsulatus* Bath, *Methylomonas methanica* MC09, *Methylomicrobium alcaliphilum* and *Methylocystis* sp. ATCC 49242).

The presence and constitutive expression of genes involved in phosphate transport, polyphosphate synthesis and utilization (ABC-type phosphate transport system, polyphosphate kinase, adenylate kinase and exopolyphosphatase) (Table 5) suggest that strain SolV is able to store polyphosphate as energy and phosphorus reserve.

Table 5. Transcription of genes involved in carbon and energy storage in “*Ca. M. fumariolicum*” strain SolV

Enzyme	Gene name	GenBank identifier	Expression level (RPKM)		
			Cells at μ_{\max}	N ₂ fixing cells	O ₂ limited cells
Glycogen synthase 2	<i>glgA</i>	Mfum_1010040	306	242	346
1,4-alpha-glucan-branching enzyme	<i>glgB</i>	Mfum_170041	154	91	110
Malto-oligosyltrehalose trehalohydrolase	<i>glgB</i>	Mfum_170046	162	128	81
Glucose-1-phosphate adenylyltransferase	<i>glgC</i>	Mfum_1020013	391	158	416
Glucan phosphorylase	<i>glgP1</i>	Mfum_1020098	656	447	843
	<i>glgP2</i>	Mfum_220010	113	98	122
	<i>glgP3</i>	Mfum_880004	447	382	450
	<i>glgX</i>	Mfum_40003	381	218	263
	<i>gdb</i>	Mfum_200059	256	246	106
Glycogen debranching enzyme					
ABC-type phosphate transport system, permease	<i>pstA</i>	Mfum_300005	81	45	98
Phosphate import ATP-binding protein	<i>pstB</i>	Mfum_300006	137	99	249
ABC-type phosphate transport system, permease	<i>pstC</i>	Mfum_300004	72	35	83
ABC-type phosphate transport system, periplasmic component	<i>pstS</i>	Mfum_300003	108	97	129
Exopolyphosphatase	<i>gppA1</i>	Mfum_1010048	581	430	486

Table 5 proceeds on next page.

Table 5. Transcription of genes involved in carbon and energy storage in “*Ca. M. fumariolicum*” strain SoIV (continuation)

Enzyme	Gene name	GenBank identifier	Expression level (RPKM)		
			Cells at μ_{\max}	N ₂ fixing cells	O ₂ limited cells
Polyphosphate kinase	<i>gpp42</i>	Mfum_1020105	101	63	101
	<i>ppk</i>	Mfum_1030014	266	206	197
Exopolysphatase-related protein		Mfum_550017	506	283	404
Adenylate kinase	<i>adk</i>	Mfum_210014	247	88	170

The mRNA expression is expressed as RPKM according to Mortazavi *et al.* (2008). Changes in expression in the chemostat cultures (N₂ fixing cells or O₂ limited cells) compared to batch culture cells growing at μ_{\max} are indicated by shading: up-regulation > 2 times (dark grey), down-regulation < 0.5 (light grey).

Nitrogen metabolism

Ammonium, nitrate & amino acid metabolism

Based on the genome and supported by the transcriptome data the main route for ammonium assimilation in “*Ca. M. fumariolicum*” occurs via glutamine synthase (*glnA*)/glutamate synthase (*gltB*) and/or the alanine and glutamate dehydrogenases (*ald*, *gdh*). Expression values of *ald* and *gdh* were about 3 to 5 fold lower compared to *glnA* and *gltB* under the conditions tested (Table 6). Also the genes encoding the glutamine-hydrolyzing carbamoyl-phosphate synthase (*carA* and *carB*) were constitutively expressed. This enzyme converts glutamine and carbon dioxide into glutamate and carbamoyl-phosphate. The latter substrate can be fed into the urea cycle. Except for the gene encoding arginase all other genes (*argDHFG*) encoding enzymes of the urea cycle were present and constitutively expressed. The most likely function of this partial cycle will be arginine synthesis. For strain V4 it was suggested that the ornithine needed can be supplied by 4-aminobutyrate aminotransferase through a part of the TCA cycle and glutamate synthesis (Hou *et al.*, 2008). In strain SolV, the gene encoding 4-aminobutyrate aminotransferase is also present and expressed. Other methylotrophs possess neither arginase nor *ArgD* (Hou *et al.*, 2008).

The genes encoding nitrate/nitrite transporters and the assimilatory nitrite and nitrate reductases showed very low expression levels (8 to 117), probably due to the absence of nitrate in the growth media used. The ammonium transporter gene (*amtB* type) is 3-4 fold up-regulated in N₂ fixing cells, which reflects increased ammonium scavenging under nitrogen limited conditions.

Nitrogen fixation

The genomes of strain SolV and strain V4 show a complete set of genes necessary for N₂ fixation (Hou *et al.*, 2008; Khadem *et al.*, 2012 b). Most of these genes and their organization in putative operons resemble those of *M. capsulatus* Bath (Ward *et al.*, 2004), a gammaproteobacterial methanotroph that has been shown to fix atmospheric N₂ (Oakley & Murrell, 1991). N₂ fixation is widely distributed among methanotrophs as shown by the presence of both *nifH* gene

fragments and acetylene reduction activity in a variety of alpha- and gammaproteobacterial methanotrophic strains (Auman *et al.*, 2001). Also the deep-sea anaerobic methane-oxidizing Archaea were shown to fix N₂ and share the products with their sulfate-reducing bacterial symbionts (Dekas *et al.*, 2009).

Gene expression data of strain SolV showed that all the genes involved in nitrogen fixation were up-regulated only in absence of ammonium and nitrate, indicating the effect of nitrogen availability on the expression of these genes (Table 7). The genes encoding for the nitrogenase (*nifH*, *nifD*, *nifK*) were 100 to 325-fold up-regulated, while the gene involved in regulation (*nifA*) and the Fe/Mo cofactor biosynthesis genes showed 30 to 235-fold increased expression levels. Our previous physiological studies already confirmed that nitrogenase was active in N₂ fixing chemostat cultures (Khadem *et al.*, 2010).

Growth on atmospheric nitrogen in the chemostat was only observed when the dO₂ was below 0.5 % oxygen saturation. Our previous batch incubations in the presence of ammonium and 0.5 % O₂ saturation resulted in doubling time of 10 h (Khadem *et al.*, 2010). This indicates that in N₂ fixing chemostat cultures, this low oxygen was not growth limiting. Maintaining a low oxygen concentration in both batch and chemostat is required for an active nitrogenase, since this enzyme is irreversibly damaged by O₂ (Robson & Postgate, 1980). Low oxygen requirement for N₂ fixation was also demonstrated for other proteobacterial methanotrophs (Dedysh *et al.*, 2004; Murrell & Dalton, 1983; Takeda, 1988). The effect of high oxygen concentration on the expression of genes encoding N₂ fixing enzymes, in absence of ammonium/nitrate still needs to be addressed in strain SolV.

Methanotrophic hydrogenases are considered to have a role in N₂ fixation or CH₄ oxidation. The role of hydrogenase as a source of reducing power for CH₄ oxidation was demonstrated in *M. capsulatus* Bath (Hanczár *et al.*, 2002). Hydrogen uptake and evolution activities during N₂ fixation were reported for strain 41 of the *Methylosinus* type (De Bont, 1976) and *Methylocystis* T-1 (Takeda, 1988), respectively. However, knock out studies of *ΔhupSL* encoding for the large and small subunit of the Ni/Fe-dependent hydrogenase in *M. capsulatus* Bath, did not show differences in viability under nitrogen fixing and non-nitrogen fixing conditions in comparison to the wild type strain (Caski *et al.*, 2001). Based on these results, the authors suggested that the hydrogenase is probably regulated by oxygen availability rather than by the hydrogen generated by the nitrogenase

enzyme complex. Our expression data also show an increased expression under both nitrogen fixing and oxygen limited conditions (Table 7). Since under oxygen limitation the nitrogen fixing genes were not expressed, while the hydrogenase encoding genes were expressed to even higher levels, oxygen seems to be the regulatory factor for the latter set of genes.

The PII signal-transduction proteins (encoded by *glnB* and *glnK*) are used to transduce the nitrogen status of the cell to the NtrB-NtrC two-component regulatory system and the σ^{54} -dependent *amtB* promoters to tune *nif* gene transcription (for a detailed overview see Dixon & Kahn, 2004). The *glnB* gene of strain SolV was highly expressed under all conditions and slightly up-regulated (1.5 fold) under N₂ fixing conditions. Expression of *glnK* was overall about 5-fold lower than the expression of *glnB* and 3-fold down-regulated under nitrogen fixing conditions. In addition genes encoding for uridylyltransferase (*glnD*), NtrB and NtrC showed expression levels under the three conditions tested which did not significantly differ (Table 6). This suggests that in strain SolV the PII proteins are involved in sensing and regulating the status of fixed nitrogen in the cell.

Transcription of the *nif* genes is regulated by *nifA* and *nifL* genes (Dixon & Kahn, 2004). The expression of *nifA* is regulated by oxygen and/or fixed nitrogen and *nifL* gene is involved in oxygen sensing. We could not identify a *nifL* gene in the genome of strain SolV (Khadem *et al.*, 2012 b). However, *nifA* is present and was 30-fold up-regulated under N₂ fixing conditions.

Nitrogenase is believed to be sensitive for reactive oxygen species (ROS), and during nitrogen fixation the level of ROS is reduced by up-regulation of ROS-detoxifying genes. In *Gluconacetobacter diazotrophicus* up-regulation of these genes was observed during nitrogen fixation (Alquéres *et al.*, 2010). Although, in the genome of strain SolV two *sodA* genes encoding for superoxide dismutases can be identified, they both are highly expressed under all conditions tested (RPKM values: Mfum_810007, 797 ± 163 ; Mfum_980001, 961 ± 669), but expression seems to be 1.5 to 3 fold lower under N₂ fixing and O₂ limited conditions.

Nitrosative stress

The pMMO enzyme involved in the first step of CH₄ oxidation in methanotrophs, also oxidizes ammonium which results in the formation of the intermediate hydroxylamine (NH₂OH) (Hanson & Hanson, 1996; Nyerges & Stein, 2009 and references therein; Stein & Klotz, 2011). Ammonia-oxidizers can relay electrons from hydroxylamine oxidation to the quinone pool to drive energy production and cellular growth (Klotz & Stein, 2008), but methanotrophs lack this relay and cannot produce energy from this oxidation. Since hydroxylamine is a highly toxic intermediate, methanotrophs rely on mechanisms to quickly remove it. In their natural habitat the “*Ca. M. fumariolicum*” cells are confronted with varying nitrogen levels (1-28 mM (Khadem *et al.*, 2010)) which means that the cells have to balance assimilation and tolerance to reactive-N. Detoxification can be achieved by conversion of hydroxylamine back to ammonium or to nitrite through the use of a hydroxylamine reductase enzyme (HAO). The nitrite in turn can be converted to N₂O via NO by putative denitrifying enzymes (nitrite reductase and NO-reductase, Campbell *et al.*, 2011). Genes involved in these conversions may include *hao*, *cytL*, *cytS*, *nirB*, *nirD*, *nirS* or *nirK*, *norB* and *norC*. The genes *hao*, *norB* and *norC* were shown to be present in the genomes of the verrucomicrobial methanotrophs (Hou *et al.*, 2008; Khadem *et al.*, 2012 b), while a *nirK* homolog was only found in strain SolV. The gene inventory in methanotrophic bacteria for handling hydroxylamine or other toxic nitrosating intermediates and for those encoding putative denitrifying enzymes is diverse and unpredictable by phylotype or taxon (Stein & Klotz, 2011).

In our study we found that although expressed under all conditions tested, expression of *hao*, *norB* and *norC* were 1.5 to 4.5 fold lower under nitrogen fixing conditions (Table 6), which makes sense in view of the expected lower ammonium levels in the cells. However, for *nirK* expression was low (RPKM = 63 to 72) except for the cells grown under oxygen limitation (RPKM = 200).

Table 6. Transcription of genes involved in nitrogen metabolism in “*Ca. M. fumariolicum*” strain SolV

Enzyme	Gene name	GenBank identifier	Expression level (RPKM)		
			Cells at μ_{\max}	N ₂ fixing cells	O ₂ limited cells
Glutamine synthetase	<i>glnA</i>	Mfum_90015	1542	1052	725
Glutamine synthetase regulatory protein P-II	<i>glnB</i>	Mfum_90016	1039	1701	914
UTP:GlnB (Protein PII) uridylyltransferase	<i>glnD</i>	Mfum_230007	169	111	145
Nitrogen regulatory protein PII	<i>glnK</i>	Mfum_140026	166	60	203
Alanine dehydrogenase	<i>ald</i>	Mfum_290047	248	279	256
Glutamate dehydrogenase	<i>gdhA</i>	Mfum_810044	436	182	500
Glutamate synthase alpha chain	<i>gltB</i>	Mfum_940063	1343	1360	1355
Glutamate synthase beta chain	<i>gltD</i>	Mfum_270076	133	114	125
Ornithine/acetylornithine aminotransferase	<i>argDI</i>	Mfum_190040	736	736	410
Argininosuccinate lyase	<i>argD2</i>	Mfum_1010035	383	421	410
	<i>argH</i>	Mfum_970020	226	186	107
Ornithine carbamoyltransferase	<i>argF</i>	Mfum_1010036	286	267	375
Argininosuccinate synthase	<i>argG</i>	Mfum_270005	725	527	678
Carbamoyl-phosphate synthase small chain	<i>carA</i>	Mfum_270024	450	340	479
Carbamoyl-phosphate synthase large chain	<i>carB</i>	Mfum_700048	395	267	504

Table 6 proceeds on next page.

Table 6. Transcription of genes involved in nitrogen metabolism in “*Ca. M. fumariolicum*” strain SolV (continuation)

Enzyme	Gene name	GenBank identifier	Expression level (RPKM)		
			Cells at μ_{\max}	N ₂ fixing cells	O ₂ limited cells
Ammonium transporter	<i>amtB</i>	Mfum_430001_160001 ^a	343	1143	420
Nitrate ABC transporter, nitrate-binding protein	<i>tauA</i>	Mfum_140012	28	117	33
Nitrate transporter	<i>nasA</i>	Mfum_140017	22	26	16
Assimilatory nitrate reductase large subunit	<i>bisC</i>	Mfum_140014	13	14	8
Assimilatory nitrite reductase	<i>nirB</i>	Mfum_140015	14	40	13
Ferredoxin subunit of nitrite reductase	<i>nirD</i>	Mfum_140016	32	18	16
Signal transduction histidine kinase with PAS domain	<i>ntrB</i>	Mfum_920004	283	294	250
Signal transduction response regulator, NtrC family	<i>ntrC1</i>	Mfum_110018	90	76	67
	<i>ntrC2</i>	Mfum_170043	116	110	111
	<i>ntrC3</i>	Mfum_260013	623	361	525
	<i>ntrC4</i>	Mfum_920003	225	154	216
Hydroxylamine oxidoreductase	<i>haoA</i>	Mfum_970027	357	124	568
Nitric oxide reductase B subunit	<i>norB</i>	Mfum_970100	261	120	342
Nitric-oxide reductase subunit C	<i>norC</i>	Mfum_970099	192	93	139

^a Mfum_430001 and Mfum_160001 encode the N- and C-terminal part, respectively.

Table 6 proceeds on next page.

Table 6. Transcription of genes involved in nitrogen metabolism in “*Ca. M. fumariolicum*” strain SolV (continuation)

Enzyme	Gene name	GenBank identifier	Expression level (RPKM)		
			Cells at μ_{\max}	N ₂ fixing cells	O ₂ limited cells
Nitrite reductase (NO-forming)	<i>nirK</i>	Mfum_270071	72	63	200
DNA-binding response regulator, NarL family	<i>mxnB</i>	Mfum_1030004	232	74	142
DNA-binding response regulator, LuxR family	<i>citB1</i>	Mfum_790006	1760	5611	4679
DNA-binding response regulator, LuxR family	<i>citB2</i>	Mfum_580001	394	200	239

The mRNA expression is expressed as RPKM according to Mortazavi *et al.* (2008). Changes in expression in the chemostat cultures (N₂ fixing cells or O₂ limited cells) compared to batch culture cells growing at μ_{\max} are indicated by shading: up-regulation > 2 times (dark grey), down-regulation < 0.5 (light grey).

Table 7. Transcription of genes involved in nitrogen fixation in “*Ca. M. fumariolicum*” strain SolV

Enzyme	Gene name	GenBank identifier	Expression level (RPKM)		
			Cells at μ_{\max}	N ₂ fixing cells	O ₂ limited cells
Nitrogenase iron protein	<i>nifH</i>	Mfum_690040	69	22651	80
Nitrogenase molybdenum-iron protein alpha chain	<i>nifD</i>	Mfum_690039	87	14359	65
Nitrogenase molybdenum-iron protein beta chain	<i>nifK</i>	Mfum_690038	35	3348	34
Nitrogenase Mo/Fe cofactor biosynthesis protein NifE	<i>nifE</i>	Mfum_690037	77	5370	67
Nitrogenase Mo/Fe cofactor biosynthesis protein NifN	<i>nifN</i>	Mfum_690036	64	3677	52
Protein NifX	<i>nifX</i>	Mfum_690035	100	2831	26
Nif-specific regulatory protein	<i>nifA</i>	Mfum_690018	123	1080	109
Nitrogenase Mo/Fe cofactor biosynthesis protein NifB	<i>nifB</i>	Mfum_690029	19	3316	14
Pyruvate-flavodoxin oxidoreductase	<i>nifJ</i>	Mfum_940083	149	133	185
NifQ family protein	<i>nifQ</i>	Mfum_690020	65	270	22
Cysteine desulfurase	<i>nifS1</i>	Mfum_690022	93	801	87
	<i>nifS2</i>	Mfum_90010	159	133	116
	<i>nifS3</i>	Mfum_190023	681	491	486
	<i>nifS4</i>	Mfum_970062	162	275	145
	<i>nifS5</i>	Mfum_310028	226	151	264
NifU-like protein involved in Fe-S cluster formation	<i>nifU</i>	Mfum_310029	54	16	79

Table 7 proceeds on next page.

Table 7. Transcription of genes involved in nitrogen fixation in “*Ca. M. fumariolicum*” strain SolV (continuation)

Enzyme	Gene name	GenBank identifier	Expression level (RPKM)		
			Cells at μ_{\max}	N ₂ fixing cells	O ₂ limited cells
Nitrogenase-stabilizing/protective protein NifW	<i>nifW</i>	Mfum_690011	62	2260	43
	<i>nifZ</i>	Mfum_690023	158	1373	50
Electron transfer flavoprotein beta chain	<i>fixA</i>	Mfum_690010	60	3311	73
Electron transfer flavoprotein alpha chain	<i>fixB</i>	Mfum_690009	81	3043	69
Flavoprotein-ubiquinone oxidoreductase	<i>fixC</i>	Mfum_690008	101	3632	100
Ferredoxin-like protein	<i>fixX</i>	Mfum_690007	126	2917	135
Nitrogen fixation protein FixU	<i>fixU</i>	Mfum_690015	164	2265	91
Fe-S cluster assembly scaffold protein, HesB/SufA family	<i>sufA1</i>	Mfum_690026	40	2301	22
	<i>sufA2</i>	Mfum_810040	149	43	71
	<i>sufA3</i>	Mfum_1020116	214	143	183
FeS cluster assembly protein SufB	<i>sufB</i>	Mfum_970056	1099	2409	622
FeS cluster assembly protein SufD	<i>sufD</i>	Mfum_970057	663	2169	279
FeS cluster assembly protein SufE family	<i>sufE</i>	Mfum_110022	375	209	219
FeS4 cluster protein with leucine rich repeats		Mfum_690024	88	1884	61
Ferredoxin-like protein in <i>nif</i> region	<i>frxA</i>	Mfum_690027	112	7892	46
Uptake hydrogenase large subunit	<i>hupB</i>	Mfum_50004	92	372	1840

Table 7 proceeds on next page.

Table 7. Transcription of genes involved in nitrogen fixation in “*Ca. M. fumariolicum*” strain SoIV (continuation)

Enzyme	Gene name	GenBank identifier	Expression level (RPKM)		
			Cells at μ_{\max}	N ₂ fixing cells	O ₂ limited cells
Uptake hydrogenase small subunit	<i>hupS</i>	Mfum_50003	186	997	2955
Nickel/iron-hydrogenase I, small subunit	<i>hyaA</i>	Mfum_870019	2380	4157	4280
Nickel/iron-hydrogenase I, large subunit	<i>hyaB</i>	Mfum_870018	2566	1879	3595
Ni,Fe-hydrogenase I cytochrome b subunit	<i>hyaC</i>	Mfum_50005	122	593	984
[NiFe] hydrogenase Ni incorporation protein HypA	<i>hypA</i>	Mfum_730023	119	110	95
[NiFe] hydrogenase Ni incorporation-associated protein HypB	<i>hypB</i>	Mfum_870009	421	335	692
[NiFe] hydrogenase metallocenter assembly protein HypC	<i>hypC</i>	Mfum_870006	830	600	321
[NiFe] hydrogenase expression/formation protein HypD	<i>hypD</i>	Mfum_870005	1159	893	1246
[NiFe] hydrogenase metallocenter assembly protein HypE	<i>hypE</i>	Mfum_870004	424	476	759
[NiFe] hydrogenase metallocenter assembly protein HypF	<i>hypF</i>	Mfum_870007	92	81	167
Hydrogenase expression protein HupH	<i>hupH</i>	Mfum_50006	160	631	879
Hydrogenase expression/formation protein HoxQ	<i>hoxQ</i>	Mfum_730017	177	169	136
Hydrogenase maturation protease	<i>hycI</i>	Mfum_730022	69	44	89

The mRNA expression is expressed as RPKM according to Mortazavi *et al.* (2008). Changes in expression in the chemostat cultures (N₂ fixing cells or O₂ limited cells) compared to batch culture cells growing at μ_{\max} are indicated by shading: up-regulation > 2 times (dark grey), down-regulation < 0.5 (light grey).

Conclusion

In this study we analyzed the genome wide changes in expression during three different growth conditions which helped very much to understand the physiology of “*Ca. Methylacidiphilum fumariolicum*” strain SolV.

The analysis indicated that the two of the three *pmoCAB* operons are probably regulated by oxygen, although the effect of other factors like growth rate, cell density can not be excluded. The results point to a regulation of the *pmoCAB1/pmoCAB2* genes by the oxygen concentration.

Further, the hydrogen produced during N₂ fixation can be recycled, and that nitrosative stress is counter acted.

The obtained information will be a guide to design future physiological and biochemical studies.

Acknowledgments

Ahmad F. Khadem was supported by Mosaic grant 62000583 from the Netherlands Organisation for Scientific Research (NWO).

Mike S. M. Jetten is supported by European Research Council, grant number 232937.

Supplementary material

The supplementary material for this chapter (article) can be found online at:

http://www.frontiersin.org/Evolutionary_and_Genomic_Microbiology/10.3389/fmicb.2012.00266/abstract

File S1. Housekeeping genes to test robustness of transcriptome data.

File S2. RNA-Seq analysis of “*Ca. Methylacidiphilum fumariolicum*” SolV grown under different conditions.

Chapter Seven

Summary & outlook



Picture by Ahmad F. Khadem.

Summary & Outlook

Methane (CH₄) is an important fossil fuel for households and industry, but also a trace gas in the atmosphere (Forster *et al.*, 2007; Houghton *et al.*, 1996). Methane shows a strong infrared absorption and the atmospheric methane directly affects the climate as a greenhouse gas, being 20 times more effective than carbon dioxide (CO₂) (Denman *et al.*, 2007; Shindell *et al.*, 2009). Global warming is a worldwide concern and therefore it is important to increase knowledge of sources and sinks for methane. In addition complete knowledge of the global element cycles in marine, soil and aquatic habitats is especially important in the assessment of the future consequences of human impact on ecosystems worldwide (Conrad, 1996).

Methane is emitted to the atmosphere from natural ecosystems (wetlands, ruminants, termites) or as a result of anthropogenic activities (rice paddies, landfills, coal mining). It is produced by methanogenic Archaea during decomposition of organic matter under anaerobic conditions (Schink, 1997; Thauer, 1998). In addition to this biogenic production, significant amounts of geological methane, produced within the Earth's crust, are released to the atmosphere. Emissions from geothermal areas like seeps, mud volcanoes, mud pots and fumaroles add up to an annual production of 45-75 Tg methane (Castaldi & Tedesco, 2005; Kvenvolden & Rogers, 2005). Although the concentration of methane in the atmosphere has been steadily increasing over the past 300 years, it is maintained at a low level considering the amounts of methane produced.

Methane-oxidizing microbes (also known as methanotrophs, see below) are assumed to be the major players in keeping the methane balance on our planet. Fundamental knowledge about methanotrophic bacteria is important since they are sinks for methane diffusing from both biogenic (degradation of organic matter) and abiogenic (seeps and geothermal areas) sources. They form a biofilter reducing methane emissions to the atmosphere. This makes them targets in strategies to combat global climate change. In addition, methanotrophic bacteria can be applied to treat odorous air streams and the methane monooxygenases of methanotrophs have unique ability to catalyze reactions of environmental and perhaps commercial importance (Semrau *et al.*, 2011).

The discovery of the verrucomicrobial aerobic methanotrophs

Methanotrophy occurs under both anaerobic and aerobic conditions. Anaerobic oxidation can be performed by consortia of methane-oxidizing Archaea and sulfate-reducing bacteria or nitrite-reducing bacteria (Boetius *et al.*, 2000; Ettwig *et al.*, 2008; Raghoebarsing *et al.*, 2006; Valentine & Reeburgh, 2000).

The obligate aerobic methanotrophs form a unique group of bacteria which utilize methane as sole source of energy and carbon (Hanson & Hanson, 1996). Until 2007, the phylogenetic distribution of the aerobic methanotrophs was limited to the *Alphaproteobacteria* and *Gammaproteobacteria* (Hanson & Hanson, 1996). Proteobacterial aerobic methanotrophs are widespread in natural environments (such as fresh and marine waters and sediments, soils and rice paddies) where they feed on the methane produced by methanogens in the anoxic zones of these environments. Most of them are neutrophilic or mesophilic (Trotsenko & Khmelenina, 2002; Tsubota *et al.*, 2005; Dedysh *et al.*, 2000; Dedysh *et al.*, 2002; Dedysh *et al.*, 2007).

Very recently (late 2007 to early 2008), aerobic methanotrophs belonging to the *Verrucomicrobia* phylum were isolated from the Solfatara at Pozzuoli near Naples (Italy), Hell's Gate, Tikitere (New Zealand) and Uzon Caldera, Kamchatka, (Russia) (Dunfield *et al.*, 2007; Islam *et al.*, 2008; Pol *et al.*, 2007). For these novel thermoacidophilic aerobic methanotrophs, the genus name *Methylocidiphilum* was proposed (Op den Camp *et al.*, 2009). So far the *Methylocidiphilum* genus is represented by three strains; *Methylocidiphilum fumariolicum* strain SolV, *Methylocidiphilum infernorum* strain V4 and *Methylocidiphilum kamchatkense* strain Kam1. All three strains are well adapted to the harsh volcanic environment (Op den Camp *et al.*, 2009; Pol *et al.*, 2007), being able to thrive at very low methane and oxygen concentrations and pH values as low as 1. This exciting discovery was a complete surprise to most microbiologists. It has revealed that the ability of bacteria to oxidize methane is much more diverse than has previously been assumed in terms of ecology, phylogeny and physiology (Hanson & Hanson, 1996). In addition, this discovery showed that natural geological sources such as mud volcanoes are also important sinks for methane. It was the first time that representatives of the widely distributed *Verrucomicrobia* phylum were coupled to a geochemical cycle. The verrucomicrobial aerobic methanotrophs may be

significant players in geochemical carbon cycling. Because the discovery of these microbes is very recent their potential is still unexplored and they will harbor biochemically very exciting pathways.

This thesis focuses on the biochemistry and physiology of one of the verrucomicrobial aerobic methanotrophs, *Methylophilum fumariolicum* strain SolV. In this study several approaches like genomics, electron microscopy, mRNA analyses, ¹³C-labelling experiments etc., were combined to unravel the metabolism of strain SolV in molecular detail.

The draft genome of *Methylophilum fumariolicum* SolV

Although the biodiversity within the *Verrucomicrobia* phylum is assumed to be very large, little is known about their physiology and only ten genome sequences are available, including those of *M. infernorum* strain V4 and the draft genome of *M. fumariolicum* strain SolV (Hou *et al.*, 2008; Khadem *et al.*, 2012 b; van Passel *et al.*, 2011; Wagner & Horn, 2006).

In **Chapter Two** of this thesis, the draft genome of strain SolV was described. The nucleotide sequence of the genome of strain SolV was unraveled using Next Generation Sequencing technology. The genome analysis of strain SolV has shown that there are similarities but also differences between the verrucomicrobial and proteobacterial methanotrophs. If we look at the nitrogen metabolism we see that both types of methanotrophs contain genes involved in nitrogen (N₂) fixation. In the area of the carbon metabolism, we see more differences. In the genome of strain SolV, three different operons (*pmoCAB*) encoding the three subunits of membrane-bound methane monooxygenases (pMMO) has been identified, along with a different (uncommon) methanol dehydrogenase. The pMMO is a crucial enzyme involved in the first step of the methane oxidation pathway, the conversion of methane to methanol. It is known that proteobacterial methanotrophs are able to assimilate carbon for biomass production, starting from formaldehyde, a substance which is produced during the oxidation of methane. There are two pathways for the assimilation of this formaldehyde, the ribulose monophosphate (RuMP) pathway, in which all biomass is derived from formaldehyde and the serine pathway with biomass derived from carbon dioxide and formaldehyde. The essential genes that encode these two assimilation pathways were not found in the genome of strain

SolV. Instead, genes encoding for enzymes involved in the Calvin-Benson-Bassham (CBB) cycle were shown to be present in the genome. This suggested that strain SolV can fix carbon dioxide for biomass synthesis. Also, genes involved in carbon storage in the form of glycogen were identified. The genome data formed the basis for the physiological studies (Chapter three, four and five) and the transcriptome analyses (Chapter six).

N₂-fixation by *Methylocacidiphilum fumariolicum* SolV

Knowledge on atmospheric nitrogen (N₂) fixation by methanotrophs is needed to understand their role in nitrogen cycling in different environments. Based on genetic and biochemical evidence, N₂ fixation capabilities were shown to be broadly distributed among aerobic and anaerobic methanotrophs (Auman *et al.*, 2001; Dekas *et al.*, 2009).

Since *M. fumariolicum* SolV is a novel thermoacidophilic aerobic methanotroph, the aim of this study was to elucidate nitrogen fixation by this microorganism. In **Chapter Three**, nitrogen fixation by strain SolV is presented. In this study, growth experiments (in batch and chemostat), were combined with nitrogenase activity tests (acetylene reduction to ethylene), and phylogenetic analysis of the *nifD* genes (encoding the nitrogenase enzyme). The nitrogenase enzyme is responsible for breaking the N-N bond and the formation of ammonium (NH₄⁺), and is crucial for nitrogen fixation. The results showed that strain SolV can fix nitrogen in chemostat cultures only under low oxygen concentration (0.5 % dissolved oxygen) and in absence of ammonium. This low oxygen concentration was shown to be required for an optimal nitrogenase activity. Based on the acetylene (C₂H₂) assay and the growth experiments, the nitrogenase of strain SolV seems extremely oxygen sensitive compared to most proteobacterial methanotrophs. The activity of nitrogenase was not inhibited by ammonium concentrations up to 94 mM. This chapter is the first report on physiology of N₂ fixation within the *Verrucomicrobia* phylum.

CO₂ fixation by *Methylophilum fumariolicum* SolV

Carbon fixation by methanotrophs has been a topic of research for decades, and the assimilation via the CBB cycle by proteobacterial aerobic methanotrophs is unlikely, because CBB is associated with high ATP requirements (Chistoserdova *et al.*, 2009).

Chapter Four focusses on carbon dioxide fixation by strain SolV. For this study, strain SolV was grown in batch and chemostat cultures. The mRNA from the cells was used for a transcriptome analysis, while also ¹³C-labeling experiments and ribulose-1,5-bisphosphate carboxylase/oxygenase (RuBisCO, the first and key enzyme of the CBB cycle) activity tests were performed. To measure the activity of RuBisCO a stable isotope method was developed. The results showed that the genes involved in the CBB cycle, were highly expressed, especially the two genes encoding for the large and small subunits of RuBisCO. The ¹³C-labeling experiments showed clearly that carbon dioxide is the carbon source for strain SolV. The activity test of RuBisCO was only positive in the supernatant fraction of the cell-free extract, which indicates that the enzyme is a cytosolic protein, being not present in carboxysomes (organelles within the cell that are involved in carbon dioxide fixation). By making use of gel electrophoresis and size-exclusion chromatography, it was demonstrated that RuBisCO probably consist of 8 small (16-kDa) and 8 large (54-kDa) subunits. Phylogenetic analysis including the *cbbL* gene from strain SolV, encoding for the large subunit of RuBisCO, showed that the verrucomicrobial RuBisCO's represent a new type (suggested name: type IE).

Glycogen storage in *Methylophilum fumariolicum* SolV

It is known that methanotrophs start to store carbon, when nitrogen becomes limiting and carbon is in access. Many studies have been focusing on the polyhydroxybutyrate (PHB) storage and its role in methanotrophs (Pieja *et al.*, 2011 a and b). In contrast detailed studies about glycogen production and its role in methanotrophs are sparse (Eshinimaev *et al.*, 2002; Linton & Cripps, 1978) and the presence of glycogen is reported only based on microscopical observations.

The storage of carbon in the form of glycogen after ammonium exhaustion is described in **Chapter Five**. For this study, fed-batch cultures of strain SolV were

used. The cells were harvested at different time points during the growth period and were used for electron microscopy, elementary analysis, and biochemical analysis of protein and glycogen levels. Growth experiments showed that after the exhaustion of the ammonium, optical density (measured at 600 nm) and dry weight of strain SolV continued to increase for another 7 days. The cell number increased only till 35 hours after the depletion of ammonium, and then stopped. The elemental analysis (measuring the ratio of carbon/nitrogen), showed that after ammonium exhaustion total nitrogen (mg per ml cell culture) did not increase, while the total amount of carbon (mg per ml cell culture) was still increasing linearly (although with decreasing speed), pointing to a possible carbon storage. This was confirmed with an electron microscopic (specific staining), and biochemical analysis (glucose measurement after enzymatic digestion) of glycogen. These analyses have shown that strain SolV, immediately starts to accumulate glycogen after depletion of ammonium. The importance of glycogen for strain SolV was demonstrated on the basis of growth experiments under substrate limitation. The results indicate that glycogen containing cells remained vital for long periods in the absence of methane. Based on the analysis of ^{13}C carbon dioxide released from cells containing ^{13}C -labeled glycogen, it could be concluded that the cells are consuming the stored glycogen in the absence of methane, but that this was not linked to growth (increase in cell number).

Whole genome transcriptome analysis of *Methylobacillus thermophilus* SolV

Cells grown under different conditions are the basis for the transcriptome analysis described in **Chapter Six**. Exponentially growing cells in bottles (with methane, carbon dioxide, oxygen and ammonium in excess), nitrogen-fixing cells in the chemostat (no ammonium, and 0.5 % dissolved oxygen) and oxygen-limited cells in the chemostat (with ammonium, methane and carbon dioxide in excess) were compared with each other. The annotated genome (Chapter two) formed the basis for the transcriptome analysis. Under nitrogen-fixing conditions, all genes involved in this pathway are up-regulated. Under all conditions tested, the genes involved in the CBB cycle are highly expressed. These results underscored the importance of this cycle for the cell in the formation of biomass. Two of the three

pmoCAB operons, encoding for the methane monooxygenases (pMMO's), showed differential expression. This appears to be dependent on the oxygen concentration. The third operon was not expressed under any of the conditions tested in this study.

In conclusion this thesis describes a number of important properties of *Methylophilum fumariolicum* strain SolV, a representative of the recently discovered methanotrophic *Verrucomicrobia*. The work performed is necessary to assess the environmental importance of these microbes as a methane sink in volcanic areas. The available draft genome, together with the transcriptome data of cells from three different culture conditions, is very helpful for future design of physiological experiments. Based on these data several future studies could be suggested (see below).

- **Dealing with nitrosative stress.** If we want to understand the methane fluxes from the geothermal areas, it is important to understand the verrucomicrobial methanotrophs and their controlling environmental factors. Beside the availability of methane and oxygen, nitrogen can have an important role in methane oxidation and can be either an inhibiting or stimulating factor. There are several studies with contradictory findings about the inhibition, stimulation or absence of effect of ammonium based N-fertilization on methanotrophs (Shrestha *et al.*, 2010). In our study optimal cultivation of strain SolV in the laboratory needs the addition of Fangaia soil extract to the growth medium. In this study highly variable ammonium concentrations (1 to 28 mM) were measured in soil extracts sampled during different visits of the Solfatara. This might indicate that dry seasons or heavy rain falls might influence the concentration of fixed nitrogen. In the future more studies are required about the availability of fixed nitrogen in the Solfatara ecosystem and the effect of ammonium concentration on strain SolV. This study will help to predict the emission of methane into the atmosphere from geothermal areas. In the draft genome of strain SolV, genes for nitrite reduction (*nirK*) and nitric oxide reduction (*norB*, *norC*), were identified but the inventory to encode nitrous oxide reduction was missing. A *haoAB* gene cluster encoding hydroxylamine oxidase was identified, suggesting the capability of nitrification and

nitrosative stress handling (Nyerges *et al.*, 2010; Nyerges & Stein, 2009; Stein & Klotz, 2011).

- **The C2 metabolism of *M. fumariolicum*.** In the draft genome of *M. fumariolicum* SolV genes encoding for acetate kinase (*ackA*) and acetyl coenzyme A synthase (*acsA*) were identified (Chapter Two) and shown to be expressed (Chapter six). If these data can be further validated by growth experiments on acetate, demonstrating that strain SolV is able to assimilate C2 compounds, and thus should be regarded as a facultative methanotroph (Semrau *et al.*, 2011).
- **Autotrophic growth.** The ¹³C-labeling experiments in chemostat cultures have demonstrated that carbon dioxide was the carbon source for strain SolV (Chapter Four). To provide the ultimate proof that *M. fumariolicum* is an autotrophic microorganism, knockout and complementation studies are required, for which a genetic system has to be developed. In addition the presence of a hydrogenase gene cluster in the genome of strain SolV (Chapter Two) points towards the possibility of using hydrogen gas (H₂) as an alternative electron donor and the possibility of chemolithotrophic growth or the use of hydrogen to provide reducing equivalents for methane oxidation.
- **Differential regulation of the three *pmoCAB* operons.** One of the *pmoCAB* operons was not expressed under the different conditions tested in the transcriptome analysis (Chapter six). Thus far it became clear that the oxygen concentration has an effect on the expression of the other operons. It could be hypothesized that the available methane concentration is a trigger for the *pmoCAB3* operon, or this pMMO may have a function in oxidizing higher alkanes. Growth studies in methane limited chemostat cultures or batch cultures with higher alkanes (propane, butane) as substrates may provide answers.

- **Analysis of the ultrastructure.** Detailed analysis of the ultrastructure, including the cellular localization of the enzymes involved in methane oxidation, especially the pMMO enzyme, would be very interesting, since the verrucomicrobial methanotrophs lack the internal membrane structures, like those found in proteobacterial methanotrophs.
- **Detection of the verrucomicrobial methanotrophs.** For the detection of microorganisms in the environment, it is important to identify a marker gene suitable for that particular microorganism. The availability of a large database of 16S ribosomal RNA gene sequences makes this gene a good marker to detect microorganisms at different taxonomic levels. In addition and as a complementary method, the *pmoA* gene is used to detect aerobic methanotrophs in the environment (McDonald *et al.*, 2008). This functional gene is more unique to the physiology and metabolism of the proteobacterial aerobic methanotrophs and is found in all genera of the proteobacterial methanotrophs, except for *Methylocella silvestris* BL2 (Chen *et al.*, 2010). A phylogenetic tree of the proteobacterial aerobic methanotrophs based on *pmoA* gene sequences corresponds very well with 16S ribosomal RNA phylogeny, except for *Crenothrix polyspora* (Stoecker *et al.*, 2006). No amplification of the verrucomicrobial methanotrophic *pmoA* gene was observed, when using the standard *pmoA* gene primer system. Since the proteobacterial *pmoA* gene primer contained multiple mismatches to all of the *pmoA* genes in the verrucomicrobial methanotrophic strains, these genes were only identified by full genome sequencing. Pol *et al.* (2007) were able to detect some related *Methylacidiphilum*-like *pmoA* sequences in Solfatara soil, but only when the PCR stringency was greatly reduced. These results suggests that the failure to detect *Verrucomicrobia*-like *pmoA* genes in previous microbial ecology studies does not necessarily mean that this type of bacteria were absent from the environments studied. The discovery of the novel verrucomicrobial pMMO's has made clear that designing new primers is worthwhile and urgently needed.

Since the methods described above cannot distinguishes between living and dead microorganisms, the presence of active methanotrophs can also be

assessed by stable isotope probing (SIP) and phospholipid fatty-acid labeling (PFAL). These techniques rely on the incorporation of the labeled methane into DNA/RNA or lipids, respectively (McDonald *et al.*, 2008 and references therein). However, the autotrophic nature of the verrucomicrobial methanotrophs has large consequences for their detection in the environment. The use of SIP and PFAL methods will overlook the involvement of these autotrophic methanotrophs especially in environments with high carbon dioxide concentrations. The *cbbL* genes are usually applied as a molecular marker to study the distribution and diversity of autotrophic bacteria. The verrucomicrobial RuBisCO type has not been detected before by molecular approaches. This can be explained by the mismatches observed in this study for all the available RuBisCO primer sets (Alfreider *et al.*, 2009; Elsaied *et al.*, 2007; Selesi *et al.*, 2007; Tourova *et al.*, 2010). In the future, research into the occurrence of methanotrophic *Verrucomicrobia* in colder and less acidic regions could be started by developing novel specific primer sets to detect phylogenetic (16S ribosomal RNA) and functional gene markers (e.g. *pmoA*, *cbbL*).

References

Picture by Ahmad F. Khadem.



References

- Alfreider, A., Vogt, C., Geiger-Kaiser, M. & Psenner, R. (2009).** Distribution and diversity of autotrophic bacteria in groundwater systems based on the analysis of RubisCO genotypes. *Syst Appl Microbiol* **32**, 140-150.
- Alquéres, S. M. C., Oliveira, J. H. M., Nogueira, E. M., Guedes, H. V., Oliveira, P. L., Camara, F., Baldani, J. I. & Martins, O. B. (2010).** Antioxidant pathways are up-regulated during biological nitrogen fixation to prevent ROS-induced nitrogenase inhibition in *Gluconacetobacter diazotrophicus*. *Arch Microbiol* **192**, 835-841.
- Anthony, C. (1982).** The biochemistry of methylotrophs. London, UK: Academic Press.
- Auman, A. J., Speake, C. C. & Lidstrom, M. E. (2001).** nifH sequences and nitrogen fixation in type I and type II methanotrophs. *Appl Environ Microbiol* **67**, 4009-4016.
- Baani, M. & Liesack, W. (2008).** Two isozymes of particulate methane monooxygenase with different methane oxidation kinetics are found in *Methylocystis* sp. strain SCZ. *Proc Natl Acad Sci USA* **105**, 10203-10208.
- Badger, M. R. & Bek, E. J. (2008).** Multiple Rubisco forms in proteobacteria: their functional significance in relation to CO₂ acquisition by the CBB cycle. *J Exp Bot* **59**, 1525-1541.
- Barnes, R. O. & Goldberg, E. D. (1976).** Methane production and consumption in anoxic marine-sediments. *Geology* **4**, 297-300.
- Baxter, N. J., Hirt, R. P., Bodrossy, L., Kovacs, K. L., Embley, T. M., Prosser, J. I. & Murrell, J. C. (2002).** The ribulose-1,5-bisphosphate carboxylase/oxygenase gene cluster of *Methylococcus capsulatus* (Bath). *Arch Microbiol* **177**, 279-289.
- Beal, E. J., House, C. H. & Orphan, V. J. (2009).** Manganese- and iron-dependent marine methane oxidation. *Science* **325**, 184-187.
- Belova, S. E., Baani, M., Suzina, N. E., Bodelier, P. L. E., Liesack, W. & Dedysh, S. N. (2011).** Acetate utilization as a survival strategy of peat-inhabiting *Methylocystis* spp. *Environ Microbiol Rep* **3**, 36-46.
- Bird, I. F., Cornelius, M. J., Keys, A. J. & Whittingham, C. P. (1978).** Intramolecular labeling of sucrose made by leaves from [¹⁴C] carbon dioxide or [3-¹⁴C] serine. *Biochem J* **172**, 23-27.
- Boden, R., Cunliffe, M., Scanlan, J., Moussard, H., Kits, K. D., Klotz, M. G., Jetten, M. S. M., Vuilleumier, S., Han, J. & other authors (2011).** Complete genome sequence of the aerobic marine methanotroph *Methylomonas methanica* MC09. *J Bacteriol* **193**, 7001-7002.
- Boetius, A., Ravenschlag, K., Schubert, C. J., Rickert, D., Widdel, F., Gieseke, A., Amann, R., Jorgensen, B. B., Witte, U. & other authors (2000).** A marine microbial consortium apparently mediating anaerobic oxidation of methane. *Nature* **407**, 623-626.
- Böttcher, M. E., Oelschlager, B., Hopner, T., Brumsack, H. J. & Rullkötter, J. (1998).** Sulfate reduction related to the early diagenetic degradation of organic matter and "black spot" formation in tidal sandflats of the German Wadden Sea (southern North Sea): stable isotope (¹³C, ³⁴S, ¹⁸O) and other geochemical results. *Org Geochem* **29**, 1517-1530.
- Bowien, B. & Kusian, B. (2002).** Genetics and control of CO₂ assimilation in the chemoautotroph *Ralstonia eutropha*. *Arch Microbiol* **178**, 85-93.

- Bowman, J. P., Sly, L. I., Nichols, P. D. & Hayward, A. C. (1993).** Revised taxonomy of the methanotrophs: description of *Methylobacter* gen-nov, emendation of *Methylococcus*, validation of *Methylosinus* and *Methylocystis* species, and a proposal that the family *Methylococcaceae* includes only the group I methanotrophs. *Int J Syst Bacteriol* **43**, 735-753.
- Bradbury, S. & Stoward, P. J. (1967).** The specific cytochemical demonstration in the electron microscope of periodate-reactive mucosubstances and polysaccharides containing vic-glycol groups. *Histochemie* **11**, 71-80.
- C**ampbell, M. A., Nyerges, G., Kozlowski, J. A., Poret-Peterson, A. T., Stein, L. Y. & Klotz, M. G. (2011). Model of the molecular basis for hydroxylamine oxidation and nitrous oxide production in methanotrophic bacteria. *FEMS Microbiol Lett* **322**, 82-89.
- Cannon, G. C. & Shively, J. M. (1983).** Characterization of a homogenous preparation of carboxysomes from *Thiobacillus neapolitanus*. *Arch Microbiol* **134**, 52-59.
- Castaldi, S. & Tedesco, D. (2005).** Methane production and consumption in an active volcanic environment of Southern Italy. *Chemosphere* **58**, 131-139.
- Chaudhuri, R. R., Yu, L., Kanji, A., Perkins, T. T., Gardner, P. P., Choudhary, J., Maskell, D. J. & Grant, A. J. (2011).** Quantitative RNA-Seq analysis of the *Campylobacter jejuni* transcriptome. *Microbiol-Sgm* **157**, 2922-2932.
- Chen, Y., Crombie, A., Rahman, M. T., Dedysh, S. N., Liesack, W., Stott, M. B., Alam, M., Theisen, A. R., Murrell, J. C. & other authors (2010).** Complete genome sequence of the aerobic facultative methanotroph *Methylocella silvestris* BL2. *J Bacteriol* **192**, 3840-3841.
- Chistoserdova, L. (2011).** Modularity of methylotrophy, revisited. *Environ Microbiol* **13**, 2603-2622.
- Chistoserdova, L., Chen, S. W., Lapidus, A. & Lidstrom, M. E. (2003).** Methylotrophy in *Methylobacterium extorquens* AM1 from a genomic point of view. *J Bacteriol* **185**, 2980-2987.
- Chistoserdova, L., Kalyuzhnaya, M. G. & Lidstrom, M. E. (2009).** The expanding world of methylotrophic metabolism. *Annu Rev Microbiol* **63**, 477-499.
- Conrad, R. (1996).** Soil microorganisms as controllers of atmospheric trace gases (H₂, CO, CH₄, OCS, N₂O, and NO). *Microbiol Rev* **60**, 609-640.
- Conrad, R. (2009).** The global methane cycle: recent advances in understanding the microbial processes involved. *Environ Microbiol Rep* **1**, 285-292.
- Croucher, N. J. & Thomson, N. R. (2010).** Studying bacterial transcriptomes using RNA-Seq. *Curr Opinion Microbiol* **13**, 619-624.
- Csaki, R., Hanczár, T., Bodrossy, L., Murrell, J. C. & Kovacs, K. L. (2001).** Molecular characterization of structural genes coding for a membrane bound hydrogenase in *Methylococcus capsulatus* (Bath). *FEMS Microbiol Lett* **205**, 203-207.
- D**alton, H. & Whittenbury, R. (1976). Acetylene reduction technique as an assay for nitrogenase activity in methane oxidizing bacterium *Methylococcus capsulatus* strain Bath. *Arch Microbiol* **109**, 147-151.
- Damm, E. & Budéus, G. (2003).** Fate of vent-derived methane in seawater above the Håkon Mosby mud volcano (Norwegian Sea). *Mar Chem* **82**, 1-11.
- Dando, P. R., Ohara, S. C. M., Schuster, U., Taylor, L. J., Clayton, C. J., Baylis, S. & Laier, T. (1994).** Gas seepage from a carbonate-cemented sandstone reef on the Kattegat coast of Denmark. *Mar Pet Geol* **11**, 182-189.

- Davis, J. B., Coty, V. F. & Stanley, J. P. (1964). Atmospheric nitrogen fixation by methane-oxidizing bacteria. *J Bacteriol* **88**, 468-472.
- De Bont, J. A. M. (1976). Hydrogenase activity in nitrogen-fixing methane-oxidizing bacteria. *Antonie van Leeuwenhoek* **42**, 255-259.
- De Bont, J. A. M. & Mulder, E. G. (1976). Invalidity of acetylene reduction assay in alkane utilizing, nitrogen-fixing bacteria. *Appl Environ Microbiol* **31**, 640-647.
- Dedysh, S. N., Belova, S. E., Bodelier, P. L. E., Smirnova, K. V., Khmelenina, V. N., Chidthaisong, A., Trotsenko, Y. A., Liesack, W. & Dunfield, P. F. (2007). *Methylocystis heyeri* sp nov., a novel type II methanotrophic bacterium possessing 'signature' fatty acids of type I methanotrophs. *Int J Syst Evol Micr* **57**, 472-479.
- Dedysh, S. N., Ricke, P. & Liesack, W. (2004). NifH and NifD phylogenies: an evolutionary basis for understanding nitrogen fixation capabilities of methanotrophic bacteria. *Microbiol-Sgm* **150**, 1301-1313.
- Dedysh, S. N., Khmelenina, V. N., Suzina, N. E., Trotsenko, Y. A., Semrau, J. D., Liesack, W. & Tiedje, J. M. (2002). *Methylocapsa acidiphila* gen. nov., sp nov., a novel methane-oxidizing and dinitrogen-fixing acidophilic bacterium from Sphagnum bog. *Int J Syst Evol Micr* **52**, 251-261.
- Dedysh, S. N., Knief, C. & Dunfield, P. F. (2005). *Methylocella* species are facultatively methanotrophic. *J Bacteriol* **187**, 4665-4670.
- Dedysh, S. N., Liesack, W., Khmelenina, V. N., Suzina, N. E., Trotsenko, Y. A., Semrau, J. D., Bares, A. M., Panikov, N. S. & Tiedje, J. M. (2000). *Methylocella palustris* gen. nov., sp nov., a new methane-oxidizing acidophilic bacterium from peat bags, representing a novel subtype of serine-pathway methanotrophs. *Int J Syst Evol Micr* **50**, 955-969.
- Dekas, A. E., Poretsky, R. S. & Orphan, V. J. (2009). Deep-Sea Archaea fix and share nitrogen in methane-consuming microbial consortia. *Science* **326**, 422-426.
- Denman, K. L., G. Brasser, A. Chidthaisong, P. Ciais, P. M. Cox, R. E. Dickinson, D. Hauglustaine, C. Heinze, E. Holland & other authors (2007). Couplings between changes in the climate system and biogeochemistry. In *Climate change 2007: The physical science basis Contribution of working group I to the fourth assessment report of the intergovernmental panel on climate change*, PP 499-587. Cambridge: Cambridge University Press.
- Dixon, R. & Kahn, D. (2004). Genetic regulation of biological nitrogen fixation. *Nat Rev Microbiol* **2**, 621-631.
- Dunfield, P. F. (2006). The soil methane sink. In *Greenhouse Gas Sinks*, PP 152-170. Edited by Reay, D., Hewitt, C.N., Smith, K. & Grace, J. Wallingford, UK: CABI Publishing.
- Dunfield, P. F., Belova, S. E., Vorobev, A. V., Cornish, S. L. & Dedysh, S. N. (2010). *Methylocapsa aurea* sp. nov., a facultative methanotroph possessing a particulate methane monooxygenase, and emended description of the genus *Methylocapsa*. *Int J Syst Evol Microbiol* **60**, 2659-2664.
- Dunfield, P. F., Khmelenina, V. N., Suzina, N. E., Trotsenko, Y. A. & Dedysh, S. N. (2003). *Methylocella silvestris* sp nov., a novel methanotroph isolated from an acidic forest cambisol. *Int J Syst Evol Micr* **53**, 1231-1239.
- Dunfield, P. F., Yuryev, A., Senin, P., Smirnova, A. V., Stott, M. B., Hou, S. B., Ly, B., Saw, J. H., Zhou, Z. M. & other authors (2007). Methane oxidation by an extremely acidophilic bacterium of the phylum Verrucomicrobia. *Nature* **450**, 879-883.

- Edgar, R. C. (2004).** MUSCLE: multiple sequence alignment with high accuracy and high throughput. *Nucleic Acids Res* **32**, 1792-1797.
- Elsaied, H. E., Kimura, H. & Naganuma, T. (2007).** Composition of archaeal, bacterial, and eukaryal RuBisCO genotypes in three Western Pacific arc hydrothermal vent systems. *Extremophiles* **11**, 191-202.
- Erikstad, H. A., Jensen, S., Keen, T. J. & Birkeland, N. K. (2012).** Differential expression of particulate methane monooxygenase genes in the verrucomicrobial methanotroph '*Methylococcoides burtonii*' Kam1. *Extremophiles* **16**, 405-409.
- Eshinimaev, B. T., Khmelenina, V. N., Sakharovskii, V. G., Suzina, N. E. & (2002).** Physiological, biochemical, and cytological characteristics of a haloalkalitolerant methanotroph grown on methanol. *Microbiology* **71**, 512-518.
- Etiopie, G. & Klusman, R. W. (2002).** Geologic emissions of methane to the atmosphere. *Chemosphere* **49**, 777-789.
- Etiopie, G., Oehler, D. Z. & Allen, C. C. (2011).** Methane emissions from Earth's degassing: Implications for Mars. *Planet Space Sci* **59**, 182-195.
- Ettwig, K. F., Butler, M. K., Le Paslier, D., Pelletier, E., Mangenot, S., Kuypers, M. M. M., Schreiber, F., Dutilh, B. E., Zedelius, J. & other authors (2010).** Nitrite-driven anaerobic methane oxidation by oxygenic bacteria. *Nature* **464**, 543-550.
- Ettwig, K. F., Shima, S., van de Pas-Schoonen, K. T., Kahnt, J., Medema, M. H., Op den Camp, H. J. M., Jetten, M. S. M. & Strous, M. (2008).** Denitrifying bacteria anaerobically oxidize methane in the absence of *Archaea*. *Environ Microbiol* **10**, 3164-3173.
- Ettwig, K. F., van Alen, T., van de Pas-Schoonen, K. T., Jetten, M. S. M. & Strous, M. (2009).** Enrichment and molecular detection of denitrifying methanotrophic bacteria of the NC10 phylum. *Appl Environ Microbiol* **75**, 3656-3662.
- Felsenstein, J. (1985).** Confidence limits on phylogenies: an approach using the bootstrap. *Evolution* **39**, 783-791.
- Forster, P., Ramaswamy, V., Artaxo, P., Bernsten, T., Betts, R. A., Fahey, D. W., Haywood, J., Lean, J., Lowe, D. C. & other authors (2007).** Changes in atmospheric constituents and in radiative forcing. In *Climate change 2007: The physical science basis Contribution of working group I to the fourth assessment report of the intergovernmental panel on climate change*, PP 129-234. Cambridge: Cambridge University Press.
- Girguis, P. R., Cozen, A. E. & De Long, E. F. (2005).** Growth and population dynamics of anaerobic methane-oxidizing archaea and sulfate-reducing bacteria in a continuous-flow bioreactor. *Appl Environ Microbiol* **71**, 3725-3733.
- Girguis, P. R., Orphan, V. J., Hallam, S. J. & De Long, E. F. (2003).** Growth and methane oxidation rates of anaerobic methanotrophic archaea in a continuous-flow bioreactor. *Appl Environ Microbiol* **69**, 5472-5482.
- Gonzales, A. D., Light, Y. K., Zhang, Z. D., Iqbal, T., Lane, T. W. & Martino, A. (2005).** Proteomic analysis of the CO₂-concentrating mechanism in the open-ocean cyanobacterium *Synechococcus* WH8102¹. *Can J Bot* **83**, 735-745.

- H**anczár, T., Csaki, R., Bodrossy, L., Murrell, J. C. & Kovacs, K. L. (2002). Detection and localization of two hydrogenases in *Methylococcus capsulatus* (Bath) and their potential role in methane metabolism. *Arch Microbiol* **177**, 167-172.
- Hanson, R. S. & Hanson, T. E. (1996).** Methanotrophic bacteria. *Microbiol Rev* **60**, 439-471.
- Hendrickson, E. L., Beck, D. A. C., Wang, T. S., Lidstrom, M. E., Hackett, M. & Chistoserdova, L. (2010).** Expressed genome of *Methylobacillus flagellatus* as defined through comprehensive proteomics and new insights into methylotrophy. *J Bacteriol* **192**, 4859-4867.
- Heyer, J., Berger, U., Hardt, M. & Dunfield, P. F. (2005).** *Methylohalobius crimeensis* gen. nov., sp. nov., a moderately halophilic, methanotrophic bacterium isolated from hypersaline lakes of Crimea. *Int J Syst Evol Micr* **55**, 1817-1826.
- Hinrichs, K.-U. & Boetius, A. (2002).** The anaerobic oxidation of methane : new insights in microbial ecology and biogeochemistry. In *Ocean Margin Systems*, PP 457-477. Edited by Wefer, G., Billet, D., Hebbeln, D., Jorgensen, B. B., Schluter, M. & van Weering, T. Heidelberg, Germany: Springer-Verlag.
- Hou, S. B., Makarova, K. S., Saw, J. H. W., Senin, P., Ly, B. V., Zhou, Z. M., Ren, Y., Wang, J. M., Galperin, M. Y. & other authors (2008).** Complete genome sequence of the extremely acidophilic methanotroph isolate V4, *Methylacidiphilum infernorum*, a representative of the bacterial phylum *Verrucomicrobia*. *Biol Direct* **3**, 26.
- Houghton, J. T., Meira Filho, L. G., Callander, B. A., Harris, N., Kattenberg, A. & Maskell, K. (1996).** In *Climate Change 1995: The Science of Climate Change, IPCC*, PP 572. Cambridge: Cambridge University Press.
- Houweling, S., Kaminski, T., Dentener, F., Lelieveld, J. & Heimann, M. (1999).** Inverse modeling of methane sources and sinks using the ad joint of a global transport model. *J Geophys Res [Atmos]* **104**, 26137-26160.
- Howard, J. B. & Rees, D. C. (1996).** Structural basis of biological nitrogen fixation. *Chem Rev* **96**, 2965-2982.
- Hu, S. H., Zeng, R. J., Burow, L. C., Lant, P., Keller, J. & Yuan, Z. G. (2009).** Enrichment of denitrifying anaerobic methane oxidizing microorganisms. *Environ Microbiol Rep* **1**, 377-384.
- I**guchi, H., Yurimoto, H. & Sakai, Y. (2011). *Methylovulum miyakonense* gen. nov., sp. nov., a type I methanotroph isolated from forest soil. *Int J Syst Evol Micr* **61**, 810-815.
- Islam, T., Jensen, S., Reigstad, L. J., Larsen, O. & Birkeland, N. K. (2008).** Methane oxidation at 55 °C and pH 2 by a thermoacidophilic bacterium belonging to the *Verrucomicrobia* phylum. *Proc Natl Acad Sci USA* **105**, 300-304.
- J**oye, S. B., Boetius, A., Orcutt, B. N., Montoya, J. P., Schulz, H. N., Erickson, M. J. & Lugo, S. K. (2004). The anaerobic oxidation of methane and sulfate reduction in sediments from Gulf of Mexico cold seeps. *Chem Geol* **205**, 219-238.
- Juretschko, S., Timmermann, G., Schmid, M., Schleifer, K. H., Pommerening-Roser, A., Koops, H. P. & Wagner, M. (1998).** Combined molecular and conventional analyses of nitrifying bacterium diversity in activated sludge: *Nitrosococcus mobilis* and *Nitrospira*-like bacteria as dominant populations. *Appl Environ Microbiol* **64**, 3042-3051.

- K**aluzhnaya, M., Khmelenina, V., Eshinimaev, B., Suzina, N., Nikitin, D., Solonin, A., Lin, J. L., McDonald, I., Murrell, C. & other authors (2001). Taxonomic characterization of new alkaliphilic and alkalitolerant methanotrophs from soda lakes of the Southeastern Transbaikal Region and description of *Methylobaculum buryatense* sp.nov. *Syst Appl Microbiol* **24**, 166-176.
- Kalyuzhnaya, M. G., Martens-Habbena, W., Wang, T. S., Hackett, M., Stolyar, S. M., Stahl, D. A., Lidstrom, M. E. & Chistoserdova, L. (2009).** *Methylobaculum* link methanol oxidation to denitrification in freshwater lake sediment as suggested by stable isotope probing and pure culture analysis. *Environ Microbiol Rep* **1**, 385-392.
- Kartal, B., Maalcke, W. J., de Almeida, N. M., Cirpus, I., Gloerich, J., Geerts, W., Op den Camp, H. J. M., Harhangi, H. R., Janssen-Megens, E. M. & other authors (2011).** Molecular mechanism of anaerobic ammonium oxidation. *Nature* **479**, 127-130.
- Kelly, D. P., Anthony, C. & Murrell, J. C. (2005).** Insights into the obligate methanotroph *Methylobaculum capsulatus*. *Trends Microbiol* **13**, 195-198.
- Khadem, A. F., Pol, A., Jetten, M. S. M. & Op den Camp, H. J. M. (2010).** Nitrogen fixation by the verrucomicrobial methanotroph '*Methylobaculum fumariolicum*' SolV. *Microbiol-Sgm* **156**, 1052-1059.
- Khadem, A. F., Pol, A., Wiczorek, A. S., Jetten, M. S. M. & Op den Camp, H. J. M. (2012 a).** Metabolic regulation of "*Ca. Methylobaculum fumariolicum*" SolV cells grown under different nitrogen and oxygen limitations. *Front Microbiol* **3**, 266.
- Khadem, A. F., Pol, A., Wiczorek, A., Mohammadi, S. S., Francoijs, K. J., Stunnenberg, H. G., Jetten, M. S. M. & Op den Camp, H. J. M. (2011).** Autotrophic methanotrophy in Verrucomicrobia: *Methylobaculum fumariolicum* SolV uses the Calvin-Benson-Bassham cycle for carbon dioxide fixation. *J Bacteriol* **193**, 4438-4446.
- Khadem, A. F., Wiczorek, A. S., Pol, A., Vuilleumier, S., Harhangi, H. R., Dunfield, P. F., Kalyuzhnaya, M. G., Murrell, J. C., Francoijs, K-J. & other authors (2012 b).** Draft genome sequence of the volcano-inhabiting thermoacidophilic methanotroph *Methylobaculum fumariolicum* strain SolV. *J Bacteriol* **194**, 3729-3730.
- Khalil, M. & Shearer, M.J. (2000).** Atmospheric Methane: Its role in the global environment. In *Sources of methane: an overview*, PP 98-111. Edited by Khalil, M. New York: Springer-Verlag.
- Khmelenina, V. N., Kalyuzhnaya, M. G., Sakharovsky, V. G., Suzina, N. E., Trotsenko, Y. A. & Gottschalk, G. (1999).** Osmoadaptation in halophilic and alkaliphilic methanotrophs. *Arch Microbiol* **172**, 321-329.
- Kip, N., Ouyang, W. J., van Winden, J., Raghoebarsing, A., van Niftrik, L., Pol, A., Pan, Y., Bodrossy, L., van Donselaar, E. G. & other authors (2011).** Detection, isolation, and characterization of acidophilic methanotrophs from Sphagnum Mosses. *Appl Environ Microbiol* **77**, 5643-5654.
- Klotz, M. G. & Stein, L. Y. (2008).** Nitrifier genomics and evolution of the nitrogen cycle. *FEMS Microbiol Lett* **278**, 146-456.
- Knittel, K. & Boetius, A. (2009).** Anaerobic oxidation of methane: progress with an unknown process. *Annu Rev Microbiol* **63**, 311-334.
- Kvenvolden, K. A. & Rogers, B. W. (2005).** Gaia's breath - global methane exhalations. **22**, 579-590.
- L**aemmli, U. K. (1970). Cleavage of structural proteins during assembly of head of bacteriophage T4. *Nature* **227**, 680-685.

- Leak, D. J., Stanley, S. H. & Dalton, H. (1985).** Implication of the nature of methane monooxygenase on carbon assimilation in methanotrophs. In *microbial gas metabolism, mechanistic, metabolic and biotechnological aspects*, PP 201-208. Edited by Poole, R. K. & Dow, C. S. London: Academic Press.
- Lelieveld, J., Crutzen, P. J. & Dentener, F. J. (1998).** Changing concentration, lifetime and climate forcing of atmospheric methane. *Tellus Ser B-Chem Phys Meteorol* **50**, 128-150.
- Linton, J. D. & Cripps, R. E. (1978).** Occurrence and identification of intracellular polyglucose storage granules in *Methylococcus* NCBI 11083 grown in chemostat culture on methane. *Arch Microbiol* **117**, 41-48.
- Liu, Y. C. & Whitman, W. B. (2008).** Metabolic, phylogenetic, and ecological diversity of the methanogenic archaea. *Ann N Y Acad Sci* **112**, 171-189.
- Luesken, F. A., van Alen, T. A., van der Biezen, E., Frijters, C., Toonen, G., Kampman, C., Hendrickx, T. L. G., Zeeman, G., Temmink, H. & other authors (2011).** Diversity and enrichment of nitrite-dependent anaerobic methane oxidizing bacteria from wastewater sludge. *Appl Microbiol Biotechnol* **92**, 845-854.
- Mackintosh, M. E. (1978).** Nitrogen fixation by *Thiobacillus ferrooxidans*. *J Gen Microbiol* **105**, 215-218.
- Malashenko, Y. R., Pirog, T. P., Romanovskaya, V. A., Sokolov, I. G. & Grinberg, T. A. (2001).** Search for methanotrophic producers of exopolysaccharides. *Appl. Biochem Microbiol* **37**, 599-602.
- Malone, J. H. & Oliver, B. (2011).** Microarrays, deep sequencing and the true measure of the transcriptome. *BMC Biology* **9**, 34.
- Martens, C. S. & Berner, R. A. (1974).** Methane production in interstitial waters of sulfate-depleted marine sediments. *Science* **185**, 1167-1169.
- McDonald, I. R., Bodrossy, L., Chen, Y. & Murrell, J. C. (2008).** Molecular ecology techniques for the study of aerobic methanotrophs. *Appl Environ Microbiol* **74**, 1305-1315.
- Mortazavi, A., Williams, B. A. McCue, K., Schaeffer, L. & Wold, B. (2008).** Mapping and quantifying mammalian transcriptomes by RNA-Seq. *Nature Meth* **5**, 621-628.
- Moss, A. R., Jouany, J. P. & Newbold, J. (2000).** Methane production by ruminants: its contribution to global warming. *Ann Zootech* **49**, 231-253.
- Murrell, J. C. & Dalton, H. (1983).** Nitrogen fixation in obligate methanotrophs. *J Gen Microbiol* **129**, 3481-3486.
- Murrell, J. C., Gilbert, B. & McDonald, I. R. (2000).** Molecular biology and regulation of methane monooxygenase. *Arch Microbiol* **173**, 325-332.
- Murrell, J. C. & Jetten, M. S. M. (2009).** The microbial methane cycle. *Environ Microbiol Rep* **1**, 279-284.
- Newton, W. E. (2007).** Physiology, biochemistry, and molecular biology of nitrogen fixation. In *Biology of The Nitrogen Cycle*, PP 109-129. Edited by Bothe, H. Ferguson, S. J. & Newton, W. E. Amsterdam: Elsevier B.V.
- Niemann, H., Duarte, J., Hensen, C., Omoregie, E., Magalhaes, V. H., Elvert, M., Pinheiro, L. M., Kopf, A. & Boetius, A. (2006).** Microbial methane turnover at mud volcanoes of the Gulf of Cadiz. *Geochim Cosmochim Acta* **70**, 5336-5355.

- Niewöhner, C., Hensen, C., Kasten, S., Zabel, M. & Schulz, H. D. (1998). Deep sulfate reduction completely mediated by anaerobic methane oxidation in sediments of the upwelling area off Namibia. *Geochim Cosmochim Acta* **62**, 455-464.
- Norris, P. R., Murrell, J. C. & Hinson, D. (1995). The potential for diazotrophy in iron- and sulfur-oxidizing acidophilic bacteria. *Arch Microbiol* **164**, 294-300.
- Nyerges, G., Han, S. K. & Stein, L. Y. (2010). Effects of ammonium and nitrite on growth and competitive fitness of cultivated methanotrophic bacteria. *Appl Environ Microbiol* **76**, 5648-5651.
- Nyerges, G. & Stein, L. Y. (2009). Ammonia cometabolism and product inhibition vary considerably among species of methanotrophic bacteria. *FEMS Microbiol Lett* **297**, 131-136.
- O**akley, C. J. & Murrell, J. C. (1988). *nifH* genes in the obligate methane oxidizing bacteria. *FEMS Microbiol Lett* **49**, 53-57.
- Oakley, C. J. & Murrell, J. C. (1991). Cloning of nitrogenase structural genes from the obligate methanotroph *Methylococcus capsulatus* (Bath). *FEMS Microbiol Lett* **78**, 121-126.
- Oh, J. I. & Bowien, B. (1998). Structural analysis of the *fds* operon encoding the NAD(+)-linked formate dehydrogenase of *Ralstonia eutropha*. *J Biol Chem* **273**, 26349-26360.
- Op den Camp, H. J. M., Islam, T., Stott, M. B., Harhangi, H. R., Hynes, A., Schouten, S., Jetten, M. S. M., Birkeland, N. K., Pol, A. & other authors (2009). Environmental, genomic and taxonomic perspectives on methanotrophic *Verrucomicrobia*. *Environ Microbiol Rep* **1**, 293-306.
- Orphan, V. J., House, C. H., Hinrichs, K. U., McKeegan, K. D. & De Long, E. F. (2002). Multiple archaeal groups mediate methane oxidation in anoxic cold seep sediments. *Proc Natl Acad Sci USA* **99**, 7663-7668.
- P**etersen, J. M. & Dubilier, N. (2009). Methanotrophic symbioses in marine invertebrates. *Environ Microbiol Rep* **1**, 319-335.
- Pieja, A. J., Rostkowski, K. H. & Criddle, C. S. (2011 a). Distribution and selection of poly-3-hydroxybutyrate production capacity in methanotrophic Proteobacteria. *Microb Ecol* **62**, 564-573.
- Pieja, A. J., Sundstrom, E. R. & Criddle, C. S. (2011 b). Poly-3-hydroxybutyrate metabolism in the Type II methanotroph *Methylocystis parvus* OBBP. *Appl Environ Microbiol* **77**, 6012-6019.
- Pol, A., Heijmans, K., Harhangi, H. R., Tedesco, D., Jetten, M. S. M. & Op den Camp, H. J. M. (2007). Methanotrophy below pH 1 by a new *Verrucomicrobia* species. *Nature* **450**, 874-879.
- Postgate, J. R., & Eady, R. R. (1988). The evolution of biological nitrogen fixation. In *Nitrogen Fixation: Hundred Years After*, PP 31-40. Edited by Bothe, H., de Bruijn, F. J. & Newton, W. E. Stuttgart: Gustav Fischer.
- Price, G. D., Coleman, J. R. & Badger, M. R. (1992). Association of carbonic anhydrase activity with carboxysomes isolated from the cyanobacterium *Synechococcus* PCC7942¹. *Plant Physiol* **100**, 784-793.

- Raghoebarsing, A. A., Pol, A., van de Pas-Schoonen, K. T., Smolders, A. J. P., Ettwig, K. F., Rijpstra, W. I. C., Schouten, S., Damste, J. S. S., Op den Camp, H. J. M. & other authors (2006).** A microbial consortium couples anaerobic methane oxidation to denitrification. *Nature* **440**, 918-921.
- Raghoebarsing, A. A., Smolders, A. J. P., Schmid, M. C., Rijpstra, W. I. C., Wolters-Arts, M., Derksen, J., Jetten, M. S. M., Schouten, S., Damste, J. S. S. & other authors (2005).** Methanotrophic symbionts provide carbon for photosynthesis in peat bogs. *Nature* **436**, 1153-1156.
- Rahalkar, M., Bussmann, I. & Schink, B. (2007).** *Methylosoma difficile* gen. nov., sp nov., a novel methanotroph enriched by gradient cultivation from littoral sediment of Lake Constance. *Int J Syst Evol Micr* **57**, 1073-1080.
- Rappe, M. S. & Giovannoni, S. J. (2003).** The uncultured microbial majority. *Annu Rev Microbiol* **57**, 369-394.
- Reeburgh, W. S. (1976).** Methane consumption in Cariaco Trench waters and sediments. *Earth Planet Sci Lett* **28**, 337-344.
- Reeburgh, W. S. (1996).** Soft spots in the global methane budget. In *Microbial growth on C₁ compounds*, PP 334-352. Edited by Lidstrom, M. E. & Tabita, F.R. Dordrecht: Kluwer academic publishers.
- Reynolds, E. S. (1963).** The use of lead citrate at high pH as an electron-opaque stain in electron microscopy. *J Cell Biol* **17**, 208-212.
- Robson, R. L. & Postgate, J. R. (1980).** Oxygen and hydrogen in biological nitrogen fixation. *Annu Rev Microbiol* **34**, 183-207.
- Rudnick, P., Meletzus, D., Green, A., He, L. H. & Kennedy, C. (1997).** Regulation of nitrogen fixation by ammonium in diazotrophic species of Proteobacteria. *Soil Biol Biochem* **29**, 831-841.
- Saitou, N. & Nei, M. (1987).** The neighbor-joining method: A new method for reconstructing phylogenetic trees. *Mol Biol Evol* **4**, 406-425.
- Schink, B. (1997).** Energetics of syntrophic cooperation in methanogenic degradation. *Microbiol Mol Biol Rev* **61**, 262-280.
- Schönheit, P., Brandis, A. & Thauer, R. K. (1979).** Ferredoxin degradation in growing *Clostridium pasteurianum* during periods of iron deprivation. *Arch Microbiol* **120**, 73-76.
- Segers, R. (1998).** Methane production and methane consumption: a review of processes underlying wetland methane fluxes. *Biogeochemistry* **41**, 23-51.
- Selesi, D., Pattis, I., Schmid, M., Kandeler, E. & Hartmann, A. (2007).** Quantification of bacterial RubisCO genes in soils by *cbbL* targeted real-time PCR. *J Microbiol Methods* **69**, 497-503.
- Semrau, J. D., Chistoserdov, A., Lebron, J., Costello, A., Davagnino, J., Kenna, E., Holmes, A. J., Finch, R., Murrell, J. C. & other authors (1995).** Particulate methane monooxygenase genes in methanotrophs. *J Bacteriol* **177**, 3071-3079.
- Semrau, J. D., DiSpirito, A. A. & Vuilleumier, S. (2011).** Facultative methanotrophy: false leads, true results, and suggestions for future research. *FEMS Microbiol Lett* **323**, 1-12.
- Semrau, J. D., DiSpirito, A. A. & Yoon, S. (2010).** Methanotrophs and copper. *FEMS Microbiol Rev* **34**, 496-531.

- Shindell, D. T., Faluvegi, G., Koch, D. M., Schmidt, G. A., Unger, N. & Bauer, S. E. (2009). Improved attribution of climate forcing to emissions. *Science* **326**, 716-718.
- Shrestha, M., Shrestha, P. M., Frenzel, P. & Conrad, R. (2010). Effect of nitrogen fertilization on methane oxidation, abundance, community structure, and gene expression of methanotrophs in the rice rhizosphere. *Isme Journal* **4**, 1545-1556.
- Singh, J. S. (2011). Methanotrophs: the potential biological sink to mitigate the global methane load. *Curr Sci* **100**, 29-30.
- Sivan, O., Adler, M., Pearson, A., Gelman, F., Bar-Or, I., John, S. G. & Eckert, W. (2011). Geochemical evidence for iron-mediated anaerobic oxidation of methane. *Limnol Oceanogr* **56**, 1536-1544.
- Sivan, O., Schrag, D. P. & Murray, R. W. (2007). Rates of methanogenesis and methanotrophy in deep-sea sediments. *Geobiology* **5**, 141-151.
- Stanley, S. H. & Dalton, H. (1982). Role of ribulose-1,5-bisphosphate carboxylase/oxygenase in *Methylococcus capsulatus* (Bath). *J Gen Microbiol* **128**, 2927-2935.
- Stein, L. Y. & Klotz, M. G. (2011). Nitrifying and denitrifying pathways of methanotrophic bacteria. *Biochem Soc Trans* **39**, 1826-1831.
- Stoecker, K., Bendinger, B., Schoning, B., Nielsen, P. H., Nielsen, J. L., Baranyi, C., Toenshoff, E. R., Daims, H. & Wagner, M. (2006). Cohn's *Crenothrix* is a filamentous methane oxidizer with an unusual methane monooxygenase. *Proc Natl Acad Sci USA* **103**, 2363-2367.
- Stolyar, S., Costello, A. M., Peebles, T. L. & Lidstrom, M. E. (1999). Role of multiple gene copies in particulate methane monooxygenase activity in the methane-oxidizing bacterium *Methylococcus capsulatus* Bath. *Microbiol-Uk* **145**, 1235-1244.
- T**abita, F. R., Satagopan, S., Hanson, T. E., Kreel, N. E. & Scott, S. S. (2008). Distinct form I, II, III, and IV Rubisco proteins from the three kingdoms of life provide clues about Rubisco evolution and structure/function relationships. *J Exp Bot* **59**, 1515-1524.
- Takeda, K. (1988). Characteristics of a nitrogen fixing methanotroph, *Methylocystis* T-1. *Antonie van Leeuwenhoek* **54**, 521-534.
- Tamura, K., Dudley, J., Nei, M. & Kumar, S. (2007). MEGA4: Molecular evolutionary genetics analysis (MEGA) software version 4.0. *Mol Biol Evol* **24**, 1596-1599.
- Tamura, K., Peterson, D., Peterson, N., Stecher, G., Nei, M. & Kumar, S. (2011). MEGA5: Molecular evolutionary genetics analysis using maximum likelihood, evolutionary distance, and maximum parsimony methods. *Mol Biol Evol* **28**, 2731-2739.
- Tavormina, P. L., Orphan, V. J., Kalyuzhnaya, M. G., Jetten, M. S. M. & Klotz, M. G. (2011). A novel family of functional operons encoding methane/ammonia monooxygenase-related proteins in gammaproteobacterial methanotrophs. *Environ Microbiol Rep* **3**, 91-100.
- Taylor, S., Ninjoor, V., Dowd, D. M., & Tappel, A. L. (1974). Cathepsin B2 measurement by sensitive fluorometric ammonia analysis. *Anal Biochem* **60**, 153-162.
- Thauer, R. K. (1998). Biochemistry of methanogenesis: a tribute to Marjory Stephenson. *Microbiol-Sgm* **144**, 2377-2406.
- Thomsen, T. R., Finster, K. & Ramsing, N. B. (2001). Biogeochemical and molecular signatures of anaerobic methane oxidation in a marine sediment. *Appl Environ Microbiol* **67**, 1646-1656.

- Toukdarian, A. E. & Lidstrom, M. E. (1984). Nitrogen metabolism in a new obligate methanotroph, '*Methylosinus*' strain 6. *J Gen Microbiol* **130**, 1827-1837.
- Tourova, T. P., Kovaleva, O. L., Sorokin, D. Y. & Muyzer, G. (2010). Ribulose-1,5-bisphosphate carboxylase/oxygenase genes as a functional marker for chemolithoautotrophic halophilic sulfur-oxidizing bacteria in hypersaline habitats. *Microbiol-Sgm* **156**, 2016-2025.
- Treude, T., Kruger, M., Boetius, A. & Jorgensen, B. B. (2005). Environmental control on anaerobic oxidation of methane in the gassy sediments of Eckernförde Bay (German Baltic). *Limnol Oceanogr* **50**, 1771-1786.
- Treude, T., Niggemann, J., Kallmeyer, J., Wintersteller, P., Schubert, C. J., Boetius, A. & Jorgensen, B. B. (2005). Anaerobic oxidation of methane and sulfate reduction along the Chilean continental margin. *Geochim Cosmochim Acta* **69**, 2767-2779.
- Treude, T., Orphan, V., Knittel, K., Gieseke, A., House, C. H. & Boetius, A. (2007). Consumption of methane and CO₂ by methanotrophic microbial mats from gas seeps of the anoxic Black Sea. *Appl Environ Microbiol* **73**, 2271-2283.
- Trotsenko, Y. A. & Khmelenina, V. N. (2002). Biology of extremophilic and extremotolerant methanotrophs. *Arch Microbiol* **177**, 123-131.
- Tsubota, J., Eshinimaev, B. T., Khmelenina, V. N. & Trotsenko, Y. A. (2005). *Methylothermus thermalis* gen. nov., sp nov., a novel moderately thermophilic obligate methanotroph from a hot spring in Japan. *Int J Syst Evol Micr* **55**, 1877-1884.
- Tyson, G. W. , Lo, I., Baker, B.J., Allen, E. E., Hugenholtz, P., & Banfield, J. F. (2005). Genome-directed isolation of the key nitrogen fixer *Leptospirillum ferrodiazotrophum* sp. nov. from an acidophilic microbial community. *Appl Environ Microbiol* **71**, 6319-6324.
- V**alentine, D. L. & Reeburgh, W. S. (2000). New perspectives on anaerobic methane oxidation. *Environ Microbiol* **2**, 477-484.
- Vallenet, D., Engelen, S., Mornico, D., Cruveiller, S., Fleury, L., Lajus, A., Rouy, Z., Roche, D., Salvignol, G. & other authors (2009). MicroScope: a platform for microbial genome annotation and comparative genomics. *Database-the Journal of Biological Databases and Curation*.
- van Niftrik, L., Geerts, W. J. C., van Donselaar, E. G., Humbel, B. M., Webb, R. I., Fuerst, J. A., Verkleij, A. J., Jetten, M. S. M. & Strous, M. (2008). Linking ultrastructure and function in four genera of anaerobic ammonium-oxidizing bacteria: cell plan, glycogen storage, and localization of cytochrome c proteins. *J Bacteriol* **190**, 708-717.
- van Niftrik, L., Geerts, W. J. C., van Donselaar, E. G., Humbel, B. M., Webb, R. I., Harhangi, H. R., Op den Camp, H. J. M., Fuerst, J. A., Verkleij, A. J. & other authors (2009). Cell division ring, a new cell division protein and vertical inheritance of a bacterial organelle in anammox planctomycetes. *Mol Microbiol* **73**, 1009-1019.
- van Passel, M. W. J., Kant, R., Zoetendal, E. G., Plugge, C. M., Derrien, M., Malfatti, S. A., Chain, P. S. G., Woyke, T., Palva, A. & other authors (2011). The genome of *Akkermansia muciniphila*, a dedicated intestinal mucin degrader, and its use in exploring intestinal metagenomes. *PLoS One* **6**, e16876.
- Vigliotta, G., Nutricati, E., Carata, E., Tredici, S. M., De Stefano, M., Pontieri, P., Massardo, D. R., Prati, M. V., De Bellis, L. & other authors (2007). *Clonothrix fusca* Roze 1896, a filamentous, sheathed, methanotrophic gamma-proteobacterium. *Appl Environ Microbiol* **73**, 3556-3565.

- Vorobev, A. V., Baani, M., Doronina, N. V., Brady, A. L., Liesack, W., Dunfield, P. F. & Dedysh, S. N. (2011). *Methyloferula stellata* gen. nov., sp nov., an acidophilic, obligately methanotrophic bacterium that possesses only a soluble methane monooxygenase. *Int J Syst Evol Micr* **61**, 2456-2463.
- W**agner, M. & Horn, M. (2006). The *Planctomycetes*, *Verrucomicrobia*, *Chlamydiae* and sister phyla comprise a superphylum with biotechnological and medical relevance. *Curr Opin Biotechnol* **17**, 241-249.
- Wang, Z., Gerstein, M. & Snyder, M. (2009). RNA-Seq: a revolutionary tool for transcriptomics. *Nature Rev Genet* **10**, 57-63.
- Wanner, U. & Egli, T. (1990). Dynamics of microbial-growth and cell composition in batch culture. *FEMS Microbiol Rev* **75**, 19-44.
- Ward, N., Larsen, O., Sakwa, J., Bruseth, L., Khouri, H., Durkin, A. S., Dimitrov, G., Jiang, L. X., Scanlan, D. & other authors (2004). Genomic insights into methanotrophy: the complete genome sequence of *Methylococcus capsulatus* (Bath). *PLoS Biol* **2**, e303.
- Weiss, R. F. (1974). Carbon dioxide in water and seawater: the solubility of a non-ideal gas. *Mar Chem* **2**, 203-215.
- Wilson, W. A., Roach, P. J., Montero, M., Baroja-Fernandez, E., Munoz, F. J., Eydollin, G., Viale, A. M. & Pozueta-Romero, J. (2010). Regulation of glycogen metabolism in yeast and bacteria. *FEMS Microbiol Rev* **34**, 952-985.
- Wise, M. G., McArthur, J. V. & Shimkets, L. J. (2001). *Methylosarcina fibrata* gen. nov., sp nov and *Methylosarcina quisquiliarum* sp nov., novel type I methanotrophs. *Int J Syst Evol Micr* **51**, 611-621.
- Wu, Z. J., Zhou, H. Y., Peng, X. T. & Chen, G. Q. (2006). Anaerobic oxidation of methane: Geochemical evidence from pore-water in coastal sediments of Qi'ao Island (Pearl River Estuary), southern China. *Chinese Science Bulletin* **51**, 2006-2015.
- Y**eates, T. O., Kerfeld, C. A., Heinhorst, S., Cannon, G. C. & Shively, J. M. (2008). Protein-based organelles in bacteria: carboxysomes and related microcompartments. *Nat Rev Microbiol* **6**, 681-691.
- Yimga, M. T., Dunfield, P. F., Ricke, P., Heyer, J. & Liesack, W. (2003). Wide distribution of a novel pmoA-like gene copy among type II methanotrophs, and its expression in *Methylocystis* strain SC2. *Appl Environ Microbiol* **69**: 5593-5602.
- Young, J.P.W. (1992). Phylogenetic classification of nitrogen-fixing organisms. In *Biological Nitrogen Fixation*, PP 43-86. Edited by Stacey, G, Evans, H. J. & Burris, R. H. New York: Chapman & Hall.
- Z**ehnder, A. J. B. & Brock, T. D. (1980). Anaerobic methane oxidation - occurrence and ecology. *Appl Environ Microbiol* **39**, 194-204.
- Zehr, J. P., Jenkins, B. D., Short, S. M. & Steward, G. F. (2003). Nitrogenase gene diversity and microbial community structure: a cross-system comparison. *Environ Microbiol* **5**, 539-554.
- Zhivotchenko, A. G., Nikonova, E. S. & Jorgensen, M. H. (1995). Effect of fermentation conditions on N₂ fixation by *Methylococcus capsulatus*. *Bioprocess Biosyst Eng* **14**, 9-15.

Nederlandse samenvatting

(Dutch summary)



Kweken van *Methylophilum fumariolicum* stam SolV onder specifieke conditie.

Foto door Ahmad F. Khadem.

Nederlandse samenvatting

Methaan (CH_4) is na koolstofdioxide (CO_2) het belangrijkste broeikasgas. De toename van beide gasen in de atmosfeer zorgt voor opwarming van de aarde. Methaan in de atmosfeer is afkomstig van zowel natuurlijke als antropogene bronnen. Methaan wordt geproduceerd door methanogene Archaea, die actief zijn bij de afbraak van organisch materiaal onder anaërobe omstandigheden. Daarnaast wordt er ook (niet-biologisch) methaan gevormd tijdens geothermale processen. Gelukkig komt niet al dit geproduceerde methaan in de atmosfeer terecht. Een groot gedeelte van het geproduceerde methaan wordt afgebroken door methaanoxiderende bacteriën (ook bekend als methanotrofe bacteriën). Aërobe methanotrofe bacteriën zijn micro-organismen die methaan als energie- en koolstofbron gebruiken. Tot 2007 konden alle toendertijd bekende genera van aërobe methanotrofen geplaatst worden binnen de Proteobacteriën. In dit proefschrift echter worden de resultaten van vier jaar onderzoek aan een nieuwe, niet proteobacteriële methanotroof, *Methyloacidiphilum fumariolicum* stam SolV, beschreven. Dit micro-organisme werd geïsoleerd uit een monster afkomstig uit een vulkanisch gebied in Italië, dicht bij Naples en werd in 2007 beschreven. Fylogenetische analyse gebaseerd op het 16S ribosoomaal RNA gen heeft laten zien, dat stam SolV samen met twee andere stammen (V4 en Kam1), die geïsoleerd werden uit vulkanische gebieden in Rusland en Nieuw-Zeeland, een nieuw type methanotrofen vertegenwoordigen die behoren tot de *Verrucomicrobia*. Alle drie stammen zijn goed aangepast aan de barre vulkanische omgeving en kunnen leven op zeer lage concentraties methaan en zuurstof, bij hoge temperaturen (50-95 °C) en pH waarden van 1. Het was voor het eerst dat representanten van de *Verrucomicrobia*, waarvan bekend is dat ze in hoge aantallen en in veel gebieden op aarde voorkomen, gekoppeld konden worden aan een geochemische cyclus. Omdat methaan bijdraagt aan het broeikaseffect, is het belangrijk dat we onze kennis over methaanoxiderende bacteriën uitbreiden. Om de biochemie en fysiologie van *Methyloacidiphilum fumariolicum* stam SolV te ontrafelen, heb ik in mijn onderzoek verschillende technieken zoals genoom-, transcriptoom analyses, elektronen microscopie en ^{13}C -labelingsexperimenten uitgevoerd.

In **Hoofdstuk Twee** van dit proefschrift wordt het genoom van stam SolV beschreven. De basepaar volgorde van het genoom van stam SolV werd met behulp van ‘next generation sequencing’ in kaart gebracht. De genoom analyse van stam SolV heeft laten zien, dat er overeenkomsten maar ook verschillen zijn tussen de verrucomicrobiële en de proteobacteriële methanotrofen. Als we kijken naar het stikstofmetabolisme zien we dat beide typen methanotrofen genen bevatten die betrokken zijn bij de stikstof (N_2) fixatie. Op het gebied van het koolstofmetabolisme zien we grotere verschillen. In het genoom van stam SolV werden maar liefst drie verschillende operonen (*pmoCAB*) coderend voor de drie subunits van membraan gebonden methaanmonooxygenases (pMMO) geïdentificeerd, samen met een afwijkend methanol dehydrogenase. Het pMMO is een cruciaal enzym betrokken bij de eerste stap van de methaanoxidatieroute, de omzetting van methaan in methanol. Het is bekend dat proteobacteriële methanotrofen koolstof kunnen assimileren voor biomassa productie, startend vanaf formaldehyde, een stof die geproduceerd wordt tijdens de oxidatie van methaan. Hiervoor bestaan twee routes, de ribulose monofosfaat route (RuMP; alle biomassa is afkomstig van formaldehyde) en de serine route (biomassa is afkomstig van formaldehyde en koolstofdioxide). De essentiële genen die voor deze twee assimilatie routes coderen werden niet gevonden in het genoom van *Methylophilum fumariolicum* stam SolV. In plaats daarvan bleken genen die coderen voor enzymen betrokken bij de Calvin-Benson-Bassham (CBB) route aanwezig in het genoom. Dit suggereerde dat stam SolV koolstofdioxide kan fixeren voor biomassa synthese. Ook genen betrokken bij opslag van koolstof in de vorm van glycogeen werden geïdentificeerd. De genoom data vormden de basis voor fysiologische studies (Hoofdstuk drie, vier en vijf) en transcriptoom analyses (Hoofdstuk zes).

In **Hoofdstuk Drie** wordt de stikstoffixatie door stam SolV gepresenteerd. In deze studie werden groeiexperimenten (in batch en chemostaat) gecombineerd met nitrogenase activiteitstesten (acetyleen reductie naar ethyleen) en fylogenetische analyse van de *nifDHK* genen (die coderen voor het nitrogenase enzym). Het nitrogenase enzym zorgt voor het verbreken van de N-N binding en de vorming van ammonium (NH_4^+), en is cruciaal voor de stikstoffixatie. De resultaten laten zien dat stam SolV alleen onder lage zuurstofconcentratie (0.5 % opgeloste zuurstof) en in afwezigheid van ammonium stikstof kan fixeren. Het nitrogenase van de verrucomicrobiële methanotrofen lijkt gevoeliger voor zuurstof dan het nitrogenase van proteobacteriële methanotrofen.

Hoofdstuk Vier beschrijft de koolstofdioxidefixatie door stam SolV. Ook voor deze studie werd stam SolV gekweekt onder batch en chemostaat condities. Het messenger RNA uit de cellen werd gebruikt voor een transcriptoom analyse, terwijl daarnaast ook ^{13}C -labelingsexperimenten en ribulose-1,5-bisphosphate carboxylase/oxygenase (RuBisCO) activiteitstesten werden uitgevoerd. De resultaten lieten zien dat de genen betrokken bij de CBB route, hoog tot expressie kwamen, vooral de twee genen coderend voor RuBisCO, het belangrijke eerste enzym van de CBB route. ^{13}C -labelingsexperimenten maakten duidelijk dat koolstofdioxide de koolstofbron is voor stam SolV. De RuBisCO activiteitstest was alleen positief in de supernatant fractie van het celvrij extract, wat er op duidt dat het enzym vrij in de cel voorkomt en niet in carboxysomen (organellen in de cel die betrokken zijn bij koolstofdioxidefixatie). Door gebruik te maken van gelelektroforese en size-exclusion chromatografie, kon aangetoond worden dat RuBisCO waarschijnlijk uit 8 kleine (16-kDa) en 8 grote (54-kDa) subunits bestaat. Fylogenetische analyse van het RuBisCO gen *cbbL* liet zien dat er sprake is van een nieuw type RuBisCO (gesuggereerde naam: type IE).

De opslag van koolstof in de vorm van glycogeen na ammoniumuitputting wordt beschreven in **Hoofdstuk Vijf**. Voor deze studie werden fed-batch kweken gebruikt. De cellen werden geoogst op verschillende tijdstippen tijdens de groei en gebruikt voor elektronen microscopie, elementaire- en biochemische analyses van eiwit- en glycogeengehalten. De groeiexperimenten lieten zien dat na het opraken van het ammonium de toename in optische dichtheid (gemeten bij 600 nm) en drooggewicht van stam SolV nog gedurende 7 dagen doorging. Het cel aantal steeg nog slechts 35 uur na het opraken van het ammonium, en stopte vervolgens. De elementaire analyse (geeft de verhouding koolstof / stikstof aan), heeft laten zien, dat na ammoniumuitputting de totale hoeveelheid stikstof (mg per ml celcultuur) niet meer toenam, terwijl de totale hoeveelheid koolstof (mg per ml celcultuur) nog steeds lineair toenam (weliswaar met afnemende snelheid). Dit wees op een mogelijke koolstofopslag. Dit werd bevestigd met een elektronen microscopische (specifieke kleuring) en biochemische analyse (glucose meting). Deze analyses hebben laten zien, dat stam SolV, direct begint met glycogeen te accumuleren, na het opraken van het ammonium. Het belang van glycogeen voor stam SolV werd aangetoond aan de hand van groeiexperimenten onder substraatlimitatie. De resultaten wijzen er op, dat glycogeen bevattende cellen vitaler bleven gedurende lange periodes (40 dagen) bij afwezigheid van methaan. Gebaseerd op de analyse van vrijkomend ^{13}C -koolstofdioxide uit met ^{13}C -glycogeen opgeladen cellen kon geconcludeerd worden, dat de cellen glycogeen consumeerden in afwezigheid van methaan, maar dat dit niet gekoppeld was aan groei (toename in aantal cellen).

Cellen gekweekt onder verschillende omstandigheden vormen de basis voor de transcriptoom analyse beschreven in **Hoofdstuk Zes**. Exponentieel groeiende cellen in flessen (met methaan, koolstofdioxide, zuurstof en ammonium in overmaat), stikstof fixerende cellen in de chemostaat (met methaan, koolstofdioxide en 0.5 % opgelost zuurstof, maar geen ammonium) en zuurstof gelimiteerde cellen in de chemostaat (met ammonium, methaan en koolstofdioxide in overmaat) werden met elkaar vergeleken. Het geannoteerde genoom (Hoofdstuk twee) vormde de basis voor de transcriptoom analyses en de fysiologische studies (Hoofdstuk drie, vier en vijf) werden verder onderbouwd. Onder stikstof fixerende condities werden alle genen betrokken bij deze route geactiveerd. Onder alle omstandigheden kwamen de genen betrokken bij de CBB route hoog tot expressie. Dit resultaat onderbouwt het belang van deze route voor de cel bij de vorming van biomassa. Twee van de drie operonen met *pmo* genen lieten differentiële expressie zien, die afhankelijk lijkt te zijn van de zuurstofconcentratie. Het derde operon kwam onder geen van de geteste condities tot expressie.

Dit proefschrift beschrijft een aantal belangrijke eigenschappen van *Methylophilum fumariolicum* stam SolV, een vertegenwoordiger van de recent ontdekte methanotrofe *Verrucomicrobia*, met als doel de rol van deze micro-organismen als methaan consumeerders in vulkanische gebieden beter te begrijpen. In **Hoofdstuk Zeven** wordt een samenvatting gegeven van de resultaten en worden suggesties gedaan voor vervolgonderzoek. Speerpunten voor dit onderzoek zouden kunnen zijn:

- de mogelijkheden van stam SolV bij het omgaan met “nitrosative stress”.
- het C2 metabolisme (o.a. het gebruik van acetaat) van stam SolV.
- de mogelijkheden tot autotrofe groei op waterstofgas (H_2) als alternatieve elektronendonator.
- de differentiële regulatie van de drie pMMO coderende *pmoCAB* operonen.
- gedetailleerde analyse van de ultrastructuur inclusief de cellulaire localisatie van de enzymen betrokken bij methaan-oxidatie.
- onderzoek naar het voorkomen van methanotrofe *Verrucomicrobia* in koudere en minder zure gebieden door het ontwikkelen van specifieke primer sets (*pmoA*, *cbbL*, 16S ribosoomaal RNA etc.) en biomarkers.



Size exclusion chromatography.
Foto door Ahmad F. Khadem.

Dankwoord

(Acknowledgments)



Picture by Ahmad F. Khadem.

Dankwoord

Ik was ongeveer 15 jaar oud toen ik naar Nederland kwam. Dankzij God en een aantal mensen heb ik mijn middelbare school af kunnen maken, ondanks het feit dat mijn Nederlandse taal nog gebrekkig was. Daarom wil ik alle leraren van het Ulenhof College en in het bijzonder de heer Bouke Hellinga, mevrouw Beatrijs Ouwehand en de heer Alex de Jong bedanken. Deze mensen hebben hun uiterste best gedaan, waardoor ik me snel de Nederlandse taal eigen kon maken zodat ik kon studeren.

Na het behalen van het vwo-diploma begon ik aan mijn studie Biologie. Gedurende mijn Bachelor heb ik veel met Klaas Heijmans samengewerkt en veel geleerd. Al gauw kwam ik er achter, dat microbiologie in het bijzonder mij aantrok. Dit heb ik te danken aan mijn favoriete docent dr. Jan Keltjens die mij de principes van redox reacties heeft geleerd terwijl ik daar een hekel aan had. Mijn Masterstages bij de afdeling microbiologie van Nijmegen en Wageningen waren heel leerzaam. Daarom wil ik mijn begeleiders in Nijmegen, prof. dr. ir. Mike Jetten, dr. Huub Op den Camp, dr. Marjan Smeulders en dr. Marcel Zandvoort en in Wageningen, prof. dr. ir. Fons Stams, prof. dr. ir. Piet Lens, dr. ir. Roel Meulepas en dr. ir. Christian Jagersma, bedanken voor hun begeleiding en de hulp bij de voorbereiding van het promotietraject.

Dankzij de beurs van NWO-Mozaïek die ik in 2008 kreeg en de afdeling microbiologie van Nijmegen kon ik aan mijn promotie beginnen. Daarom wil ik prof. dr. ir. Mike Jetten, dr. Huub Op den Camp en dr. Arjan Pol bedanken voor hun begeleiding gedurende mijn promotie onderzoek. Naast mijn begeleiders wil ik ook al die mensen bedanken die mij met de analyses hebben geholpen of die de analyses voor mij hebben uitgevoerd, Katinka van de Pas-Schoonen, Laura van Niftrik, Harry R. Harhangi, Muriel van Teeseling, Jelle Eygensteyn, Naomi de Almeida, Mingliang Wu en Dick van Aalst.

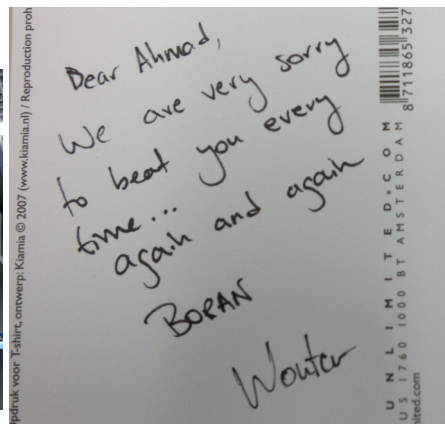
Ook heb ik een zeer leuke tijd gehad met Boran Kartal, Harry R. Harhangi, Wouter Maalcke, Adam Wieczorek en Daan Speth, onder andere door al die mooie wedstrijden tafelvoetbal.

Het was ook heel plezierig om in de labaratorium mijn werktafel te delen met Maartje van Kessel en tegenover ons Nardy Kip en Suzanne Haaijer. Bedankt voor de mooie tijd.

Katharina Ettwig, het was mij een genoegen om in jouw proefschrift te lezen dat ik jouw lievelingsstudent was en ik weet zeker dat Boran Kartal ook hetzelfde dacht, maar nooit toegaf. Als dank heb ik besloten om jullie te gaan helpen bij de cursus Ecological Microbiology.

Graag wil ik Katinka van de Pas-Schoonen, Theo van Alen en Marjan Smeulders bedanken voor hun handige tips toen ik een moeilijke tijd had met mijn pittige zoontje Hamza.

Ik dank jullie allemaal.



Acknowledgments

I want to thank the following ladies for allowing me to be the only guy in their office and of course for the nice time I had with them: Lina Russ, Naomi de Almeida, Marjan Smeulders, Francisca Luesken, Mingliang Wu and Jia Yan.

I want to thank Olivia Rasigraf for the nice teamwork during the Ecological Microbiology course.

Also I want to thank John Hermans, Wim Geerts, Marianne Uijt de Haag, Erwin van der Biezen, Ronald van den Heuvel, Rob de Graaf, Baoli Zhu, Sarah Neumann, Ziye Hu and Ke Ji for all their support and interest.

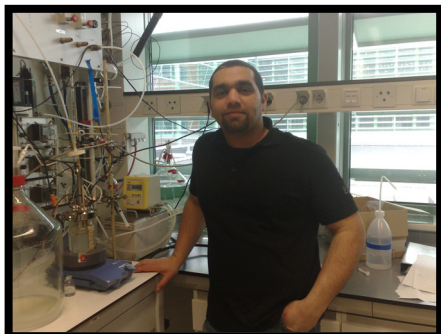
I want to thank my students who helped me with my experiments, Seyed S. Mohammadi, Joey Kampman and Iris van Leeuwen and wish you good luck in the future.

Thank you all.

Ahmad F. Khadem 2012.

Curriculum Vitae & List of publications

Curriculum Vitae



Ahmad Fouad Khadem was born on the 15th of April 1981 in Baghdad, Iraq.

In 1995 he came to the Netherlands. After finishing the secondary school (havo and vwo), he studied biology and in 2006 he obtained his Bachelor of Science from Radboud University Nijmegen.

After two years of specialization in microbiology he obtained his Master of Science in 2008. For his Master of Science degree he worked at the microbiology departments of Radboud University Nijmegen and Wageningen University.

In 2008, he received a Mosaic grant (62000583) from the Dutch Organisation for Scientific Research (NWO), and he started his Ph.D. at the department of microbiology, Radboud University Nijmegen under the supervision of Prof. dr. ir. Mike S. M. Jetten, Dr. Huub J. M. Op den Camp and Dr. Arjan Pol. The results of his Ph.D. are presented in this thesis.

E-mail: khadem.a.f@hotmail.com

List of publications

- Khadem, A. F., Pol, A., Jetten, M. S. M. & Op den Camp, H. J. M. (2010).** Nitrogen fixation by the verrucomicrobial methanotroph '*Methylocacidiphilum fumariolicum*' SolV. *Microbiol-Sgm* **156**, 1052-1059.
- Khadem, A. F., Pol, A., Wieczorek, A. S., Jetten, M. S. M. & Op den Camp, H. J. M. (2012).** Metabolic regulation of “*Ca. Methylocacidiphilum fumariolicum*” SolV cells grown under different nitrogen and oxygen limitations. *Front Microbiol* **3**, 266.
- Khadem, A. F., Pol, A., Wieczorek, A., Mohammadi, S. S., Francoijs, K. J., Stunnenberg, H. G., Jetten, M. S. M. & Op den Camp, H. J. M. (2011).** Autotrophic methanotrophy in *Verrucomicrobia*: *Methylocacidiphilum fumariolicum* SolV uses the Calvin-Benson-Bassham cycle for carbon dioxide fixation. *J Bacteriol* **193**, 4438-4446.
- Khadem, A. F.^a, van Teeseling, M. C. F.^a, van Niftrik, L., Jetten, M. S. M., Op den Camp, H. J. M. & Pol, A. (2012).** Genomic and physiological analysis of carbon storage in the verrucomicrobial methanotroph “*Ca. Methylocacidiphilum fumariolicum*” SolV. *Front Microbiol* **submitted**.
- Khadem, A.F., Wieczorek, A.S., Pol, A., Vuilleumier, S., Harhangi, H.R., Dunfield, P.F., Kalyuzhnaya, M.G., Murrell, J.C., Francoijs, K. J. & other authors (2012).** Draft genome sequence of the volcano-inhabiting thermoacidophilic methanotroph *Methylocacidiphilum fumariolicum* strain SolV. *J Bacteriol* **194**, 3729-3730.
- Meulepas, R. J. W., Jagersma, C. G., Khadem, A. F., Buisman, C. J. N., Stams, A. J. M. & Lens, P. N. L. (2009).** Effect of environmental conditions on sulfate reduction with methane as electron donor by an Eckernförde Bay enrichment. *Environ Sci Technol* **43**, 6553-6559.
- Meulepas, R. J. W., Jagersma, C. G., Khadem, A. F., Stams, A. J. M. & Lens, P. N. L. (2010).** Effect of methanogenic substrates on anaerobic oxidation of methane and sulfate reduction by an anaerobic methanotrophic enrichment. *Appl Microbiol Biotechnol* **87**, 1499-1506.

Smeulders, M. J., Barends, T. R. M., Pol, A., Scherer, A., Zandvoort, M. H., Udvarhelyi, A., Khadem, A. F., Menzel, A., Hermans, J. & other authors (2011). Evolution of a new enzyme for carbon disulphide conversion by an acidothermophilic archaeon. *Nature* **478**, 412-419.

^a Both authors contributed equally.

Conference proceedings

Khadem, A. F., Pol, A., Harhangi, H., Jetten, M. S. M. & Op den Camp, H. J. M. (2009). Methanotrophy under extreme conditions: Biochemistry and physiology of *Methylacidiphilum fumariolicum* SolV. *Antonie Van Leeuwenhoek* **95**, 74.

Khadem, A. F., Pol, A., Harhangi, H., Jetten, M. S. M. & Op den Camp H. J. M. (2010). Methanotrophy under extreme conditions: Biochemistry and physiology of *Methylacidiphilum fumariolicum* SolV. *Nederlands Tijdschrift voor Medische Microbiologie* **18**, 55.

Khadem, A. F., Pol, A., Mohammadi, S. S., Wieczorek, A., Jetten, M. S. M. & Op den Camp, H. J. M. (2011). *Methylacidiphilum fumariolicum* SolV uses the Calvin cycle for carbon assimilation. *Nederlands Tijdschrift voor Medische Microbiologie* **19**, 39.

وتمت مقارنة هذه الخلايا مع بعضها البعض، واستند الباحث في ذلك الى شرح الجينوم الذي ذكر في الفصل الثاني الذي يمثل الاساس لتحليلات الترنسكريبتوم ويثبت التجارب الفزيولوجية (الواردة في الفصل الثالث و الرابع و الخامس).

تحت ظروف تثبيت النتروجين نلاحظ ان جميع الجينات التي تسهم في هذه العملية جرى تفعيلها (التعبير الجيني)، وفي ظل جميع الظروف كان تعبير الجينات المسؤولة في دورة (CBB) عالية. هذه النتيجة تثبت أهمية هذه الدورة للخلية في تكوين الكتلة الحيوية. وظهرت التحاليل ان اثنان من اصل ثلاثة مشاغل (*pmoCAB*) الموجودة في الجينوم تُظهر فرقا في التعبير الجيني الذي يبدو أنه يعتمد على تركيز الأوكسجين. اما المشغل الثالث فلم ياتي بأي تغيير في التعبير الجيني في ظل الظروف المختبرية.

إن هذه الاطروحة تصف عددا من الخصائص المهمة لسلالة SolV التي تمثل الميثانوتروفس الهوائية في شعبة الـ (*Verrucomicrobia*) المكتشفة مؤخراً وكان الهدف من هذه التجارب فهم دور هذه البكتيريا كمُسْتَهْلِك لغاز الميثان في المناطق البركانية. في **الفصل السابع** جرى تلخيص النتائج وتقديم عدداً من الاقتراحات للتجارب المستقبلية، وكانت اولويات هذه البحوث هي:

- امكانيات سلالة SolV للتعامل مع اجهاد الـ (Nitrosative).
- التمثيل الغذائي C2 (بما في ذلك استخدام أسيتات) من سلالة SolV.
- إمكانات النمو الحقيقي ذاتية التغذية على الهيدروجين (H_2) كجهة بديلة مانحة للإلكترونات.
- تنظيم اختلاف التعبير الجيني في مشاغل (*pmoCAB*) التي ترمز الى ثلاثة انزيمات (pMMO).
- تحليل مفصل للتركيب الدقيق بما في ذلك موقع الانزيمات التي تشارك في اكسدة الميثان داخل الخلايا.
- البحث في احتمالية ظهور الميثانوتروفس الهوائية في شعبة الـ (*Verrucomicrobia*) في مناطق أكثر برودة وأقل حامضية من خلال تطوير مجموعات مشرع محددة (Primer sets) تستهدف جينات معينة (وهذه الجينات هي: *pmoA*، *cbbl*، الحمض النووي الريبسي (16S)، (الخ)، والمؤشرات الحيوية.

ومن الله التوفيق.

على حرية هذا الانزيم في داخل الخلية ويكون غير موجود في الكاربوكسيسوم (العضيات الموجودة داخل الخلايا التي تساعد في تثبيت ثاني أكسيد الكربون و تكون موجودة في أنواع معينة من البكتيريا). ويمكننا ملاحظة ان انزيم (RuBisCO) يتكون من ٨ وحدات صغرى (١٦-kDa) و ٨ وحدات كبرى (٥٤-kDa). وكانت وسائل البحث تتمثل باستخدام هلام كهربائي (تستخدم فيه تقنية خاصة لفصل البروتينات عن طريق تطبيق مجال كهربائي في وسط هلامي)، وحجم الاستبعاد اللوني (يُفصل بين الجسيمات على أساس الحجم، وبالتالي فإنها تكون مفيدة لتقنية البروتينات). وظهر تحليل النشوء والتطور من الجين (*cbbL*) الذي يرمز الى الوحدات الكبرى لانزيم (RuBisCO) ان هناك نوعا جديدا من هذا الانزيم (والاسم المقترح لتسميته به: نوع IE).

إن تخزين الكربون في شكل جليكوجين في ظل نضوب الأمونيوم يتم توضيحه في **الفصل الخامس**. في هذه الدراسة جرى تنمية سلالة SolV في ناظم كيميائي حسب طريقة (fed-batch)، حيث تُحصَد الخلايا في أوقات مختلفة خلال فترة النمو، وأُستخدِم المِجْهر الإلكتروني، وتحليل العناصر، والتحليل البايوكيميائي من البروتين والجليكوجين. وأظهرت نتائج التجارب الفيزيولوجية، انه بعد نفاذ الأمونيوم ان الزيادة في الكثافة البصرية (يقاس بـ ٦٠٠ نانومتر) والوزن الجاف لسلالة SolV استمر حتى ٧ أيام، وزيادة عدد الخلايا استمر ما يقارب ٣٥ ساعة بعد نضوب الأمونيوم ثم توقفت عن النمو. وأظهر نتائج تحليل العناصر (أي نسبة الكربون/ النيتروجين)، بعد نضوب الأمونيوم، ان اجمالي كمية النيتروجين بمقدار مليغرام/مليتر من الخلايا لم تزد، في حين أن اجمالي كمية الكربون بمقدار مليغرام/مليتر من الخلايا يزداد، ويستمر بالزيادة خطأً في الرسم البياني (ولو مع خفض السرعة)، ويمكن ان تكون هذه اشارة لتخزين الكربون في الخلايا. وهذا ما أكدته تحليل نتائج المِجْهر الإلكتروني (صبغة محددة)، والتحليل البايوكيميائي (قياس الغلوكوز) وهذه التحليلات اظهرت لنا ان الخلايا المنتجة في سلالة SolV يجري انتاج وتراكم الجليكوجين فيها بعد استنفاد الأمونيوم. وقد أظهرت أهمية الجليكوجين في سلالة SolV بالرجوع إلى تجارب النمو تحت تقييد الركيزة. وأشارت النتائج إلى أن الخلايا المحتوية على الجليكوجين، كانت أكثر قوة وقابلة للنمو لفترات طويلة (٤٠ يوماً) بعد تقييد الميثان. واستناداً على تحليل (^{13}C) - ثاني أكسيد الكربون، المنبعث من الخلايا التي تحتوي على (^{13}C) - الجليكوجين، استنتج الباحث أن الجليكوجين في الخلايا كان يُستهلك في حالة عدم وجود غاز الميثان، ولكن هذه النتيجة لا علاقة لها بالنمو (الزيادة في أعداد الخلايا).

وصف الفصل السادس أساس تحليل الترنسكريبتوم من خلال اجراء التجارب على خلايا نمت في ظل ظروف مختلفة، وكالاتي:

- خلايا تنمو نمواً مطرداً في زجاجات تحتوي على مركبات مُعينة (الميثان، وثاني أكسيد الكربون، والأوكسجين، والأمونيوم) بكميات مفرطة.
- خلايا مُثَبَّتة للنيتروجين في نظام كيميائي الذي يحتوي على تركيز محدد من المغذيات المطلوبة (٥،٠ ٪ الأوكسجين المذاب، الميثان، ثاني أكسيد الكربون) بدون الأمونيوم.
- خلايا محدودة الأوكسجين في نظام كيميائي اخر الذي يحتوي على تركيز محدد من المغذيات المطلوبة (الأمونيوم، والميثان، وثاني أكسيد الكربون).

الايض الكربوني. حُدد في الجينوم ثلاثة انواع مختلفة من المشاغل (المشغل: هو مجموعة من الجينات متجاورة لها وظائف متعلقة بعملية حيوية مشتركة) تسمى بـ (*pmoCAB*) ترمز لثلاثة اجزاء تُكون الانزيم (*Particulate Methane MonoOxygenase: pMMO*) وحُدد ايضا انزيم نازع الميثانول (*Methanol dehydrogenase*). ان انزيم (*pMMO*) مهم للمشاركة في الخطوة الاولى من عملية أكسدة الميثان الى الميثانول، ومن المعروف ان الكربون الموجود في الميثانوتروفس الهوائية في شعبة البروتيوبكتيريا يمكن استيعابه لإنتاج الكتلة الحيوية بدءاً من مادة الفورمالديهايد (وهي المادة التي تُنتج خلال أكسدة الميثان). وهنا توجد طريقتان، طريقة الريبولوز احادي الفوسفات (وتتكون الكتلة الحيوية فقط من الفورمالديهايد) وطريقة *serine* (الكتلة الحيوية تتكون من الفورمالديهايد وثاني أكسيد الكربون). إن وجود الجينات الضرورية في هاتين الطريقتين لم يُعثر عليها في جينوم سلالة *SoIV*، وبدلاً من ذلك وُجدت جينات ترمز إلى إنزيمات تشارك في دورة (*Calvin-Benson-Bassham : CBB*) وهذا أشار إلى أن سلالة *SoIV* يمكنها تثبيت ثاني أكسيد الكربون لتركيب الكتلة الحيوية. وحُددت الجينات المسؤولة عن تخزين الكربون على شكل جليكوجين. ومن هنا شكلت بيانات الجينوم الأساس للتجارب الفزيولوجية (كما سنرى في الفصل الثالث و الرابع و الخامس)، وتحليل الترنسكريبتوم (يراجع: الفصل السادس).

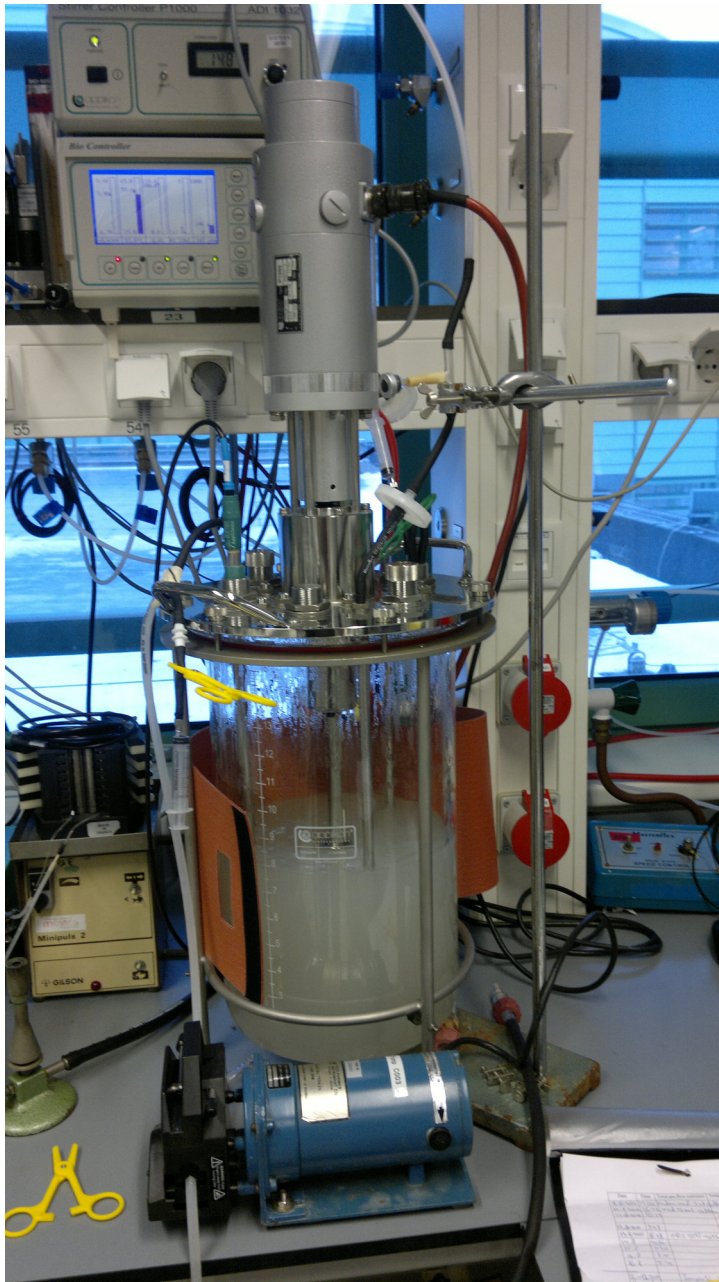
تناول الفصل الثالث دراسة تثبيت النتروجين عن طريق سلالة *SoIV*، وأجريت التجارب الفزيولوجية في زجاجات وناظم كيميائي (وهو جهاز تجري فيه تكاثر مضبوط للجراثيم بلا حدود بواسطة جريان مستمر للوسط الذي يحتوي على تركيز محدد من المغذيات المطلوبة)، جنباً الى جنب مع فحوصات نشاط الانزيم (*nitrogenase*) (أي اختزال الاستيلين الى اثيلين)، ودراسة النشوء والتطور لجينات (*nifDHK*) (التي ترمز إلى أنزيم الـ *nitrogenase*). هذا الأنزيم مسؤول عن كسر الرابطة (*N-N*) وتشكيل الامونيوم (NH_4^+) وهو مهم لتثبيت النتروجين. وقد بينت النتائج أن سلالة *SoIV* في ظل تركيز الأوكسجين المنخفض (٥،٠ ٪ الأوكسجين المذاب)، وفي حالة عدم وجود الأمونيوم تستطيع تثبيت النيتروجين. يكون انزيم الـ (*nitrogenase*) في الميثانوتروفس الهوائية من شعبة الـ (*Verrucomicrobia*) اكثر حساسية للأوكسجين من انزيم الـ (*nitrogenase*) في الميثانوتروفس الهوائية من شعبة البروتيوبكتيريا.

وبحث الفصل الرابع عملية تثبيت ثاني أكسيد الكربون عن طريق سلالة *SoIV*، وأستُخدمت زجاجات وناظم كيميائي لنمو سلالة *SoIV*، واستُخدم أيضاً مرسال الحمض النووي الريبسي (*mRNA*) من الخلايا لتحليل الترنسكريبتوم وكذلك اجريت تجارب استُخدم فيها غاز (^{13}C) - ميثان وغاز (^{13}C) - ثاني أكسيد الكربون، ونشاط انزيم (*RuBisCO*) وهو مختصر لاسم الانزيم الريبولوز ثنائي الفوسفات كربوكسيلاز / أوكسيجيناز. أن الجينات المسؤولة عن دورة (*CBB*)، أظهرت درجة عالية للتعبير الجيني حسب نتائج تحليل الترنسكريبتوم، وبالأخص اثنين من الجينات التي ترمز الى (*RuBisCO*) وهو اهم انزيم في دورة (*CBB*). إن التجارب التي اجريت باستخدام (^{13}C) - ميثان و(^{13}C) - ثاني أكسيد الكربون، اثبتت ان سلالة *SoIV* تستخدم ثاني أكسيد الكربون كمصدر لانتاج الكربون في الكتلة الحيوية. وكان اختبار النشاط لانزيم (*RuBisCO*) ايجابيا فقط في الجزء الطائف من البروتين المستخلص من الخلايا (عملية استخلاص البروتين من الخلايا البكتيرية وتسمى هذه العملية بـ (*Preperation of Cell Free Extract*))، مما يدل

المخلص

يعتبر غاز الميثان (CH_4) من اهم الغازات الدفيئة او غازات الاحتباس الحراري بعد ثاني أوكسيد الكربون (CO_2)، إن زيادة هذين الغازين في الغلاف الجوي يؤدي الى ارتفاع درجة حرارة الارض. يأتي غاز الميثان من المصادر الطبيعية والبشرية، وتنتجُ الاحياء الدقيقة المعروفة باسم العتائق او الاركيا (methanogenic Archaea)، التي تنشط في تحليل المواد العضوية تحت الظروف اللاهوائية وتعتبر هذه الطريقة البيولوجية في الإنتاج، بالإضافة إلى إنتاجه بالطريقة غير البيولوجية حيث يتكون غاز الميثان في عمليات إنبعاث الطاقة الحرارية الأرضية حيث يبدأ تحليل المواد العضوية في درجات حرارة عالية (> 80 درجة مئوية). لحسن الحظ، لا يذهب كل هذا الميثان الناتج الى الجو فهناك جزء كبير منه تستعمله الاحياء الدقيقة المعروفة ببكتيريا الميثانوتروفس (methanotrophs)، وهي كائنات حية دقيقة تستعمل الميثان كمصدر للطاقة والكربون لتكوين الكتلة الحيوية، و يمكنها أن تنمو هوائيا أو لا هوائيا، وأنواعها الهوائية تصنف تحت شعبة البروتوبكتيريا (Proteobacteria) حتى عام ٢٠٠٧. تضم هذه الاطروحة نتاج اربعة سنوات من البحوث العلمية على نوع جديد من الميثانوتروفس الهوائية الذي لا يقع تحت تصنيف شعبة البروتوبكتيريا ويسمى هذا النوع الجديد بـ (*Methylococcus* strain SolV). أُحضرت عينة البحث هذه من البكتيريا من منطقة بركانية في ايطاليا بالقرب من نابولي، ونُشر اول بحث علمي وصف هذا النوع من البكتيريا في عام ٢٠٠٧. وقد تبين في تحليل النشوء والتطور استنادا إلى جينات الحمض النووي الريبي (16S) ان سلالة SolV تُمثل مع اثنين من سلالات أخرى (Kam1 وV4) أُحضرتا من المناطق البركانية في روسيا ونيوزيلندا، وبذلك تعتبر هذه السلالات انواعا جديدة من الميثانوتروفس الهوائية التي تنتمي الى شعبة الـ (*Verrucomicrobia*). وتكيف هذه السلالات الثلاثة بشكل جيد مع البيئة البركانية القاسية، وتكون قادرة على النمو في كميات منخفضة جدا من تركيز غازي الميثان والاكسجين وتكون درجة الحموضة (الرقم الهيدروجيني pH) منخفضة جدا تصل الى ١، ودرجات حرارة عالية جدا تصل الى مئة درجة مئوية. الـ (*Verrucomicrobia*) تعرف بانها ذات اعداد كبيرة، وتكون موجودة في مناطق كثيرة على الارض، ولان التجارب اثبتت أن أنواعاً معينة من الميثانوتروفس الهوائية تنتمي الى هذه الشعبة فيذلك نستطيع ربطها بالدورة الجيوكيميائية. ولان غاز الميثان يسهم في ظاهرة الاحتباس الحراري فمن المهم ان نزيد معرفتنا بالبكتيريا المؤكسدة لغاز الميثان، وعلى هذا الاساس استعملنا تقنيات مختلفة لدراسة الكيمياء الحيوية و الفيزيولوجيا لسلالة SolV مثل : تحليل الجينوم و الترנסكربتوم وإستخدام المجهر الالكتروني وإجراء تجارب استُخدِم فيها غازي (^{13}C) - ميثان و (^{13}C) - ثاني أوكسيد الكربون.

تضمن **الفصل الثاني** من هذه الاطروحة تعريف الجينوم الخاص بسلالة SolV وتحديد تسلسل زوج قاعدة من الجينوم بواسطة (next generation sequencing). وأظهر تحليل الجينوم بان هناك أوجه تشابه، واختلافات بين الميثانوتروفس الهوائية في شعبة البروتوبكتيريا والميثانوتروفس الهوائية في شعبة الـ (*Verrucomicrobia*). اذا نظرنا الى الايض النتروجيني يمكننا ان نرى ان كلا النوعين من الميثانوتروفس الهوائية يحتوي على الجينات التي تشارك في تثبيت النتروجين (N_2)، بينما نلاحظ اختلافات اكبر في منطقة



الناظم الكيميائي الذي استُخدم في عمليات نمو سلالة SolV.
ألتقط الصورة : أحمد فؤاد كاظم.

الملخص

(Arabic summary)

المشرف:

Prof. dr. ir. Mike S. M. Jetten.

مساعدین المشرف:

Dr. Huub J. M. Op den Camp.

Dr. Arjan Pol.

لجنة اطروحة الدكتوراه:

Prof. dr. Titti Mariani.

Prof. dr. ir. Fons Stams (Wageningen University).

Dr. Paul L. E. Bodelier (The Netherlands Institute of Ecology (NIOO-KNAW), Wageningen).

أكسدة الميثان تحت ظروف قاسية

دراسة الكيمياء الحيوية والفيزيولوجيا لسلالة SolV

اطروحة الدكتوراه

للحصول على درجة الدكتوراه من جامعة

Radboud University Nijmegen, Holland

وبناء على تفويض من رئيس الجامعة

البروفيسور الدكتور S. C. J. J. Kortmann

ووفقاً لقرار مجلس عمداء الكليات لمناقشة الاطروحة

علناً في يوم الاربعاء المصادف (٥ كانون الاول ٢٠١٢)

في الساعة ١٠:٣٠.

لـ

أحمد فؤاد كاظم

١٥ نيسان ١٩٨١

بغداد - العراق

الحمد لله رب العالمين والصلاة والسلام على خير خلقه محمد وعلى آله الطيبين الطاهرين
 طلب علم هذا الكتاب كان بالتوسل الى الله عز وجل وبالنبي (ص) وآله (عليهم السلام) وهذا ما شجعني ان
 اطلب من الله ما طلبه الامام السجاد (عليه السلام) في دعائه المشهور "مكارم الأخلاق".

"اللَّهُمَّ صَلِّ عَلَى مُحَمَّدٍ وَآلِهِ وَلَا تَرْفَعْنِي فِي النَّاسِ دَرَجَةً إِلَّا حَطَّطْتَنِي عِنْدَ نَفْسِي مِثْلَهَا وَلَا تُخَذِّبْ لِي عِزًّا
 ظَاهِرًا إِلَّا أَحَدَّثْتَ لِي ذِلَّةً بَاطِنَةً عِنْدَ نَفْسِي بِقَدْرِهَا"

أهدي كتابي هذا الى صاحب العصر والزمان الحجة المهدي (عجل الله فرجة الشريف وسهل مخرجه)
 والى ابي الشهيد الدكتور فؤاد كاظم غيدان الربيعي والى امي الغالية لدورهما الكبير في حياتي
 واشكر زوجتي العزيزة والأهل والأقارب.

بِسْمِ اللَّهِ الرَّحْمَنِ الرَّحِيمِ

